Catalytic wet oxidation of organic wastes using platinum catalysts

DOI:

[10.6100/IR575845](10.6100/IR575845)

Document status and date:
Published: 01/01/2004

Document Version:
Publisher's PDF, also known as Version of Record (includes final page, issue and volume numbers)

Please check the document version of this publication:

• A submitted manuscript is the version of the article upon submission and before peer-review. There can be important differences between the submitted version and the official published version of record. People interested in the research are advised to contact the author for the final version of the publication, or visit the DOI to the publisher's website.
• The final author version and the galley proof are versions of the publication after peer review.
• The final published version features the final layout of the paper including the volume, issue and page numbers.

Link to publication

Catalytic wet oxidation of organic wastes using platinum catalysts

PROEFSCHRIFT

ter verkrijging van de graad van doctor aan de
Technische Universiteit Eindhoven, op gezag van de
Rector Magnificus, prof.dr. R.A. van Santen, voor een
commissie aangewezen door het College voor
Promoties in het openbaar te verdedigen op
donderdag 3 juni 2004 om 16.00 uur

door

Zacharia Peter Gikira Masende

geboren te Bariadi, Tanzania

Dit proefschrift is goedgekeurd door de promotoren:

prof.dr.ir. J.C. Schouten
en
prof.dr.ir. F.J.J.G. Janssen

Copromotor:
dr.ir. B.F.M. Kuster

Dedicated to my parents

SUMMARY

The problems of water quality in developing countries are in most cases caused by agricultural activities, rapid urbanization, and expanding industries. Tanzania is one of the developing countries, which faces water pollution due to growing industrial activities. Generally, there are very few wastewater treatment facilities. The most widely used treatment systems in Tanzania include stabilization ponds, and natural and constructed wetlands, all using biological processes. The effluents from chemical and related industries contain organic compounds, which cannot be treated by conventional biological oxidation. The process industries that have a significant wastewater effluent include refining, chemicals, petrochemicals, pharmaceuticals, agrochemicals, and pulp and paper industries. The organic pollutants e.g. phenol, are toxic and cause considerable damage and threat to the ecosystem in water bodies and to the human health.

Catalytic wet oxidation (CWO) of organic waste in water using noble metal catalysts seems to be a promising and an environmental friendly method to improve water quality. The process uses air as the oxidant, which is contacted with the organic compound over a catalyst at elevated temperatures and pressures. The CWO process is capable of converting oxygenate organic contaminants ultimately to carbon dioxide and water. However, one of the major drawbacks of noble metal catalysts, such as platinum, is deactivation during liquid phase oxidation. Furthermore, catalytic wet oxidation technology is, at present, not available in Tanzania.

This thesis describes the study undertaken on the application of platinum catalysts for catalytic wet oxidation (CWO) of organic wastes in water. The emphasis is on the evaluation of activity, selectivity, and stability of platinum catalysts for use in liquid phase oxidation of organic (oxygenates) compounds. It is also envisaged to enhance and consolidate research and strengthen institutional capability in catalytic oxidation of wastewater in Tanzania. The approach covered experimental investigation of four types of platinum catalysts on different support materials, namely Pt/graphite, Pt/TiO_2, Pt/Al_2O_3, and Pt/activated carbon (AC). The performances of these catalysts were studied using three model reactions, namely phenol oxidation, maleic acid oxidation, and malonic acid oxidation.

The experimental work was partly performed at the Laboratory of Chemical Reactor Engineering, Eindhoven University of Technology, the Netherlands, using a continuous

stirred tank (CSTR) slurry reactor. Since the research was a so-called "sandwich programme", part of the work was also carried out at the University of Dar es Salaam in Tanzania, whereby research equipment and analytical facilities have been installed and tested for CWO studies. Analysis of gas samples was performed by means of on-line gas chromatography (GC), an oxygen sensor and a gas analyser, whereas the liquid samples were analysed using high performance liquid chromatography (HPLC).

The oxidation of phenol using Pt/graphite has shown that the activity of the Pt/graphite catalyst, and hence the selectivity to the oxidation products, is influenced by the degree of oxygen coverage of the platinum surface. Full conversion of phenol to CO_2 and H_2O is mostly favoured on a partly oxidised platinum surface. It was found that complete oxidation of phenol to CO_2 and H_2O is achieved at a temperature of 150°C, when the reaction proceeds within the range of stoichiometric oxygen excess to phenol from 0 to 80%. At a residual oxygen partial pressure above 150 kPa, deactivation of platinum catalysts was observed which leads to the formation of insoluble matter from the reaction intermediates. Increasing the reaction temperature enhances the activity of the platinum catalyst and also the reaction rate. When insufficient oxygen is used, the oxidation of phenol favours the formation of refractory acids, e.g. acetic acid and succinic acid, which are difficulty to oxidize.

A practical operation window in which high selectivity to CO_2 and H_2O can be achieved, and catalyst deactivation avoided, has been determined from the experimental data. Also a reaction pathway for phenol oxidation over platinum catalysts has been proposed. It was further found that high conversions of phenol and high selectivities to CO_2 were favoured when the reaction was carried out in the mass transport limited regime. A model, which predicts the performance of oxidation of the organic waste over platinum catalyst in the mass transport limited regime and within the practical operation window, has been developed and validated.

The aqueous phase degradation of malonic acid over Pt/graphite proceeds via homogeneous and catalytic decarboxylation to CO_2 and acetic acid. The disappearance rate of malonic acid during non-catalysed decarboxylation in the absence of oxygen increases with the increase in temperature, whereas complete conversion to CO_2 and acetic acid was achieved at 160°C. The catalytic oxidation of malonic acid showed no significant influence on the disappearance rate, while the carbon selectivity to CO_2 increased. Several possible kinetic models have been developed and evaluated. The optimum kinetic model for malonic acid decarboxylation was able to describe the kinetic experiments adequately.

The oxidation of maleic acid over a Pt/graphite catalyst showed a performance similar to phenol oxidation. At an impeller speed of 1200 rpm and a catalyst concentration of 10 kg_{cat}/m_L^3 of Pt/graphite, a high conversion of maleic acid (above 95%) was obtained when the reaction was carried out at 150°C with S.E. between 0 and 100%. At high residual oxygen partial pressure above 150 kPa, deactivation of Pt/graphite was observed. It was further found that high performance of the catalyst and high selectivity of maleic acid oxidation to CO_2 was obtained in the mass transport limited regime. A catalytic wet oxidation model, which describes the oxidation of maleic acid for these conditions, has been developed.

The evaluation of the influence of catalyst support has shown that the differences in activity of platinum catalysts in the liquid phase oxidation of organic wastes seem to be related to the metal dispersion and porosity of the catalyst support. Pt/graphite catalyst (metal dispersion of 5.3%) is the most effective and stable catalyst for liquid phase oxidation, and also deactivates slowly compared to Pt/TiO_2 (15.3%), Pt/Al_2O_3 (19.5%), and Pt/AC (19.0%). During phenol oxidation, deactivation by fouling seems to be severe for "mixed" type catalysts such as Pt/TiO_2, Pt/Al_2O_3, and Pt/AC. Despite the differences of morphological properties of the supports, the activity of platinum catalysts for phenol oxidation decreased in the order $Pt/graphite > Pt/TiO_2 > Pt/Al_2O_3$, and for maleic acid oxidation, $Pt/graphite > Pt/Al_2O_3 > Pt/AC$.

Finally, it can be concluded that platinum catalysts are effective for liquid phase oxidation of organic compounds and can be applied for catalytic wastewater treatment systems. To avoid the deactivation of the catalyst and maintain high catalyst activity, reaction needs to be carried out in a properly defined operation window. Consequently, a Continuous Stirred Tank Reactor (CSTR), or a Slurry Bubble Column (SBC) with improved mixing, are the best reactor types to use for this process. The results of the research described in this thesis contribute to a more efficient and environmental friendly technology of treating industrial wastewater.

SAMENVATTING

Waterkwaliteitsproblemen in ontwikkelingslanden worden in de meeste gevallen veroorzaakt door landbouwactiviteiten, snelle verstedelijking en industriële groei. Tanzania is één van de ontwikkelingslanden, die zich geconfronteerd ziet met waterverontreiniging door toenemende industriële activiteit. Over het algemeen zijn er zeer weinig afvalwaterzuiveringsinstallaties. De meest algemeen gebruikte zuiveringssystemen zijn stabilisatievijvers, en natuurlijke en aangelegde moeraslanden, welke alle gebruik maken van biologische processen. Het afvalwater van de chemische en aanverwante industrie bevat organische stoffen, die niet met de gebruikelijke biologische oxidatie kunnen worden behandeld. De procesindustrie met een belangrijke hoeveelheid afvalwater omvat olieraffinage, de chemische, petrochemische, farmaceutische, agrochemicaliën, en de papier- en pulpindustrie. De organische verontreinigingen, zoals fenol, zijn giftig, veroorzaken aanzienlijke schade, en zijn een bedreiging voor het ecosysteem in waterpartijen, en voor de gezondheid van de mens.

Katalytische natte oxidatie (CWO) van organische afvalstoffen in water, met behulp van edelmetaalkatalysatoren, lijkt een veelbelovende en milieuvriendelijke methode te zijn voor de verbetering van de waterkwaliteit. Het proces maakt gebruik van lucht als oxidatiemiddel, welke met de organische verbinding in contact wordt gebracht over een katalysator bij verhoogde temperatuur en druk. Het CWO-proces is in staat om zuurstofbevattende, organische verontreinigingen uiteindelijk tot kooldioxide en water om te zetten. Echter, één van de belangrijkste nadelen van edelmetaalkatalysatoren, zoals platina, is deactivering tijdens oxidatie in de vloeistoffase. Bovendien is katalytische natte oxidatie technologie momenteel niet beschikbaar in Tanzania.

Dit proefschrift beschrijft de uitgevoerde studie naar de toepassing van platina katalysatoren voor katalytische natte oxidatie van organische afvalstoffen in water. De nadruk ligt op de evaluatie van activiteit, selectiviteit en stabiliteit van platina katalysatoren voor gebruik in vloeistoffase-oxidatie van organische (zuurstofbevattende) verbindingen. Er is ook voorzien in verbetering en integratie van onderzoek, en versterking van de institutionele capaciteit voor katalytische oxidatie van afvalwater, in Tanzania. De aanpak betrof een experimenteel onderzoek naar vier types platinakatalysatoren op verschillende dragermaterialen, namelijk, Pt/grafiet, Pt/TiO$_2$, Pt/Al$_2$O$_3$, en Pt/actieve kool (AC). Het gedrag van deze katalysatoren werd

bestudeerd gebruikmakende van drie modelreacties, namelijk, fenoloxidatie, maleinezuur-oxidatie, en malonzuuroxidatie.

Het experimentele werk werd gedeeltelijk uitgevoerd in het Laboratorium voor Chemische Reactortechnologie van de Technische Universiteit Eindhoven, Nederland, gebruikmakende van een continue geroerde tank (CSTR) slurry reactor. Aangezien het onderzoek viel binnen een zogenaamd "sandwich programma", werd een gedeelte van het werk ook uitgevoerd aan de Universiteit van Dar es Salaam in Tanzania, waarbij onderzoeksapparatuur en analytische faciliteiten zijn geïnstalleerd en getest voor CWO-studies. Gasmonsters werden geanalyseerd met behulp van on-line gaschromatografie (GC), een zuurstofsensor en een gasanalysator, terwijl de vloeistofmonsters werden geanalyseerd met vloeistofchromatografie (HPLC).

De oxidatie van fenol over Pt/grafiet heeft aangetoond dat de activiteit van de Pt/grafietkatalysator, en derhalve de selectiviteit naar de oxidatieproducten, wordt beïnvloed door de mate van zuurstofbedekking van het platina-oppervlak. Volledige omzetting van fenol naar CO_2 en H_2O is het meest gunstig op een gedeeltelijk geoxideerd platina-oppervlak. Er is gevonden dat volledige oxidatie van fenol tot CO_2 en H_2O kan worden bewerkstelligd bij een temperatuur van 150°C, indien de reactie verloopt in het bereik van de stoïchiometrische zuurstof overmaat tot fenol van 0 tot 80%. Bij een rest zuurstofdruk boven 150 kPa, werd deactivering van de platinakatalysatoren waargenomen, hetgeen leidt tot de vorming van onoplosbare stoffen uit de tussenproducten van de reactie. Toename van de reactietemperatuur verhoogt de activiteit van de platinakatalysator, evenals de snelheid van de reactie. Wanneer onvoldoende zuurstof wordt gebruikt, begunstigt de oxidatie van fenol de vorming van hardnekkige zuren, zoals azijnzuur en barnsteenzuur, die moeilijk zijn te oxideren.

Een praktisch bedrijfsvenster, waarbinnen een hoge selectiviteit naar CO_2 en H_2O kan worden bereikt, en katalysatordeactivering kan worden vermeden, is vastgesteld uit de experimentele gegevens. Het reactienetwerk voor fenoloxidatie over platinakatalysatoren is eveneens voorgesteld. Ook werd gevonden dat goede omzetting van fenol en hoge selectiviteit naar CO_2 werd begunstigd, indien de reactie werd uitgevoerd onder stofoverdrachtslimitering. Een model, welke de prestatie voor oxidatie van de organische afvalstof over een platinakatalysator binnen het praktisch bedrijfsvenster voorspelt, is ontwikkeld en gevalideerd.

De afbraak van malonzuur over Pt/grafiet in de waterige fase, verloopt via homogene en katalytische decarboxylatie tot CO_2 en azijnzuur. De verdwijnsnelheid van malonzuur tijdens

de niet-katalytische decarboxylatie in afwezigheid van zuurstof, neemt toe met toenemende temperatuur, en volledige omzetting tot CO_2 en azijnzuur werd bereikt bij 160°C. De katalytische oxidatie van malonzuur vertoonde geen belangrijke invloed op de verdwijnsnelheid, maar de koolstofselectiviteit naar CO_2 nam toe. Verschillende mogelijke kinetische modellen zijn ontwikkeld en op waarde geschat. Het beste kinetische model voor malonzuurdecarboxylatie, was in staat de kinetische experimenten voldoende te beschrijven.

De oxidatie van maleïnezuur over een Pt/grafietkatalysator vertoonde eenzelfde gedrag als de fenoloxidatie. Bij een roersnelheid van 1200 rpm en een katalysatorconcentratie van 10 kg_{cat}/m_L^3 Pt/graphite werd een hoge omzetting van maleïnezuur (boven 95%) verkregen, indien de reactie werd uitgevoerd bij 150°C en een stoïchiometrische overmaat (S.O.) tussen 0 en 100%. Bij een hoge rest zuurstofpartiaaldruk, boven 150 kPa, werd deactivering van Pt/grafiet waargenomen. Verder werd gevonden dat een goede prestatie van de katalysator en een hoge selectiviteit voor maleïnezuuroxidatie tot CO_2 werd verkregen, onder stoftransport-limiterende omstandigheden. Een katalytisch natte-oxidatie model, dat de oxidatie van maleïnezuur onder deze omstandigheden beschrijft, is ontwikkeld.

De evaluatie van de invloed van de katalysatordrager heeft aangetoond, dat de verschillen in activiteit van platinakatalysatoren voor de vloeistoffase oxidatie van organische afvalstoffen, gerelateerd schijnen te zijn aan de metaaldispersie en de porositeit van de katalysatordrager. Pt/grafietkatalysator (metaaldispersie 5.3%) is de meest effectieve en stabiele katalysator voor vloeistoffase oxidatie, welke slechts langzaam deactiveert vergeleken met Pt/TiO$_2$ (15.3%), Pt/Al$_2$O$_3$ (19.5%), en Pt/AC (19.0%). Tijdens fenoloxidatie lijkt deactivering door verstopping ernstig te zijn voor de "gemengde" types katalysatoren zoals Pt/TiO$_2$, Pt/Al$_2$O$_3$, en Pt/AC. Ondanks de verschillen in morfologische eigenschappen van de dragermaterialen, nam de activiteit van platinakatalysatoren voor fenoloxidatie af in de volgorde Pt/grafiet > Pt/TiO$_2$ > Pt/Al$_2$O$_3$, en voor maleïnezuuroxidatie Pt/grafiet > Pt/Al$_2$O$_3$ > Pt/AC.

Tenslotte kan worden vastgesteld dat platinakatalysatoren doeltreffend zijn voor de vloeistoffase-oxidatie van organische verbindingen en kunnen worden toegepast in katalytische afvalwaterzuiveringssystemen. Om deactivering van de katalysator te vermijden en hoge katalysatoractiviteit te handhaven dient de reactie te worden uitgevoerd binnen een duidelijk afgebakend bedrijfsvenster. Dientengevolge zijn een Continue Geroerde Tankreactor (CSTR), of een Slurry Bellenkolom (SBC), welke goede mengers zijn, de beste reactortypes om voor dit proces te gebruiken. De resultaten van het onderzoek, die in dit proefschrift beschreven zijn, dragen bij tot een efficiëntere en milieuvriendelijkere technologie voor de behandeling van industrieel afvalwater.

TABLE OF CONTENTS

1
INTRODUCTION

There is increasing environmental concern worldwide regarding the disposal of wastewater containing non-biodegradable organic compounds. Since most pollutants do not respect national boundaries, a worldwide effort to monitor their movement and to develop tools to prevent them from polluting environmental components or to remediate consequent pollution is desirable. This introductory chapter presents the context of the research and the objectives for undertaking catalytic wet oxidation studies using platinum catalysts. This chapter provides an overview of the water pollution problems and challenges related to water pollution in developing countries, Tanzania being an example. It highlights sandwich research undertaken between Eindhoven University of Technology in the Netherlands and University of Dar es Salaam in Tanzania.

1.1   General

Water is the most precious natural resource that exists on our planet as over 70% of the Earth's surface is covered by water. The oceans contain 97% of the earth's water, while the remaining 3% is classified as fresh water. Seventy-nine percent of this surface fresh water is stored as ice and glaciers and 20% as groundwater. The remaining freshwater, which is about 1% of the world's total, is contained in lakes, rivers, soil moisture etc., as shown in Fig. 1.1. It can be seen that the water available for humankind use is very small as such it needs to be protected from all forms of contamination.

Surface water is the resource for the provision of drinking water, irrigation water for agricultural activities, and process water for industrial activities. Since water means new potential, new hope for a better tomorrow and new life, human settlement and development has concentrated around water resources. As such the most densely populated and commercially developed areas are the shorelines of oceans, lakes and rivers (Scheren, 2003).

oceans
97%

fresh
water
3%

(a) All water

ice caps
&
glaciers
79%

EASF
1%

ground
water
20%

(b) Fresh water

lakes
52%

soil
moisture
38%

WWLO
1%

rivers
1%

AWV
8%

(c) Easily accessible surface water
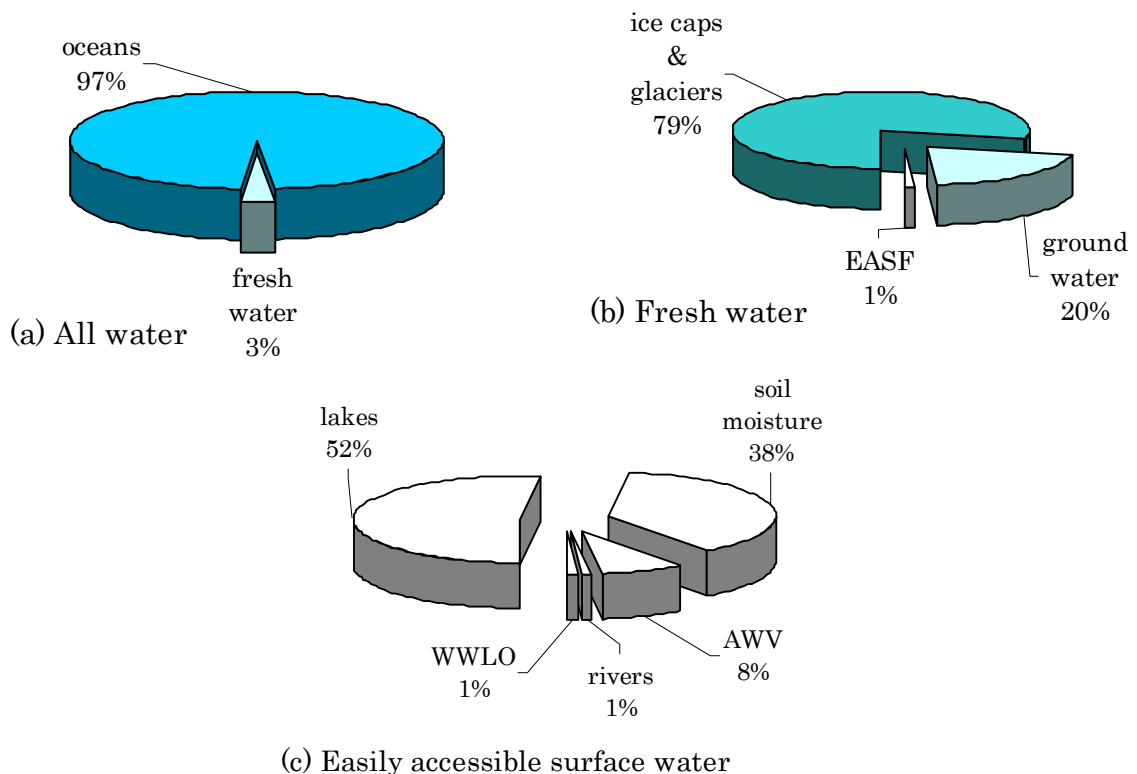
Fig. 1.1. Distribution of the world's water. Abbr.: EASF: easily accessible surface fresh water; AWV: atmospheric water vapour; WWLO: water within living organisms.

Although on the one hand this fact is recognized, on the other hand it is disregarded by polluting rivers, lakes and oceans, since the same water bodies are used as depository of wastes. During use, water becomes contaminated with various kinds of substances. In many regions, particularly in parts of the developing world, poverty combined with rapid population growth is leading to widespread degradation of water resources. At the same time, rapid urbanization and industrialization in many developing countries are creating high levels of water pollution associated with harmful industrial effluents and sewage discharges. Agricultural activities have created problems in water receiving bodies due to run-off, which bring with them pesticides and fertilizers (Shiklomanov, 1997). Since only a little amount of water is available for human needs, it is therefore important to preserve water resources in order to enhance both current and future potential.

In order to manage environmental pollution at global level, the United Nations Environmental Program (UNEP) in 1972 was designed to be the "environmental conscience of the United Nations". In response to this, towards the end of the 20th Century, environmental legislation in most, if not all countries has been enacted to safeguard environmental integrity. Legislation has put in place stringent regulations regarding environmental and health quality standards, especially on the utilisation of water resources. However, even with these stringent measures pollution of water resources is still a major problem. In order to combat water pollution, it is important to understand the sources of and problems related to polluting agents.

1.1.1. *Major sources of water pollution*

Water pollution occurs when a body of water is adversely affected due to the addition of large amounts of material to the water. When it is unfit for its intended use, water is considered polluted. The source of water pollution may be a point or a non-point source. Point sources of water pollution occur when harmful or toxic substances are emitted directly into a water body at a single point of discharge. The oil spill from the then Tanzanian Italian Petroleum Refinery (TIPER) in Tanzania well illustrates a point source. A non-point source delivers pollutants via a wide area. An example of this type of water pollution is when pesticides or fertilizers are washed from agricultural fields by rain, run-off into a water body such as lake or river. While pollution arising from non-point sources accounts for the majority of contaminants in streams and lakes, it is much more difficult to control. Table 1.1 shows a summary of major pollution sources and their effects. The level of nutrients such as nitrates and phosphorus in the freshwater ecosystems and toxicity due to pesticides is still a problem in the world.

Table 1.1
Common water pollutants and their effects (Shiklomanov, 1997; UNEP/GEMS, 1995)

POLLUTANT	PRIMARY SOURCE	EFFECTS
Organic matter	Industrial wastewater and domestic sewage	Depletes oxygen from the water column as it decomposes, stressing or suffocating aquatic life.
Excess nutrients (nitrates, phosphorous)	Run-off from agricultural lands and urban areas	Over-stimulates growth of algae (a process called eutrophication), which then decomposes, robbing the water oxygen and harming aquatic life. High levels of nitrates in drinking water lead to illness in humans
Heavy metals	Industries and mining sites	Persists in freshwater environments, like river sediments and wetlands, for long periods. Accumulates in the tissue of fish and shellfish. Toxic to both aquatic organisms and humans who eat them
Microbial contaminants (e.g. cryptosporidium, cholera and other bacteria, amoebae, etc.)	Domestic sewage, cattle, natural sources	Spreads infectious diseases through contaminated water supplies, causing millions of cases of diarrhoea diseases and intestinal parasites, and providing one of the principal causes of childhood mortality in the developing world
Toxic organic compounds (oil, pesticides, some plastics, industrial chemicals)	Wide variety of sources, from industrial sites, to automobiles, to farmers and domestic gardeners	Displays a range of toxic effects in aquatic fauna and humans, from mild immune suppression, to acute poisoning, or reproductive failure
Dissolved salts (salinization)	Leached from alkaline soils by over-irrigation, or drawn into coastal aquifers from over-drafting of groundwater	Leads to salt build-up in soils, which kills crops or cuts yields. Renders freshwater supplies undrinkable
Acid precipitation or acid run-off	Deposition of sulphate particles, mostly from coal combustion. Acid run-off from mine tailings and sites	Acidifies lakes and streams, which harms or kills aquatic organisms and leaches heavy metals such as aluminum from soils into water bodies
Silt and suspended particles	Soil erosion and construction activities on watersheds	Reduces water quality for drinking and recreation and degrades aquatic habitats by smothering them with silt, disrupting spawning, and interfering with feeding
Thermal pollution	Fragmentation of rivers by dams and reservoirs, slowing water and allowing it to warm. Industrial uses such as cooling towers	Affects oxygen levels and decomposition rate of organic matter in water column. May shift the species composition of a river or lake

In most cases, the major causes of these contaminants are the increased use of pesticides, manure and industrial fertilizer in agriculture. In the USA, for example, agriculture is the greatest source of pollution degrading the quality of surface waters like rivers and lakes as shown in Table 1.2 (Carpenter *et al.*, 1998). Similarly, despite some positive trends in Europe, the overall state of many European rivers with respect to nutrient concentrations remains poor (EEA, 1998). Dissolved nutrients act as fertilizers, stimulating algal blooms and eutrophication of many inland waters. Dissolved nitrates in drinking water can also harm human health.

While most industrialized countries have greatly reduced the effects of these pollutants from point sources such as factories and sewage treatment plants, in most developing countries like Tanzania the traditional pollution sources like sewage are still a major problem particularly near urban centres (Scheren, 2003; Shiklomanov, 1997). An estimated 90 percent of wastewater in developing countries is still discharged directly into rivers and streams without any waste processing treatment (Mato, 2002; WMO, 1997). Other pollutants like pesticides and fertilizers pollute the water receiving body in both urban centres and agricultural areas.

Table 1.2
Nitrogen and phosphorous discharge into U.S. surface waters from point and non-point sources (in thousands of metric tons per annum) (Carpenter *et al.*, 1998)

SOURCE	NITROGEN	PHOSPHORUS
Non-point sources		
Crop lands	3,204	615
Pastures	292	95
Rangelands	778	242
Forests	1,035	495
Other rural lands	659	170
Other non-point sources	695	68
Total non-point discharges	6,663	1,658
Total point sources	1,495	330
Total discharge (point + non-point)	8,158	2,015
Non-point as a percentage of total	82%	84%

Agricultural activities in Tanzania pollute waters through the application of pesticides, herbicides and fertilizers. The use of pesticides and fertilizers in Tanzania has been increasing over the last 10-15 years and it is likely to continue increasing in the future (Marwa, 1996). A large amount of expired pesticides are improperly stored in some parts of the country, thus causing a threat to the aquatic environment. Another significant water pollutant comes from persistent organic pollutants such as

polychlorinated biphenyls (PCBs), which are considered to be one of mankind's most dangerous pollutants. The extremely high toxicity of some of this class of compounds results from the compounds' high stability to chemical agents (resistance to degradation) and their potential to bioaccumulation in living organisms (Filippis *et al.*, 1999).

1.1.2. Industrial wastewater

Industrial activities have been fast expanding for the past decades in Tanzania. In Tanzania, most industries commenced during the colonial and post-independence period and were established without adequate environmental consideration. These industries include, among others, petrochemical, chemical, and pharmaceutical industries, which use both natural and synthetic organic chemicals. Water pollution is caused by both synthesis and the application of industrial products in such areas as: nutrition, transportation, accommodation and energy exploitation. Although not always acknowledged, chemical activity is indispensable to sustaining life; also it is needed to achieve and maintain a high standard of living. Examples of products needed in modern life include medicaments, cleaning and disinfecting products, cosmetics, stabilizers, artificial fertilizers, pesticides, fuel, batteries, polymers (thermoplastics, thermosetting resins, elastomers, fibres), paint and dyes. These product classes inevitably result into pollution during their production, use and disposal (Patnaik, 1999).

Improper discharge of wastewater containing toxic organic compounds such as phenol and its derivatives presents a major threat to the environment and must be prevented because of the extreme toxicity to aquatic life even at concentration levels of the order of 1.0 ppm (Wang, 1992; Lee and Carberry, 1992). These reasons call for the development of more feasible, effective and efficient effluent treatment technologies, which accomplish the destruction of these wastes into non-toxic or biodegradable end products.

1.1.3. Catalytic wet oxidation (CWO)

Wastewater produced in many industrial processes contains organic compounds such as phenol and its derivatives, which cannot be treated by conventional biological oxidation. Other processes such as chemical oxidation, electrochemical treatment, photo-catalytic oxidation, photo-electrochemical oxidation, and wet oxidation processes under sub- and supercritical conditions and incineration have been tested in

developed countries (Mishra *et al.*, 1995). The application of a particular method depends on, among others, the nature of the pollutant, the concentration of the pollutant, the desired removal efficiency, effectiveness, ability to form secondary toxic product and cost. Current literature shows that among the wastewater treatment techniques, catalytic wet oxidation (CWO) of organic wastes in water seems to be effective and promising (Luck, 1999; Matatov-Meytal and Sheintuch, 1998; Mishra *et al.*, 1995).

Catalytic wet oxidation is a reaction involving an organic compound in water and oxygen over a catalyst. Heterogeneous oxidation involves intensive contacting of an organic compound in solution with oxygen over a solid catalyst. Heterogeneous systems have the advantages over homogenous systems because the catalysts can be separated much more easily after the process. Although many studies have shown that metal oxide catalysts of transitional metals like Zn, Cu, Mn etc., are very effective for the removal of organic wastes, the use of noble metal catalysts for liquid phase oxidation is preferred since no leaching or dissolution of the active metal occurs even in hot and acidic conditions (Gallezot, 1997; Luck, 1999).

Among the noble metal catalysts reported for liquid phase oxidation, platinum-supported catalysts seem to be promising. Platinum catalysts are well-known to be effective during aqueous phase oxidation of alcohols (Besson and Gallezot, 2000; Kluytmans *et al.*, 2000; Mallat and Baiker, 1994) and ammonia (Ukropec *et al.*, 1999). However, there is still meagre information on the application of platinum catalysts for CWO of organic pollutants (Gomes *et al.*, 2000; Chollier *et al.*, 1999; Harmsen *et al.*, 1997; Gallezot *et al.*, 1996). Furthermore, in wet oxidation, the deactivation of platinum catalysts in liquid phase oxidation is not clearly addressed.

1.1.4. Mechanisms and reaction pathways

Many attempts have been made to study reaction mechanisms for pure organic compounds during liquid phase oxidation. For engineering purposes, it is important to quantify the reaction rate by identifying the major oxidation pathways as well as understanding the reaction controlling steps. Knowledge of the reaction pathway also offers the possibility of manipulation of the oxidation to allow more complete destruction of waste organic compounds in water, or perhaps the preferential production of a particular product through appropriate variation of the process conditions. According to Gallezot (1997), catalytic oxidations of organic molecules can proceed via different mechanisms, namely: (1) enzymatic oxidation; (2) free

radical auto-oxidations initiated by transition metal cations; (3) metal ion oxidation of coordinated substrates; (4) oxygen transfer to the substrate mediated by metaloxo or peroxo complexes and (5) oxidative dehydrogenation on metal surfaces. In alcohol oxidations, oxidative dehydrogenation on metal surfaces is commonly reported (Gallezot, 1997; Mallat and Baiker, 1994). The mechanism of alcohol oxidation on a noble metal catalyst involves the dehydrogenation of the organic substrate on the metal surface, while oxygen is needed to scavenge the adsorbed hydrogen from the surface.

Phenol and its derivatives have been the subject of many studies in CWO as a model reaction. Studies on the mechanisms for oxidation of phenol require some knowledge of the short-lived intermediates as well as the final reaction products. For transition metal oxide catalysts, the reaction is believed to occur by free-radical initiation on the catalyst surface, homogeneous propagation, and either a homogeneous or a heterogeneous termination process. Radical initiation could occur by dissociative adsorption of phenol or hydroperoxide decomposition on the catalyst (Mishra *et al.*, 1995). Sadana and Katzer (1974) found that, during phenol oxidation, the oxidation involves an induction period, in which the generation of radicals is poor, followed by a higher steady-state activity period with a fast free-radical reaction regime. These mechanisms are likely to occur even for noble metal catalysts.

Generally, the reaction intermediates reported on phenol oxidation catalyzed by supported metal oxides, like copper, zinc, manganese and other metal catalysts, are similar to those of non-catalysed phenol oxidation. The reaction products that have been reported from the oxidation of phenol by oxygen and ozone can be attributed to three classes: primary intermediates (hydroquinone, catechol, *p*-benzoquinone, o-benzoquinone), secondary intermediates (maleic acid, formic acid, pyruvic acid, oxalic acid, oligomers of primary intermediates), and end products (formic acid, acetic acid, carbon dioxide and water). Phenol reaction networks in supercritical water oxidation (SCWO) have been recently reviewed (Savage, 2000), in which the formation of dimers and other intermediates like single-ring compounds (e.g. hydroquinone), ring-opening products (e.g. maleic acid, glyoxylic acid, acetic acid and other organic acids) and gases (e.g. CO, CO_2) are reported. Some of these partial oxidation products and intermediates, especially the dimers, are relatively more toxic than phenol. Fig. 1.2 gives the summary of a variety of partial oxidation and polymerisation products observed during wet oxidation. The oxidation of phenol has in most cases involved oxidation, decarboxylation, dehydration and rearrangement of the molecules or some combination of these steps (Matatov-Meytal and Sheintuch, 1998; Pintar and Levec, 1992; Devlin and Harris, 1984; Sadana and Katzer, 1974).

While platinum catalysts have the potential to change the reaction pathways of organic compounds to the desired end products, CO_2 and H_2O, there is still limited information on the oxidation routes as well as the catalytic mechanisms.

Fig. 1.2. Possible reaction pathways for phenol oxidation in liquid phase adapted from literature (Savage, 1999; Matatov-Meytal and Sheintuch, 1998; Pintar and Levec, 1992; Devlin and Harris, 1984; Sadana and Katzer, 1974). Possible reaction steps: 1 - oxidation; 2 - C-C bond cleavage; 3 - decarboxylation; 4 -hydration; 5 - transfer hydrogenation; 6 - dehydration; 7 - molecular coupling or polymerisation. Compounds in bracket: suggested intermediates not positively identified during phenol oxidation.

1.1.5. Oxidizing agents

The type of oxidant for a given organic compound may influence both the reaction mechanism and pathway. The most reported oxidizers for oxidation of dilute aqueous solutions of organic compounds are: hydrogen peroxide, the hydroperoxyl radical, the hydroxyl radical, the ozone radical ion, ozone and atomic oxygen. Some researchers, including Gould and Weber (1976), have used ozone (O_3) to oxidize phenol. The majority of work using ozone to oxidize phenol has been carried out at ambient temperatures, since ozone is a powerful oxidant even at low temperatures. In wet oxidation reactions, the two commonly used oxidants have been oxygen (either molecular oxygen or in air) and hydrogen peroxide. Other oxidizers are widely used in advanced oxidation processes (AOP's) due to the fact that these processes aim at in-situ production of the oxidizers.

In wet oxidation, water with dissolved oxygen is used to oxidize the target compound. The main reactions are described in equations (1.1)-(1.8). Hydroxyl radicals are produced from the dissociation and oxidation of water according to equations (1.1) & (1.2). Hydroperoxyl radicals are formed from the oxidation of water (Eq. 1.2) and the target compound RH (Eq. 1.6). Hydroxyl radicals are also produced from hydrogen peroxide (Eq. 1.4) and from the reaction of atomic oxygen with the target compound (Eq. 1.8). Hydrogen peroxide is produced by the recombination of hydroperoxyl radicals (Eq. 1.3) or by the reaction of hydroperoxyl radicals with the target compound (Eq. 1.7). Atomic oxygen is produced from the dissociation of oxygen (Eq. 1.5). Although the hydroperoxyl radical is less reactive than the hydroxyl radical, it plays an important role because of its relative abundance.

$$H_2O \rightarrow OH + H \tag{1.1}$$
$$H_2O + O_2 \rightarrow OH + HO_2 \tag{1.2}$$
$$2HO_2 \rightarrow H_2O_2 + O_2 \tag{1.3}$$
$$H_2O_2 \rightarrow 2OH \tag{1.4}$$
$$O_2 \rightarrow 2O \tag{1.5}$$
$$RH + O_2 \rightarrow R + HO_2 \tag{1.6}$$
$$RH + HO_2 \rightarrow R + H_2O_2 \tag{1.7}$$
$$RH + O \rightarrow R + OH \tag{1.8}$$

During catalytic wet oxidation (CWO), oxygen may participate in reaction either as an adsorbed species on the catalyst surface or as a part of the lattice oxygen present in metal oxides (Matatov-Meytal and Sheintuch, 1998). Both free radical (homolytic) and

ionic (heterolytic) oxidation reaction mechanisms have been proposed for the oxidation of aromatic compounds, resulting in a ring-opening reaction.

1.1.6. *Deactivation of platinum catalysts*

Catalyst deactivation is a major concern for catalyst users and manufactures. Although there is little information on the application of platinum catalysts for the oxidation of organic wastes in water, comprehensive reviews (Besson and Gallezot, 2003; Mallat and Baiker, 1994) report deactivation of platinum metal catalysts during liquid phase oxidation of alcohols and carbohydrates. The possible mechanisms for deactivation include: sintering of metal particles, leaching of active components, poisoning of active sites by reactants or by-products, metal oxidation, inactive metal or metal oxide deposition. It is most likely that all deactivation mechanisms lead to a decrease in the active platinum surface area and hence to a decrease in the reaction rate.

It is, however, important to note that the reaction medium and conditions, such as pH, reactants, intermediates and end products, all play an important role in the activity and selectivity decay of the catalyst. The deactivation of metal catalysts also depends on the reducing potential of the organic compound, e.g. the deactivation is much lower for aldehyde than for alcohols (Gallezot, 1997). It has also been reported, for example, that the dissolution of platinum ions is enhanced in the presence of carbohydrates, because they can act as a sequestering agent (Vleeming *et al.*, 1997; Angyal, 1973). The balance of the reactants on the metal surface during aqueous phase oxidation is also important since the organic compound and oxygen are both adsorbed on the metal surface, as explained in the literature (Gallezot, 1997).

The deactivation of the catalyst by over-oxidation is caused by the exposure of the platinum surface to oxygen, resulting in the formation of inactive surface platinum oxide (Schuurman *et al.*, 1992; Dirkx and Van der Baan, 1981). This type of deactivation depends on the composition, structure and texture of the catalyst. Small metal particles (<2 nm) deactivate more readily because of a stronger affinity to oxygen (Besson and Gallezot, 2003). The sintering of metal particles is caused by the migration and redeposition of atoms leading to particle growth (Ostwald ripening) and a smaller active platinum surface (Vleeming *et al.*, 1997; Schuurman *et al.*, 1992). Schuurman *et al.* (1992) also observed leaching of platinum metal from Pt/C during oxidation of carbohydrates. They also found it to be dependent on the reaction medium, such as the oxidation potential and the acidity of the solution. Catalytic site covering or blocking is caused by deposition of carbonaceous species such as

polymeric and by-products on the surface of the metal catalyst, which prevents the reactant access.

Several remediation steps for catalyst deactivation have been suggested in the literature. According to Mallat and Baiker (1994), the vulnerability of noble metals to poisoning can be changed by the addition of promoters such as Bi, Pb and Sn. Furthermore, it has been suggested that promoters also can protect noble metals against over-oxidation (Besson and Gallezot, 2000).

1.2   Research objectives and methodology

The main objective of this research was to investigate the applicability and effectiveness of platinum catalysts for catalytic oxidation of organic wastes in water. Specific objectives were:

❑ *to evaluate the activity, selectivity and stability of platinum catalysts for use in catalytic wet oxidation of organic wastes, in particular phenol, maleic acid and malonic acid, as model compounds;*

❑ *to investigate the effect of reactant loads on the catalyst activity and selectivity, and the reaction mechanisms;*

❑ *to study the effects of mass transfer on the reaction rate and the reaction networks and the implication on reactor and process design.*

In this work, catalyst deactivation studies were focused on the influence of reactants on platinum catalysts. It was therefore the hypothesis of this research that during the oxidation of organic wastes in water, and possibly other oxidation reactions, there is a properly defined operation window in which higher activity of platinum catalysts and hence the selectivity to the desired product would be maintained.

1.2.1. Relevance of the research to Tanzania

While water quality appears to be degraded with agricultural expansion, rapid urbanization and expanding industry in developing countries like Tanzania, it is unfortunate that little information is available to evaluate the extent to which chemical contamination has impacted the health of people and of freshwater ecosystems. According to the World Meteorological Organization (WMO, 1997), the total surface water withdrawal in Tanzania during the year 1994 was 1.2 km^3, of which the percent withdrawals by sector were: agriculture (89%), domestic (9%) and industry (2%).

These data are obliviously changing rapidly due to expanding industry and agriculture. Furthermore, Tanzania has a population of about 34.4 million (according to the 2002 National Census), of whom 75-80% live in rural areas. It is estimated that the water supply coverage is 50% and 42% for urban and rural, respectively. Inadequate supply of quality water in urban centres, characterized by frequent interruptions, forces people to use alternative sources, in some cases, of inferior quality. Although many methods have been studied or developed for the destruction and/or recovery of reusable materials and chemicals, such technologies are not available in most developing countries, such as Tanzania.

The information obtained from this research is relevant to both developed and developing countries, like Tanzania. Such information will provide useful insight into integrating chemical/ biological treatment systems in Tanzania. The information is also useful to allow a systematic approach to be used in deciding on the degree of chemical oxidation necessary to convert the starting organics into biodegradable molecules. Also this information will help in designing appropriate reactors and processes, and in selecting suitable catalysts and/or support for long-term application, thereby lowering the cost of the catalyst. Whether the application of platinum catalysts in CWO of organic pollutants will become feasible will depend on, among others, understanding the reaction mechanisms and choosing the proper operation window, in which the catalyst life would compromise to its cost.

1.2.2. Methodology

This work has been carried out under a sandwich program, whereby part of the work has been done at the Laboratory of Chemical Reactor Engineering at the Eindhoven University of Technology (TU/e) in the Netherlands and part was done at the Department of Chemical & Process Engineering at the University of Dar es Salaam (UDSM) in Tanzania. In both locations, the same reactor set-ups were used. Catalytic wet oxidation of model compounds was studied in a continuous flow three-phase slurry reactor (CSTR). Analyses of liquid samples were performed by means of HPLC techniques, while an online GC, an O_2 sensor and an online gas analyser were used for analysis of the gas stream.

Commercially available platinum catalysts on different support materials, namely: Pt/graphite (5 wt%) from Johnson Matthey, and Pt/TiO$_2$ (5 wt%), Pt/Al$_2$O$_3$ (5 wt%), and Pt/active carbon (5 wt%) from Engelhard, were used in this study. According to the manufacturers' information, Pt/graphite is "eggshell" type, whereby the platinum

metals are distributed on the outer surface or edges of the pores. Other catalysts, namely, Pt/active carbon, Pt/Al$_2$O$_3$ and Pt/TiO$_2$ are "mixed" type, whereby platinum metal is located partly on the surface/edges and deeper in the pores.

The model reactions were chosen based on the characteristics of common or typical industrial wastewater and well-known compound classes. The model reactions were phenol oxidation, maleic acid oxidation and malonic acid oxidation. Fig.1.3 shows the molecular structures of the model compounds. These compounds represent typical pollutants present in the aqueous environment, and offer a range of composition, physical and chemical properties, susceptibilities to oxidation and potential for deactivation of noble metal catalysts. In addition, phenol represents the family of oxygenated ring compounds and maleic acid represents unsaturated dicarboxylic acids, while malonic acid represents saturated carboxylic acids.

(a) phenol   (b) maleic acid   (c) malonic acid
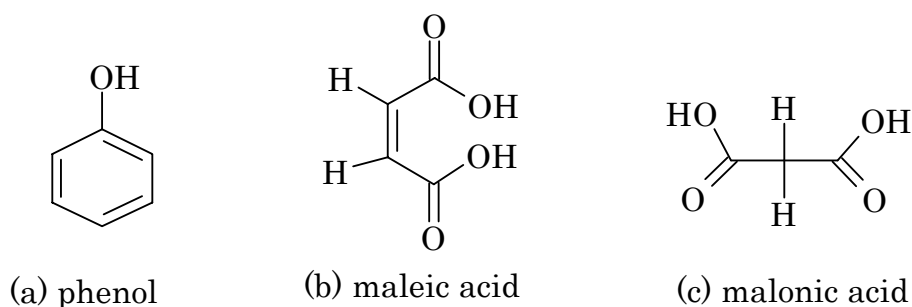
Fig. 1.3. Molecular structure of the model organic compounds for CWO using platinum catalysts.

1.2.3. Institutional capacity building

The recent emergence of environmental concerns in developing countries needs to be supplemented with capacity building in terms of expertise and technical support from developed countries. The research presented in this thesis was financially supported by the Dutch Government under the MHO Programme through the EVEN Project, a joint project between the University of Dar es Salaam in Tanzania and Eindhoven University of Technology in the Netherlands. One of the objectives of the EVEN project was to enhance and consolidate research and strengthen institutional capability in catalytic oxidation of wastewater in Tanzania. Therefore, as part of the capacity building in catalytic wastewater treatment research, dedicated research equipment and analytical facilities have been installed, tested and used at the University of Dar es Salaam in Tanzania.

1.3   Structure of the thesis

Most of the chapters in this thesis have been published in various journals.

The advantages and drawbacks of the various conventional and non-conventional methods for wastewater treatment are discussed in Chapter 2 of this thesis. The influences of reaction parameters, which include temperature, reactants concentrations, and reaction start-up procedures, on the performance of the platinum catalysts, are also discussed in this chapter. Furthermore, a practical operation window in which complete conversion of phenol to CO_2 and H_2O could be achieved and high activity of platinum catalysts could be maintained is proposed. This chapter has been published in "Applied Catalysis B: Environmental, 41 (2003) 247".

The influence of different supports for platinum catalyst during CWO of organic wastes is discussed in Chapter 3. The results on phenol oxidation using Pt/graphite, Pt/TiO_2 and Pt/Al_2O_3 were obtained at the Laboratory of Chemical Reactor Engineering, Eindhoven University of Technology, while malonic acid reaction and maleic acid oxidation using Pt/graphite, Pt/Al_2O_3 and Pt/AC were obtained from experiments performed at the Department of Chemical and Process Engineering, University of Dar es Salaam. The deactivation of the catalysts is clearly related to the increase in metal dispersion of the catalyst. This chapter has been submitted to the special issue on CWO of organic wastes in "Topics in Catalysis, (2004)".

In Chapter 4, a detailed investigation on the reaction mechanisms and pathways during phenol oxidation using Pt/graphite is presented. In addition, oxidation of individual compounds identified during phenol oxidation as intermediates was carried out. The role of the oxygen load on the activity of the catalyst is discussed in depth. In this chapter, the catalytic mechanism and reaction pathways for phenol oxidation over platinum catalysts are proposed. This chapter has been published in "Catalysis Today, 79-80 (2003) 357".

Development of the model that predicts the performance of Pt/graphite during phenol oxidation in a CSTR is discussed in Chapter 5. The influences of such factors as impeller speed, catalyst concentration, residence times, and molar flow rate for liquid solutions on reaction rate and selectivity to CO_2 are discussed. Furthermore, the mass transfer and reaction rate constants are determined. The model, which involves a mass transport equation for phenol and oxygen, predicts the experimental data adequately. This chapter was presented during ISCRE-17 and has been submitted for publication in "Chemical Engineering Science, (2004)".

In Chapter 6 several kinetic models for malonic acid reaction were developed and evaluated. A mass transfer assessment for the kinetic data was performed. This part was not considered in Chapter 5. This chapter has been submitted for publication in "Applied Catalysis B: Environmental, (2004)".

Additional model description for maleic acid oxidation using Pt/graphite is presented in Chapter 7. The model incorporates the mass transport of oxygen and maleic acid to the catalyst surface. This chapter has been submitted for publication in "Applied Catalysis B: Environmental, (2004)".

Finally, the main conclusions of this thesis are summarised in Chapter 8. This chapter also gives some recommendations for further research and/or future work. The implications of the major findings, such as the practical operation window, reaction mechanisms of model compounds, the mass transfer effects and reaction kinetics, on the reactor and process design for the platinum catalysed wet oxidation (Pt-CWO) process, are presented.

Nomenclature

AOP	advanced oxidation process
AWV	atmospheric water vapour
CSTR	continuous stirred tank reactor
CWO	catalytic wet oxidation
EASF	easily accessible surface fresh water
EVEN	capacity building in Environmental Engineering
GC	gas chromatography
HPLC	high performance liquid chromatography
MHO	The Dutch Joint Financing Programme for Cooperation in Higher Education
PCB	polychlorinated biphenyl
SCWO	supercritical water oxidation
TIPER	Tanzanian Italian Petroleum Refinery
WWLO	water within living organisms

References

Besson, M. and Gallezot, P. Catal. Today 57 (2000) 127.

Carpenter, S., Caraco, N., Correll, D., Howarth, R., Sharpley, A. and Smith, V. Nonpoint Pollution of Surface Waters with Phosphorous and Nitrogen, Issues in Ecology (1998) Washington, DC: Ecological Society of America.

Chollier, M.J., Epron, F., Lamy-Pitara, E. and Barbier, J., Catal. Today 48 (1999) 291.

EEA (European Environment Agency). Europe's Environment: The Second Assessment. Copenhagen, Denmark: European Environment Agency. (1998) 194-196.

Filippis, P.D., Scarsella, M. and Pochetti, F., Ind. Eng. Chem. Res. 38 (1999) 380-384.

Gallezot, P., Catal. Today 37 (1997)405.

Gallezot, P., Laurain, N. and Isnard, P. Appl. Catal. B 9 (1996) L11.

Harmsen, J.M.A., Jelemensky, L., van Andel-Schefer, P.J.M., Kuster, B.F.M.and Marin, G.B., Appl. Catal. A 165 (1997) 499.

Kluytmans, J.H.J., Markusse, A.P., Kuster, B.F.M., Marin, G.B. and Schouten, J.C., Catal. Today 57 (2000) 143.

Lee, S.H. and Carberry, J.B., Water Environ. Res. 64 (1992) 682.

Levec, J. and Pintar, A., Catal. Today 24 (1995) 51.

Luck, F., Catal. Today 53 (1999) 81.

Mallat, T. and Baiker, A., Catal. Today 19 (1994) 247.

Markusse, A.P., Kuster, B.F.M. and Schouten, J.C., Stud. Surf. Sci. Catal. 126 (1999) 273.

Marwa, P.B., Industrial Development and National Environmental Policy (Ed.). Framework In: Mwandosya, M.J.; Luhanga, M.L., Mugurusi, E.K.(Ed.), Environmental Protection and Sustainable Development. CEEST, Dar es Salaam, (1996).

Matatov-Meytal, Yu.I. and Sheintuch, M., Ind. Eng. Chem. Res. 37 (1998) 309.

Mato, R.R.A.M. Groundwater Pollution in Urban Dar es Salaam, Tanzania. Assessing Vulnerability and Protection Priorities. Ph.D. Thesis, Eindhoven University of Technology, Eindhoven, (2002).

Mishra, V.S., Mahajani, V.V. and Joshi, J.B., Ind. Eng. Chem. Res. 34 (1995) 2.

Patnaik, P., A Comprehensive Guide to the Hazardous Properties of Chemical Substances, 2nd Edn., New York: Wiley (1999) 835-865.

Santos, A., Yustos, P., Durban, B. and Garcia-Ochoa, F., Catal. Today 66 (2001) 511.

Scheren, P.A.G.M. Integrated Water Pollution Assessment in Data- and Resource- Poor Situations. Lake Victoria and Gulf of Guinea Case Studies. Ph.D. Thesis, Eindhoven University of Technology, Eindhoven, (2003).

Shiklomanov, I.A. Comprehensive Assessment of the Freshwater Resources of the World: Assessment of Water Resources and Water Availability in the World. Stockholm, Sweden: World Meteorological Organization and Stockholm Environment Institute (1997) 34-36.

Ukropec, R., Kuster, B.F.M., Schouten, J.C. and van Santen, R.A., Appl. Catal. B 23 (1999) 45.

UNEP/GEMS (United Nations Environment Program Global Environment Monitoring System/Water). Water Quality of World River Basins. Nairobi, Kenya: UNEP (1995) 33-35.

Wang, Y.T., Water Environ. Res. 64 (1992) 268.

WMO (World Meteorological Organization). Comprehensive Assessment of the Freshwater Resources of the World. Stockholm, Sweden: WMO and Stockholm Environment Institute (1997) 11.

2

PLATINUM CATALYSED WET OXIDATION OF PHENOL IN A STIRRED SLURRY REACTOR: A PRACTICAL OPERATION WINDOW

Abstract

The catalytic performance of graphite supported platinum (5-wt.%) catalyst in liquid phase oxidation has been studied using a continuous stirred tank (CSTR) slurry reactor in order to determine the proper operation window. The study was carried out in a temperature range of 120 to 180 °C and in a total pressure range of 1.5 to 2.0 MPa. Other operational variables employed were oxygen partial pressure (0.01-0.8 MPa), initial phenol feed concentration (0.005-0.07M), and catalyst concentration from 1 to 10 $kg_{cat}.m_L^{-3}$. It was found that the extent of oxygen coverage on the platinum surface determines the reaction pathway and selectivity to CO_2 and H_2O. Complete oxidation of phenol to CO_2 and H_2O could be achieved at 150 °C when the reaction proceeds within the range of weight specific oxygen loads of 0.15 to 0.35 $mol.s^{-1}.kg_{Pt}^{-1}$ and at stoichiometric oxygen excess in the range of 0 to 80%. The activity of the platinum catalyst remained high when the residual partial pressure of oxygen in the reactor was kept below 150 kPa. Higher residual oxygen partial pressure resulted into deactivation of the platinum catalyst (over-oxidation), which was temporary and could be reversed at reducing conditions. The formation of p-benzoquinone, followed by the formation of polymeric products was also favoured at higher oxygen load, which resulted into permanent deactivation of the platinum catalyst (poisoning). While the platinum surface was vulnerable to poisoning by carbonaceous compounds when insufficient oxygen was used, a fully reduced platinum surface favoured the formation of acetic and succinic acids which are difficult to oxidize. Higher temperatures can enhance the activity of the platinum catalyst, while at lower temperatures catalyst deactivation occurs with increased formation of polymeric products and lower selectivity to CO_2 and H_2O. In order to maintain the catalyst within the proper operation window, a CSTR is the preferred reactor.

Keywords: Catalytic wet oxidation; Phenol oxidation; Platinum catalyst; Operation window; Catalyst deactivation

2.1.   Introduction

The increasing awareness on the importance of clean environment to human health in both developing and developed countries has necessitated more studies in search of feasible solutions for treating toxic wastewaters. In Tanzania most of the industries commenced during the colonial and post-independence period and were established without adequate environmental consideration. These industries include amongst others petrochemical, chemical, and pharmaceutical industries, which use different natural and synthetic organic chemicals. Phenol and its derivatives are used in these industries in the production of a wide range of consumer goods and materials such as: plasticizers, herbicides, insecticides, dyes, rubber chemicals, flavours, insulating foams, binders, adhesives, laminates, impregnating resins, raw materials for varnishes, emulsifiers, and detergents. Improper discharge of wastewater containing toxic organic compounds such as phenol and its derivatives presents a major threat to the environment and must be prevented because of the extreme toxicity for aquatic life even at concentration levels of the order of 1.0 ppm (Wang, 1992; Lee and Carberry, 1992). Although several methods are being developed for treatment of wastewaters, such technologies are not available in most of the developing countries like Tanzania. This reason calls for the development of more feasible, effective and efficient effluent treatment technologies, which accomplish the destruction of these wastes into non-toxic or biodegradable end products. In this work, phenol has been used as a characteristic effluent component, since it is not only a common pollutant in industrial waste streams, but also it is considered as a worst-case model compound for water pollution studies.

2.1.1. Wastewater treatment techniques

Numerous techniques are available for treatment of wastes in liquid phase, such as chemical treatment, physical treatment, biological treatment, and incineration, which can be used either in isolation or in combination. However, the main problem in reducing water pollution lies on how to remove toxic organic compounds, which are too concentrated for biological remediation but are too dilute for economical chemical or physical treatment, or incineration. Wet oxidation processes are considered to be attractive for removal of toxic compounds and organic loads in the range of about 10 to 100 g/l (Debellefontaine *et al.*, 1996).

Wet oxidation processes can be carried out at conditions below or above the vapour-liquid critical point of water ($374^{o}C$ and 22.1 MPa). While a high temperature is

required to attain a rapid rate of reaction, an increase in temperature will also increase the saturated water vapour pressure, which means that a higher pressure is required to maintain the liquid phase. Wet air oxidation (WAO) is carried out below the critical point of water, typically at 200 - 320ºC and 2.0 – 20.0 MPa (Mishra *et al.*, 1995). When compared to incineration, the WAO process creates minimal air pollution problems as the contaminants remain in the aqueous phase. The WAO process generally produces low molecular weight oxygenated compounds, like acetic and propionic acids, ethanol, etc. (Luck, 1999). Supercritical water oxidation (SCWO) processes are carried out at supercritical conditions. A recent review (Savage, 1999) on SCWO processes shows that complete and rapid oxidation of phenol as well as other organics can be achieved. Although higher efficiency for destruction of organic contaminants may be achieved in SCWO than in WAO, SCWO is usually a too expensive process to install and operate, because of the severe conditions employed, and the requirement of construction materials that are resistant to the high corrosion rates. The application of suitable catalysts may enhance reaction rates, reduce residence times, lower temperatures required for treatment, and also provide control over competing reaction pathways.

2.1.2. *Catalytic wet oxidation*

Catalytic wet oxidation (CWO) of organic compounds and organic-containing wastewaters over homogeneous or heterogeneous catalysts can be carried out under much milder conditions (80-200ºC; 0.1-2 MPa) than non-catalysed processes. Although homogeneous catalytic systems using transition metal catalysts (especially salts of Cu, Fe, Mn) are generally more effective than solid catalysts, the dissolved catalysts however, are in many cases toxic and their use requires a separation step such as precipitation to remove or recover the catalyst ions from the treated effluent (Matatov-Meytal and Sheintuch, 1998). Due to this, heterogeneous catalysed wet oxidation seems to be more promising since only one down-stream separation step, filtration, is required to remove the catalyst from the liquid phase.

The application and efficiency of several supported and unsupported non-noble (transition) metal oxides and noble metals for catalytic wet oxidation of organic pollutants have been well reviewed (Luck, 1999; Matatov-Meytal and Sheintuch, 1998; Levec and Pintar, 1995). The use of metal oxides of, for example copper, manganese, vanadium, and chromium in liquid phase oxidation processes is, however, limited due to loss of activity by leaching of the metal in the hot acidic reaction medium (Santos *et al.*, 2001; Matatov-Meytal and Sheintuch, 1998; Mishra *et al.*,

1995). Supported noble metal catalysts (including Pt, Pd, Ru, Rh, Ir, etc.) are generally less vulnerable to deactivation by leaching of the active metal and present higher overall activities for the oxidation of pollutants (Luck, 1999).

Among the noble metal catalysts reported for liquid phase oxidation, platinum supported catalysts seem to be promising (Ukropec *et al.*, 1999; Markusse *et al.*, 1999; Maugans and Akgerman, 1997). Platinum catalysts were found to be effective during aqueous phase oxidation of low molecular weight organic carboxylic acids (Gomes *et al.*, 2000; Chollier *et al.*, 1999; Harmsen *et al.*, 1997), ammonia (Ukropec *et al.*, 1999), and alcohols (Markusse *et al.*, 1999). However, data on the application of platinum catalysts for CWO, especially for phenols, is still limited. Maugans and Akgerman (1997) reported that high conversion of phenol was achieved during catalytic oxidation over Pt/TiO_2 in a batch slurry reactor; however, full conversion of the total organic carbon (TOC) was not obtained. This was attributed to the presence of side reactions, which lead to the formation of stable acids that do not readily degrade. The effect of oxygen and phenol loads on the activity of the catalyst and selectivity to CO_2 and H_2O was not clearly revealed.

2.1.3. *Objective of this work*

Although platinum catalysts have been reported to be effective during catalytic liquid phase oxidation of ammonia (Ukropec *et al.*, 1999) and alcohols (Markusse *et al.*, 1999; Mallat and Baiker, 1994), rapid loss of catalyst activity with a surplus of oxygen (over-oxidation) was also observed. There is no clearly defined operation window proposed yet, in which deactivation of the catalyst is minimized and high selectivity is maintained. Furthermore, the mechanism of platinum catalysed oxidation of phenol is not fully explained yet in literature. Whether the application of platinum catalysts in catalytic wet oxidation (CWO) of organic pollutants will become feasible, will depend on, amongst others, understanding the reaction mechanisms and choosing the proper operation window, in which the catalyst life would compromise to its cost.

The objective of this study was to investigate the effectiveness of supported platinum catalyst for liquid phase oxidation of phenol in a CSTR. The influence of initial phenol concentration and oxygen partial pressure, reactor start-up methods, catalyst mass, and temperature has been studied in order to identify the proper operation window for total oxidation to CO_2 and H_2O. Experiments were performed in a continuous stirred slurry reactor in which the catalyst activity was monitored during the measurement period.

2.2. Experimental

2.2.1. Chemicals and catalyst

Phenol and all other chemicals used in this research were p.a. from Merck. Deionised water was used as a solvent. The liquid phase oxidation of phenol by oxygen was investigated using a commercially available catalyst, graphite supported platinum (5 wt % Pt/G, Johnson Matthey JM287). The average graphite particle size was 7 μm and 95% of the particles were smaller than 15 μm, as confirmed by particle size measurement (Coulter LS 130 apparatus). Other catalyst specifications include: metal surface area of 0.66 $m^2.g^{-1}$ sample, metal dispersion 5.3%, and B.E.T. surface area of 15 $m^2.g^{-1}$. The platinum metal content of the catalyst was determined by means of UV/VIS spectrophotometer after dissolving from the support by boiling the catalysts in aqua regia, forming a stable yellow Sn-Pt complex (Charlot, 1961). The platinum content of the fresh Pt/G catalyst was 4.73% by weight. Determination of long-term stability in liquid phase and topographical characterisation were not part of this work.

2.2.2. Experimental set-up

The experiments were conducted in a continuous flow stirred slurry reactor (CSTR) in a temperature range of 120 to 180°C and in a total pressure range of 1.5 to 2.0 MPa. Other experimental and reactor operating conditions were as listed in Table 2.1. The reactor is a 500 ml volume autoclave (Autoclave Engineers, Zipperclave Hastelloy) with two internal baffles, thermowell, cooling coil, two separate liquid inlets, a liquid outlet with catalyst filters (filter type: Millipore HV 0.45 μm and a stainless steel 0.5 μm), immersion-pipe for level measurement, and a gas dispersion impeller. The reactor set-up is schematically presented in Fig. 2.1. During reaction the reactor was kept at constant temperature within $\pm 0.3^o$C, in a wide range of temperatures, by a heating element around the reactor. The pressure in the reactor was kept constant by using a backpressure regulator. The composition of the outlet gas was determined by using an O_2 sensor and on-line GC. The liquid outlet of the reactor contains a proportional valve, which is controlled by a PID-level controller. The liquid samples were analysed by an on-line HPLC for residual phenol concentration and intermediate reaction products. During the experiments the flow rate of phenol feed solution was kept constant. Moreover, the flow rate of gas entering the reactor was also kept constant. The composition of the gas leaving the reactor was varying, depending on the O_2 consumption and CO_2 formation in the reactor.

Table 2.1
Standard reactor operating conditions

|	Standard	Range
Temperature, °C	150	120 - 180
Total pressure, MPa	1.8	1.5 – 2.0
Oxygen partial pressure, MPa	0.5	0.01 – 0.8
Oxygen flow rate (at room conditions), ml/min	40	0 - 80
Nitrogen flow rate (at room conditions), ml/min	90	10 -120
Initial phenol concentration, mol/m^3	20	5 - 70
Liquid flow rate, ml/min	10	5 - 20
Volume of liquid in the reactor, ml	350	350
Mass of 5% Pt/graphite in the reactor, kg/m$_L^3$	6	0 - 10
Particle mean diameter (> 95% particles), μm	7	< 15
pH	Uncontrolled	2 - 7
Stirrer speed, rpm	1200	350 -1800
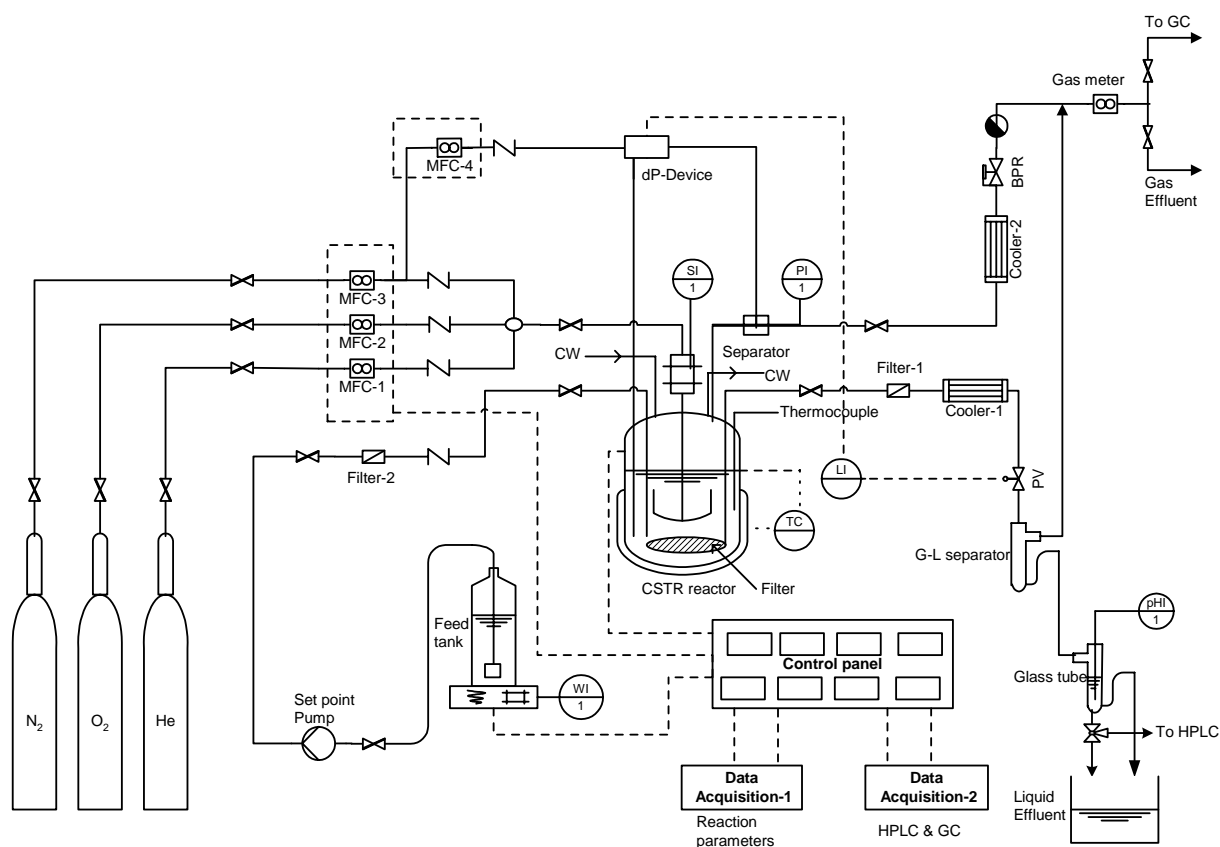
Fig. 2.1. A schematic presentation of the high-pressure CSTR. Abbreviations- BPR: backpressure regulator; CV: on/off valve; d*P*: differential pressure; LI: level indicator; MFC: mass flow controller; PI: pressure indicator; pHI: pH indicator; RV: relief/vent valve; SI: stirrer speed indicator; TC: temperature controller; TI: temperature indicator; WI: weight indicator.

2.2.3. *Reactor start-up procedure*

Three different procedures for reactor start-up were tested. In the first procedure (O_2-FIRST), a given mass of dry catalyst was introduced into the reactor with 350 ml of water. After closing the reactor, a mixture of oxygen and nitrogen was introduced into the reactor at a given flow rate and the mixture was stirred at a low speed of 350 rpm to keep the catalyst in suspension without causing any gas dispersion. After the oxygen in the gas outlet has reached a steady state concentration, the pressure was set at the desired value on the backward pressure regulator. The reactor was pressurized and heating of the reactor was started. When the reaction temperature and pressure were attained, the speed of the stirrer was increased to the desired value and the liquid feed valve was opened to allow the flow of phenolic solution into the reactor. The reaction was monitored by taking liquid and gas samples at given time intervals.

Similarly, in the second start-up procedure (Ph-FIRST), the catalyst was introduced into the reactor with 350 ml of water only. Then after closing the reactor, nitrogen gas was introduced into the reactor at a given flow rate and the reactor was pressurized and heated. After the desired reactor pressure and temperature were reached, phenol solution containing the specified concentration was fed to the reactor by the HPLC pump. When steady state concentration of phenol in the reactor was reached, a mixture of oxygen and nitrogen was fed to the reactor at a given flow rate and the reaction was monitored for the whole experimental period.

The third start-up procedure (O_2-Ph-SIM) involved simultaneous feed of both oxygen and phenol at reaction condition. The catalyst was introduced into the reactor with 350 ml of water, then the reactor was fed with nitrogen gas at a given flow rate to pressurize before heating was started. When the desired reactor pressure and temperature were reached, both the liquid phenol solution and the gas mixture with oxygen at a given flow rate, were fed to the reactor and the reaction was monitored. Both liquid and gas samples were taken and analysed at given time intervals.

2.2.4. *Analysis of liquid and gas*

In each experiment, the progress of the reaction and the catalytic activity were monitored by the measurement of the reactor effluent composition as a function of time. At appropriate intervals the composition of the outlet liquid samples was determined by an on-line HPLC set-up (Spectra Physics), which consists of HPLC pumps (SP 8800), sample valves, column heaters, detectors and an integrator (DataJet CH2). Phenol and

other aromatic compounds were analysed in a 300 x 4.6 ID mm Lichroma SS column, slurry packed with a Benson type of cation-exchange resin (Ca^{++}) using a UV detector. Water was used as eluent with a flow rate of 1.5 ml/min. The oven heater was set at a temperature of $80^{\circ}C$. Carboxylic acids were analysed in a 300 x 8 ID mm RSpak KC-811 column using a refractometer detector (Waters R401). The oven temperature was set at $40^{\circ}C$ and the mobile phase used was 0.1% H_3PO_4/H_2O at a flow rate of 1.0 ml/min. Gases were analysed using an on-line GC (HP 5890A Series II), equipped with a 10 m Molsieve 5A wide bore (Chrompack) column, a 25 m Porapak Q wide bore (Chrompack) column, a thermal conductivity detector (TCD) and an integrator (DataJet CH2). For the quantification of the analysed gases, nitrogen gas, which was fed together with feed gases to the reactor, was used as a standard while helium was used as carrier gas.

2.2.5. Data analysis

The molar flow rates of oxygen gas and phenol solution were calculated based on the overall oxidation reaction as expressed in equation (2.1):

$$C_6H_5OH + 7\,O_2 \rightarrow 6\,CO_2 + 3\,H_2O \tag{2.1}$$

The molar feed ratio for complete oxidation of phenol to CO_2 and H_2O is equivalent to the stochiometric ratio, ν, of oxygen to phenol. The percentage stoichiometric oxygen excess to phenol (S.E.) used in this study is defined according to equation (2.2) as:

$$S.E. = \frac{\left[\left(F_{O2}/F_{Ph}\right) - \nu\right]}{\nu} \times 100\ \% \tag{2.2}$$

All notations and abbreviations used are listed in the notation section. The weight specific oxygen load (S.O.L.) is defined as the ratio of the molar oxygen feed rate (mol/s) to the weight of platinum (kg) used during the liquid phase oxidation of phenol as expressed in equation (2.3a). Similarly, the weight specific phenol load (S.P.L.) is defined as the ratio of molar phenol feed rate (mol/s) to the weight of platinum (kg) used during oxidation of phenol as expressed in equation (2.3b).

$$S.O.L. = \frac{F_{O_2}}{W_{Pt}} \tag{2.3a} \qquad\qquad S.P.L. = \frac{F_{Ph}}{W_{Pt}} \tag{2.3b}$$

The liquid and gas analyses data obtained from the slurry CSTR were evaluated to give phenol disappearance rate as well as conversion and selectivity to CO_2 and H_2O. The net specific disappearance rate of phenol was calculated by:

$$R_{w,Ph} = \frac{F_V^L}{W}\left(C_{Ph,in} - C_{Ph}\right) - \frac{V_L}{W}\frac{dC_{Ph}}{dt} \tag{2.4}$$

The accumulation term (dC_{ph}/dt) is useful to get relevant rate data also at non-steady state conditions. This term is important especially when different start-up procedures are employed and is calculated as a derivative of the residual phenol concentration-time curve. The percentage phenol conversion is defined using the expression:

$$X_{Ph} = \frac{R_{W,Ph} \cdot W}{F_V^L \cdot C_{Ph,in}} \times 100\%$$ (2.5)

The rates of formation of reaction intermediates and end products were similarly calculated by:

$$R_{w,i} = \frac{F_V^L}{W} C_{W,i} + \frac{V_L}{W} \frac{dC_i}{dt}$$ (2.6)

The percentage molar selectivity of phenol to reaction intermediates and end products was calculated based on total carbon and constant volumetric liquid flow rate, by the expression:

$$S_i = \frac{N_{Ci} \cdot R_{W,i}}{6 \cdot R_{W,ph}} \times 100\%$$ (2.7)

For all experimental data, carbon balance calculations were carried out to check the accuracy and reliability of the experiments. Vaporization of phenol could be neglected. The carbon balance was verified after every experiment. The typical range was 95-100%, which was considered acceptable since it is within the experimental errors for HPLC and GC analyses.

2.2.6. Oxygen mass transfer

Several criteria can be used for checking the absence of mass transfer limitations, for example setting a maximum deviation of 5% or a minimum degree of saturation, Γ_L, of 0.95 as reported in the literature (Fogler, 1999; Beenackers and van Swaaij, 1993). However, for catalytic oxidation it is useful to know the oxygen concentration at the catalyst particle surface. Sequential calculations were performed to determine the oxygen concentrations in the bulk liquid and at the catalyst surface as explained in literature (Fogler, 1999). The mass transfer resistance in the gas phase was neglected. The net consumption rate of oxygen (or disappearance rate) by the oxidation of phenol was calculated by:

$$R_{O_2}^{cons} = v \cdot \left(R_{w,Ph} \right) \cdot W$$ (2.8)

The stoichiometric factor, v, is 7 for complete oxidation of phenol to CO_2 based on equation (2.1). For a reactor that is perfectly mixed, the oxygen mass transfer equals the consumption of oxygen by the oxidation of phenol. The bulk liquid oxygen concentration can be calculated from the equation (2.9) for oxygen transport from the gas-liquid interphase to the bulk liquid:

$$R_{O_2}^{cons} = k_L \cdot a \cdot V_L \cdot \left(C_{O_2,sat} - C_{O_2,b} \right) \tag{2.9}$$

The solubility of oxygen in liquid at a given temperature, expressed as mole fraction of oxygen, χ_{O2}, in liquid at the standard pressure (P^0) of 101.325 kPa was calculated using a semi-empirical correlation of Battino (1981). The oxygen concentration in liquid, which is in equilibrium with the gas phase, was calculated by:

$$C_{O_2,sat} = \frac{\rho_{H2O}}{M_{H2O} \cdot P^0} \cdot \chi_{O_2} \cdot P_{O_2} \tag{2.10}$$

The reactor used in this work was equipped with a special gas dispersion impeller. The minimum value of $k_L a$ can be estimated from equation (2.9) when the concentration driving force is set at maximum, i.e. the bulk liquid concentration ($C_{O_2,b}$) is equal to zero for a given value of $C_{O_2,sat}$. Similarly, for a perfectly mixed bulk liquid, the oxygen mass transfer to the catalyst surface equals the consumption of oxygen by the oxidation of phenol. The concentration of reactant X at the catalyst surface is calculated from equation (2.11) where the rate of mass transfer from the bulk solution to the external surface of catalyst particles is calculated as:

$$R_X = k_{S,X} \cdot a_{LS} \cdot W \cdot \left(C_{X,b} - C_{X,s} \right) \tag{2.11}$$

The mass transfer coefficient from liquid to solid, $k_{S,X}$, is calculated from the dimensionless Sherwood number as given by Sano *et al.* (1974):

$$Sh = \varphi_C \left(2 + 0.4 \mathrm{Re}^{\frac{1}{4}} Sc^{\frac{1}{3}} \right) \tag{2.12}$$

where *Sh* the Sherwood number expressed in equation (2.13a) as:

$$Sh = \frac{k_{S,X} \cdot d_P}{D_X} \tag{2.13a} \qquad Sc = \frac{\mu_L}{\rho_L \cdot D_X} \tag{2.13b}$$

with *2 ≤ Sh < 10*, where *X* is the reactant. The Carman factor, φ_C, is a correction factor for the geometry of the particle. The catalyst particles were assumed to be spherical (i.e. φ_C is 1) which is the conservative assumption. The Schmidt number, Sc, was calculated using equation (2.13b). The Reynolds number based on the Kolmogoroff theory for isotropic turbulence is given by:

$$Re = \frac{N_P D_i^5 N^3 d_P^4 \rho_L^3}{\mu_L^3 V_L} \tag{2.14}$$

in which N_p is the impeller power number, D_i is the impeller diameter, N is the impeller revolution speed, d_p is the particle size of the solid, ρ_L is the density of liquid, and μ_L is the dynamic viscosity of the liquid. The weight specific liquid-solid interface area is given by:

$$a_{LS} = \frac{6}{d_p \cdot \rho_p} \tag{2.15}$$

in which ρ_p is the density of the dry particle which can be calculated from the particle porosity, ε_p, and the volumetric mass of the support, ρ_s, as:

$$\rho_P = \rho_s \left(1 - \varepsilon_P\right) \qquad (2.16)$$

The significance of internal mass transfer limitations can be assessed using the Weisz-Prater modulus criteria (Fogler, 1999). However, the type of catalyst used in this study is the "egg-shell" catalyst where the active sites are mainly located in the outer shell. Thus calculations of oxygen diffusion resistance become useless. Detailed calculations and assessment of oxygen mass transfer and its implication on phenol oxidation is reported elsewhere (Masende *et al.*, 2004).

2.3. Results and discussion

The experiments were selected to cover a wide range of conditions. This range as well as the standard experimental conditions is given in Table 2.1. The activity of platinum catalysts during liquid phase oxidation may be influenced by the amount of oxygen in the reactor (Ukropec *et al.*, 1999; Markusse *et al.*, 1999; Mallat and Baiker, 1994) as well as the oxidation intermediates and end products. The purpose of this work is to find the proper operation window for high phenol conversion to CO_2 and H_2O. It was therefore necessary to carry out studies under intrinsic and non-intrinsic kinetics conditions as well. The verification and assessment of oxygen mass transfer limitations as described in Section 2.2.6 are reported in Section 2.3.7.

Results obtained from blank experiments in which solutions of only water and Pt/graphite catalyst were tested for about 6h at 700 kPa oxygen partial pressure and 180°C, proved the absence of oxidation and showed the stability of graphite at these conditions. Studies on long-term stability and topographical characterisation of the catalyst were not part of this work.

Experiments performed at 150°C and total pressure of 1.8 MPa under nitrogen gas and without catalyst showed no measurable phenol conversion (~0.5% of initial phenol) indicating absence or negligible thermal degradation of phenol at liquid residence time of 35 min. When oxygen gas was fed to the reactor in the same run, a very faint yellowish liquid, ascribed to the presence of *p*-benzoquinone, was observed with a slight change in pH from 5.6 (of phenol) to 5.0 at steady state condition. The low phenol conversion (< 2%) observed could be attributed to either homogeneous reaction of phenol with oxygen at reaction conditions or reaction caused by presence of impurities in the solution or catalytic activity of the reactor material. Traces (<1% of initial phenol) of *p*-benzoquinone, maleic acid, and succinic acid were identified.

These results show that the extent of thermal degradation, and homogeneous reaction of phenol with oxygen at standard experimental conditions, is relatively small. Non-oxidative reaction also may take place to some extent initiated by the catalyst, which is likely to cause catalyst deactivation, probably through polymerisation. In Table 2.2 a list of reaction intermediates and end products detected in this study is given. The influence of such factors as reaction start-up method, oxygen partial pressure, initial phenol concentration, temperature, and catalyst mass, on the selectivity of the reaction to CO_2, and other main intermediates are reported in the next sections.

Table 2.2
Reaction intermediates and end products during phenol oxidation

Compound	Formula	High P_{O_2} (S.E.[a] > 80%)			Low P_{O_2} (0<S.E.[a]<80%)		
		A[b]	B[b]	C[b]	A[b]	B[b]	C[b]
Phenol	C_6H_5OH						
p-benzoquinone	$C_6H_4O_2$	++	++	++	+(0)	+(0)	-
Maleic acid	cis-HO_2C-CH=CH-CO_2H	++	++	++	+(0)	+(0)	-
Fumaric acid	trans-HO_2C-CH=CH-CO_2H	+	+	+	-	-	-
Succinic acid	HO_2C-$(CH_2)_2$-CO_2H	+	+	+	+	+	+
Malonic acid	HO_2C-CH_2-CO_2H	-	-	-	+	+	+
Acetic acid	CH_3-CO_2H	+	+	+	+	+	+
Glyoxylic acid	$CHOCO_2H$	++	++	+	+(0)	+(0)	-
Oxalic acid	HO_2C-CO_2H	++	++	+	+(0)	+(0)	-
Insoluble compounds	Not identified	++	++	+	-	-	-
Carbon dioxide	CO_2	++	++	++	+++	+++	+++

Selectivity: +++, highest; ++, high; +, low; (0), only at start of reaction; -, not detected.
[a]S.E.: the stoichiometric oxygen excess to phenol.
[b]Start-up procedures- A: O_2-FIRST; B: Ph-FIRST; and C: O_2-Ph-SIM.

2.3.1. Influence of reaction start-up procedure

The sensitivity of the platinum catalyst to the sequence of initial exposure to the reactants was investigated at standard experimental conditions and initial oxygen partial pressure of 400 kPa. Three different start-up methods, namely 'first oxygen then phenol' (O_2-FIRST), 'first phenol then oxygen' (Ph-FIRST), and 'simultaneous feed of oxygen and phenol' (O_2-Ph-SIM) were investigated. It was found that reaction start-up with the O_2-Ph-SIM method gave the highest phenol conversion of over 99% while a lower steady state conversion of 83% was obtained when the Ph-FIRST method was used as shown in Fig. 2.2(a). In the O_2-FIRST start-up method, phenol conversion of 84% was observed at the beginning of the reaction, which increased gradually to reach over 97% at steady state conditions. As the residual oxygen partial pressures for all methods remained at the same level of ca. 50 kPa, the observed

difference in phenol conversion can be explained by the effect of the sequence of initial exposure of the catalyst to the reactants.
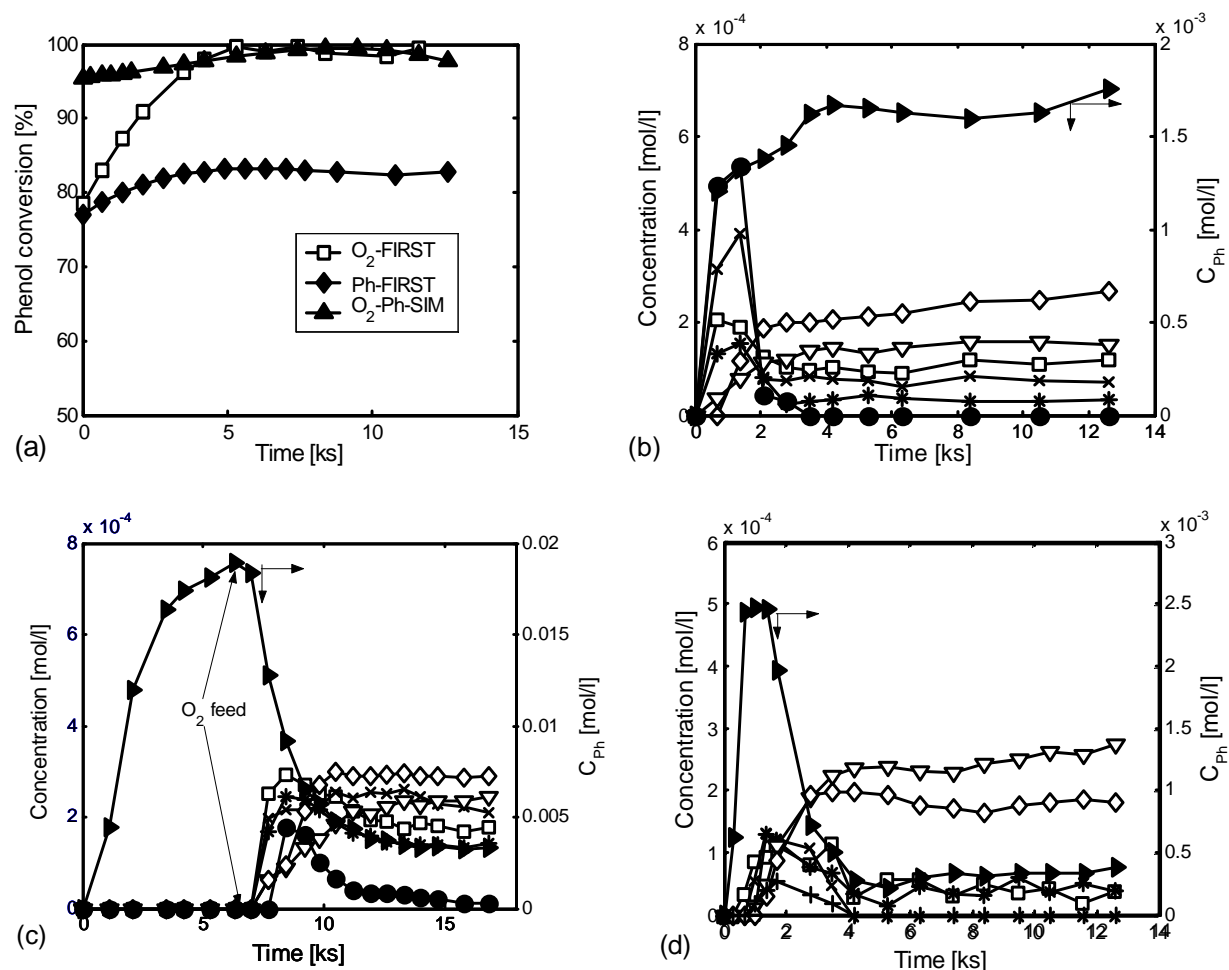

Fig. 2.2. Influence of reactor start-up methods at standard conditions (Table 2.1) with S.E.=20% and S.O.L.=0.27 mol.s^{-1}.kg$_{Pt}^{-1}$: conversion (a); concentration: (b) O$_2$-FIRST (c) Ph-FIRST (d) O$_2$-Ph-SIM methods. Symbols: (►) phenol, (●) *p*-benzoquinone, (□) oxalic acid, (x) maleic acid, (*) glyoxylic acid, (∇) succinic acid, (◊) acetic acid, and (+) malonic acid.

The formation of intermediates and end products during the reaction period when the O$_2$-FIRST start-up method is used is shown in Fig. 2.2(b). High concentrations of *p*-benzoquinone and maleic acid were detected during the first 70 min in a yellowish coloured effluent. Afterwards, the liquid effluent became colourless, with a change in pH from 3.2 to 4. The main steady state oxidation products detected in the liquid were succinic and acetic acids, while oxalic and glyoxylic acids appeared in trace amounts.

The somewhat lower initial conversion obtained when the O$_2$-FIRST method is used, could be attributed to a pre-oxidised surface of the platinum catalyst. The increase in phenol conversion after 70 min can be explained by the reducing effect on the catalyst

of the phenol solution entering the reactor, which indicates that more active sites of platinum catalyst were available for reaction after being regenerated by phenol. The formation of *p*-benzoquinone at the start of the oxidation is possibly due to oxygen insertion in the benzene ring or attack by OH radicals at the *para* position of the phenol molecule (Alnaizy and Akgerman, 2000).

The reaction proceeded differently when the Ph-FIRST method was used. In Fig. 2.2(c) the oxidation intermediates and end products similar to those obtained with the O_2-FIRST method, are shown. The relatively low phenol conversion achieved when the Ph-FIRST method is used, can be explained by the presence of irreversibly adsorbing organic species and carbonaceous fragments resulting from phenol on a free platinum surface, before oxygen is injected into the reactor. Recovery or regeneration of the poisoned active sites of the catalyst seems to be difficult. As the reaction proceeds, the residual platinum active sites are easily over-oxidised, and this could explain why *p*-benzoquinone is formed. The deactivation of platinum catalysts at oxygen free conditions has also been observed during alcohol oxidation (Markusse *et al.*, 2000; Vleeming *et al.*, 1997).

Fig. 2.2(d) shows the reaction intermediates and products for the O_2-Ph-SIM start-up method. Succinic and acetic acids are the main products formed at residual oxygen partial pressure of 50 kPa at a pH of 4. Both maleic and malonic acids are formed in trace amounts only during a reaction period of 70 min, that is two times the liquid residence time. The high conversion observed in the simultaneous feed method clearly shows that the catalytic activity and the mechanism of platinum catalysed phenol oxidation to CO_2 and H_2O is influenced by the reaction start-up procedure. The residual phenol concentrations of $1.7.10^{-3}$, $3.5.10^{-3}$, and $0.4.10^{-3}$ mol/l measured for O_2-FIRST, Ph-FIRST, and O_2-Ph-SIM methods, respectively, suggest that reaction start-up with simultaneous feed of oxygen and phenol is the preferred method. The O_2-Ph-SIM method therefore, unless otherwise stated, was used in the rest of the investigation. Table 2.2 shows the influence of the reaction start-up procedures on the selectivity and distribution of oxidation products. In the next sections, the optimum conditions to obtain high selectivity to CO_2 an H_2O are discussed.

2.3.2. Influence of oxygen load

The effect of oxygen partial pressure on phenol oxidation was investigated at standard conditions (Table 2.1) using the O_2-Ph-SIM start-up method but with oxygen partial pressures within the 10 to 800 kPa range. In Fig. 2.3 typical results are presented on

the influence of oxygen load, expressed as stoichiometric excess (S.E.), on phenol conversion with the corresponding CO_2 formation, concentration of intermediate compounds at steady state, pH, and residual oxygen partial pressures. It can be seen in Fig. 2.3(a) that phenol conversion of over 95% is achieved when the supply of oxygen is close to the stoichiometric amount for phenol oxidation. When the oxygen supplied for the reaction is twice the stoichiometric amount, low phenol conversion and selectivity to CO_2 are observed. This low conversion when surplus of oxygen is used could be due to the high oxygen load on the platinum catalyst, thus affecting the catalytic reaction. As expected, lower conversions were also observed when the reaction was carried out with sub stoichiometric amount of oxygen, as shown in Fig. 2.3(a). In Fig.2.3(b) the influence of oxygen load on the CO_2 formation is presented. When the residual oxygen partial pressure (see Fig. 2.3d) in the reactor is lower than 100 kPa, the formation of CO_2 increases with the increase in residual oxygen pressure. However, less CO_2 was formed at residual oxygen pressures above 200 kPa.
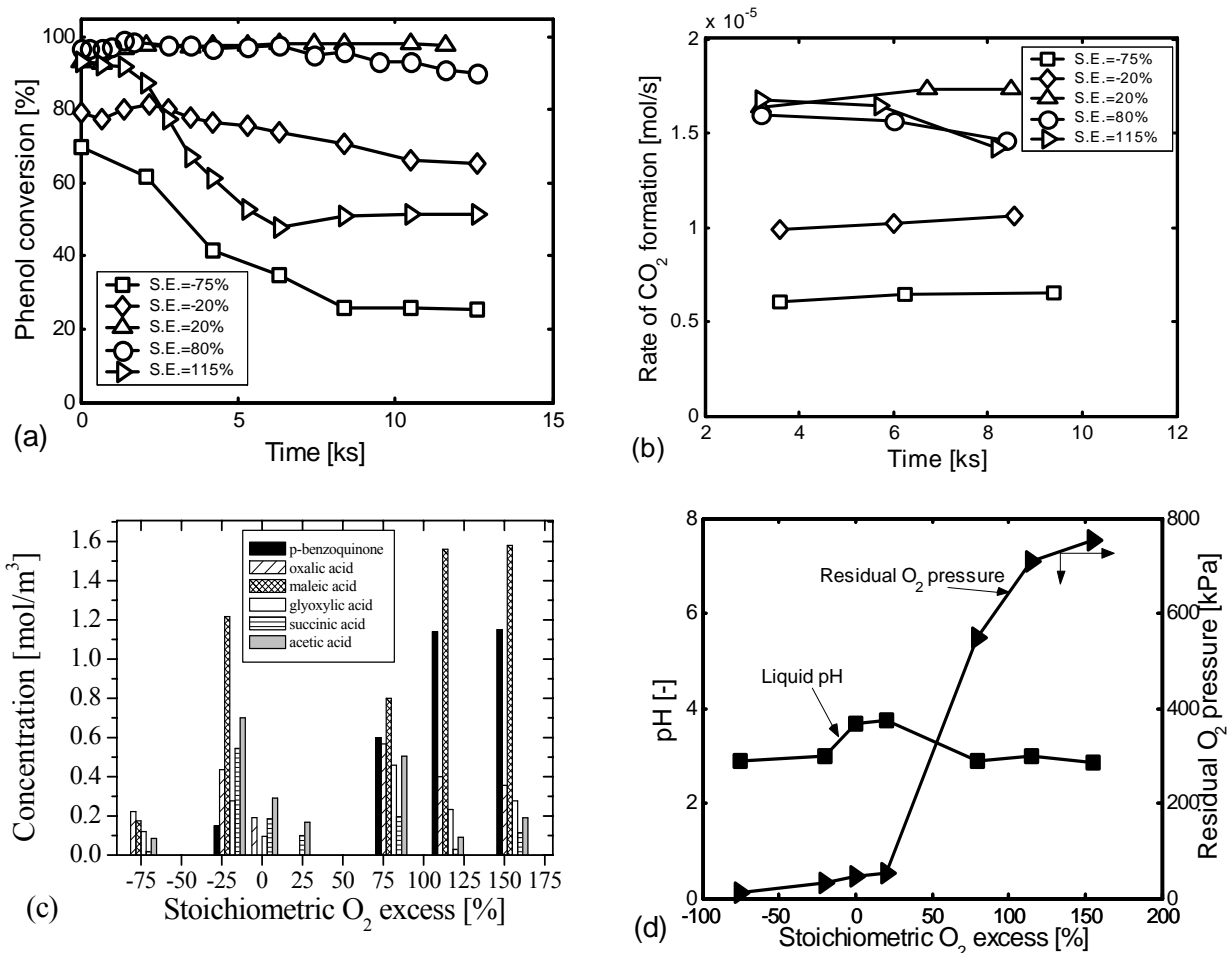

Fig. 2.3. Influence of oxygen load on phenol oxidation at standard conditions (Table 2.1) using the O_2-Ph-SIM start-up method on: (a) phenol conversion, (b) CO_2 formation, (c) selectivity of reaction intermediates at steady state (after 105 min), and (d) corresponding residual oxygen partial pressure and pH at steady state.

These results suggest that there is a maximum oxygen load for the platinum catalyst in order to get high selectivity to CO_2. The steady state concentrations of reaction intermediates and end products are shown in Fig. 2.3(c) with the corresponding pH and residual oxygen partial pressures in Fig. 2.3(d). It can be seen that when insufficient oxygen is fed, the reaction is dominated by the formation of low molecular weight carboxylic acids, which corresponds to the observed low pH with low selectivity to CO_2. There is however, a dramatic change in the formation of reaction intermediates as the residual oxygen partial pressures in the reactor changes. As can be seen in Figs. 2.3(c) and (d), within the residual oxygen pressure range of 20 to 40 kPa, neither *p*-benzoquinone nor maleic acid were detected in the colourless liquid effluent.

The pH of 3.8 is within the range for water saturated with CO_2, indicating that mainly CO_2 was present in the liquid. At high residual oxygen partial pressures, both *p*-benzoquinone and maleic acid were detected in high concentrations in the brownish coloured liquid effluent, as shown in Fig. 2.3(c). As the intensity of the brownish colour in the liquid effluent increased, insoluble compounds, attributed to polymeric products, are also formed in addition to the increase of the *p*-benzoquinone concentration. These results support the hypothesis that the extent of oxygen coverage on the platinum surface influences the selectivity of the reaction as was already suggested in Section 2.3.1.

2.3.3. Influence of phenol load

The influence of the phenol feed concentration was investigated at standard experimental conditions (Table 2.1). Also a set of experiments was carried out at 165°C and the molar flow rate ratio of oxygen to phenol was kept constant at a stoichiometric oxygen excess of 20%. This implies that as the phenol feed concentration was changed, the oxygen load also was changed to maintain the same oxygen to phenol ratio. It was found that with phenol feed concentrations up to 0.05 mol/l, the disappearance rate of phenol increased with increasing feed concentration as is seen in Fig. 2.4(a). At a phenol feed concentration of 0.065 mol/l, a remarkable, gradual decline in the reaction rate was observed. Also such a high phenol load resulted in a lower rate of formation of CO_2, as can be seen in Fig. 2.4(b). In the liquid effluent, obtained when phenol oxidation was carried out with 0.02 and 0.035 mol/l phenol feed solutions, neither *p*-benzoquinone nor maleic acid were detected, while considerable amounts of *p*-benzoquinone and maleic acid were observed for phenol feed concentration of 0.065 mol/l. In Fig. 2.4(c) the residual phenol concentrations for different phenol feed concentrations are shown. It is observed that the residual phenol

concentration increases from 0 to 0.034 mol/l at 10 and 175 min, respectively, when phenol solution of 0.065 mol/l is used, while a decrease in residual phenol concentration from ca. 0.007 to 0 mol/l is observed at 30 and 105 min, respectively, for 0.035 mol/l phenol solution. Similar trend is observed when phenol solution of 0.02 mol/l is used. It was further observed that higher catalyst activity was maintained when the residual partial pressure in the reactor was below 150 kPa (see Fig. 2.4(d)) otherwise deactivation occurred.
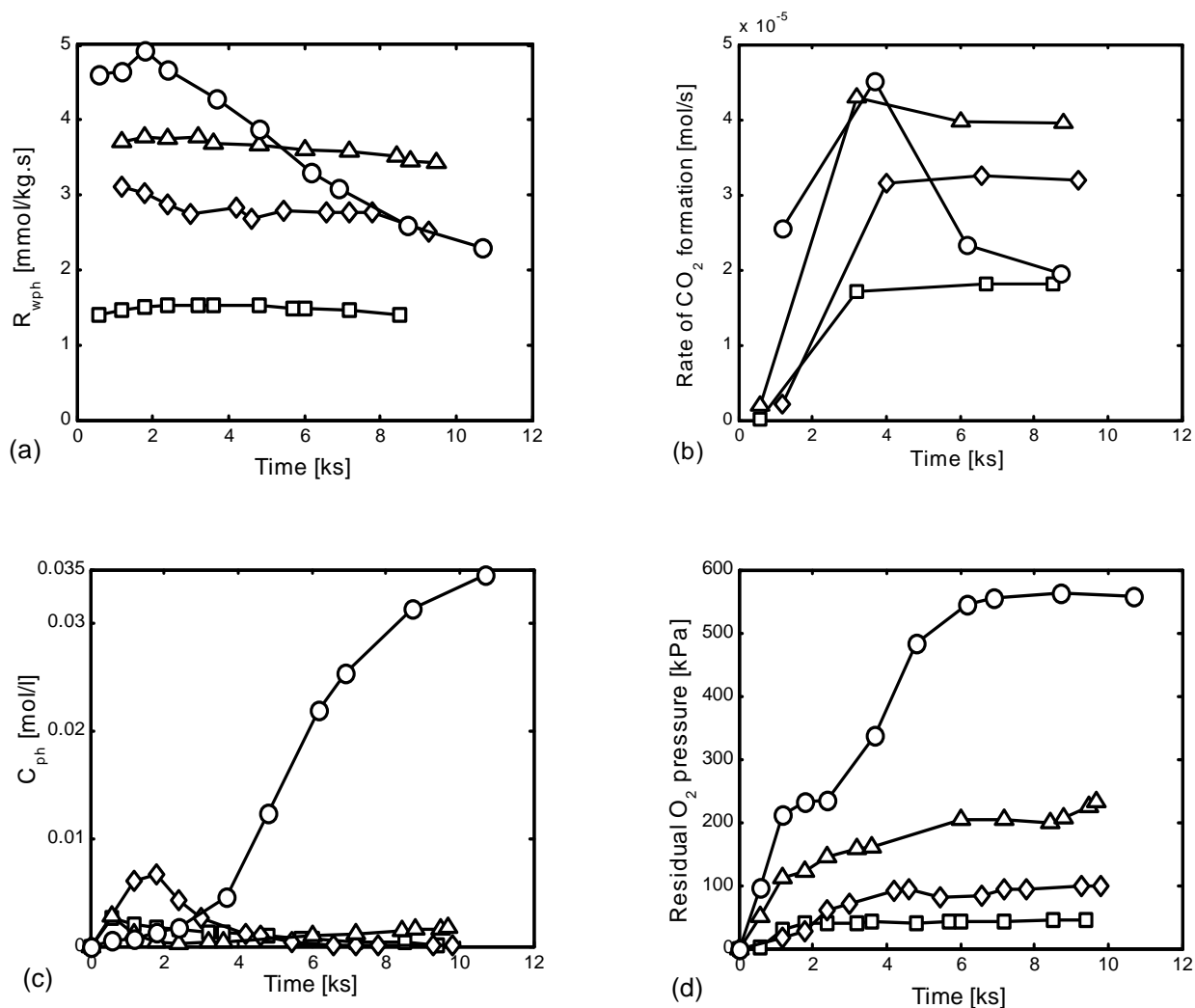

Fig. 2.4. Influence of initial phenol concentration at standard conditions (Table 1) and 165°C using the O_2-Ph-SIM start-up method on: (a) phenol disappearance rate, (b) rate of CO_2 formation, (c) residual phenol concentration, and (d) corresponding residual oxygen partial pressure. Symbols: ($\square$) C_{ph} =0.02, S.O.L. = 0.265, ($\lozenge$) C_{ph} = 0.035, S.O.L. = 0.484, (Δ) C_{ph} = 0.05, S.O.L. = 0.670, and (O) C_{ph} = 0.065, S.O.L. = 0.860, where C_{ph} in [mol/l] and S.O.L. in [mol.s^{-1}.kg$_{Pt}^{-1}$].

The observed decline in the reaction rate and the rate of formation of CO_2, at higher phenol feed concentrations can be explained either by the too limited amount of the catalyst needed to fully convert phenol at these conditions, or by the high residual

oxygen partial pressures, leading to catalyst deactivation as explained in the previous section. The increasing residual phenol concentration when a 0.065 mol/l phenol solution is used proves that catalyst deactivation takes place. The decrease in residual phenol concentration from ca. 0.007 to 0 mol/l at 30 and 105 min, respectively, when a 0.035 mol/l phenol solution was used indicates the presence of catalyst reactivation. This also suggests that when the reaction is carried out with proper oxygen and phenol loads, platinum catalyst deactivation can be avoided. The activity of platinum catalyst during phenol oxidation and higher selectivity to CO_2 can be maintained when the reaction is carried out at a residual oxygen partial pressure below 150 kPa.

2.3.4. *Influence of temperature*

The influence of temperature on the reaction rate and the selectivity of the phenol oxidation reaction was studied in the temperature range of 120 to 180°C. The molar flow ratio of oxygen to phenol was kept constant at a stoichiometric oxygen excess of 80% for all experiments. Typical results on the influence of temperature on phenol conversion are shown in Fig. 2.5(a). It was found that at temperatures above 150°C, phenol conversion to CO_2 and H_2O of 99% and higher was attained, while at 135 and 120°C, phenol conversions were 60% and 42% respectively, after 105 min of reaction time. In an additional experiment at 150°C with a stoichiometric oxygen excess of 20%, over 99% conversion of phenol was achieved, in contrast to the experiment with a stoichiometric oxygen excess of 80%. Similar temperature dependence was observed for the rate of CO_2 formation as can be seen in Fig. 2.5(b). When phenol oxidation is carried out with a stoichiometric oxygen excess of 80%, higher rates of formation of CO_2 were observed at temperatures above 150°C and reached a maximum at 180°C, while it drops down for temperatures below 150°C. However, a comparable rate of CO_2 formation to that at 180°C was obtained when a reaction was carried out at 150°C with a stoichiometric oxygen excess of 20%. In Fig. 2.5(c) the residual phenol concentration at different temperatures is shown. Analysis of the liquid samples obtained at higher temperatures showed low residual phenol concentrations with trace amounts of low molecular weight carboxylic acids. Neither *p*-benzoquinone nor maleic acid were detected in the liquid samples obtained at 165 and 180°C, which had an average pH of 3.9.

However, at lower temperatures the residual phenol concentration increased gradually, while a decline in the activity of the platinum catalyst was observed. Analysis of the liquid effluent obtained at 120°C, which was characterised by a brownish colour, showed increased formation of *p*-benzoquinone, maleic acid, and insoluble

(polymeric) products. No attempt was made to identify the composition of the insoluble (polymeric) compounds formed in this work.
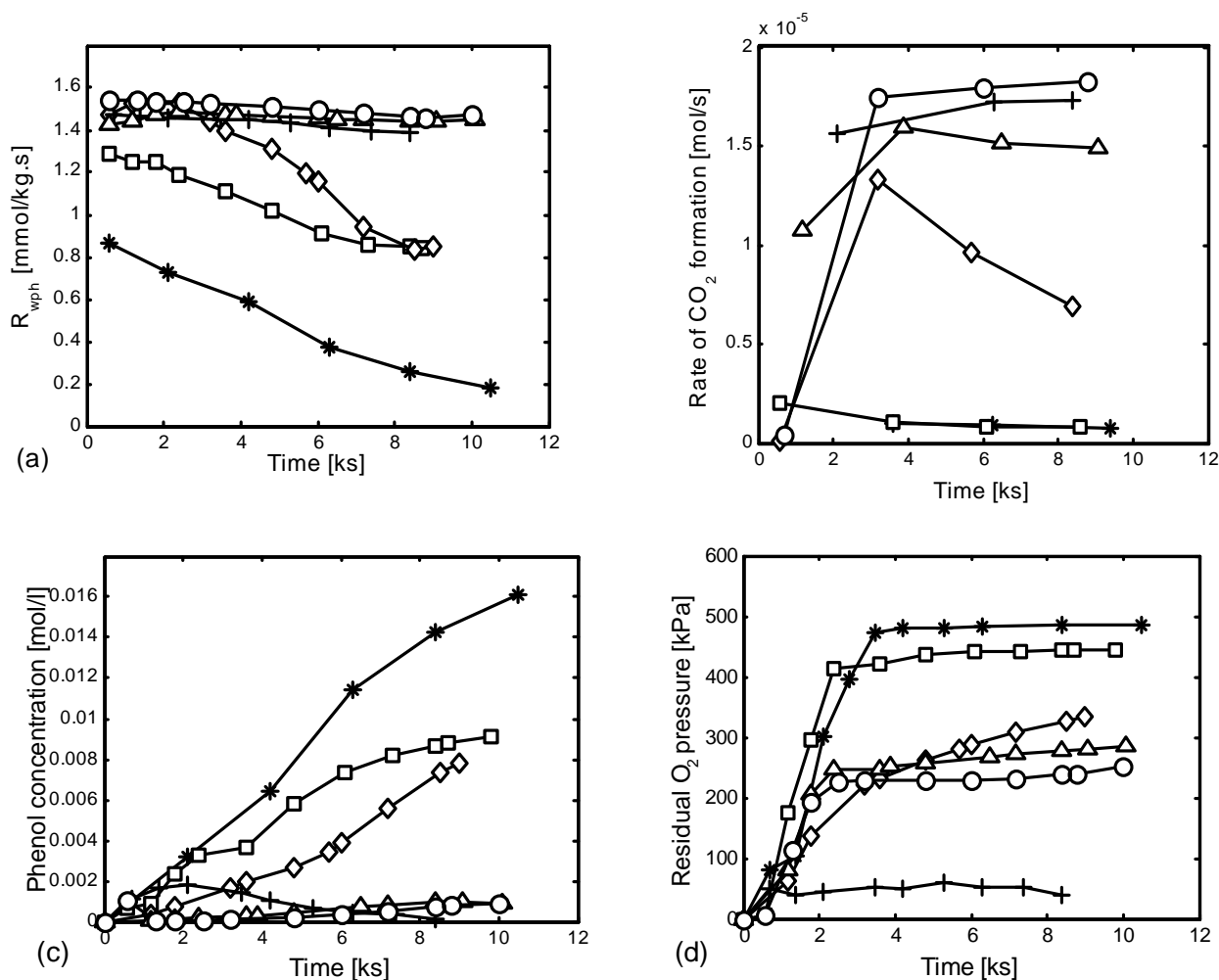

Fig. 2.5. Influence of temperature on phenol oxidation at standard conditions (Table 1) using the O_2-Ph-SIM start-up method on: (a) phenol disappearance rate, (b) rate of CO_2 formation, (c) residual phenol concentration, and (d) corresponding residual oxygen partial pressure. Symbols: (*) 120°C, S.E.= 80% (□) 135°C, S.E.= 80%, (◊) 150°C, S.E.= 80%, (+) 150°C, S.E.= 20%, (Δ) 165°C, S.E.= 80%, and (O) 180°C, S.E.= 80%.

The increase in the residual phenol concentration (see Fig. 2.5(c)) indicates the presence of catalyst deactivation during phenol oxidation at S.E. of 80%. Although the increase in residual phenol concentration is remarkable at lower temperatures, gradual increase albeit small is also observed at higher temperatures. The possible explanation for the presence of deactivation could be due to higher residual oxygen partial pressure, i.e. above 200 kPa, as can be seen in Fig. 2.5(d). The high phenol conversion and low residual oxygen partial pressure observed at a stoichiometric oxygen excess (S.E.) of 20%, as compared to S.E. of 80% both at 150°C, proves again that the extent of oxygen coverage on the platinum catalyst clearly affects the catalytic activity of the

platinum and selectivity to CO_2 and H_2O. It can be inferred from the above observations that at 150 °C and above the conversion of phenol and hence the reaction rate is so high that mass transfer of oxygen becomes the rate limiting.
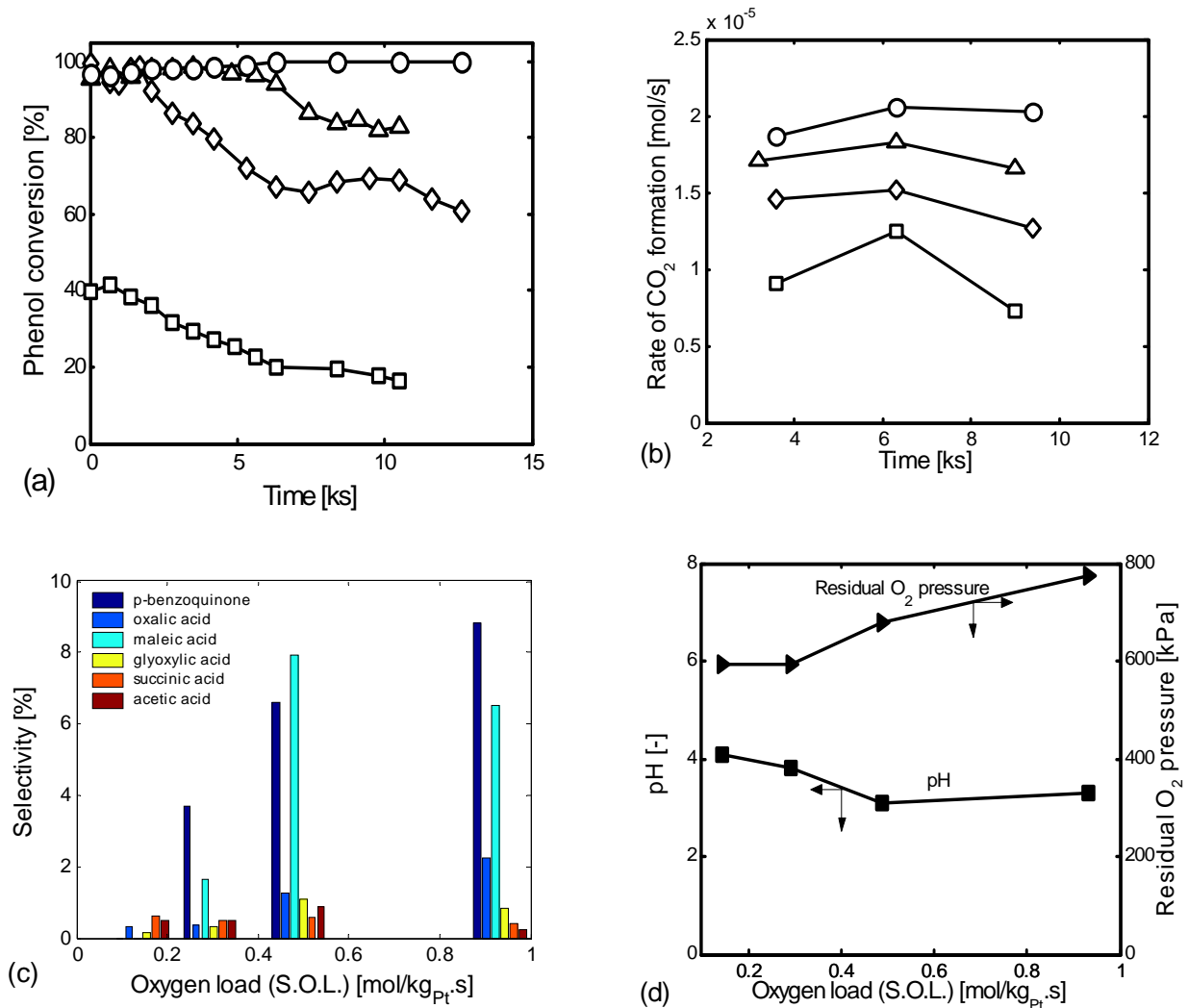

Fig. 2.6. Influence of catalyst mass and specific oxygen load (S.O.L.) during phenol oxidation using the O_2-Ph-SIM start-up method at standard reaction conditions (Table 2.1) on: (a) phenol conversion, (b) rate of CO_2 formation, (c) selectivity of reaction intermediates at steady state (after 105 min), and (d) corresponding residual oxygen partial pressure and pH at steady state. Symbols: (□) W= 3 g, S.E.= 120%, S.O.L.= 0.933, (◊) W= 6 g, S.E.= 120%, S.O.L.=0.489, (Δ) W= 10 g, S.E.= 120%, S.O.L.= 0.293, and (O) W= 10 g, S.E.= 20%, S.O.L.=0.145, where S.O.L. in $[mol.s^{-1}.kg_{Pt}^{-1}]$.

2.3.5. Influence of catalyst amount

The influence of the catalyst amount on the rate of phenol oxidation and the selectivity was studied at standard conditions (Table 2.1) with 3, 6, and 10 $kg.m^{-3}$ of catalyst. The ratio of the molar flow rates of oxygen and phenol was kept constant at a stoichiometric oxygen excess of 120%. It was found that the conversion of phenol

increased as the amount of catalyst increased. However, the relationship between the conversion and the catalyst concentration does not appear to be linear as can be seen in Fig. 2.6(a). A low phenol conversion of 20% was obtained at steady state when 3 kg.m^{-3} of catalyst was used. This can be explained by a combined effect of high residual oxygen pressure, and an insufficient amount of catalyst used.

With 10 kg.m^{-3} of catalyst, phenol conversion of over 99% was obtained during the first 105 min of reaction time, however after 105 min a gradual decline in conversion was noted, reaching 82% after 175 min. Similarly, using 3 kg.m^{-3} of catalyst, over 90% phenol conversion was obtained during the first 70 min of reaction time, dropping down to 65% after 175 min. Again, the decline in phenol conversion could be due to the high residual oxygen partial pressure in the reactor leading to over-oxidation of the catalyst. In order to check this, an additional experiment was carried out with 10 kg.m^{-3} of catalyst and a stoichiometric oxygen excess of 20%. It was found that 100% of phenol conversion to CO_2 and H_2O was achieved and maintained during the whole period of reaction as is shown in Fig. 6(a). Furthermore, this experiment gave the highest CO_2 evolution rate, as can be seen in Fig. 2.6(b). Fig. 2.6(c) compares the distribution of reaction intermediates and end products at steady state, while the corresponding residual oxygen partial pressure and liquid effluent pH are shown in Fig. 2.6(d). When 3 kg.m^{-3} of catalyst was used, catalyst deactivation occurred. In addition to the formation of polymeric products, analysis of the brownish coloured liquid showed increased formation of *p*-benzoquinone, maleic acids, and other low molecular weight acids.

These results provide evidence that a high oxygen load may decrease the activity of the catalyst and may affect the selectivity to CO_2 and H_2O. The non-linearity observed when the amount of catalyst was increased above 6 kg.m^{-3} leads to the conclusion that only part of the catalyst particles is taking place in the reaction.

2.3.6. Operation window

Analysis of the experimental data demonstrated that complete oxidation of phenol to CO_2 and H_2O is achieved at 150°C when the reaction proceeds within the range of molar specific oxygen loads (S.O.L.), i.e. molar oxygen feed rate (mol/s) to weight of platinum in the reactor (kg) of 0.15 to 0.35 mol.s^{-1}.kg$_{Pt}^{-1}$ and at a stoichiometric oxygen excess (S.E.) in the range of 0 to 80%. Fig. 2.7(a) summarizes the observed effects of oxygen and phenol loads on platinum catalysed phenol oxidation. The graph indicates the limits of the practical operation window for high phenol conversion and

selectivity to CO_2 and H_2O. When the reaction is carried out at low stoichiometric excess of oxygen (S.E. < 0%), phenol oxidation is dominated by the formation of low molecular weight carboxylic acids, such as succinic and acetic acids which are difficulty to oxidize, and catalyst deactivation is due to irreversible adsorption of carbonaceous compounds. Stoichiometric oxygen excess (S.E.) above 80% results into increased formation of mainly *p*-benzoquinone and maleic acid, which is accompanied by polymer formation.
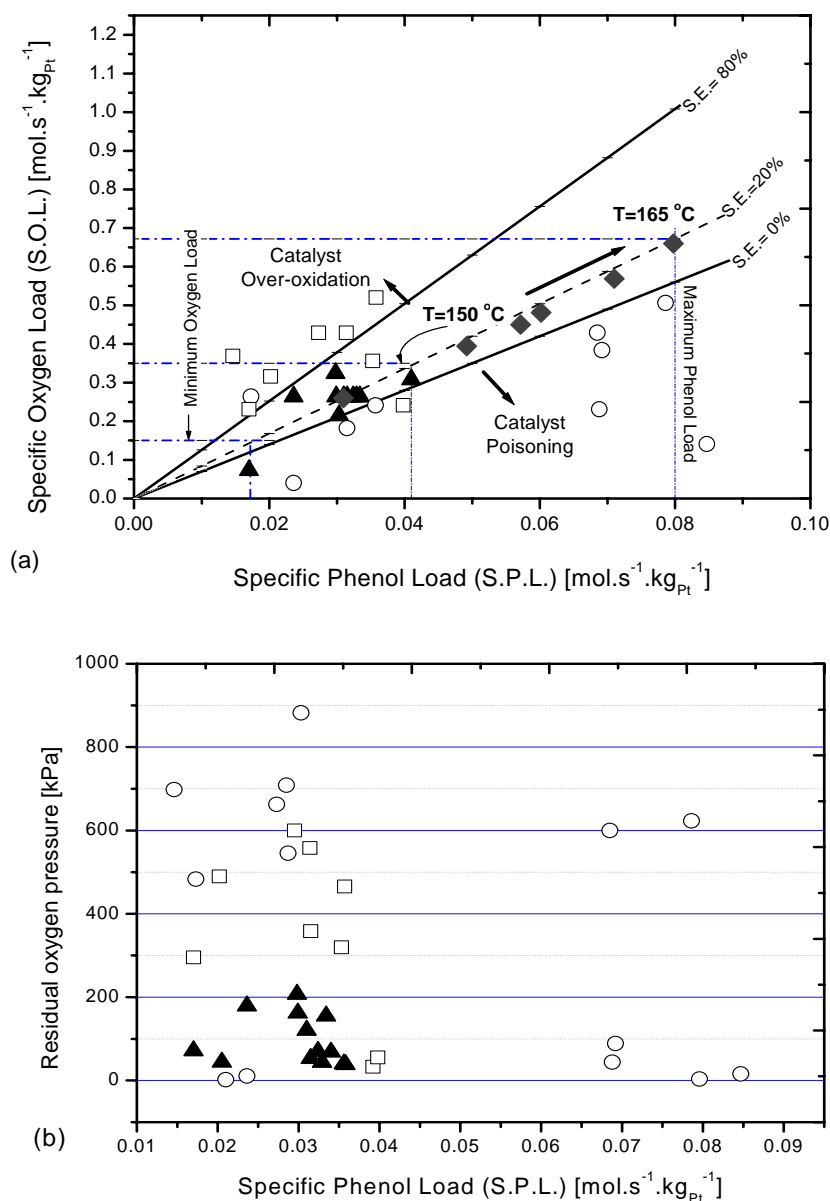
Fig. 2.7. Operating window for platinum catalysed phenol oxidation. Conditions: Catalyst; 5 wt% Pt/graphite, P_T= 1.8 MPa, F_{VL}= 10 ml/min, V_L= 350 ml and 1200 rpm. (a) Specific phenol load (S.P.L.) versus specific oxygen load (S.O.L.), and (b) Specific phenol load (S.P.L.) versus residual oxygen partial pressure. Symbols: (O) X_{ph} < 70%, (□) 70 < X_{ph} < 95%, (▲) X_{ph} > 95 % at 150ºC, and (♦) X_{ph} > 95 % at 165ºC.

The deactivation of the catalyst is possibly due to high oxygen load, which causes over-oxidation of the platinum catalyst (Markusse *et al.*, 2000; Ukropec *et al.*, 1999; Mallat and Baiker, 1994). When the S.E. is kept constant within the limits of the operation window, increasing the amount of catalyst in the reactor can reduce both the oxygen (S.O.L.) and phenol (S.P.L.) loads, which also enhances phenol conversion to CO_2 and H_2O. The use of higher amount of catalyst however could result into a costly process. The minimum S.O.L. of 0.15 $mol.s^{-1}.kg_{Pt}^{-1}$ (which corresponds to S.P.L. of 0.017 $mol.s^{-1}.kg_{Pt}^{-1}$ at S.E. of 20%) was obtained from the experimental data when the amount of catalyst was fixed at 6 $kg_{cat}.m^{-3}$. For the reactor with liquid volume of $3.5.10^{-4}$ m^3 the reaction becomes oxygen-supply limited when lower S.O.L. are used.

Also the influence of reaction temperature on phenol oxidation using S.E. of 20% is indicated in the operating window in Fig. 2.7(a). The activity of platinum catalyst is enhanced by the increase in temperature as indicated with the arrow. Complete phenol conversion to CO_2 and H_2O is attained at S.O.L. of 0.670 $mol.s^{-1}.kg_{Pt}^{-1}$ when the reaction is carried out at 165 and 180°C as compared to a maximum S.O.L. of 0.0.350 $mol.s^{-1}.kg_{Pt}^{-1}$ when the reaction is carried out at 150°C. In addition to the practical operation limits of oxygen and phenol loads, which are related to S.E., the residual oxygen partial pressure in the reactor perhaps is the most important from an engineering point of view. In Fig. 2.7(b) the relationship between the residual oxygen partial pressure and the specific phenol load (S.P.L.) is shown. The observed experimental data indicate that higher phenol conversion to CO_2 and H_2O is achieved when the residual partial pressure of oxygen in the reactor is kept below 150 kPa. Residual oxygen partial pressures above 200 kPa result into catalyst deactivation by over-oxidation as previously explained. To verify whether the practical operation window is under the "intrinsic" kinetic reaction regime or the mass transfer limited regime, preliminary assessment of the gas/liquid transfer of oxygen was carried out as explained in the next section.

2.3.7. *Verification of oxygen mass transfer*

An operating regime where there is absence of gas/liquid mass transfer limitation in the liquid phase is the one in which the reactant conversion does not vary with further increase of the stirring speed (Zlokarnik, 2001; Kluytmans *et al.*, 2000; Perego and Peratello, 1999). Preliminary test was carried out at standard conditions (Table 1) and S.E. 80% at different impeller speed in the range of 600 to 1800 rpm. The stirrer speed of 1200 rpm was chosen since it gives sufficient mass transfer rate to obtain good

conversions. The influence of stirring speed on oxygen mass transfer and hence reaction rate was not the subject of this paper.

During the catalytic oxidation of phenol, it is assumed that, oxygen mass transfer proceeds in series subsequent steps from the gas phase to the liquid phase and to the catalyst particle surface. Pore diffusion resistance on Pt/graphite catalyst was neglected since the catalyst is the eggshell type where the active sites are mainly located at the outer shell. The mass transfer resistance in the gas phase was also neglected. Only the experimental data related to the influence of oxygen load were considered and treated according to equations (2.8)-(2.16). The $k_L a$ value of 0.3 s^{-1} was estimated from experimental data set and using equation (2.9), where the bulk liquid oxygen concentration was assumed to be zero as the minimum value. Typical values for $k_L a$ are in the range of 0.1 - 0.5 s^{-1} for both industrial and laboratory slurry reactors (Beenackers and van Swaaij, 1993). The diffusion coefficient used is 1.16.10^{-8} m^2/s for oxygen and 7.65.10^{-9} m^2/s for phenol, which were estimated as described in literature (Perry *et al.*, 1997). The values of $k_{S,X}$ for oxygen and phenol were estimated from the Sherwood numbers, 3.6 and 2.8, respectively, after performing iterative calculations.

Fig. 2.8(a) shows the relationships of the phenol conversion and S.E. for selected experimental data. It is clear that at S.E. below 0%, as for experiment number L1 to L4, low phenol conversions are due to limited oxygen-supply. It can be seen in Fig. 2.8(b) that the corresponding oxygen concentration at the catalyst surface is practically 0 mol/m^3 and this is the reason for the high concentration of phenol at the catalyst surface. It is clear also that higher phenol conversion was achieved for experiments number L5 to L12 when the S.E. was set in the range of 0 to 40%. The corresponding oxygen concentration at the catalyst surface was experimentally less than 1 mol/m^3. It can be seen further that low phenol conversion was obtained for experiments number L13 to L15 which were carried out at S.E. above 80%. Higher oxygen and phenol concentrations at the catalyst surface were also observed in these experiments.

These results prove that high phenol conversion to CO_2 is achieved when the reaction is carried out within a properly defined operation window, which is under the oxygen mass transfer limited regime. For experiments number L5 to L12 the average ratio for $C_{O_2,b}/C_{O_2,sat}$ and $C_{O_2,s}/C_{O_2,b}$ is 0.64 and 0.98, respectively, which indicates that the gas to liquid mass transfer is limiting. When the residual (bulk liquid) phenol concentration is compared to the catalyst surface phenol concentration, no significant concentration gradient is observed which proves that phenol transport to the catalyst surface is not limiting. This holds for all experiments performed within and outside the operation

window. The low phenol conversion observed at S.E. above 80%, which corresponds to the higher oxygen concentration at the catalyst surface, proves the negative influence of higher oxygen load on platinum catalysed phenol oxidation. A detailed study on oxygen mass transfer limitation during phenol oxidation is reported elsewhere (Masende et al., 2004). A general treatment on the use of gas inducing impellers for improved gas-liquid mass transfer is given by Zlokarnik (2001).

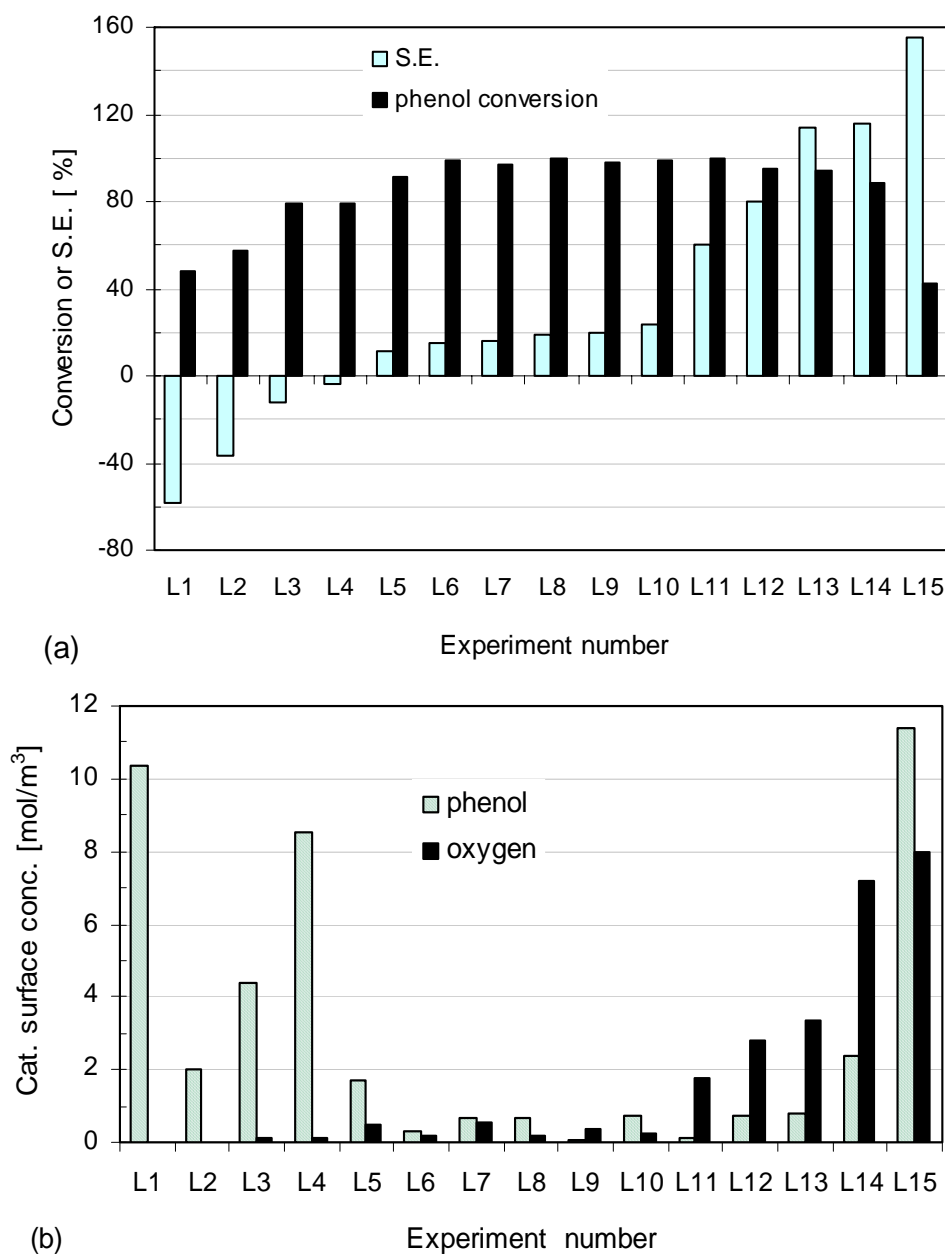Fig. 2.8. Verification of mass transfer limitations. Only the experimental data related to the influence of oxygen load are considered: (a) phenol conversion and the corresponding stoichiometric oxygen excess (S.E.) and (b) concentration of phenol and oxygen at the catalyst surface. Conditions: 6 kg_{cat}/m^3 catalyst (5 wt% Pt/graphite), P_T= 1.8 MPa, F_{VL}= 10 ml/min, V_L= 350 ml, T= 150 °C and 1200 rpm.

2.4.   Conclusions

It has been found that Pt/graphite can be efficiently applied for liquid phase oxidation of phenol. A practical operation window is determined in which high selectivity to CO_2 and H_2O can be achieved and catalyst deactivation avoided. It has been found that complete oxidation of phenol to CO_2 and H_2O can be achieved at 150°C when the reaction proceeds within the range of weight specific oxygen loads of 0.15 to 0.35 $mol.s^{-1}.kg_{Pt}^{-1}$ and at stoichiometric oxygen excess in the range of 0 to 80%. The activity of platinum catalyst remained high when the residual partial pressure of oxygen in the reactor was kept below 150 kPa at 1200 rpm. With a volumetric reaction rate ($R_{O_2}^{cons}$) of $2.29.10^{-5}$ mol/s, $k_L a = 0.3$ s^{-1} and $Sh = 3.6$, the oxygen partial pressure of 150 kPa corresponds to the oxygen concentration of 1.67 mol/m^3 in the bulk liquid and 1.64 mol/m^3 at the catalyst surface.

At higher residual oxygen partial pressure, the activity of platinum catalyst dropped as a result of deactivation by so-called over-oxidation. This type of deactivation was temporary and could be reversed at reducing conditions. The over-oxidation of the platinum surface, however, favoured the formation of *p*-benzoquinone leading to the formation of polymeric products, which resulted into permanent deactivation of the catalyst (poisoning). At lower stoichiometric oxygen excess, poor phenol conversion is observed with increased formation of intermediate compounds and the platinum catalyst may become vulnerable to poisoning by carbonaceous compounds. At conditions of limited supply of oxygen (a fully reduced platinum surface) the phenol oxidation reaction favours the formation of acetic and succinic acids which are difficult to oxidize. Also for the phenol oxidation reaction it might be worthwhile to test the influence of promoter metals like Bi, Pb and Sn. These promoters change the vulnerability of noble metals to poisoning (Mallat and Baiker, 1994). Furthermore, it has been suggested that promoters also can protect noble metals against over-oxidation (Besson and Gallezot, 2000). Lower sensitivity to poisoning (Mallat and Baiker, 1994) and enhancement of the dehydrogenation activity (Kluytmans *et al.*, 2000), form most likely the origin of this protecting action.

Increasing the reaction temperature can enhance the activity of the platinum catalyst. At temperatures below 150°C, catalyst deactivation occurs with increased formation of polymeric products and lower selectivity to CO_2 and H_2O. It was further found that when a high amount of catalyst was used, only part of the platinum catalyst participates in the reaction while at a lower catalyst amount a non-linear dependence

of the disappearance rate of phenol on the increase in the amount of catalyst was observed.

A proper choice of the reactor start-up procedure needs to be made as it influences the initial activity of the catalyst. Reaction start-up with 'simultaneous feed' of reactants once reaction conditions are reached is to be preferred when compared to 'first phenol then oxygen', and 'first oxygen then phenol' methods. Preliminary assessment of the gas/liquid mass transfer limitations show that high selectivity to CO_2 is most likely favoured under oxygen mass transfer limited regime. In order to maintain the catalyst within the proper operation window, a CSTR is the preferred reactor. Also, the residual phenol concentration in the reactor should be kept low, otherwise deactivation of the catalyst may occur.

Acknowledgements

Nomenclature

a	volumetric gas-liquid interfacial surface area [m^2/m^3]
a_{LS}	weight specific liquid-solid interfacial surface area [m^2/kg]
C_i	concentration of the compound i [mol/m^3]
$C_{O_2,sat}$	oxygen concentration in the liquid at the gas-liquid interphase [mol/m^3]
$C_{O_2,b}$	bulk liquid oxygen concentration [mol/m^3]
$C_{O_2,s}$	oxygen concentration at the catalyst surface [mol/m^3]
C_{Ph}	concentration of phenol in aqueous solution [mol/m^3]
CWO	catalytic wet oxidation
d_p	the powder size of the solid [m]
D_{O_2}	diffusion coefficient of oxygen into water [m^2/s]
D_i	impeller diameter [m]
F_i	molar flow rate of compound i [mol/s]
F_V	volumetric flow rate [m^3/s]
F_V^L	volumetric flow rate of liquid [m^3/s]
k_L	gas/liquid mass transfer coefficient [m/s]
k_S	liquid/solid mass transfer coefficient [m/s]

M_{H_2O} molecular mass of water [kg/mol]

N impeller revolution speed [s^{-1}]

$N_{C,i}$ number of carbon atoms in compound i [-]

N_p the impeller power number (= 5)

O₂-FIRST   oxygen feed first then phenol

O₂-Ph-SIM   simultaneous feed of oxygen and phenol

P pressure [Pa]

Ph-FIRST   phenol feed first then oxygen

P^o standard pressure of 101.325 [kPa]

P_{O_2} partial pressure of oxygen [Pa]

P_T total pressure in the reactor [Pa]

Re Reynolds number [-]

$R_{O_2}^{cons}$ rate of oxygen consumption by reaction [mol/s]

$R_{O_2}^{max}$ maximum transfer rate of oxygen from the gas phase to the liquid phase [mol/s]

$R_{w,Ph}$ specific disappearance rate of phenol [mol/s.kg]

R_X rate of mass transport of reactant X [mol/s]

Sc   Schmidt number [-]

SCWO   supercritical water oxidation

S_i selectivity to compound i [%]

S.E.   stoichiometric oxygen excess to phenol [%]

Sh Sherwood number [-]

S.O.L.   weight specific oxygen load [mol.s^{-1}.kg_{Pt}^{-1}]

S.P.L.   weight specific phenol load [mol.s^{-1}.kg_{Pt}^{-1}]

T   temperature [K]

TOC   total organic carbon

V_L volume of the liquid in the reactor [m^3]

W total mass of dry catalyst in the reactor [kg]

WAO   wet air oxidation

X_i conversion of compound i [%]

Greek letters

ε_P particle porosity [-]

φ_C Carman factor for geometry correction (= 1 for spherical shape)

ρ_{H_2O} density of water [kg/m^3]

ρ_L density of liquid [kg/m^3]

ρ_P density of the dry particle [kg/m^3]

ρ_S volumetric mass of the support [kg/m^3]

Γ_L degree of saturation in liquid phase [-]

μ_L dynamic viscosity of the liquid [Pa.s]

ν stoichiometric number of oxygen for complete phenol oxidation (= 7) [-]

χ_{O_2} mole fraction of oxygen [-]

Superscripts

cons   consumed

max   maximum

G   gas

L   liquid

Subscripts

b   bulk

C   carbon atoms

i/j   organic compound in liquid/gas streams

in   inlet to reactor

out   outlet from reactor

p   particle

Ph   phenol

Pt   platinum

R   reactor

T   total

s   solid

sat   saturated

X   related to compound X

References

Alnaizy, R. and Akgerman, A., Adv. Environ. Res. 4 (2000) 233.

Battino, R., Ed., "IUPAC Solubility Data Series, Oxygen and Ozone", Pergamon Press, Oxford, 1981, p.459.

Beenackers, A.A.C.M. and van Swaaij, W.P.M., Chem. Eng. Sci. 48 (1993) 3139.

Besson, M. and Gallezot, P., Catal. Today 57 (2000) 127.

Charlot, G., "Les méthodes de la chimie analytique", Mason, Paris, 1961, p.859

Chollier, M.J., Epron, F., Lamy-Pitara, E. and Barbier, J., Catal. Today 48 (1999) 291.

Debellefontaine, H., Chakchouk, M., Foussard, J.N., Tissot, D. and Striolo, P., Environ. Pollution 92 (1996) 155.

Fogler, H.S., "Elements of Chemical Reaction Engineering", 3rd Ed., Prentice Hall, Upper Saddle River NJ, 1999, p.577.

Gomes, H.T., Figueiredo, J.L. and Faria, J.L., Appl. Catal. B 27 (2000) L217.

Harmsen, J.M.A., Jelemensky, L., van Andel-Schefer, P.J.M., Kuster, B.F.M.and Marin, G.B., Appl. Catal. A 165 (1997) 499.

Kluytmans, J.H.J., Markusse, A.P., Kuster, B.F.M., Marin, G.B. and Schouten, J.C., Catal. Today 57 (2000) 143.

Lee, S.H. and Carberry, J.B., Water Environ. Res. 64 (1992) 682.

Levec, J. and Pintar, A., Catal. Today 24 (1995) 51.

Luck, F., Catal. Today 53 (1999) 81.

Mallat, T. and Baiker, A., Catal. Today 19 (1994) 247.

Markusse, A.P., Kuster, B.F.M. and Schouten, J.C., J. Mol. Catal. A: Chem. 158 (2000) 215.

Markusse, A.P., Kuster, B.F.M. and Schouten, J.C., Stud. Surf. Sci. Catal. 126 (1999) 273.

Masende, Z.P.G., Kuster, B.F.M., Ptasinski, K.J., Janssen, F.J.J.G., Katima, J.H.Y. and Schouten, J.C., submitted to Chem. Eng. Sci. (2004).

Matatov-Meytal, Yu.I. and Sheintuch, M., Ind. Eng. Chem. Res. 37 (1998) 309.

Maugans, C.B. and Akgerman, A., Water Res. 31 (1997) 3116.

Mishra, V.S., Mahajani, V.V. and Joshi, J.B., Ind. Eng. Chem. Res. 34 (1995) 2

Perego, C. and Peratello, S., Catal. Today 52 (1999) 133.

Perry, R.H., Green, D.W. and Maloney, J.O., Eds., " Perry's Chemical Engineers' Handbook", 7th ed., McGraw-Hill, New York , 1997, p.48

Sano, Y., Yamaguchi, N. and Adachi, T., J. Chem. Eng. Japan, 7 (1974) 255.

Santos, A., Yustos, P., Durban, B. and Garcia-Ochoa, F., Catal. Today 66 (2001) 511.

Savage, P.E., Chem. Rev. 99 (1999) 603.

Ukropec, R., Kuster, B.F.M., Schouten, J.C. and van Santen, R.A., Appl. Catal. B 23 (1999) 45.

Vleeming, J.H., Kuster, B.F.M. and Marin, G.B., Ind. Eng. Chem. Res. 36 (1997) 3541.

Wang, Y.T., Water Environ. Res. 64 (1992) 268.

Zlokarnik, M., "Stirring", John Wiley-VCH, 2001, p.180.

3

SUPPORT AND DISPERSION EFFECTS ON ACTIVITY OF PLATINUM CATALYSTS DURING WET OXIDATION OF ORGANIC WASTES

Abstract

Catalytic activity of platinum catalysts such as Pt/graphite, Pt/TiO$_2$, Pt/Al$_2$O$_3$, and Pt/active carbon was studied using a slurry phase CSTR. Three model reactions, namely, phenol, maleic acid, and malonic acid oxidation were investigated in the temperature range from 120 to 170°C and at a total reactor pressure of 1.7 MPa. Platinum on graphite was found to be most suitable for aqueous phase oxidation of phenol, maleic acid, and malonic acid. Complete conversion for both phenol oxidation as well as maleic acid oxidation to CO$_2$ was observed with Pt/graphite at stoichiometric oxygen excess close to 0% and at 150°C. The catalytic activity of platinum catalysts is significantly influenced by the surface coverage of oxygen on the platinum surface. Deactivation due to over-oxidation is gradual for Pt/graphite with a metal dispersion of 5.3% as compared to Pt/TiO$_2$, Pt/Al$_2$O$_3$ and Pt/AC, which have metal dispersions of 15.3%, 19.5% and 19.0%, respectively. It was further found that in the presence of Pt/graphite catalyst and oxygen, malonic acid reaction proceeds via non-catalysed decarboxylation, and catalytic decarboxylation to CO$_2$ and acetic acid, and catalytic oxidation to CO$_2$ and H$_2$O. Acetic acid was found to be difficult to oxidise at temperatures below 200°C.

Keywords: Platinum catalysts; Catalytic supports; Wastewater treatment; Stoichiometric oxygen excess; Platinum metal dispersion

3.1.   Introduction

Cleaning of hazardous and toxic organic wastes in water before the final disposal has acquired great importance all over the world in order to protect the human health, aquatic life, and the whole environment. The treatment of industrial wastewater, which contains organic wastes, by biological processes, is often unsuitable due to their inherent toxicity to micro-organisms. The use of traditional non-catalytic chemical processes or incineration may be too costly and energy intensive. Conventional wet air oxidation (WAO) processes usually require higher pressures (0.5 – 20 MPa) and temperatures (423 –598 K), which result in a high capital investment and a high energy consumption for operation. The application of homogeneous and heterogeneous catalysts can improve the oxidation efficiency of organic wastes in water and reaction temperatures can be reduced (Matatov-Meytal and Sheintuch, 1998; Mishra *et al.*, 1995). Homogenous catalysts are reported to be more effective in increasing the rate of oxidation, but heterogeneous catalysts are preferred because the catalyst is present as a separate phase and therefore more likely easy to separate.

Catalytic wet oxidation (CWO) using solid catalysts, involves the following steps: diffusion of the reactants to the catalytic or support surface, adsorption of the reactants onto the surface, reaction on the surface, desorption of products off the surface, and diffusion of products from the surface. Because of these steps, heterogeneous processes are usually more complicated to control. Since the catalyst surface plays an important role in adsorption and desorption, appropriate selection of both the active part and the support of the catalyst therefore can have a remarkable effect on the reaction rate.

The advantages and disadvantages of supported and unsupported non-noble (transition) metal oxides and noble metals for catalytic wet oxidation of organic pollutants have been well reviewed (Luck, 1999; Matatov-Meytal and Sheintuch, 1998; Levec and Pintar, 1995). Supported noble metal catalysts, like platinum catalysts, are generally less vulnerable to deactivation by leaching of the active metal and show higher overall activities for the oxidation of pollutants (Luck, 1999). However, platinum catalysts may suffer rapid loss of catalyst activity, which is due to either poisoning by surface impurities, or deactivation due to too high oxygen coverage (over-oxidation). It was previously found that the deactivation of a Pt/graphite catalyst could be avoided by operating the reactor within a practical operation window, whereby moderate oxygen coverage of the platinum surface could be maintained (Masende *et al.*, 2003a). The role and influence of the catalyst support

on the reaction mechanism and on the stability of the platinum catalyst were not investigated.

According to Matatov-Meytal and Sheintuch (1998) the support serves three important functions in the catalytic system, namely: to increase the surface area of the catalytic material; to decrease sintering and to improve hydrophobicity and thermal stability and chemical stability of the catalytic material; and to govern the lifetime of the catalyst. Supports may also improve the catalytic activity by acting as a co-catalyst. Reducing the crystallite size of the active metal, or increasing the dispersion, increases the active surface area. However, very small active metal particles are vulnerable to oxygen poisoning due to the high enthalpies of oxygen adsorption on small metal particles particularly under 2 nm (Beziat *et al*., 1999). Another possibility to increase activity is to increase the particle porosity. Supporting the noble metal catalyst on a metal oxide surface has been suggested to improve the activity and stability of the catalyst (Oliviero *et al.*, 2000). However, a hot and acidic medium promotes solubility of some transition metal oxides and therefore causes deactivation of the catalyst by leaching of the metal or metal oxides (Matatov-Meytal and Sheintuch, 1998). Beziat *et al.* (1999) reported a high stability of titania supported ruthenium catalyst, when used in acidic and oxidizing medium for oxidation of aqueous solutions of carboxylic acids. While noble metal catalysts supported on activated carbon are more resistant to acidic leaching than transition metal oxides (Beziat *et al*., 1999; Gallezot *et al.*, 1997), activated carbon is likely to burn off at higher temperatures (Fortuny *et al.*, 1998).

The support may influence the surface properties of the platinum particles due to platinum-support interaction. According to Gallezot *et al.* (1990), the different interaction with the graphite support of platinum particles located at the edges of basal planes and particles on top of basal planes is due to electron transfer from the graphite to the platinum particles at the edges of basal planes, resulting in a different morphology and electronic structure. The rate of liquid phase oxidation may also be influenced by the hydrophilic character of the catalyst, which is related to the number and nature of the support surface groups. This may influence the affinity of the support for the aqueous phase or the physisorption of the organic compound on the support and thereby the internal transport of the organic compound or adsorption of the organic compound on the active platinum surface (Vleeming, 1997). For catalytic wet oxidation, it is therefore worthwhile to understand not only the reaction conditions, but also the morphology, texture, and size of the catalyst support, and the location of the active metal.

The reactor configuration and the mode of operation may cause significant impact on performance of the platinum catalysts. Most of the kinetic studies in catalytic wet oxidation (CWO) have been carried out in batch reactors (Matatov-Meytal and Sheintuch, 1998; Mishra *et al.*, 1995). The advantages of batch reactors include simplicity in operation, flexibility in production and process operations, and simplicity in determination of kinetic rates (Perego and Peratello, 1999; Donati and Paludetto, 1999; Fogler, 1999). Whereas batch reactors are helpful in measuring of intrinsic kinetics in the absence of catalyst deactivation, unfortunately, most of heterogeneous catalytic reactions using noble metal catalysts, are affected by, among others, deactivation due to over-oxidation. Due to these reasons a continuous stirred tank reactor (CSTR) is preferred for quantifying simultaneously reaction and deactivation kinetics (Perego and Peratello, 1999).

In the present work, attention is focused on the understanding of the reaction mechanisms of platinum catalysts during oxidation of organic wastes in water. Different supports for platinum metal catalysts are evaluated. These include carbon-based, namely: Pt/graphite (G) and Pt/active carbon (AC), and Pt/Al_2O_3 and Pt/TiO_2, being metal oxide supports. The effect of the reaction conditions on the properties of the catalysts was investigated. Phenol was used as a model reaction since it is one of the most serious pollutants and is considered as worst case in WAO studies. Maleic acid was investigated because it is one of the intermediate products reported in the phenol reaction network. Malonic acid was also investigated since it is an intermediate to acetic acid Masende *et al.*, 2003b). The investigation was carried out in a slurry phase CSTR.

3.2.   Experimental

The experimental work was carried out at the Laboratory of Chemical Reactor Engineering at Eindhoven University of Technology (Netherlands) and at the Department of Chemical & Process Engineering at the University of Dar es Salaam (UDSM) in Tanzania. In both laboratories, the same type of reactor set-up was used. Whereas oxidation of phenol was performed at Eindhoven University of Technology, the experiments for maleic acid and malonic acid oxidation were carried out at University of Dar es Salaam. Whenever there are differences, e.g. materials and equipment used at the University of Dar es Salaam, it is stated in this chapter.

3.2.1. Chemicals and catalyst

All chemicals used in this research including phenol, maleic acid, and malonic acid were pure analytical grade from Merck and were used as received. Oxidation solutions were prepared using deionised water. Gases were of 99.99% purity (5.0 grade) from Hoekloos (Netherlands). In Tanzania, all gases (99 +%) were obtained from Tanzania Oxygen Limited (TOL). The liquid phase oxidation of organic solutions was investigated using commercially available catalysts namely, Pt/graphite (5 wt%) from Johnson Matthey, and Pt/active carbon (5 wt%), Pt/Al$_2$O$_3$ (5 wt%) and Pt/TiO$_2$ (5 wt%) from Engelhard. The metal content for both fresh and used catalysts, average catalyst particle diameter and the particle size distribution, and the morphological properties were determined as described in the next sections.

Table 3.1
Characteristics of the supported platinum catalysts

Feature	Pt/Graphite	Pt/TiO$_2$	Pt/Al$_2$O$_3$	Pt/AC
Code	5R2287	42380	7080	7002
Active metal content	5% on dry basis	5% on dry basis	5% on dry basis	5% on dry basis
Type	Reduced/Dry	Reduced/Dry	Reduced/Dry	Reduced/Dry
Carrier	Graphite powder	TiO$_2$	Al$_2$O$_3$	Carbon
Catalyst particle size distribution[a]	< 5 μm (15%)	< 15 μm (10%)	< 46 μm (10%)	< 3.16 μm (10%)
	< 10 μm (75%)	< 40 μm (50%)	< 74 μm (50%)	< 4.71 μm (50%)
	< 15 μm (95%)	< 65 μm (90%)	< 130 μm (90%)	< 6.72 μm (75%)
	> 15 μm (5%)			< 10.2 μm (90%)
Total Surface Area (B.E.T.) [m$^2 \cdot$g^{-1}]	15.0	70	110	100
Metal dispersion[b] [%]	5.3	15.3	19.5	19.0
Metallic Surface Area[b] [m$^2 \cdot$g^{-1} sample]	0.66	1.89	2.40	2.37
Metallic Surface Area[b] [m$^2 \cdot$g^{-1} metal]	13.1	37.9	48.1	47.0
Porosity[c] [%]	69.3	73.8	76.9	81.7

[a]The particle size distribution was confirmed using the Coulter LS 130 apparatus.
[b]Catalyst characterisation using ASAP 2000 series equipment
[c]Porosity measurement using AutoPore IV 9500 equipment

3.2.2. Catalyst characterisation techniques

The morphology of the catalyst particle was examined using a Scanning Electron Microscope (SEM) apparatus. The samples were prepared by forming a thin layer (70 nm) of gold on a sticky carbon support with the catalyst samples on top. The gold was added to avoid charging of the catalyst samples. The topographical analyses of different catalysts were made up to a magnification of 25,000 times. The centre of the images was preserved during magnification. The signal of the secondary electrons was

used for a topographical observation of the catalyst surface. The information on the particle shape and on the size of the catalyst support was obtained from the SEM micrographs. The average catalyst particle diameter and the particle size distribution were also measured with a Coulter LS 130 apparatus. Table 3.1 shows the results of the particle size distribution of different catalysts.

The specific surface area and metal dispersion of the platinum catalysts of different supports were analysed using the ASAP 2000 apparatus (Micromeritics Instrument Corporation). The samples for the analysis were fresh and used catalysts, which were used without any pre-treatment. The specific surface area of the catalysts was measured with a standard method of B.E.T (Brunauer, Emmet and Teller), which is based on the adsorption isotherm of nitrogen (Scholten, 1993). The porosity of catalyst support was measured by using the AutoPore IV 9500 apparatus (Micromeritics Instrument Corporation), which uses mercury as a pressure fluid. The results of B.E.T and mercury porosity measurements are shown in Table 3.1.

The platinum content of the catalysts was determined in duplicate by dissolving the platinum after boiling the catalysts in aqua regia (HCl/HNO_3, 3:1). This was followed by the removal of the nitric acid by adding hydrochloric acid and evaporating. For each sample this step was done three times. On addition of a hydrochloric acid containing tin chloride solution a stable yellow platinum tin (Sn-Pt) complex was formed by platinum ions and $SnCl_2$ in the presence of excess chlorine ions. The resulting extinction was measured by UV/VIS spectrophotometry at 403 nm (Charlot, 1961). Similarly, liquid samples were taken directly from the reactor to measure the loss of platinum metal by leaching during oxidation. In all samples hydrochloric acid was added to avoid precipitation or reduction of the platinum ions prior to measurement. The platinum metal concentration in the liquid effluent was found to be less than 1 mg/m_L^3 in all experiments whereas the maximum loss of platinum metal on the used catalyst samples was found to be less than 0.5 wt.%.

3.2.3. Oxidation experiments

The experiments were conducted in a continuous flow stirred slurry reactor (CSTR), a 500 ml autoclave (Autoclave Engineers, Zipperclave Hastelloy) that is equipped with a gas dispersion impeller. The reactor operating conditions are given in Table 3.2. During reaction, the reactor was kept at constant temperature within ± 0.3 K, in a wide range of temperatures, by a heating element around the reactor. The pressure in the reactor was kept constant by using a backpressure regulator. During the experiments

the flow rates of the phenol feed solution and the gas entering the reactor were kept constant. Details of the experimental set-up and reactor start-up procedures are reported elsewhere (Masende *et al.*, 2003a).

Table 3.2
Standard reactor operating conditions

Parameter	Standard	Range
Temperature (°C)	150	120-170
Total pressure (MPa)	1.7	1.5-1.8
Oxygen partial pressure (MPa)	0.3	0-0.5
Oxygen flow rate (at room conditions) (ml/min)	32	8-48
Nitrogen flow rate (at room conditions) (ml/min)	150	150
Initial phenol concentration (mol/m^3)	20	20
Initial maleic acid concentration (mol/m^3)	20	20
Initial malonic acid concentration (mol/m^3)	20	20
Liquid flow rate (ml/min)	10	10
Liquid volume in the reactor (ml)	350	350
Catalyst (g)	3.5	0.5-7.0
Stirrer speed (rpm)	1200	350-1400
pH	Uncontrolled	2-7

In each experiment, the progress of the reaction and the catalytic activity were monitored by measurement of the reactor effluent composition as a function of time. The liquid samples were analysed by using two HPLC set-ups (Thermo Separation Products) for residual phenol and intermediate reaction products. Phenol and other aromatic compounds were analysed in a 300 x 4.6 ID mm Lichroma SS column, packed with a Benson type of cation-exchange resin (Ca^{++}) using a UV detector, while carboxylic acids were analysed in a 300 x 8 ID mm RSpak KC-811 column using a refractometer detector (Waters R401). The same HPLC columns were used at UDSM in Tanzania with HPLC set from Merck-Hitachi. The composition of the outlet gases was analysed using an on-line gas chromatograph (GC) (HP 5890A Series II). The GC was equipped with a 10 m Molsieve 5A wide bore (Chrompack) column, a 25 m Porapak Q wide bore (Chrompack) column, a thermal conductivity detector (TCD) and an integrator (DataJet CH2). In addition, the oxygen concentration in the outgoing gas stream was determined by using an O$_2$ sensor (Orbisphere Laboratories, Switzerland). Nitrogen gas was used as a standard while helium was used as carrier gas. In Tanzania, the composition of the effluent gases (mainly O$_2$, CO$_2$ and N$_2$) was determined using an online gas analyser (Servomex, Xentra 4200) where nitrogen was an inert gas during reaction.

The experimental results were evaluated in terms of the disappearance rate of the respective compound, *i*, using the equation

$$R_{w,i} = \left(F_V^l / W\right)\left(C_{i,in} - C_i\right) - \left(V_L / W\right)\left(dC_i / dt\right) \tag{3.1}$$

with $C_i = 0$ at $t = 0$. The accumulation term, (dC_i/dt), is required especially when different start-up procedures are employed. The percentage conversion is calculated by

$$X_i(\%) = \left(R_{W,i} \cdot W\right) / \left(F_V^l \cdot C_{i,in}\right) \times 100\% \tag{3.2}$$

while the percentage selectivity (based on carbon atom) is calculated from equation (3.3) as

$$S_{\to j}(\%) = \left(n_{C,j} \cdot R_{w,j}\right) / \left(n_{C,i} \cdot R_{w,i}\right) \times 100\% \tag{3.3}$$

Detailed data analysis procedures and other definitions used in this paper are described elsewhere (Masende *et al.*, 2003a). For all experimental data, the overall carbon balance and the oxygen balance were verified after every experiment; they were within 95 - 100%, which was considered acceptable.

3.3.   Results and discussion

3.3.1. Catalyst characterisation

The results of the particle size distribution and the BET analysis for platinum supported catalysts are shown in Table 3.1. It can be observed that the metal dispersion of Pt/TiO_2 (15.3%) is approximately three times as large as the metal dispersion of Pt/graphite (5.3%). The metal dispersion of Pt/Al_2O_3 and Pt/AC catalysts is 19.5% and 19.0%, respectively. Similar trend is observed for the metallic surface area per gram sample and per gram metal. Measurement of porosity of the catalyst support also shows comparable results whereas Pt/AC is very porous (81.7%) as compared to other supports.

Fig. 3.1 shows micrographs of platinum catalysts at different magnification, which were obtained from the SEM analysis. The graphite particles have irregular shapes and consist of layers (Fig. 3.1a). The size of graphite particles was estimated using the Coulter LS 130 apparatus. It can be seen from Fig. 3.1(b) that TiO_2 particles have spherical shapes. It was also observed that the largest particles had a diameter of approximately 55 μm. Fig. 3.1(c) shows images of the platinum on alumina support in which the particles have similar spherical shapes. It was also observed that the largest particles had a diameter of approximately 160 μm. Similarly, Pt/AC particles have different physical shape as can be seen in Fig. 3.1(d). The micrographs clearly show that there are physical differences of the catalyst supports used in this study. The morphology of the support has an influence on the location of the active component, and therefore different exposure of the catalyst to the reactants is likely to affect the overall activity of the catalyst.
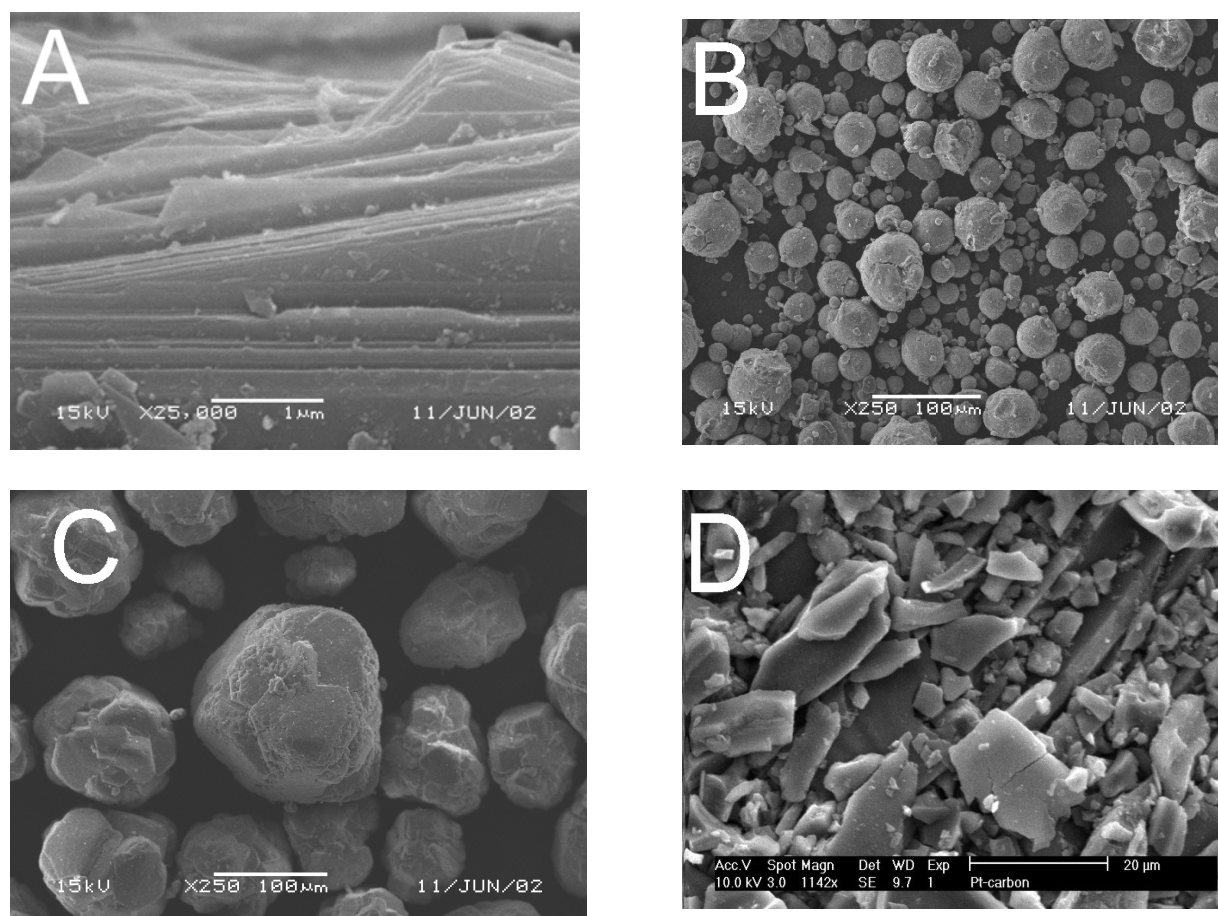
Fig. 3.1. SEM micrographs of platinum catalysts at different magnifications: (A) Pt/graphite at X25,000, (B) Pt/TiO$_2$ at X250, (C) Pt/Al$_2$O$_3$ at X250, and (D) Pt/AC at X1,142.

The location and distribution of the platinum metal depends normally on the methods and/or procedures employed during manufacturing of the catalysts. According to the manufacturers' information, Pt/graphite is an "eggshell" type whereby the platinum metals are distributed on the outer surface or edges of the pores. Other catalysts, namely: Pt/Al$_2$O$_3$, Pt/TiO$_2$, and Pt/AC are "mixed" type, i.e. platinum metals are located partly on surface/edges and deeper in pores. The effectiveness of these catalysts were examined in catalytic wet oxidation of model compounds namely, phenol, maleic acid, and malonic acid. The influences of such factors as the hydrophilic properties, and effects of the catalyst particle on mass transfer and reactor hydrodynamics were not the subject of this study.

3.3.2. *Catalytic activity during phenol oxidation*

The performances of the supported platinum catalysts were determined at temperatures of 135 and 165°C and a total reactor pressure of 1.7 MPa whereas the stoichiometric

oxygen excess (S.E.) of 20% (mol/mol) was kept constant during phenol oxidation. The overall reaction for complete oxidation of phenol to CO_2 and H_2O is given by equation (3.4)

$$C_6H_5OH + 7O_2 \rightarrow 6CO_2 + 3H_2O \qquad (3.4)$$

The reaction proceeded rather slowly at 135°C for all catalysts. Fig. 3.2a shows the oxidation results for platinum on graphite, alumina and titanium oxide in terms of conversion and selectivity to CO_2 during phenol oxidation at 135°C. Pt/graphite has a relatively high conversion of over 75% and selectivity to CO_2 of 92% at 135°C, and liquid effluent samples changed from colourless to light yellow. The yellowish colour in the liquid sample possibly is due to the formation of *p*-benzoquinone and polymer precursors. The residual partial pressure of oxygen remained almost constant for about 2 h, thereafter a gradual increase was observed. This indicates that the Pt/graphite catalyst does not loose all of its activity. About 62% conversion was attained after 1 h when Pt/TiO$_2$ was used and dropped gradually to reach 46% after 2 h, while the selectivity after 1 h was 65%. The residual oxygen partial pressure increased from 79 kPa to 123 kPa. The performance of the Pt/Al$_2$O$_3$ catalyst is low at low temperature as can be seen from Fig. 3.2(a). A low conversion of less than 10% was observed at 135°C. In addition, the effluent liquid was dark brownish in colour with suspended matter, probably polymeric products. The formation of *p*-benzoquinone indicates that few active sites are available for the catalytic reaction. The polymeric products contribute to deactivation of the catalyst by fouling.
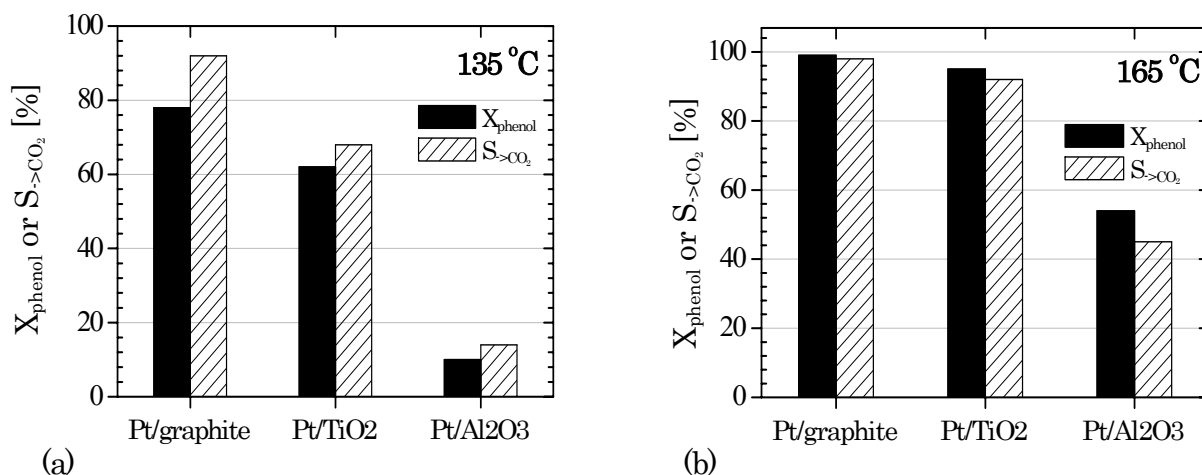

Fig. 3.2. Disappearance of phenol and selectivity to CO_2 during phenol oxidation at standard condition (Table 3.2) over different supported Pt catalysts at S.E.=20%: (a) conversion and selectivity to CO_2 at 135°C, (b) conversion and selectivity to CO_2 at 165°C.

However, at high temperature a significant change in the disappearance rate of phenol was observed. It can be seen in Fig. 3.2(b) that at 165°C high phenol conversion (>99%) and selectivity to CO_2 (98%) with Pt/graphite catalyst was obtained and the high activity of the catalyst was maintained. The effluent liquid was colourless without significant concentration of carboxylic acids or aromatic compounds (e.g. *p*-benzoquinone). Similar results were obtained with Pt/TiO$_2$ catalyst whereby phenol conversion above 95% and selectivity to CO_2 of ca. 92% was observed. Pt/Al$_2$O$_3$ catalyst gave poor performance with a conversion of 54% and selectivity to CO_2 less than 45%. The liquid effluent was characterised with the presence of a brownish colour with high concentration of *p*-benzoquinone. The formation of *p*-benzoquinone indicates over-oxidation of the active sites of the catalyst (Masende *et al.*, 2003a). In addition, deactivation of Pt/Al$_2$O$_3$ could also be explained by the formation of the less active form PtO$_2$ (Bauer *et al.,* 1993; Ostermaier *et al.,* 1976) suggested that deactivation of Pt/Al$_2$O$_3$ occurs by the formation of platinum oxides.
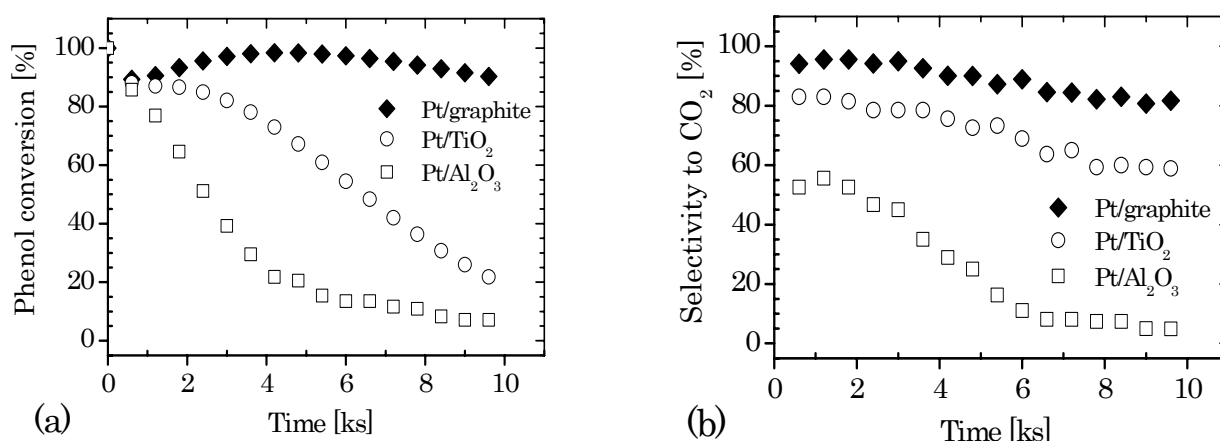

Fig. 3.3. Phenol oxidation at standard conditions (Table 3.2) over different supported Pt catalysts at 150°C, and S.E.=100%: (a) conversion and (b) selectivity to CO_2.

The influence of a high oxygen load on the platinum catalyst performance was determined at 150°C and a stoichiometric oxygen excess (S.E.) of 100%. Similar trends on the activity of the catalysts were observed as seen in Figs. 3.3. Pt/graphite catalyst shows relatively high activity and deactivation is rather slow or gradual. Once again low conversions and selectivity to CO_2 were observed for Pt/TiO$_2$ and Pt/Al$_2$O$_3$. After 8 ks the respective conversions were 93%, 31%, and 8% (Fig. 3.3a) for Pt/graphite, Pt/TiO$_2$, and Pt/Al$_2$O$_3$, whereas the selectivities (carbon basis) were 82%, 59%, and 7.5% (Fig. 3.3b), respectively. The corresponding residual oxygen partial pressures after 8 ks were 307, 524, and 572 kPa for Pt/graphite, Pt/TiO$_2$, and Pt/Al$_2$O$_3$, respectively. The effects of high residual oxygen partial pressures on the mechanisms

of platinum on graphite catalysts and phenol oxidation pathways are reported elsewhere (Masende *et al.*, 2003b).

It can be concluded from Fig. 3.2 that an increase in temperature influences the activity of the platinum catalyst. At higher temperatures, the catalyst is able to handle higher oxygen and organic loads. While on the one hand poor performances are caused by the high residual oxygen partial pressures, on the other hand the differences observed among the catalyst supports can be attributed to their differences in morphological and/or chemical properties. According to the manufacturer information, Pt/graphite is an "eggshell" catalyst with Pt metal located on the surface, while Pt/TiO_2, and Pt/Al_2O_3 are both "mixed" type with Pt metal partly on the edges and deeper in the pores. Since the experiments were performed at double the stoichiometric oxygen amount (S.E. of 100%) and sufficient degree of mixing (1200 rpm), several explanations are possible. The formation of polymer precursors is likely to cause deactivation for the inner active sites by fouling or blocking of pores for the "mixed" catalysts.

From the results, it seems that the activity of the catalyst is related to the metal dispersion and porosity. Pt/graphite with a metal dispersion of 5.3% deactivates due to over-oxidation slowly compared to Pt/TiO_2, Pt/Al_2O_3 and Pt/AC with metal dispersions of 15.3%, 19.5%, and 19.0% respectively (Table 3.1). Another possible explanation is that the support effect can be caused by platinum-support interaction, which may be larger for Pt/graphite due to electron transfer from the graphite to platinum particles. Gallezot *et al.* (1990) reported that this electron transfer results in a different morphology and electronic structure of particles located on the edges of graphite layers than for particles located elsewhere. The differences in hydrophilic character of the catalyst cannot be overruled, since it has the potential to affect the affinity of the catalyst for the aqueous phase as well as the interaction between the support and the organic compound (Vleeming, 1997). It is well known that Pt/graphite has low affinity for the aqueous phase.

3.3.3. Catalytic activity during maleic acid oxidation

The oxidation reaction of maleic acid to the desired end products CO_2 and H_2O is expressed by

$$COOH(CH)_2COOH + 3O_2 \rightarrow 4CO_2 + 2H_2O \tag{3.5}$$
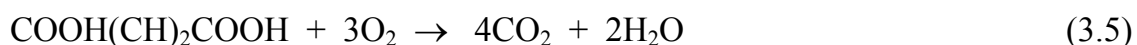
Comparative studies of catalyst supports were carried out at 150°C and stoichiometric oxygen excess (S.E.) of 100% with catalysts concentration of 6.0 kg_{cat}/m_L^3, while other reaction parameters were kept at standard conditions (Table 3.2). Results show that Pt/graphite has the best performance in terms of maleic acid conversion and selectivity to CO_2 compared to Pt/Al_2O_3 and Pt/AC (see Fig. 3.4a&b). The trends shown for residual oxygen partial pressure (Fig. 3.4c) and residual maleic acid concentration (Fig. 3.4d) indicate the presence of deactivation.

The observed deactivation of the catalyst is possibly due to the differences in properties of the supports. This is because all catalysts have the same loading of Pt metal of 5 wt%. A drop of conversion for Pt/graphite is clearly seen from 95% at after 1½ h to 81% after 3 h. The high pH of the liquid effluent (4.8), when Pt/graphite catalyst is used, indicates high conversion of maleic acid to CO_2 and H_2O. During the first 600s, low concentrations of oxalic acid were detected which disappeared afterwards. The formation of oxalic acid at the start of the reaction was also observed when Pt/Al_2O_3 and Pt/AC were used.
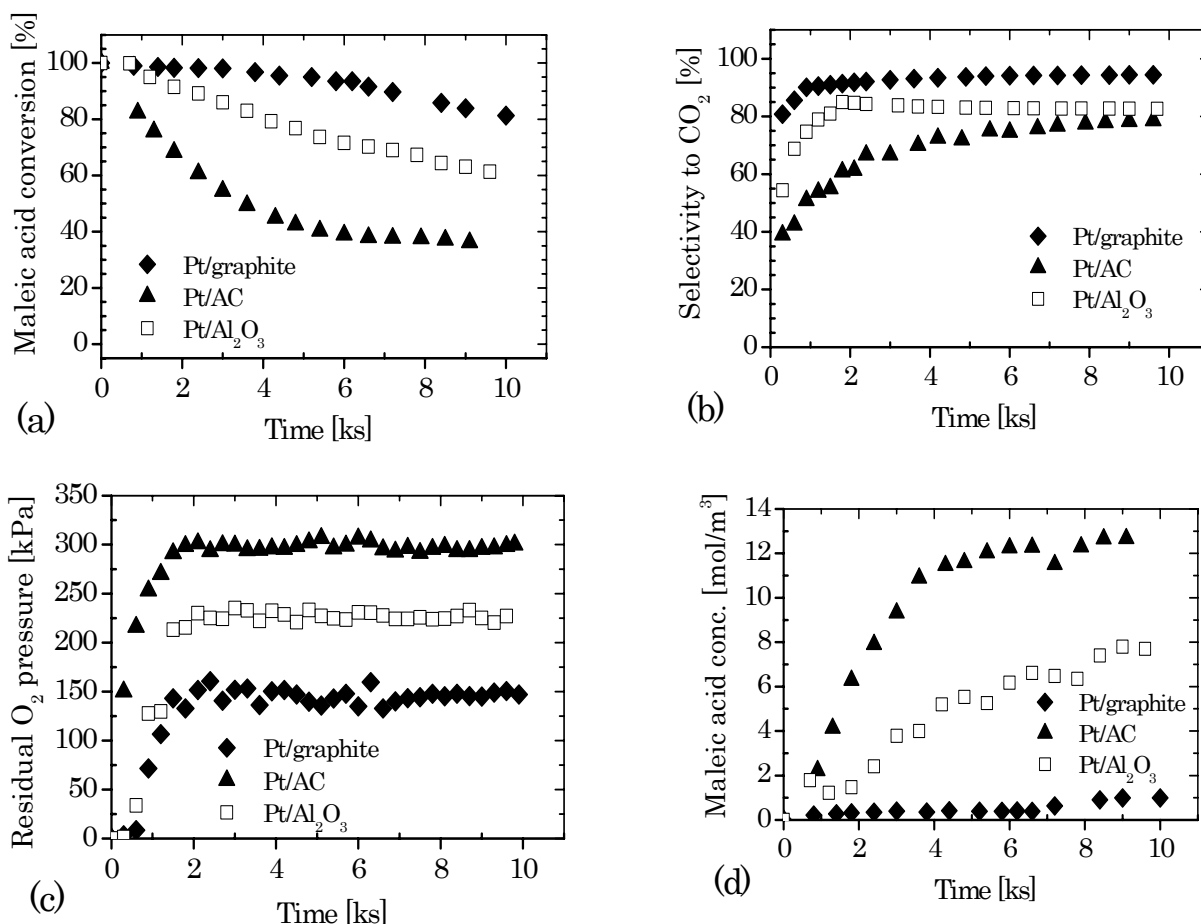

Fig. 3.4. Maleic acid oxidation at standard conditions (Table 3.2) over different supported Pt catalysts at 150°C, S.E.=100%, and 6 kg_{cat}/m_L^3 catalyst: (a) conversion, (b) Selectivity to CO_2, (c) residual O_2 pressure and (d) concentration of maleic acid.

In all three catalysts, neither acetic acid nor succinic acid were observed in the liquid effluent. The formation of oxalic acid at the beginning of the reaction is attributed to the reactor start-up method (Masende *et al.*, 2003a) whereby oxygen concentration in the liquid phase is initially low for the oxidation of maleic acid and oxalic acid. Furthermore, it can be inferred that oxidation of oxalic acid requires a partly oxidised platinum surface whereby the reaction to CO_2 proceeds via oxygen insertion (Markusse *et al.*, 1999). The absence of acetic acid and succinic acid in the liquid effluent implies that these acids cannot be formed at high oxidation potential of the platinum catalyst; possibly they can be formed under oxygen-poor conditions.

The observed high conversion of maleic acid using Pt/graphite at these conditions is probably due to a high stability of the graphite as compared to Al_2O_3 or active carbon. The differences in activity observed between Pt/graphite and Pt/Al_2O_3 again can be attributed to differences in metal dispersion as previously explained. The differences in activity between Pt/graphite and Pt/AC are possibly due to the hydrophilic character of the support. Graphite is a more hydrophobic catalyst than activated carbon (Vleeming, 1997).

Pt/graphite was used to investigate the effects of temperature and oxygen partial pressure on the catalytic activity during maleic acid oxidation. The effect of temperature on the reaction rate was studied at a stoichiometric oxygen excess of 200% in the temperature range of 120-170ºC with a catalyst concentration of 10 kg_{cat}/m_L^3 of Pt/graphite. It can be seen from Fig. 3.5(a) that the activity of the catalysts, which is expressed in terms of conversion, increases with temperature. Complete conversion of maleic acid to CO_2 and H_2O is achieved at 170ºC while at 120ºC low conversion and poor selectivity to CO_2 were obtained (see Fig. 3.5b). Fig. 3.5(c) shows the residual oxygen partial pressure in the reactor while Fig. 3.5(d) shows a similar trend on the residual maleic acid concentration.

These observations indicate that a high temperature (>140ºC) enhances the reaction and the activity of the platinum catalyst. At high temperatures the catalyst can handle higher oxygen and maleic acid loads. It was previously observed that when high oxygen loads are employed deactivation by over-oxidation takes place, however, at high temperature the activity of the catalyst was enhanced (Masende *et al.*, 2003a). In order to discriminate the effects of temperature from that of oxygen loads, further experiments were performed at different oxygen concentration, expressed as stoichiometric oxygen excess (S.E.).
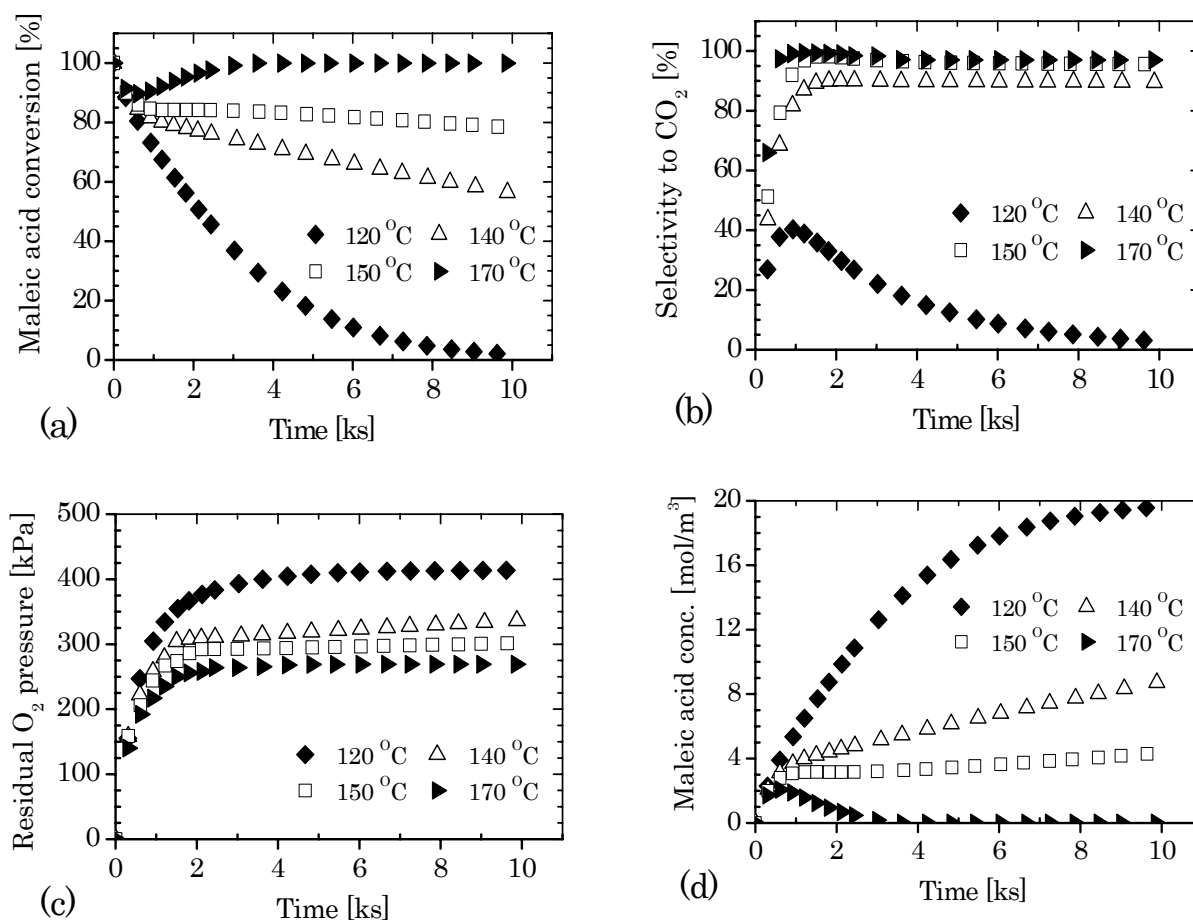
Fig. 3.5. Effect of temperature during maleic acid oxidation using Pt/graphite at standard conditions (Table 3.2) and S.E.=200%: (a) conversion, (b) Selectivity to CO_2, (c) residual O_2 pressure and (d) concentration of maleic acid.

The influence of the oxygen molar flow rate (expressed as S.E.), during maleic acid oxidation was investigated at 150°C at a catalyst concentration of 10 kg_{cat}/m_L^3 of Pt/graphite. Other parameters were maintained at standard condition (Table 3.2). It was found that the conversion of maleic acid increased with an increase in the oxygen molar flow with maximum conversion to CO_2 at S.E. of 20% (Fig. 3.6a). At high S.E. (100% and 200%) low carbon selectivity to CO_2 was obtained as seen in Fig. 3.6(b). The trend observed in Fig. 3.6(c) shows that the activity of the catalyst is decreased at very high residual oxygen partial pressure. In Fig. 3.6(d) the residual maleic acid concentration decreased with an increase in the oxygen flow for S.E. of –50%, 0%, 20%, and 100%, while a relatively high concentration was observed with S.E. of 200%.

The low activity of catalyst observed at high stoichiometric oxygen excess (e.g., S.E. of 200%) is possibly due to overoxidation of the catalyst active sites. It would have

been expected that the highest CO_2 formation be at S.E. of 200% but it is lower than when S.E. of 0% and 100% are used; obviously this is due to the loss of activity of the platinum catalyst due to very high residual oxygen pressure. These results again support our previous observation during phenol oxidation that residual oxygen partial pressure, and hence too high oxygen load, is responsible for catalyst deactivation (Masende *et al.*, 2003a,b). Detailed experimental work to elucidate the reaction pathways for phenol and maleic acid oxidation has already been reported (Masende *et al.*, 2003b).
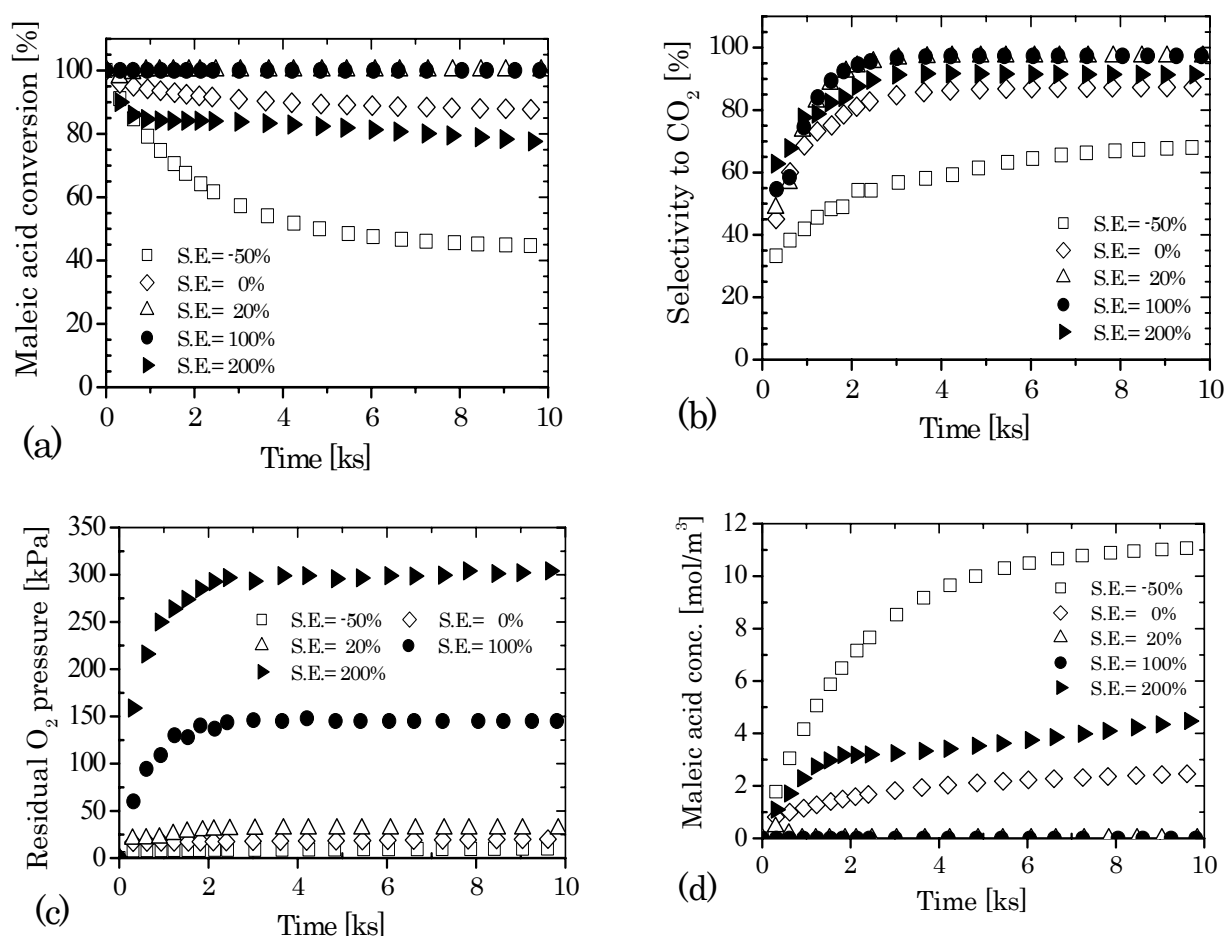

Fig. 3.6. Effect of stoichiometric oxygen excess (S.E.) during maleic acid oxidation using Pt/graphite standard conditions and at 150ºC: (a) conversion, (b) Selectivity to CO_2, (c) residual O_2 pressure and (d) concentration of maleic acid.

3.3.4. Catalytic activity during malonic acid oxidation

Fig. 3.7 shows the performance of various catalysts during malonic acid oxidation at 150°C and S.E. of 100%, while other parameters were kept at standard conditions (Table 3.2). Malonic acid conversion was 85% for Pt/graphite whereas 74-78% were obtained for both Pt/Al$_2$O$_3$ and Pt/AC as shown in Fig. 3.7(a). It was further found that

all catalysts gave comparable selectivity (carbon basis) to CO_2 within the range from 63 to 66% (Fig. 3.7b) while acetic acid was the only end products identified in liquid effluent. No other intermediates or end products were detected. Similar results were observed for residual oxygen partial pressures (Fig. 3.7c) and residual malonic acid concentration (Fig. 3.7d).
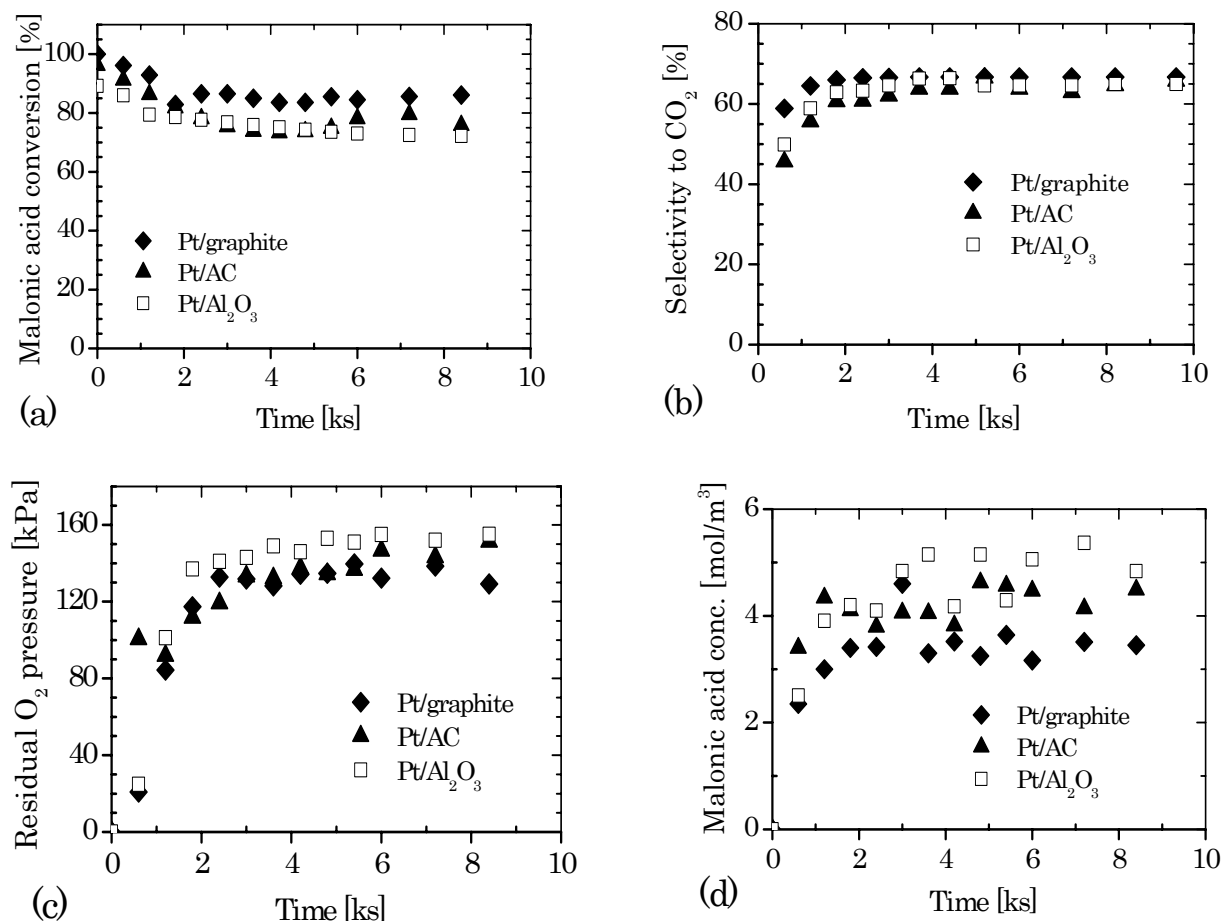

Fig. 3.7. Malonic acid reaction at standard conditions (Table 3.2) over supported Pt catalysts at 150°C, and S.E.=100%: (a) conversion, (b) selectivity to CO_2, (c) residual O_2 pressure and (d) malonic acid concentration.

It can be inferred from these results that all catalysts have comparable performance under the test conditions. Since the residual oxygen partial pressure is high in all cases (about 150 kPa) and also the selectivity to CO_2 seems to be comparable (selectivity about 66%), it can be concluded that the oxidation of malonic acid is not the only route to CO_2. It indicates that the malonic acid reaction proceeds either through catalytic decarboxylation and oxidation or via non-catalytic decarboxylation. Homogeneous decarboxylation of malonic acid in the aqueous phase can be explained as
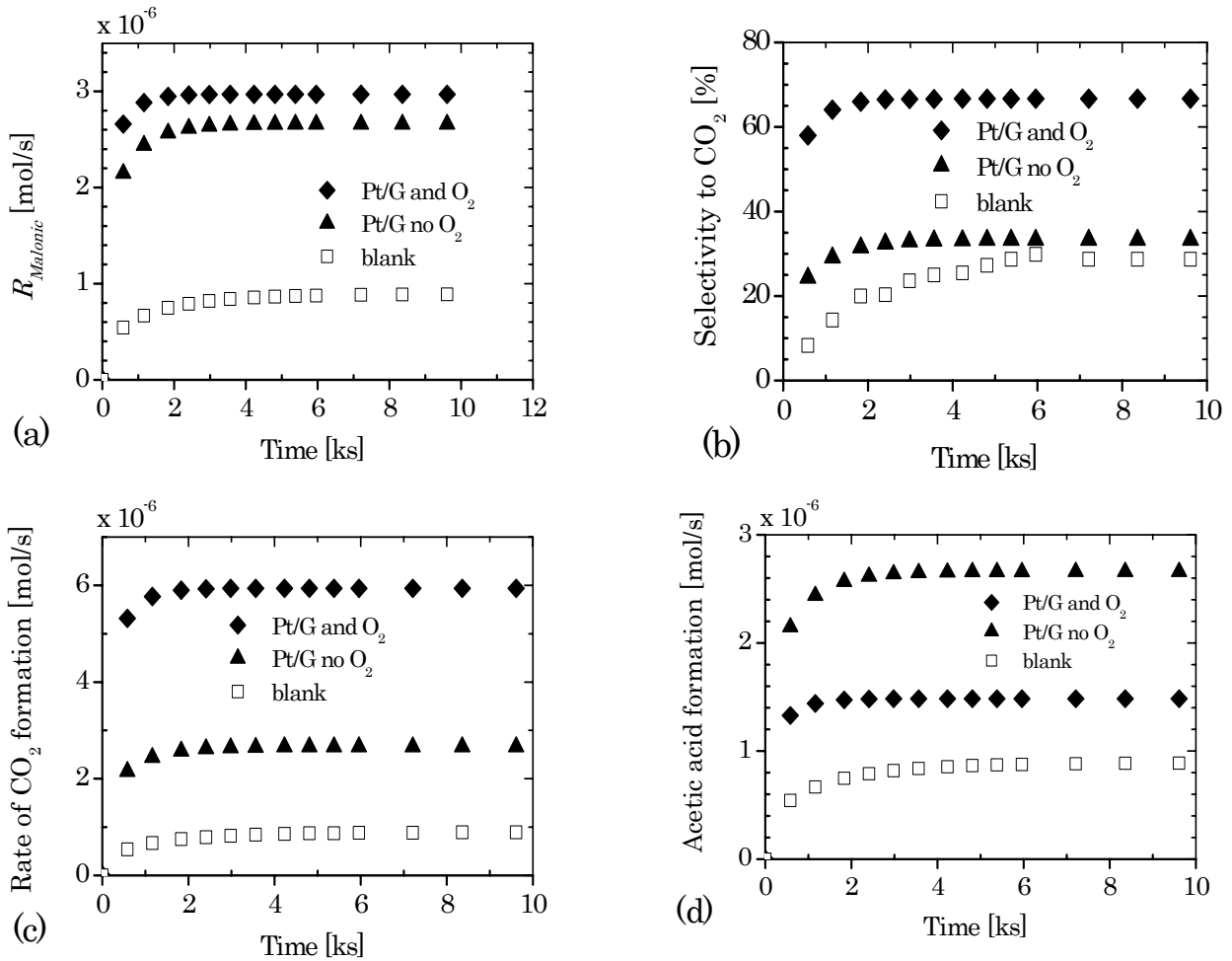
$$CH_2(COOH)_2 \rightarrow CO_2 + CH_3COOH \tag{3.6}$$
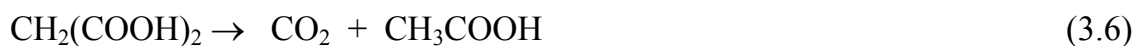
Fig. 3.8. Catalysed and non-catalysed reaction of malonic acid at 150°C, 1200 rpm, S.E.=100%, $C_{malonic}$=20 mol/m^3 and 10 kg$_{cat}$/m$_L^3$ Pt/graphite: (a) reaction rate for malonic acid, (b) selectivity to CO_2, (c) acetic acid formation and (d) CO_2 formation.

In order to investigate whether malonic acid reaction proceeds via a catalytic or a non-catalytic route, a set of experiments was carried out at 150°C with feed concentration of 20 mol/m^3. Fig. 3.8 shows the results for malonic acid when the reaction is carried out under oxygen free environment (nitrogen only) without a catalyst present, with catalyst, and when both catalyst and oxygen are employed. High conversion rates for malonic acid were obtained when a catalyst was used as can be seen in Fig. 3.8(a). During a blank experiment without oxygen (nitrogen only), about 0.88 x 10^{-6} mol/s of malonic acid degraded into CO_2 and acetic acid with molar selectivity of 100% each according to equation (3.6). However, the carbon selectivity to CO_2 was 33% after 2h (Fig. 3.8b) whereas acetic acid was 67%. Furthermore, comparable disappearance rates for malonic acid were observed during catalytic degradation without oxygen (2.66 x 10^{-6} mol/s) as well as with oxygen (2.97 x 10^{-6} mol/s). However, the carbon selectivity to CO_2 was different for catalytic degradation without oxygen (33%) as compared to catalytic oxidation (67%) of malonic acid. Similarly, a low rate of CO_2 formation was

obtained during catalytic degradation without oxygen, which reached 2.7×10^{-6} mol/s after 2h, whereas with oxygen a high rate is obtained (5.9×10^{-6} mol/s) as shown in Fig. 3.8(c). Significant differences were also observed on the rate of formation of acetic acid as shown in Fig. 3.8(d). While high rate for acetic acid formation was observed during catalytic reaction without oxygen (2.66×10^{-6} mol/s), about 1.49×10^{-6} mol/s acetic acid was attained when oxygen was added.

The results show that both homogeneous and catalytic decarboxylation give almost the same selectivity of the end products, CO_2 and acetic acid, however a high disappearance rate of malonic acid is achieved when the platinum catalyst is employed. It is further shown that when both catalyst and oxygen are used high selectivity to CO_2 is obtained, which confirms the presence of the oxidation route.

Another set of experiments was carried out at 150°C with different oxygen molar flows (i.e. S.E. of 20% and 100%) to the reactor. It was found that in all cases, the disappearance rate of malonic acid remains relatively the same, i.e. from 5.9×10^{-6} to 6.0×10^{-6} mol/s. Furthermore, the maximum carbon selectivity to CO_2 was 68%, which is the same value as observed in Fig. 3.8(b). The results show that the influence of oxygen concentration on malonic acid conversion is very small whereas the selectivity to the end products CO_2 and H_2O is increased.

The influence of the temperature was also investigated to determine its effects on the conversion of malonic acid and selectivity to CO_2 and acetic acid. The investigation was carried out with 10 kg_{cat}/m_L^3 of catalyst and in an oxygen-free environment (only nitrogen) to prevent oxidation. It is clearly seen in Fig. 3.9(a) that high temperature enhances the rate of disappearance of malonic acid. High disappearance rate of 3.2×10^{-6} mol/s for malonic acid (over 96% conversion) was achieved at 160°C while 1.3×10^{-6} mol/s (about 40% conversion) was attained 120°C. Within the range of temperatures studied, there is no significant difference in selectivity to CO_2, and the maximum achievable selectivity to CO_2 is 34% (Fig. 3.9b) and to acetic cid is 66%. Fig. 3.9(c) also shows similar temperature dependence in terms of residual maleic acid. The rate of CO_2 formation also increases with temperature as can be seen in Fig. 3.9(d). The observed increase in conversion rate of malonic acid at high temperature during decarboxylation can be attributed to the increased catalytic activity of the platinum catalyst.
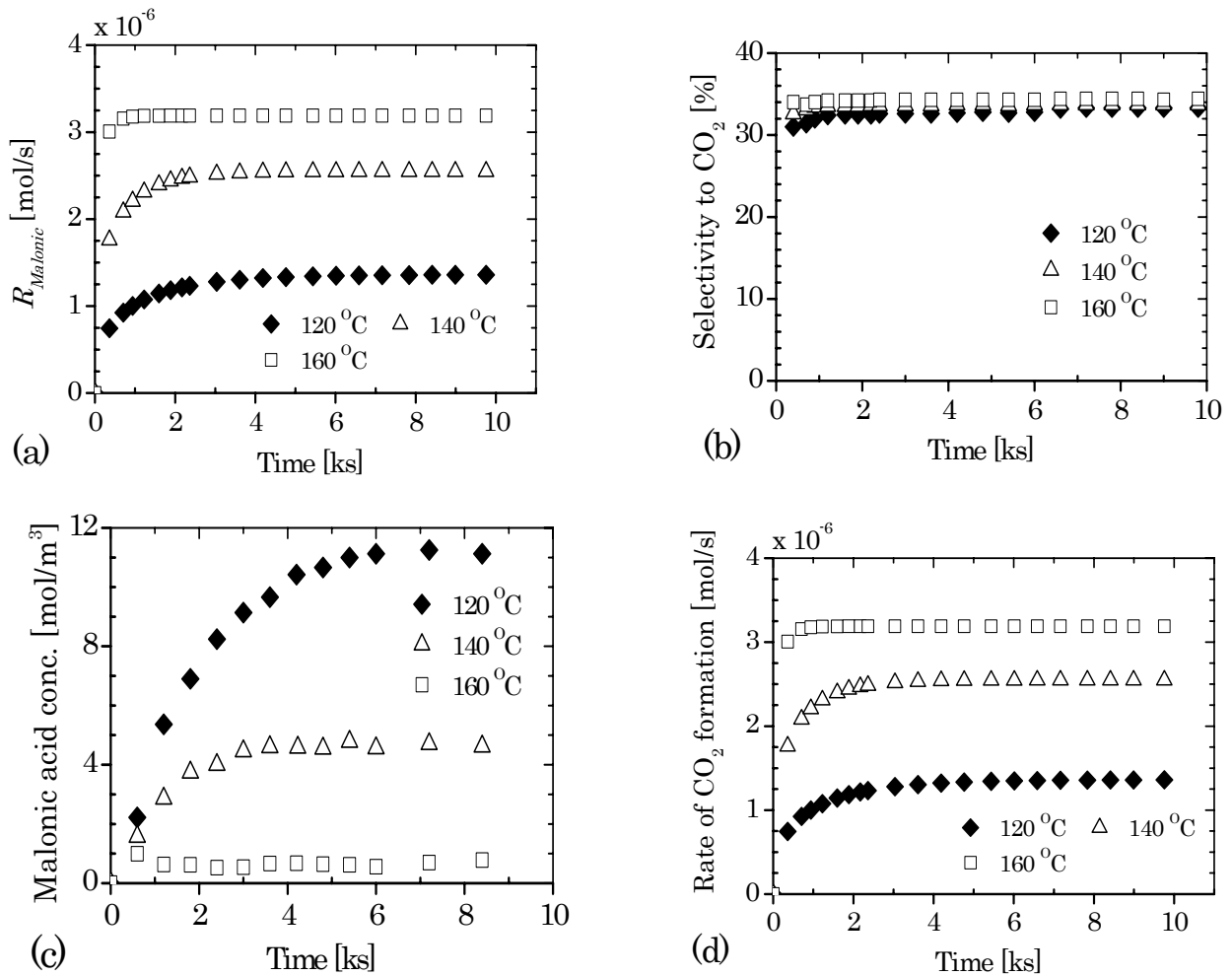
Fig. 3.9. Effect of temperature during malonic acid reaction without oxygen at 1200 rpm, $C_{malonic}$=20 mol/m^3 and 10 kg$_{cat}$/m$_L^3$ Pt/graphite (a) reaction rate for malonic acid, (b) Selectivity to CO_2, (c) concentration of malonic acid and (d) CO_2 formation.

On the basis of the observed results, it is clear that malonic acid reaction proceeds via homogenous and catalytic decarboxylation to CO_2 and acetic acid, and direct catalytic oxidation to CO_2 and H_2O. From Fig. 3.8 it appears that the homogeneous route for decarboxylation proceeds independently while the catalytic route leads to either decarboxylation and/or oxidation. Since the rate of CO_2 formation of 5.9 x 10^{-6} mol/s (Fig. 3.8d) during catalytic oxidation is twice the disappearance rate of malonic acid (2.9 x 10^{-6} mol/s), and the formation of acetic acid (1.5 x 10^{-6} mol/s) is almost half the disappearance of malonic acid, it seems that decarboxylation is not the only route. Although the catalytic mechanism for oxidation of malonic acid is not yet known, the catalytic routes can be expressed using the following equations:

decarboxylation: $CH_2(COOH)_2 \rightarrow CO_2 + CH_3COOH$ (3.7)

oxidation: $CH_2(COOH)_2 + 2O_2 \rightarrow 3CO_2 + 2H_2O$ (3.8)
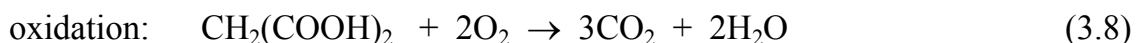
When the catalytic reaction is carried out in the presence of oxygen, each of the reaction routes takes place, i.e. homogenous and catalytic decarboxylation, and oxidation. If we assume that malonic acid does not strongly adsorb on the catalyst, and the reactor wall and other impurities have no catalytic effects, the contribution of the individual reactions can be estimated based on the rates of formation of CO_2 (Fig. 3.8c) and acetic acid (Fig. 3.8d). It was found that, when both catalyst and oxygen are used, malonic acid reaction proceeds via homogenous decarboxylation, catalytic decarboxylation (Eq. 3.7), and catalytic oxidation (Eq. 3.8). The kinetics investigation of these reactions was not the subject of this study.

During catalytic reaction of malonic acid, acetic acid once formed was stable for the whole range of experimental conditions. It seems therefore, that oxidation of malonic acid involves decarboxylation, which forms an intermediate and H_{ads} (adsorbed H-atom) that can be oxidized. This surface intermediate is possibly $-CH_2-COOH$, whereby a highly oxidised platinum surface takes the H-atom (H_{ads}) before it can recombine to form acetic acid. In absence of oxygen, the catalyst surface is in a reduced state, which means that after decarboxylation the intermediates can recombine with H-atoms, thus favouring acetic acid formation. The role of oxygen during catalytic oxidation is therefore to enhance the selectivity to the desired end products CO_2 and H_2O as well as to impair the formation of acetic acid.

3.4.   Conclusions

This work shows that the catalyst support type and the platinum dispersion have a significant effect on the reaction rate during CWO of organic wastes. Pt/graphite catalyst was found to be most effective and stable throughout the range of experimental conditions used. Pt/graphite, which has a metal dispersion of 5.3%, deactivates (over-oxidation) slowly compared to Pt/TiO₂ (15.3%), Pt/Al₂O₃ (19.5%) and Pt/AC (19.0%). Deactivation by fouling or blocking of active sites is one of the consequences of over-oxidation, particularly during phenol oxidation whereby *p*-benzoquinone and polymer precursors are formed. Deactivation by fouling seems to be severe for "mixed" type catalysts, e.g., Pt/Ti₂O₂, Pt/Al₂O₃, and Pt/AC, which also have relatively high metal dispersion and high porosity as compared to Pt/graphite catalyst. During oxidation of maleic acid at 150°C with a catalyst concentration of 6.0 kg_{cat}/m_L^3, Pt/graphite again was found to be effective followed by Pt/Al₂O₃ and Pt/AC. Furthermore, complete conversion of maleic acid to CO_2 and H_2O was achieved at 150°C and S.E. of 100% when 10 kg_{cat}/m_L^3 of Pt/graphite was used. At high

temperatures the activity of the Pt/graphite is enhanced, and complete conversion can be obtained even with high oxygen loads.

Despite the differences of the morphological properties of the catalysts, the activity of the investigated support materials for platinum catalysts decreases in the order Pt/graphite>Pt/TiO$_2$>Pt/Al$_2$O$_3$, as observed during phenol oxidation, and Pt/graphite>Pt/Al$_2$O$_3$>Pt/AC during maleic acid oxidation. It seems that the metal dispersion is one of the explanations for the differences in activity of the catalysts. The effect of platinum-support interaction however, cannot be excluded, which may be larger for Pt/graphite due to electron transfer from the graphite support to the platinum particle. Furthermore, differences in catalytic activity between Pt/graphite and Pt/Active carbon also can be attributed to the difference in hydrophilic character of the catalyst, where Pt/graphite has the lowest affinity for the aqueous phase.

The reaction of malonic acid in the presence of Pt/graphite catalyst and oxygen proceeds via homogeneous or non-catalysed decarboxylation, and catalytic decarboxylation to CO$_2$ and acetic acid, and catalytic oxidation to CO$_2$ and H$_2$O. The oxidation of malonic acid involves decarboxylation that gives intermediates, which can be oxidized at a highly oxidised platinum surface before desorption as acetic acid takes place. Without oxygen the catalyst surface is in a reduced state and this favours the intermediates to recombine with H$_{ads}$ to form acetic acid. Acetic acid, which was formed during catalytic decarboxylation, is a refractory compound that was difficulty to oxidize at the conditions tested.

Acknowledgements

Nomenclature

AC   active carbon
C_i concentration of the compound i [mol/m^3]
CWO   catalytic wet oxidation

F_i molar flow rate of compound i [mol/s]

F_V volumetric flow rate [m^3/s]

F_V^L volumetric flow rate of liquid [m^3/s]

n_C number of carbon atoms in a compound [-]

P pressure [Pa]

Pt   platinum

$R_{w,i}$ specific disappearance rate of compound i [mol/s.kg]

SCWO supercritical water oxidation

$S_{\to i}$ selectivity to compound i [%]

S.E.   stoichiometric oxygen excess to model compound [%]

T   temperature [K]

V_L volume of the liquid in the reactor [m^3]

W total mass of dry catalyst in the reactor [kg]

WAO   wet air oxidation

X_i conversion of compound i [%]

Superscripts

l   liquid

L   liquid

Subscripts

ads   adsorbed

C   carbon atoms

cat   catalyst

i/j   organic compound

in   inlet to reactor

Ph   phenol

w   weight

References

Bauer, J.E., Occelli, M.L., Williams, P.M. and McCaslin, P.C., Heterogeneous catalyst structure and function: review and implications for the analysis of dissolved organic carbon and nitrogen in natural waters, Marine Chemistry, 41 (1993) 75-89.

Beziat, J.C., Besson, M., Gallezot, P. and Durecu, S., Ind. Eng. Chem. Res. 38 (1999) 1310.

Charlot, G., "Les méthodes de la chimie analytique", Mason, Paris, 1961, p.859.

Donati, G. and Paludetto, R., Catal. Today 52 (1999) 183.

Fogler, H.S., "Elements of Chemical Reaction Engineering", 3rd Ed., Prentice Hall, Upper Saddle River NJ, 1999, p.577.

Fortuny, A., Font, J. and Fabregat, A, Appl. Catal. B 19(3-4) (1998) 165.

Gallezot, P., Chaumet, S., Perrard, A. and Insard, P., J. Catal. 168 (1) (1997) 104.

Gallezot, P., Richard, D. and Bergeret, G., in "Novel Materials in Heterogeneous Catalysis" (R.T.K. Baker and L.L. Murrel, Eds.), ACS Symposium Series,Vol. 437, p. 150. ACS, Washington D.C., 1990.

Levec, J. and Pintar, A., Catal. Today 24 (1995) 51.

Luck, F., Catal. Today 53 (1999) 81.

Markusse, A.P., Kuster, B.F.M. and Schouten, J.C., Stud. Surf. Sci. Catal. 126 (1999) 273.

Masende, Z.P.G., Kuster, B.F.M., Ptasinski, K.J., Janssen, F.J.J.G., Katima, J.H.Y. and Schouten, J.C., Appl. Catal. B 41 (2003a) 247.

Masende, Z.P.G., Kuster, B.F.M., Ptasinski, K.J., Janssen, F.J.J.G., Katima, J.H.Y. and Schouten, J.C., Catal. Today 79-80 (2003b) 357.

Matatov-Meytal, Yu.I. and Sheintuch, M., Ind. Eng. Chem. Res. 37 (1998) 309.

Mishra, V.S., Mahajani, V.V. and Joshi, J.B., Ind. Eng. Chem. Res. 34 (1995) 2.

Oliviero, L. (Jr.), Barbier, J., Duprez, D., Guerrero-Ruiz, A., Bachiller-Baeza, B. and Rodriguez-Ramos, I., Appl. Catal. B 25 (4) (2000) 267.

Ostermaier, J.J., Katzer, J.R. and Manogue, W.H., J. Catal., 41 (1976) 277.

Perego, C. and Peratello, S., Catal. Today 52 (1999) 133.

Scholten, J.J.F., in " Catalysis, An Integrated Approach to Homogeneous, Heterogeneous and Industrial Catalysis" (J.A. Moulijn, P.W.M.N. Van Leeuwen and Van Santen, Eds.), Stud. in Surface Science and Catalysis, Vol. 79, p. 419. Elsevier, Amsterdam, 1993.

Vleeming, J.H., "Deactivation of carbon-supported platinum catalysts during carbohydrate oxidation", Ph.D. thesis, Eindhoven University of Technology, Eindhoven (1997).

4

PLATINUM CATALYSED WET OXIDATION OF PHENOL IN A STIRRED SLURRY REACTOR: THE ROLE OF OXYGEN AND PHENOL LOADS ON REACTION PATHWAYS

Abstract

The catalytic wet oxidation of phenol was studied in a slurry phase CSTR using platinum on graphite support as a catalyst. The investigation was carried out in the temperature range of 120-180°C and at total pressure of 1.8 MPa, while the phenol feed concentration was varied between 5 and 70 mol/m^3, and oxygen partial pressures between 0.01 and 0.8 MPa. It was found that both the oxygen load and the stoichiometric oxygen excess determine the extent of oxygen coverage on the platinum surface, which influences the reaction pathways and selectivity to CO_2 and H_2O. A fully oxidized platinum surface resulted into catalyst deactivation (over-oxidation), which favoured the formation of p-benzoquinone and polymeric products. Whereas free platinum surface was vulnerable to poisoning by carbonaceous compounds, a fully reduced platinum surface favoured the formation of acetic and succinic acids which are difficult to oxidize. A reaction scheme for platinum catalysed phenol oxidation in liquid phase has been proposed.

Keywords: Catalytic wet oxidation; Phenol oxidation; Platinum/graphite; Wastewater treatment; Reaction network

4.1.   Introduction

The application of noble metal catalysts for liquid phase oxidation provides a potential for treatment of wastewaters containing organic pollutants. In addition to their high activity, noble metal catalysts have the advantage over the supported oxides of transition metals like copper oxide, manganese oxides etc., that no dissolution of the active component into the liquid, even in hot acidic environment, takes place (Luck, 1999; Mishra *et al.*, 1995). Other possible catalyst deactivation mechanisms that are reported to occur in commercial catalytic reactors include: deactivation by reduction of the support surface (sintering), deactivation by deposition of carbonaceous material on the catalyst surface (coking or fouling), and deactivation by irreversible adsorption on active sites by poisoning molecules (poisoning) (Luck, 1999; Fogler, 1999; Savage, 1999). Platinum catalysts have been reported to be effective during catalytic liquid phase oxidation of alcohols (Markusse *et al.*, 2000), formic acid (Harmsen *et al.*, 1997), and ammonia (Ukropec *et al.*, 1999). The main drawback for platinum metal catalysts is their rapid deactivation in the liquid phase. Deactivation mechanisms reported for platinum metal catalysts include over-oxidation and elution of the catalyst (leaching) as described by Mallat and Baiker (1994). The deactivation by over-oxidation has been explained as a result of an increase of the catalyst potential (Markusse *et al.*, 2000; Vleeming *et al.*, 1997). There is, however, limited information on the platinum activity during wet oxidation of phenolic wastewater and its influence on the reaction pathways and selectivity to end products.

Different reaction networks for liquid phase phenol oxidation have been reported in literature (Savage, 2000; Mishra *et al.*, 1995; Pintar and Levec, 1992; Devlin and Harris, 1984). The reaction pathways were derived through the identification of reaction intermediates and end products. The formation of a variety of partial oxidation and polymerisation products during wet oxidation has in most cases involved oxidation, decarboxylation, dehydration, and rearrangement of the molecules or combination of these steps.

In both catalysed and non-catalysed phenol oxidation, the ultimate partial oxidation compounds reported are low molecular mass mono- and dibasic acids such as glyoxylic, oxalic, propionic, acetic, and formic acid. Devlin and Harris (1984) proposed a reaction pathway for non-catalysed phenol oxidation in aqueous solution by molecular oxygen at 413-498 K and oxygen pressures up to 20.7 MPa, in which unsaturated acids viz. maleic acid and acrylic acid, were the main intermediates. The intermediate ring compounds, catechol, hydroquinone, and benzoquinones were not

observed under conditions of excess oxygen. Dimers such as 2-phenoxy-phenol, 4-phenoxy-phenol, 2,2-biphenol, dibenzofuran, 2-dibenzofuranol, and dibenzo-1,4-dioxin were identified during supercritical water oxidation (SCWO) of phenol (Savage, 2000).

Phenol reaction networks in SCWO have been recently reviewed (Savage, 2000), in which the formation of dimers and other intermediates like single-ring compounds (e.g. hydroquinone), ring-opening products (e.g. maleic acid, glyoxylic acid, acetic acid, and other organic acids), and gases (e.g. CO, CO_2) are reported. Some of these partial oxidation products and intermediates, especially the dimers, are relatively more toxic than phenol.

The reaction intermediates reported on phenol oxidation catalysed by supported metal oxides, like copper, zinc, and manganese and other metal catalysts, are similar to those of non-catalysed phenol oxidation (Matatov-Meytal and Sheintuch, 1998; Hamoudi *et al*., 1998; Fortuny *et al*., 1998; Pintar and Levec, 1994; Sadana and Katzer, 1974). The formation of polymeric products in liquid phase has been reported in different studies (Pintar and Levec, 1992; Ohta *et al*., 1980). Pintar and Levec (1992) reported that polymers were formed by the reaction between glyoxale and phenol, and polymerisation of the C-2 aldehyde (glyoxale). The homogeneous polymerisation was related to catalyst deactivation. Polymerisation reactions might be suppressed by use of reactors with high solid-to-liquid ratio such as a trickle-bed reactor (Pintar and Levec, 1994).

Hamoudi *et al*. (1998, 1999) reported that the use of noble-metal containing catalyst (such as platinum on alumina) generated lesser build-ups of deposits of polymeric products, which cause catalyst deactivation via physical blockage of active sites. They further suggested that platinum very likely catalyses the C-C bond rupture within organic molecules, while simultaneously it prevents polymerisation of the reactive intermediate radicals that are formed in the course of catalytic wet oxidation (CWO). The role of oxygen and phenol loads on the platinum catalyst is not well explained yet in literature. While the operation window for platinum catalysed phenol oxidation, where loss of catalyst activity is avoided, has recently been reported (Masende *et al*., 2003a), the reaction pathways for phenol oxidation over platinum catalyst are also not clearly reported in literature.

The purpose of this work was to identify the most likely pathways for platinum catalysed phenol oxidation in the liquid phase. The influence of reactant

concentrations on phenol conversion to CO_2 and H_2O, and the role and reactivity of phenol oxidation intermediates and end products have been investigated. Moreover, a reaction pathway has been proposed.

4.2.   Experimental

The liquid phase oxidation of phenol by oxygen was investigated using a commercially available catalyst, graphite supported platinum (5 wt % Pt/G, Johnson Matthey JM287). The average graphite particle size was 7 μm and 95% of the particles were smaller than 15 μm, as confirmed by particle size measurement (Coulter LS 130 apparatus). Other catalyst specifications include: metal surface area of 0.66 $m^2.g^{-1}$ sample, metal dispersion 5.3%, and B.E.T. surface area of 15 $m^2.g^{-1}$.

The experiments were conducted in a continuous flow stirred slurry reactor (CSTR), a 500 ml autoclave (Autoclave Engineers, Zipperclave Hastelloy) that is equipped with a gas dispersion impeller. During reaction, the reactor was kept at constant temperature within ± 0.3 K, in a wide range of temperatures, by a heating element around the reactor. The pressure in the reactor was kept constant by using a backpressure regulator. During the experiments the flow rates of the phenol feed solution and the gas entering the reactor were kept constant. Details of the experimental set-up and reactor start-up procedures are reported elsewhere (Masende *et al.*, 2003a). The reactor operating conditions were as given in Table 4.1.

Table 4.1
Reactor operating conditions

	Standard	Range
Temperature, °C	150	120 - 180
Total pressure, MPa	1.8	1.5 – 2.0
Oxygen partial pressure, MPa	0.5	0.01 – 0.8
Oxygen flow rate, ml/min	40	0 - 80
Nitrogen flow rate, ml/min	90	10 -120
Phenol concentration, mol/m^3	20	5 - 70
Liquid flow rate, ml/min	10	5 - 20
Liquid reactor volume, ml	350	350
Catalyst amount, kg_{cat}/m_L^3	6	1 - 30
pH	Uncontrolled	2 - 8
Stirrer speed, rpm	1200	350 -1200

In each experiment, the progress of the reaction and the catalytic activity were monitored by measurement of the reactor effluent composition as a function of time. The liquid samples were analysed by an on-line HPLC for residual phenol and intermediate reaction products. Phenol and other aromatic compounds were analysed in a 300 x 4.6 ID mm Lichroma SS column, packed with a Benson type of cation-exchange resin (Ca^{++}) using a UV detector, while carboxylic acids were analysed in a 300 x 8 ID mm RSpak KC-811 column using a refractometer detector (Waters R401). The composition of the outlet gas was determined by using an O_2 sensor and on-line GC. Nitrogen gas was used as a standard while helium was used as carrier gas.

For all experimental data, the overall carbon balance and the oxygen balance were verified after every experiment; they were within 95 - 100%, which was considered analytically acceptable.

4.3. Results and discussion

4.3.1 Influence of reactor temperature

The influence of reaction temperature on phenol oxidation and selectivity of intermediates was determined at temperatures between 120 and 180°C at standard conditions as shown in Table 4.1. It was found that at temperatures above 150°C, phenol conversion to CO_2 and H_2O of 99% and higher was attained, while at 135 and 120°C, lower phenol conversions were obtained. Neither *p*-benzoquinone nor maleic acid were detected in the liquid samples obtained at 165 and 180°C. At the lower temperatures, the residual phenol concentration increased gradually over time while a decline in the activity of the platinum catalyst was observed. The liquid effluent obtained at 120°C was characterised by a brownish colour and showed formation of *p*-benzoquinone, maleic acid, and insoluble (polymeric) products. Unless otherwise mentioned, all other experiments reported were carried out at 150°C.

4.3.2 Influence of reactant concentration

To determine the effect of the reactant concentrations on the reaction mechanism and pathway, the ratio of the molar flow rate of the reactants, expressed as percentage stoichiometric oxygen excess to phenol (S.E.), was varied. The experiments were carried out at a constant phenol feed concentration of 0.02 mol/l while the oxygen partial pressures were varied between 10 and 800 kPa. A start-up method where

phenol and oxygen are fed simultaneously to the reactor was used (Masende *et al*., 2003a).

Fig. 4.1 shows the typical results on phenol conversion at different stoichiometric oxygen excess. The oxygen load has two opposing effects on the reaction rate (Fig. 4.1(a) & (b)). At sub-stoichiometric amount of oxygen (S.E. < 0%), increasing the oxygen partial pressure, which means the dissolved oxygen concentration, enhanced the oxidation rate of phenol. Above the stoichiometric oxygen amount, the reaction rate is enhanced up to a certain point at which the oxygen concentration started to inhibit the phenol oxidation rate. The inhibitory effect observed at S.E. above 80% can be explained by the loss of activity of the platinum catalyst as a result of over-oxidation. This negative effect of a high oxygen concentration on the activity of platinum catalyst was also observed during alcohol oxidation (Markusse *et al*., 2000; Mallat and Baiker, 1994) and ammonia oxidation (Ukropec *et al*., 1999).
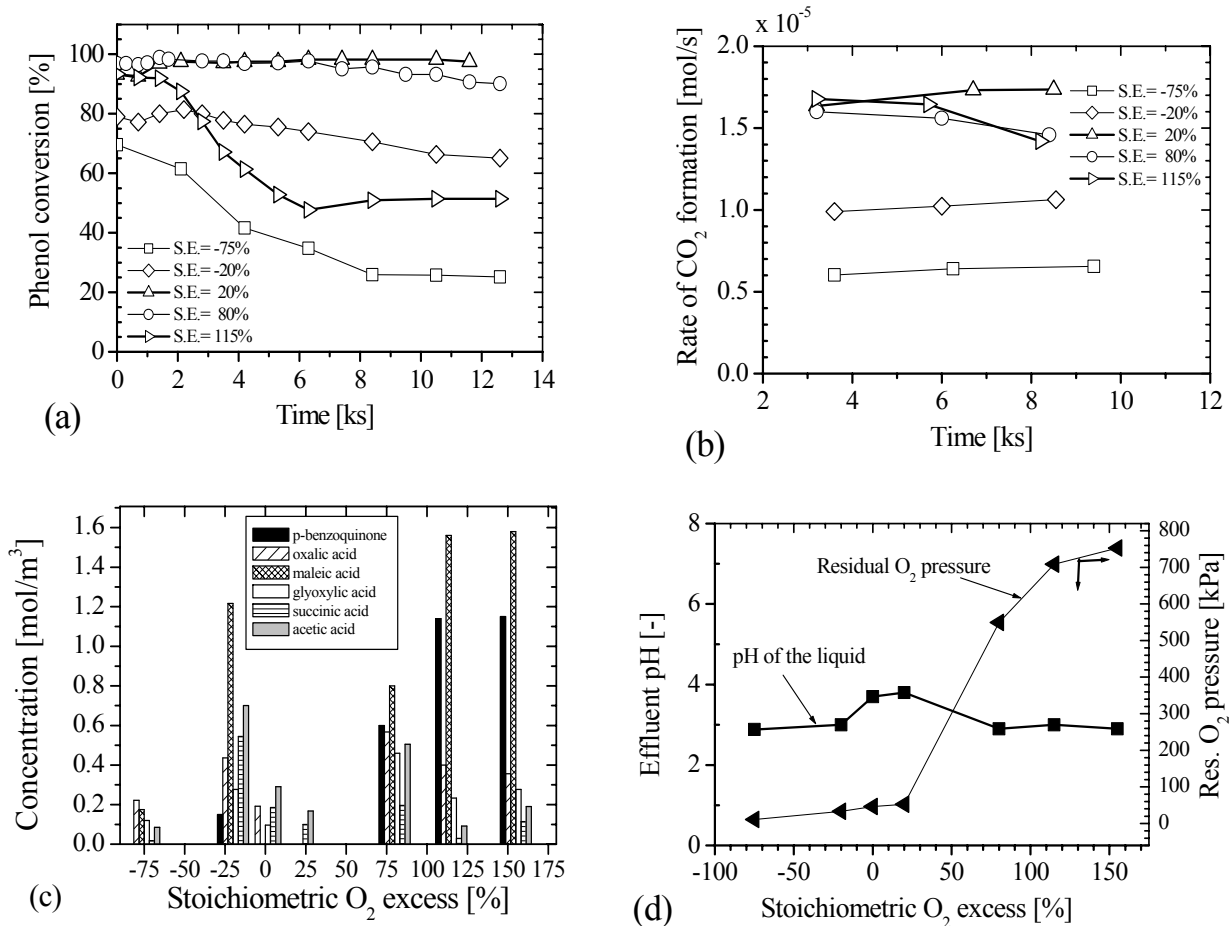

Fig. 4.1. Influence of oxygen load on phenol oxidation at standard conditions (Table 4.1) using the O_2-Ph-Sim start-up method: (a) phenol conversion, (b) CO_2 formation, (c) concentration of intermediates, (d) residual oxygen partial pressure and effluent pH.

It can be seen in Fig. 4.1(c) & (d) that when insufficient oxygen is fed, the reaction is dominated by the formation of low molecular weight carboxylic acids, while within the residual oxygen pressure range of 20 to 40 kPa, neither *p*-benzoquinone nor maleic acid were detected in the colourless liquid effluent. The pH of 3.8 is within the range for water saturated with CO_2, indicating that mainly CO_2 was present in the liquid. At high residual oxygen partial pressure, which means high oxygen concentration at the catalyst surface, both *p*-benzoquinone and maleic acid were detected in high concentrations in the brownish coloured liquid effluent. These results suggest that the extent of oxygen coverage on the platinum surface influences the reaction network and selectivity to reaction products.

Table 4.2
Reaction intermediates and end products during phenol oxidation (Masende *et al.*, 2003a)

Compound	Formula	High P_{O2} (S.E.[a] > 80%)			Low P_{O2} (0<S.E.[a]<80%)		
		A	B	C	A	B	C
Phenol	C_6H_5OH						
p- Benzoquinone	$C_6H_4O_2$	++	++	++	+(0)	+(0)	-
Maleic acid	*Cis*-HO_2C-CH=CH-CO_2H	++	++	++	+(0)	+(0)	-
Fumaric acid	*Trans*-HO_2C-CH=CH-CO_2H	+	+	+	-	-	-
Succinic acid	HO_2C-$(CH_2)_2$-CO_2H	+	+	+	+	+	+
Malonic acid	HO_2C-CH_2-CO_2H	-	-	-	+	+	+
Acetic acid	CH_3-CO_2H	+	+	+	+	+	+
Glyoxylic acid	$CHOCO_2H$	++	++	+	+(0)	+(0)	-
Oxalic acid	HO_2C-CO_2H	++	++	+	+(0)	+(0)	-
Insoluble compounds	Not identified	++	++	+	-	-	-
Carbon dioxide	CO_2	++	++	++	+++	+++	+++

[a]S.E.: The stoichiometric oxygen excess to phenol. Start-up procedures- A (O_2-First): start with oxygen feed followed by phenol; B (Ph-First): start with phenol feed followed by oxygen; and C (O_2-Ph-Sim): feeding of both oxygen and phenol at the start of the reaction. Selectivity: +++: highest; ++: high; +: low; (0): high only at start of reaction; -: not identified

4.4. Reaction intermediates and pathways

The reaction intermediates and products identified during the oxidation of phenol are listed in Table 4.2. Reactor start-up methods, at which particular end products and intermediates are found, are also given in the table. These include intermediate ring compounds, and unsaturated and saturated carboxylic acids. Although these reaction products are similar to those reported in literature (Pintar and Levec, 1992; Devlin and Harris, 1984; Sadana and Katzer, 1974), their evolution and stability during the catalytic reaction depend on whether the reaction is carried out within or outside the operation window (viz. oxygen and phenol loads) (Masende *et al.*, 2003a). In order to properly elucidate the phenol oxidation reaction network, the fate of these compounds,

namely oxalic, acetic, glyoxylic, malonic, succinic, and maleic acid, were investigated
at similar experimental conditions. In addition, muconic acid, catechol, hydroquinone,
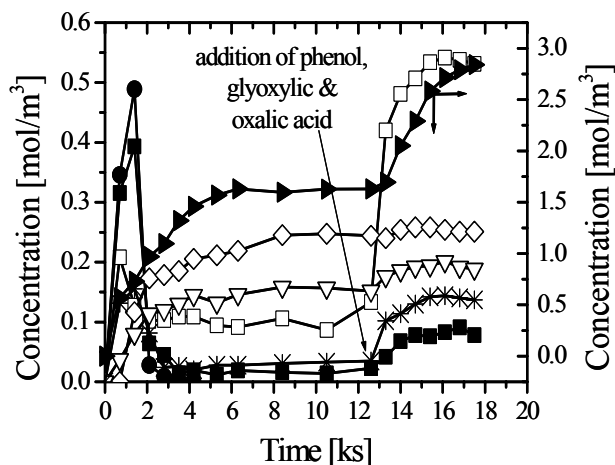and benzoquinone solutions were oxidized at the same conditions.

Fig. 4.2. In-situ oxidation of solution containing 0.02 mol/l phenol, 0.01 mol/l oxalic acid, and 0.01 mol/l glyoxylic acid using O_2-First start-up method at standard conditions (Table 4.1): phenol (►), *p*-benzoquinone (●), oxalic id (□), maleic acid (■), glyoxylic acid (*), succinic acid (∇), acetic acid (◊).
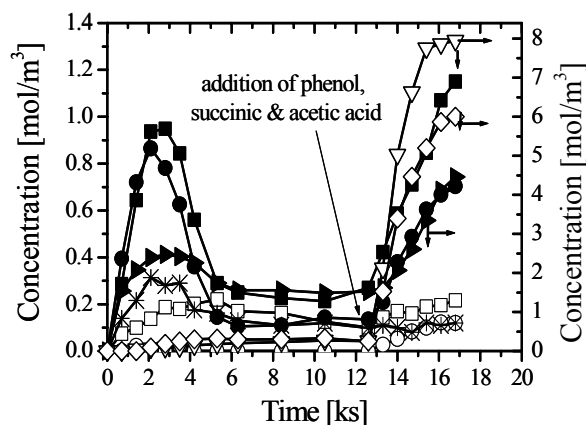
Fig. 4.3. In-situ oxidation of solution containing 0.02 mol/l phenol, 0.01 mol/l acetic acid and 0.01 mol/l succinic acid using O_2-First start-up method at standard conditions (Table 4.1): phenol (►), *p*-benzoquinone (●), oxalic acid (□), maleic acid (■), glyoxylic acid (*), succinic acid (∇), acetic acid (◊).

4.4.1. Oxidation of oxalic acid and glyoxylic acid

The oxidation of oxalic acid solution using Pt/graphite gave complete conversion to CO_2 and H_2O. Formic acid was not observed in the liquid effluent. The pH of 4.6 and the residual oxygen pressure of 300 kPa remained constant during the oxidation period indicating a high potential of the platinum surface.

The oxidation pathway of oxalic acid on platinum surface requires a high oxidation potential to split the C-C bond of the saturated acid. This is an exceptional case when compared to other platinum catalysed reactions in which the oxidation mechanism involves dehydrogenation of the C-H bond as the first step (Mallat and Baiker, 1994). These results are in accordance to Markusse *et al*. (2000) who reported that oxalic acid was easily oxidized at the oxidised platinum surface while it was difficult at a reduced platinum surface.

When oxidation of 0.02 mol/l glyoxylic acid solution was undertaken, full conversion with 100% selectivity to CO_2 was attained. The pH of 4.3 and the residual oxygen partial pressure of 290 kPa remained constant. Neither formic acid nor oxalic acid was

detected in the liquid effluent. However, this result does not exclude the possibility that oxalic acid and formic acid might be formed as intermediates especially at a reduced platinum surface. This is because at similar conditions formic acid was completely converted to CO_2 and H_2O.

In Fig. 4.2 a profile of phenol oxidation before and after replacing the feed solution with a solution containing 0.02 mol/l phenol, 0.01 mol/l oxalic acid, and 0.01 mol/l glyoxylic acid, is presented. A decline in phenol conversion from 92% to 86% before and after injection of the compounds was observed. In this case, changes before and after injection were observed in the residual partial pressure of oxygen, dropping from 50 to 30 kPa, while the pH also changed from 3.7 to 3.4. The decline in conversion was attributed to the limited amount of oxygen for competing oxidation reactions of phenol, glyoxylic, and oxalic acid. The additional formation of succinic acid, which could be due to transfer hydrogenation, and of oxalic acid due to its limited breakdown at a reduced platinum surface, supports this argument. It can further be noted that the absence of polymeric products suggests that glyoxylic acid is not a polymer precursor as suggested by others (Pintar and Levec, 1992).

4.4.2. Oxidation of acetic acid and succinic acid

The oxidation of 0.014 mol/l acetic acid solution was carried out at standard conditions (Table 4.1). There were no intermediate products detected in the liquid and the pH remained at 3.4. The residual oxygen pressure was the same as the initial value of 350 kPa, which indicates that acetic acid is stable at these experimental conditions. These observations suggest that acetic acid is an end product during platinum catalysed phenol oxidation at 150°C rather than an intermediate. The results are in agreement with those in literature whereby acetic acid is reported to be stable even above 200°C (Gomes *et al.*, 2000; Rivas *et al.*, 1999).

The oxidation of 0.02 mol/l sucinic acid solution showed that succinic acid did also not react at standard conditions. Both the pH (3.0) and the residual oxygen partial pressure remained constant. This suggests that succinic acid is also an end product rather than an intermediate product.

In Fig. 4.3 the profile of the co-oxidation of 0.01 mol/l acetic and 0.01 mol/l succinic acid in the presence of 0.02 mol/l phenol is shown. While very little acetic acid conversion could not be excluded, the results clearly indicated that succinic acid did not react. The decline of phenol conversion after injection of these acids could be

attributed either to inhibition of its reaction due to competitive adsorption or by the drop in pH from 3.4 to 2.8 caused by the unconverted acids, which could influence the oxidation potential of the platinum surface, causing the residual partial pressure of oxygen to increase from 80 to 220 kPa. The evolution of *p*-benzoquinone and maleic acid seem to result from phenol oxidation on platinum at a higher potential. The results confirmed that both succinic and acetic acid are end products during phenol oxidation.
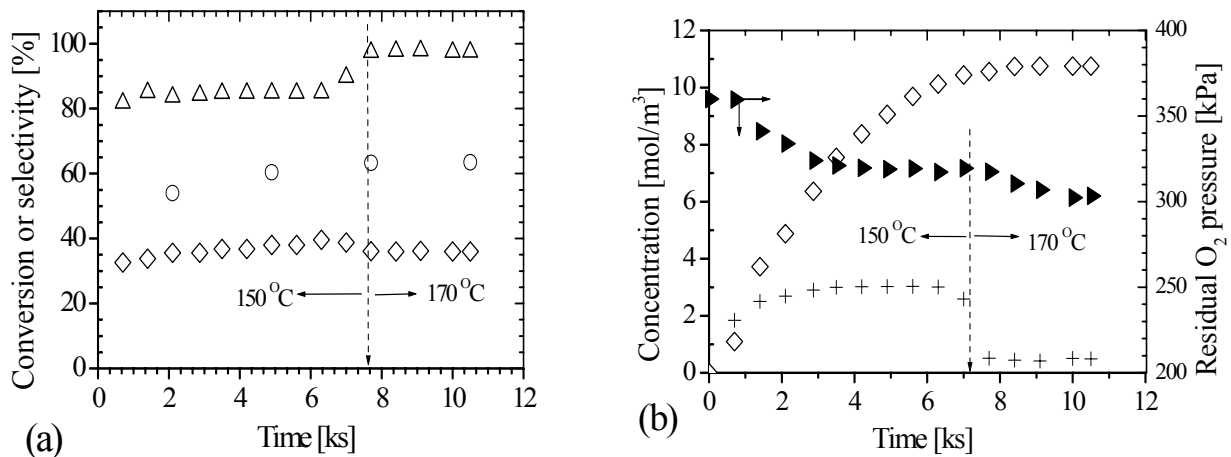

Fig. 4.4. Oxidation of 0.02 mol/l malonic acid using the O_2-Ph-Sim start-up method at standard conditions (Table 4.1) (a) malonic acid conversion (Δ), selectivity to CO_2 ($\circ$) and acetic acid ($\Diamond$), (b) concentration of malonic acid (+), and acetic acid ($\Diamond$), and residual oxygen partial pressure ($\blacktriangleleft$).

4.4.3. Oxidation of malonic acid

Fig. 4.4(a) shows the oxidation of malonic acid where conversion above 84% is achieved at 150°C and it increases to above 90% conversion at 170°C. The main end products were acetic acid and CO_2 as shown in Fig. 4.4(a) & (b) with their respective selectivities of 38% and 62%. Although malonic acid conversion increased at high temperature, the selectivity to acetic acid remained the same while the liquid effluent pH changed from 3.6 to 2.8, indicating the increase of acetic acid formation. The residual oxygen partial pressure of 320 kPa shows that little amount of oxygen is consumed during the reaction.

The results suggest that two parallel reaction routes for malonic acid exist, namely direct oxidation to CO_2 and H_2O, and decarboxylation to CO_2 and acetic acid. Decarboxylation of malonic acid is reported to be the main reaction (Santos *et al.*, 2002; Vogel *et al.*, 2000) while the contribution of direct oxidation is scarcely considered. Taking into account the feed concentration of 20 mol/m^3 of malonic acid,

the relative contributions of the two reactions were determined whereby 60% of malonic acid reacted via decarboxylation while 40% by direct oxidation. However, decarboxylation of malonic acid produces acetic acid, which is difficulty to oxidize even at 170°C. The stability of acetic acid formed from decarboxylation of malonic acid was also observed in other studies, even at 240°C (Rivas *et al.*, 1999).

4.4.4. Oxidation of maleic acid

Maleic acid, which appeared at almost all conditions, though sometimes in trace amounts, is an important compound in understanding the phenol reaction network. Fig. 4.5(a) & (b) show the profile of 0.01 mol/l maleic acid oxidation in which a steady state conversion of 80% was achieved while selectivity to CO_2 was 91% at residual oxygen partial pressure of 300 kPa. The reaction intermediates detected in the liquid samples with pH of 2.7 are succinic, acetic, and fumaric acid.
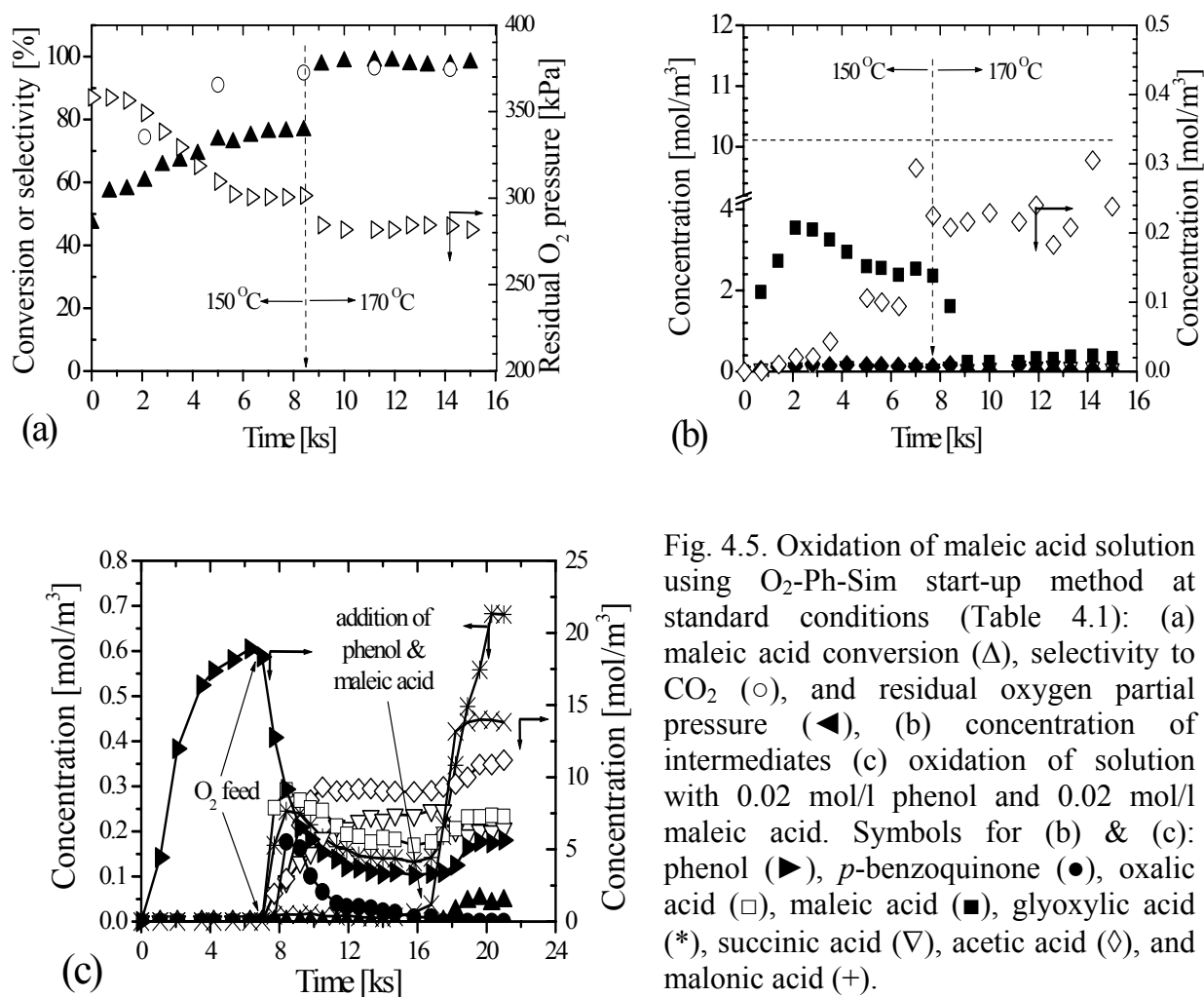

Fig. 4.5. Oxidation of maleic acid solution using O_2-Ph-Sim start-up method at standard conditions (Table 4.1): (a) maleic acid conversion (Δ), selectivity to CO_2 (○), and residual oxygen partial pressure (◄), (b) concentration of intermediates (c) oxidation of solution with 0.02 mol/l phenol and 0.02 mol/l maleic acid. Symbols for (b) & (c): phenol (►), *p*-benzoquinone (●), oxalic acid (□), maleic acid (■), glyoxylic acid (*), succinic acid (∇), acetic acid (◊), and malonic acid (+).

It can be inferred from these observations that maleic acid reacts catalytically to CO_2, probably through glyoxylic and oxalic acid, which are very reactive at the test conditions. The appearance of fumaric acid could be due to the *cis-trans*-isomerization of maleic acid. While the formation of succinic acid is explained by transfer hydrogenation, the formation of acetic acid could be due to bond cleavage followed by transfer hydrogenation.

Fig. 4.5(c) shows the influence of maleic acid on phenol oxidation, when a solution containing 0.02 mol/l of maleic acid and 0.02 mol/l phenol was oxidised. While phenol conversion dropped from 82% to 70% during 4.2 ks (double liquid residence time), the concentration of maleic acid increased with time with slight increase in the concentration of glyoxylic acid followed by oxalic acid. Fumaric acid, the isomer of maleic acid, was also formed in relatively low concentration. The decline of phenol conversion could be due to either coverage of the active catalyst sites by organic species or a lower pH.

The results suggest that glyoxylic acid is formed from maleic acid by carbon-carbon cleavage and oxidation, and that glyoxylic acid possibly reacts sequentially to CO_2 through oxalic acid. The appearance of oxalic acid could be explained by the decrease in oxidation potential of the platinum surface as a result of a lower pH, which decreased from 3.4 (before) to 2.4 (after injection).

4.4.5. Oxidation of hydroquinone

A 0.02 mol/l hydroquinone solution oxidised in the presence of Pt/graphite catalyst, easily reacted to form *p*-benzoquinone, and maleic acid with low concentrations of oxalic and acetic acid (Fig. 4.6(a)), while a selectivity to CO_2 of 76% was attained. Significant changes were observed after increasing the temperature to 170ºC in which conversion above 95% to CO_2 was attained and the pH of the effluent liquid increased to over 4.0 while the residual oxygen partial decreased (Fig. 4.6(b)). The brownish colour of the liquid effluent, which is a typical characteristic of *p*-benzoquinone also disappeared at the higher temperature. These observations are consistent with results obtained during phenol oxidation at oxygen stochiometric excess (S.E.) above 80%, thus proving that *p*-benzoquinone is an intermediate product, which agrees with others (Pintar and Levec, 1992; Devlin and Harris, 1984; Ohta *et al*., 1980; Sadana and Katzer, 1974).

The formation of *p*-benzoquinone and maleic acid seems to be sequential. Similarly, the formation of acetic acid seems to be sequential from maleic acid. In order to verify this hypothesis, a solution of 0.02 mol/l of phenol and 0.02 mol/l of *p*-benzoquinone was used as a feed after 12.6 ks of reaction. Fig. 4.7 shows the profile of oxidation intermediates before and after changing the feed solution in which a decline in phenol conversion from over 99% to 70% was observed. The colour of the liquid effluent changed from colourless to dark brownish, as the concentrations of *p*-benzoquinone, maleic acid, and oxalic acid increased. These changes were accompanied by the formation of insoluble compounds attributed to polymeric products. Whenever *p*-benzoquinone was formed insoluble compounds attributed to polymeric products were also formed, which most likely resulted in the loss of platinum catalyst activity.
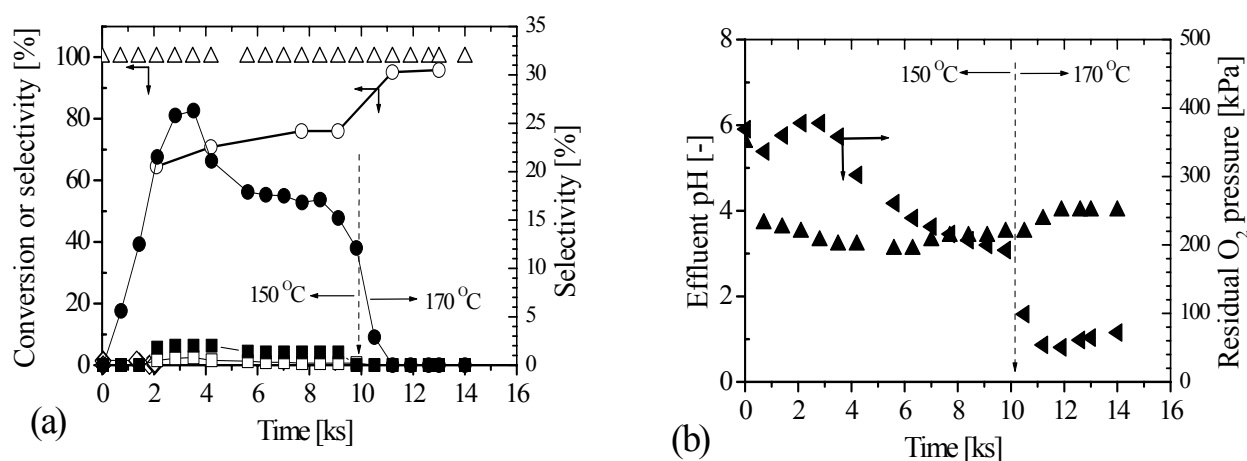

Fig. 4.6. Oxidation of a solution containing 0.02 mol/l hydroquinone using O_2-Ph-Sim start-up method at standard conditions (Table 4.1): (a) conversion of hydroquinone (Δ) and selectivity to: CO_2 ($\circ$), *p*-benzoquinone ($\bullet$), oxalic acid ($\square$), maleic acid ($\blacksquare$), glyoxylic acid (*), succinic acid (∇), acetic acid ($\diamond$), malonic acid (+), and (b) residual oxygen partial pressure ($\blacktriangleleft$), and liquid pH ($\blacktriangle$).
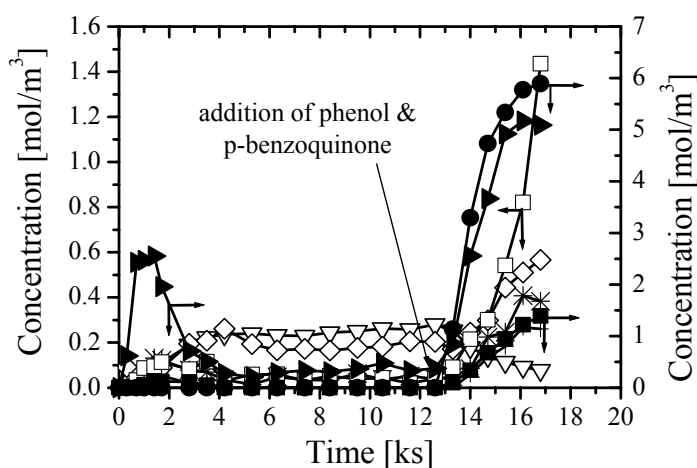

Fig. 4.7. Oxidation of a solution containing 0.02 mol/l phenol and 0.02 mol/l *p*-benzoquinone using O_2-Ph-Sim start-up method at standard conditions: phenol ($\blacktriangleright$), *p*-benzoquinone ($\bullet$), oxalic acid ($\square$), maleic acid ($\blacksquare$), glyoxylic acid (*), succinic acid (∇), acetic acid ($\diamond$), malonic acid (+).

4.4.6. Oxidation of catechol

During phenol oxidation experiments, catechol was not detected. When catechol was oxidised in a separate experiment, it was easily converted into oxidation products, mainly CO_2 (selectivity of 90%) as shown in Fig. 4.8(a). Intermediates formed in the oxidation, though in small amounts (selectivity < 5% in total), were oxalic, acetic, succinic, and malonic acid. Fig. 4.8(b) shows the pH of the liquid effluent and the corresponding residual oxygen partial pressure. Neither *o*-benzoquinone nor maleic acid were detected in the yellowish coloured liquid effluent. However, the yellowish colour can be associated with the presence of unmeasurable traces of *o*-benzoquinone since catechol is colourless under oxygen-free environments.

The possible explanation of the absence of *o*-benzoquinone could be that *o*-benzoquinone produced by oxidation reacts rapidly under ring cleavage to end products. It is most likely that during ring cleavage the splitting of C-6 to form C-4 and C-2 compounds is favoured. However, the splitting of C-6 into C-3 compounds cannot be excluded since malonic acid is also formed, although in trace amount. The formation of succinic and acetic acid proves the idea that catechol is a strong reducer, thus reduced platinum favours transfer hydrogenation reaction in addition to oxidation.
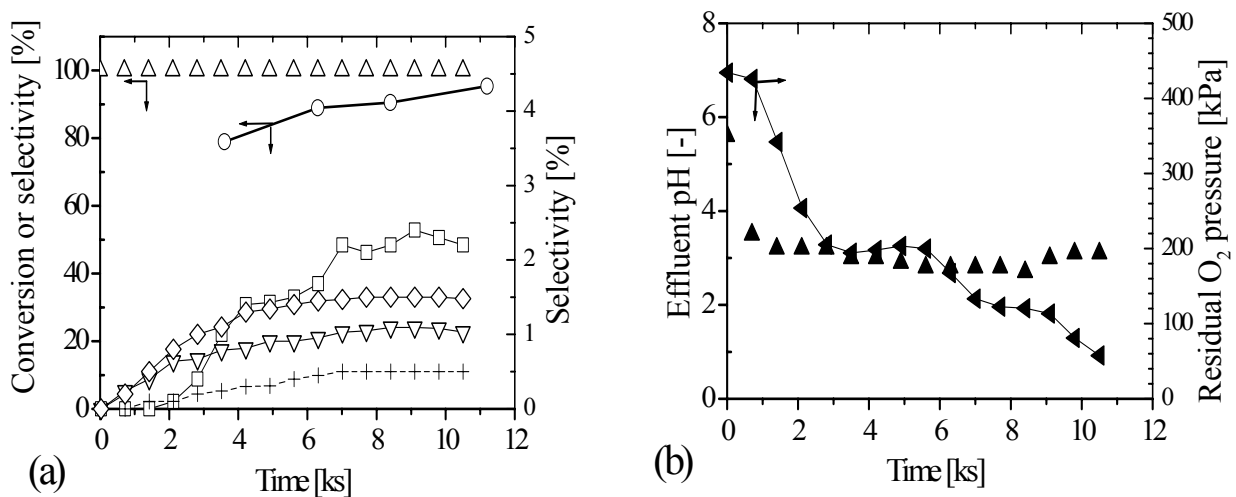

Fig. 4.8. Oxidation of 0.02 mol/l catechol using O_2-Ph-Sim start-up method at standard conditions: (a) conversion of catechol (Δ), and selectivity to CO_2 (○), oxalic acid (□), malonic acid (+), succinic acid (∇), acetic acid (◊), and (b) residual oxygen partial pressure (◄), and liquid pH (▲).
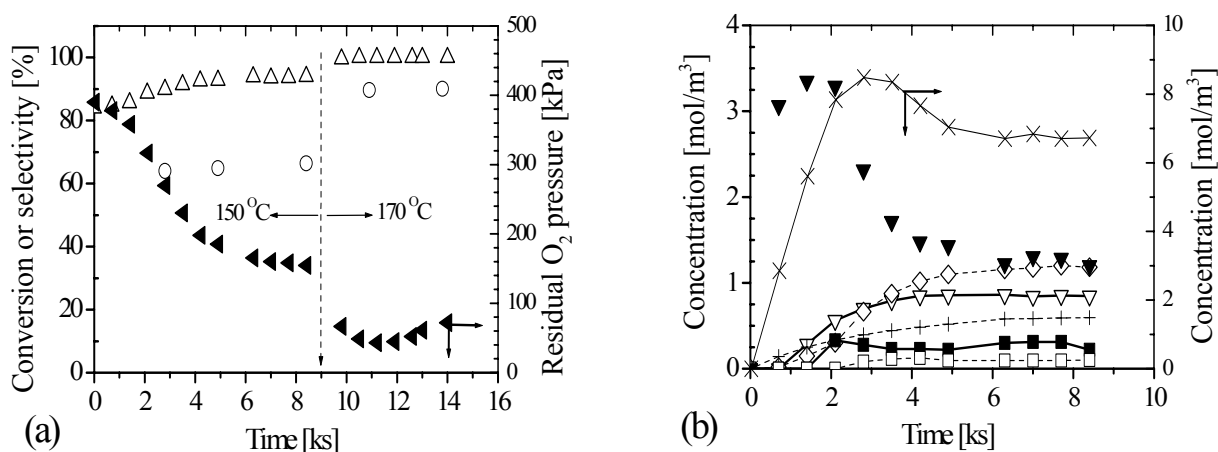
Fig. 4.9. Oxidation of 0.02 mol/l muconic acid solution using O_2-Ph-Sim start-up method at standard conditions: (a) muconic acid conversion (Δ), selectivity to CO_2 ($\circ$), and residual oxygen partial pressure ($\blacktriangleleft$), (b) concentrations of muconic acid ($\blacktriangledown$), propanoic acid (X), oxalic acid ($\square$), malonic acid (+), maleic acid ($\blacksquare$), succinic acid (∇), and acetic acid ($\diamondsuit$).

4.4.7. Oxidation of muconic acid

Although muconic acid was not detected in our experiments, it is generally considered as the intermediate compound during phenol oxidation to CO_2. Therefore, the reactivity and hence reaction intermediates during oxidation of muconic acid were investigated at standard conditions. Fig. 4.9(a) presents the reaction profile of muconic acid in which a steady state conversion of 94% and a selectivity to CO_2 of 65% were achieved. In Fig 4.9(b) the concentrations of muconic acid, and of propanoic, succinic, acetic, and malonic acid are shown. Both maleic and oxalic acid were detected in trace amounts. At 170ºC, muconic acid was fully converted with selectivity to CO_2 over 90%. The corresponding changes in the residual oxygen partial pressure are depicted in Fig. 4.9(a). The formation of propanoic acid in relatively high concentration raises doubt on whether muconic acid is a reaction intermediate in the phenol oxidation. This is due to the reason that both propanoic acid, which seems to be stable at the test conditions, and muconic acid were never detected during our phenol oxidation experiments.

### 4.4.8. Mechanistic interpretation and reaction pathways

The oxidation of phenol in aqueous solution is very complex for both non-catalytic and catalytic systems. A proposal of a complete mechanism of platinum catalysed oxidation of phenol based on the evidence presented is not yet possible. However, the

reaction intermediates and end products observed in this study (Table 4.2) provide a basis to postulate a preliminary reaction mechanism. During oxidation, phenol seems to react to either catechol or hydroquinone, which can react further to end products. The π-electrons of the phenol molecule are uniformly conjugated over the C-atoms and the O-atom, while for σ-bonds a dipole points towards the OH-group. Catalysts in the presence of oxygen can promote the formation of hydroxyl radicals, which can activate the phenol aromatic ring. This makes phenol become most reactive at the *para*-position especially for non-catalysed reactions in acidic environment. However, the reaction pathways and selectivity to CO_2 and H_2O seem to be controlled by the extent of oxygen coverage of the platinum surface.

The results strongly suggest four possible situations (see Scheme 4.1), namely: fully oxidised, partly oxidised, free, and partly hydrogen covered platinum surfaces. When the oxidation takes place on a partly oxidised surface of platinum (Scheme 4.1(b)), phenol and oxygen adsorb simultaneously and react on the platinum surface. The high potential of the platinum surface orients the phenol molecule in such a way that dehydrogenation of the *ortho*-C-H can take place followed by hydration or hydroxylation to form catechol, which reacts further through unstable *ortho*-benzoquinone and ring-cleavage compounds and finally to CO_2 and H_2O. It is well known that *ortho*-benzoquinone is fairly unstable and easily cleaved to form aliphatic compounds (Alnaizy and Akgerman, 2000). This mechanism can be maintained when the reaction is carried out within the proper operation window (Masende *et al.*, 2003a).

A fully oxidized platinum surface results in a change in the selectivity of the reaction, and favours the formation of *p*-benzoquinone as simplified in Scheme 4.1(a). Under such reaction conditions, rapid loss of catalyst activity ascribed to 'over-oxidation' has been observed although it was temporary and could be reversed at reducing conditions. When the platinum surface is fully covered with oxygen (PtO_x), it is possible that the reaction proceeds under the free radical mechanism resulting into oxygen insertion at the *para*-position of the phenol molecule to form *p*-benzoquinone. The formation of *p*-benzoquinone when high oxygen loads are employed (Fig. 4.1) confirms this mechanism. We observed further that a prolonged operation with a fully oxidised platinum surface favoured the formation of polymeric products, which resulted into permanent deactivation of the catalyst (fouling). Analogous findings have been obtained during electrochemical oxidation of aqueous phenol (Gattrell and Kirk, 1993).
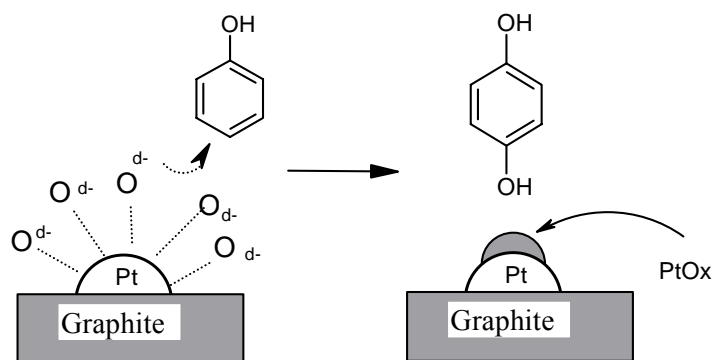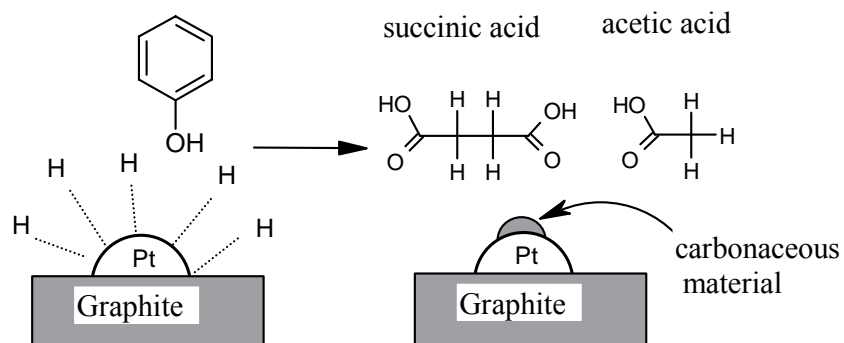
(a) Over-oxidized Pt surface. Steps: attack by OH radicals or oxygen insertion.
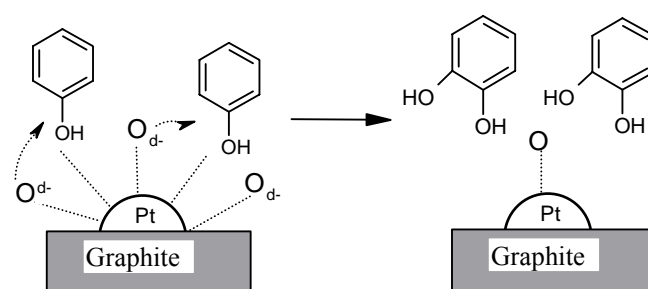
(b) Partly oxidized Pt surface. Steps: dehydrogenation, or hydroxylation.
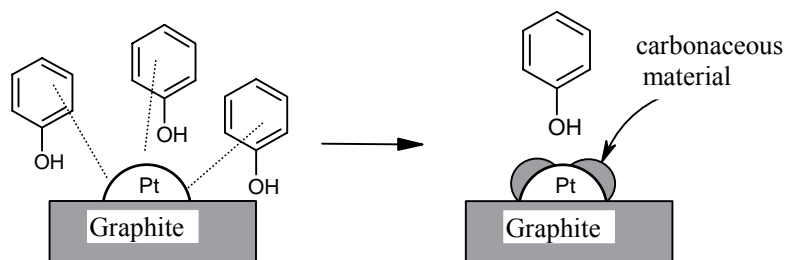
(c) Free Pt surface. Steps: carbon deposition.

(d) Partly hydrogen covered Pt surface. Steps: ring cleavage and hydrogenation.

Scheme 4.1. Mechanisms of platinum catalysed phenol oxidation.

While a free platinum surface was vulnerable to poisoning by carbonaceous compounds (Scheme 4.1(c)), a partly hydrogen covered platinum surface favoured the formation of acetic and succinic acid which are difficult to oxidize (Scheme 4.1(d)). The possible source of hydrogen in this case is phenol dehydrogenation. Also mixed situations are likely to occur during the reaction.

The mechanism of platinum catalysed oxidation of phenol, which is favoured in the presence of oxygen at the platinum active sites, seems to involve splitting of the C-H bonds. Therefore the first role of oxygen is to raise the oxidation potential of the platinum necessary for releasing of a proton from the C-H bond ready for oxidation. At low oxidation potential, platinum active sites are vulnerable to poisoning by carbonaceous matter. The second role of oxygen is possibly protection of the platinum surface from irreversible poisoning by carbonaceous matter.

It is suggested that there exist two catalytic routes for phenol oxidation. Scheme 4.2 presents the corresponding reaction network derived from the observed intermediate and end products. One route, which was clearly identified during the reaction start-up with 'oxidative' method (oxygen first fed into the reactor followed by phenol), shows that phenol reacts through hydroquinone to *p*-benzoquinone, which reacts further to maleic acid (C-4) and carboxylic acid (C-2), and finally to the end products.

However, once *p*-benzoquinone is formed, molecular coupling or polymerisation is likely to occur. This reaction route is favoured when there is a relatively high oxygen load on the platinum surface. At stoichiometric oxygen excess close to 0% the platinum catalysed reaction goes through catechol, o-benzoquinone and ring opening compounds (the second route), and finally to CO_2 and H_2O. The most favourable reaction seems to be the splitting of the C-6 ring into C-4 (e.g. maleic acid) and C-2 (e.g. glyoxylic or oxalic acid) which reacts further to end products.

The desired reaction pathway for platinum catalysed phenol oxidation is indicated by the bold arrows in Scheme 4.2. The explanation of this mechanism is not obvious, however it is logical to speculate that at S.E. within 0-80%, the platinum surface is at a relatively low oxidation potential, such that dehydrogenation and afterwards hydroxylation of the phenol molecule is favoured at the *ortho*-C-H bond to form catechol, a very reactive intermediate to carbon dioxide. As proposed earlier, catechol is a strong reducer on platinum, therefore the presence of oxygen on the platinum surface is of great importance to prevent transfer hydrogenation reaction to stable succinic and acetic acid.

Scheme 4.2. Proposed reaction scheme in this work for liquid phenol oxidation catalyzed with graphite supported platinum catalyst. *Reaction steps include: 1 - oxidation; 2 - C-C bond cleavage; 3 - decarboxylation; 4 - transfer hydrogenation; 5 - molecular coupling or polymerization.*

4.5. Conclusions

It has been shown that the activity of the Pt/graphite catalyst and hence the selectivity of the oxidation products are influenced by the degree of oxygen coverage of the platinum surface. Four situations can be postulated from the extent of oxygen coverage, namely: over-oxidised, partly oxidised, free, and reduced platinum surfaces. Full conversion of phenol to CO_2 and H_2O is mostly favoured on a partly oxidised platinum surface. The first role of oxygen is to raise the oxidation potential of the platinum necessary for releasing of a proton from the C-H bond ready for oxidation. At low oxidation potential, platinum active sites are vulnerable to poisoning by carbonaceous matter. The second role of oxygen is the protection of the platinum surface from irreversible poisoning by carbonaceous matter.

The reaction pathways for platinum catalysed oxidation of phenol are reported in this work (Scheme 4.2). At low stoichiometric oxygen excess, phenol is fully oxidised to CO_2 via catechol and o-benzoquinone. The most favourable reaction seems to be the splitting of the C-6 ring into C-4 and C-2 compounds which react to end products. Similarly, at higher stoichiometric oxygen excess, phenol reacts through hydroquinone, which forms *p*-benzoquinone. It is clearly observed that p-benzoquinone is responsible for polymer formation. In addition, it has the potential to cause deactivation of the platinum catalyst by blocking of active sites leading to over-oxidation of the residual platinum sites.

It was found that glyoxylic acid is not a polymer precursor. Furthermore, it appears that both maleic and oxalic acid might be formed through parallel reaction of *p*-benzoquinone or o-benzoquinone by carbon-carbon cleavage and oxidation. While malonic acid is formed from catechol by ring cleavage and oxidation, it reacts by direct oxidation (40%) to form CO_2 and by decarboxylation (60%) to form acetic acid and CO_2. The formation of propanoic acid in relatively high concentration, which remains stable at the test conditions, excludes muconic acid as an intermediate during phenol oxidation since both propanoic and muconic acid were never detected during phenol oxidation.

Acknowledgements

Nomenclature

CSTR	continuous stirred tank reactor
CWO	catalytic wet oxidation
GC	gas chromatography
HPLC	high performance liquid chromatography
O_2-FIRST	reactor start-up with oxygen first followed by oxygen
O_2-Ph-Sim	simultaneous feed of oxygen and phenol at start of reaction
Ph	phenol
Ph-FIRST	reactor start-up with phenol first followed by phenol
Pt	platinum

SCWO   supercritical water oxidation
S.E.   stoichiometric oxygen excess [%]

References

Alnaizy, R. and Akgerman, A., Adv. Environ. Res. 4 (2000) 233.

Devlin, H.R. and Harris, I.J., Ind. Eng. Chem. Fundam. 23 (1984) 387.

Fogler, H.S., "Elements of Chemical Reaction Engineering", 3rd Ed., Prentice Hall, Upper Saddle River NJ, 1999, p.577.

Fortuny, A., Font, J. and Fabregat, A, Appl. Catal. B 19(3-4) (1998) 167.

Gattrell, M. and Kirk, D.W., J. Electrochem. Soc. 140 (1993) 1534.

Gomes, H.T., Figueiredo, J.L. and Faria, J.L., Appl. Catal. B 27 (2000) L217.

Hamoudi, S., Belkacemi, K. and Larachi, F., Chem. Eng. Sci. 54 (1999) 3569.

Hamoudi, S., Larachi, F. and Sayari, A., J. Catal. 177 (1998) 247.

Harmsen, J.M.A., Jelemensky, L., van Andel-Schefer, P.J.M., Kuster, B.F.M. and Marin, G.B., Appl. Catal. A 165 (1997) 499.

Luck, F., Catal. Today 53 (1999) 81.

Mallat, T. and Baiker, A., Catal. Today 19 (1994) 247

Markusse, A.P., Kuster, B.F.M. and Schouten, J.C., J. Mol. Catal. A: Chem. 158 (2000) 215.

Masende, Z.P.G., Kuster, B.F.M., Ptasinski, K.J., Janssen, F.J.J.G., Katima, J.H.Y. and Schouten, J.C., Appl. Catal. B 41 (2003a) 247.

Matatov-Meytal, Yu.I. and Sheintuch, M., Ind. Eng. Chem. Res. 37 (1998) 309.

Mishra, V.S., Mahajani, V.V. and Joshi, J.B., Ind. Eng. Chem. Res. 34 (1995) 2.

Ohta, H., Goto, S. and Teshima, H., Ind. Eng. Chem. Fundam. 19 (1980) 180.

Pintar, A. and Levec, J., Chem. Eng. Sci. 47 (1992) 2395.

Pintar, A. and Levec, J., Ind. Eng. Chem. Res. 33 (1994) 3070.

Rivas, J., Kolaczkowski, S.T., Betran, F.J. and McLurgh, D.B., Appl. Catal. B 22 (1999) 279.

Sadana, A. and Katzer, J.R., Ind. Eng. Chem. Fund. 13 (1974) 127.

Santos, A., Yustos, P., Quintanilla, A., Rodriguez, S., and Garcia-Ochoa, F., Appl. Catal. B 39 (2002) 97.

Savage, P.E., Catal. Today 62 (2000) 167.

Savage, P.E., Chem. Rev. 99 (1999) 603.

Ukropec, R., Kuster, B.F.M., Schouten, J.C. and van Santen, R.A., Appl. Catal. B 23 (1999) 45.

Vleeming, J.H., Kuster, B.F.M. and Marin, G.B., Ind. Eng. Chem. Res. 36 (1997) 3541.

Vogel, F., Harf, J., Hug, A. and Von Rohr, P.R., Wat. Res. 34 (2000) 2689.

5

PLATINUM CATALYSED WET OXIDATION OF PHENOL IN A STIRRED SLURRY REACTOR: MASS TRANSFER AND REACTION KINETICS

Abstract

The catalytic performance of graphite supported platinum (5-wt.%) catalyst in liquid phase phenol oxidation has been studied in a continuous stirred tank (CSTR) slurry reactor. The study was carried out for a temperature range of 120 to 180 °C and for a total pressure range of 1.5 to 2.0 MPa. Other operational variables employed were oxygen partial pressure (0.01 - 0.8 MPa), initial phenol feed concentration (5 - 70 mol/m^3), and catalyst amount (0.2 - 12.0 g of Pt/graphite). The selectivity and activity of the platinum catalyst depend strongly on the transfer rate of oxygen to the catalyst. Carbon dioxide and water are the only products when the reaction proceeds at oxygen gas-liquid mass transfer limitation conditions. In surplus of oxygen, the side products p-benzoquinone, maleic acid, and low molecular weight carboxylic acids were detected. A model was developed that predicts the performance of phenol oxidation in a CSTR in the mass transfer limited regime and within the practical operation window.

Keywords: Catalytic wet oxidation; Phenol oxidation; Platinum catalyst deactivation; Mass transfer; Kinetics; Multiphase reactors

5.1.   Introduction

Water pollution by toxic organic compounds has become a serious environmental problem in both developed and developing countries like Tanzania. The catalytic wet oxidation of carbon containing compounds, such as phenol, leading ultimately to carbon dioxide and water, is one possible way to solve water pollution problems. The use of platinum metal catalysts for liquid phase oxidation provides a potential for treatment of wastewaters containing organic pollutants.

Platinum catalysts have been reported to be effective during catalytic liquid phase oxidation of alcohols (Markusse *et al.*, 2001; Mallat and Baiker, 1994), formic acid (Harmsen *et al.*, 1997), and ammonia (Ukropec *et al.*, 1999). However, a rapid loss of activity of platinum catalyst was observed in these studies. While platinum catalysts are widely used in hydrogenation reactions and hydro-processing, information on the application of platinum catalysts for wet oxidation of organic pollutants is still meagre. The kinetics of phenol oxidation in the liquid phase is very complex and not well understood. A wide range of reaction steps and mechanisms for phenol oxidation are reported for both catalysed and non-catalysed wet air oxidation at supercritical as well as subcritical conditions (Savage, 2000; Luck, 1999; Matatov-Meytal and Sheintuch, 1998; Mishra *et al.*, 1995; Levec and Pintar, 1995). There is little information on the activity and kinetics of platinum catalysed phenol oxidation in the liquid phase (Maugans and Akgerman, 1997). Many factors can influence the oxidation of phenol and the activity of platinum catalyst. Such factors include concentrations of reactants, reaction products, catalyst type, size and type of the catalyst supporting material, temperature, and mass transport properties of the reactor system.

While kinetic models developed so far are applicable at intrinsic kinetic conditions only, the role of mass transport of the reactants during oxidation is not adequately addressed. For platinum catalysed wet oxidation, oxygen mass transfer is of crucial importance since the behaviour of the platinum catalyst is influenced by the oxygen coverage (Markusse *et al.*, 2001; Mallat and Baiker, 1994). The operation window in which full phenol conversion and high selectivity to CO_2 can be achieved without deactivation of the catalyst has been recently reported (Masende *et al.*, 2003). It was revealed that platinum over-oxidation is the major cause of deactivation under oxygen rich conditions. When the slurry reactor was operated in the mass transport limited regime, with residual oxygen partial pressure below 150 kPa, the platinum catalyst showed high activity, while above 150 kPa the catalyst gave the same performance as

metal oxide catalysts. However, the effects of mass transfer and reaction kinetics on catalyst performance still need clarification.

The objectives of the present work are to quantify and model the performance of Pt/graphite catalyst in liquid phase oxidation of phenol. The model can be used to define adequately the operation window for phenol oxidation over platinum catalysts. Experiments were performed in a continuous stirred (CSTR) slurry reactor in which the catalyst activity was monitored. A detailed investigation of the effects of reactor operation parameters is presented. This includes the effect of stirring speed, amount of catalyst, and the concentration of oxygen and phenol in the bulk liquid as well as at the catalyst surface.

Table 5.1
Range of reactor operating conditions

	Standard	Range
Temperature, °C	150	120 - 180
Total pressure, MPa	1.8	1.5 – 2.0
Oxygen partial pressure, MPa	0.5	0.01 – 0.8
Oxygen flow rate, ml/min	40	0 - 80
Nitrogen flow rate, ml/min	90	10 -120
Phenol concentration, mol/m^3	20	5 - 70
Liquid flow rate, ml/min	10	5 - 20
Liquid reactor volume, ml	350	350
Catalyst amount, g	3.5	0.2 – 12.0
pH	Uncontrolled	2 - 7
Stirrer speed, rpm	1200	350 -1800

5.2. Experimental

The experiments were conducted in a continuous flow stirred slurry reactor (CSTR), a 500 ml autoclave (Autoclave Engineers, Zipperclave Hastelloy), which is equipped with a gas dispersion impeller. The liquid phase oxidation of phenol by oxygen was investigated using a commercially available catalyst, graphite supported platinum with 5 wt.% platinum. The diameter of 95% of the graphite particles was smaller than 15 μm, as confirmed by particle size measurement (Coulter LS 130 apparatus). Other catalyst specifications include: metal surface area of 0.66 m^2.g^{-1} sample, metal dispersion 5.3%, and B.E.T. surface area of 15 m^2.g^{-1}. The experimental conditions are given in Table 5.1.

The optimum reactor start-up method requires simultaneous feed of both oxygen and phenol at reaction condition (Masende *et al.*, 2003). The catalyst was introduced into the reactor with 350 ml of water, and then the reactor was fed with helium gas to

pressurize before heating was started. When the desired reactor pressure and temperature were reached, both the liquid phenol solution and the gas mixture with oxygen at a given flow rate, were fed to the reactor and the reaction was monitored. The outlet liquid samples were analysed by on-line HPLC (Spectra Physics), in which phenol and other aromatic compounds were analysed using a UV detector while carboxylic acids were analysed using a refractive index detector. The composition of the outlet gas was determined by an oxygen sensor and on-line GC (HP 5890A Series II). Details about the experimental set-up, reactor operating procedures, and analytical procedures are reported elsewhere (Masende *et al.*, 2003).

The data obtained from the analyses of liquid and gases from the slurry CSTR were evaluated to give the phenol disappearance rate as well as conversion and selectivity to CO_2 and H_2O. The overall oxidation reaction for phenol using oxygen gas over platinum catalyst is given by equation (5.1) as:

$$C_6H_6O + 7\,O_2 \;\rightarrow\; 6\,CO_2 + 3\,H_2O \tag{5.1}$$

The net specific disappearance rate of phenol was calculated by:

$$R_{w,Ph} = \frac{F_{V,L}}{W}\left(C_{Ph,in} - C_{Ph}\right) - \frac{V_L}{W}\frac{dC_{Ph}}{dt} \tag{5.2}$$

The accumulation term (dC_{ph}/dt) is required to get relevant rate data also at non-steady state conditions during the reactor start-up period. The percentage phenol conversion is defined using the expression:

$$X_{Ph} = \frac{R_{W,Ph} \cdot W}{F_{V,L} \cdot C_{Ph,in}} \times 100\ \% \tag{5.3}$$

The rates of formation of reaction intermediates and end products were similarly calculated by:

$$R_{w,i} = \frac{F_{V,L}}{W}C_i + \frac{V_L}{W}\frac{dC_i}{dt} \tag{5.4}$$

The rate of oxygen consumption for complete oxidation of phenol to CO_2 and H_2O can be calculated from the phenol reaction rate as:

$$R_{O_2} = 7\,R_{Ph} = 7W\,R_{w,Ph} \tag{5.5}$$

For all experimental data, the carbon balance as well as the oxygen balance was verified after every experiment and it were within 95 - 100%, which was considered analytically acceptable. The inlet gas stream is composed of oxygen, nitrogen, and helium while carbon dioxide gas is formed in the reactor. The rate of oxygen consumption in the reactor was calculated from the mole fractions of gas components entering and leaving the reactor.

5.3. Effects of reactor operation conditions

The influence of the impeller stirring speed on phenol oxidation was studied at 165 °C with 20 mol/m^3 phenol solution and stoichiometric oxygen excess of 20% using 3.5-g of Pt/graphite catalyst. Fig. 5.1 shows the dependence of the overall phenol reaction rate, expressed in terms of rate of CO_2 formation, on the stirring speed. The rate of CO_2 formation reaches a maximum value above a stirrer speed of 1200 rpm. This indicates that above this stirrer speed, the contacting of phenol and oxygen at the catalyst surface is sufficient and full phenol conversion to CO2 can be obtained. The effect of catalyst amount on the reaction rate was investigated at 165 °C by varying the catalyst amount over the range 0.2 – 12.0 g of Pt/graphite. Fig. 5.2 shows the effect of the catalyst concentration on phenol conversion to CO_2 for two feed concentrations of 5 and 20 mol/m^3 of phenol. Initially, the reaction rate increases with increase in the amount of catalyst. While the catalyst concentration of ca. 2 kg/m^3 is sufficient for full conversion of 5 mol/m^3 of phenol solution, 10 kg/m^3 of catalyst is needed for full conversion of 20 mol/m^3 of phenol.
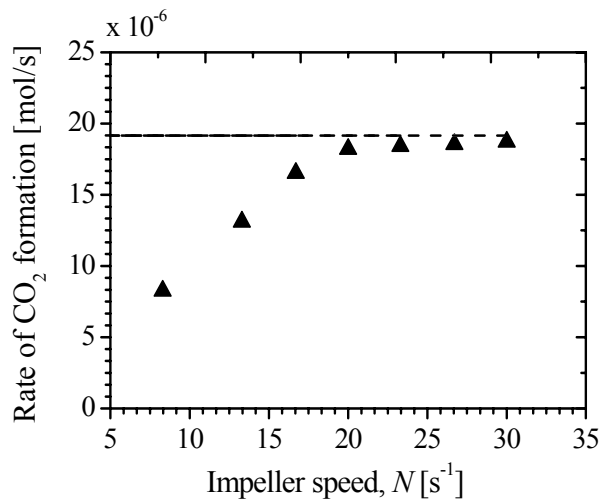
Fig. 5.1. Steady state rate of CO_2 formation at different impeller stirrer speeds during phenol oxidation: (▲) measured, and (---) stoichiometric CO_2 formation rate based on phenol feed flow. Conditions: W = 3.5 g Pt/graphite, T = 165 °C, V_L = 0.35 l, F_{vL} = 10 ml/min, $C_{ph,in}$ = 20 mol/m^3, and S.E. = 20%.
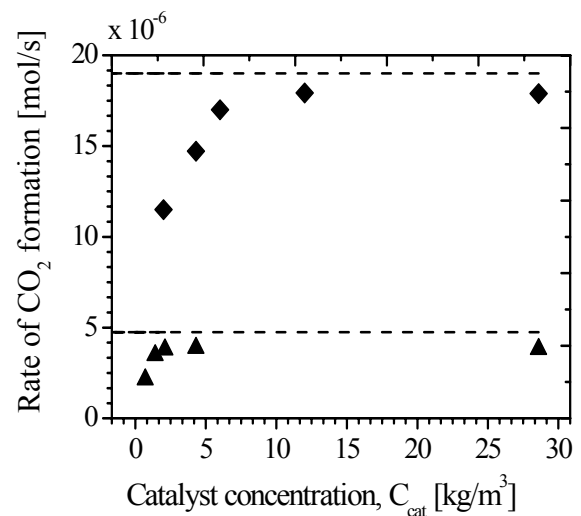
Fig. 5.2. Steady state rate of CO_2 formation at different catalyst concentrations during phenol oxidation: (▲) $C_{ph,in}$ = 5 mol/m^3, (♦) $C_{ph,in}$ = 20 mol/m^3 solution, (---) stoichiometric CO_2 formation rate. Conditions as in Fig. 5.1 and N = 20 s^{-1}.

The influence of the liquid flow rate and the initial phenol concentration was studied at stoichiometric excess of oxygen of 20%. Fig. 5.3(a) shows the reaction rate at different

molar flow rates of phenol. Both the variation in phenol concentration and the variation of liquid flow rate show the same effects, i.e. the reaction rate of phenol and hence the CO_2 formation rate increase with increasing molar flow of phenol until the catalyst activity starts declining. The effect of phenol feed concentration is depicted further in Fig. 5.3(b) in which high residual phenol concentration and oxygen partial pressure are observed at higher molar flow rate of phenol. The stagnating phenol reaction rate observed at high phenol flow rate can be explained by deactivation of the platinum catalyst as a result of the higher oxygen load.

The higher residual oxygen partial pressure in the reactor, i.e. above 150 kPa, can cause catalyst deactivation by so-called over-oxidation (Markusse *et al.*, 2001; Mallat and Baiker, 1994). This is in agreement to our previous findings (Masende *et al.*, 2003) where high activity of platinum catalyst was maintained when the residual oxygen partial pressure in the reactor was kept below 150 kPa.
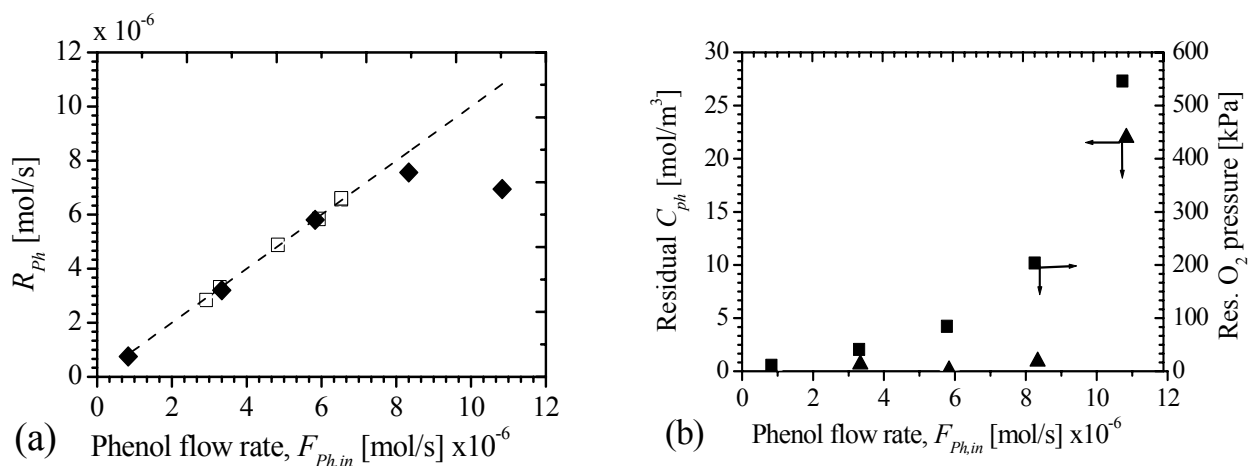
Fig. 5.3. Effect of initial phenol flow rate on: (a) steady state phenol disappearance rate, where (♦) different $C_{ph,in}$ at $F_{V,L}$ = 10 ml/min, (□) different $F_{V,L}$ with $C_{ph,in}$ = 20 mol/m³ solution, (---) theoretical phenol reaction rate; and (b) residual phenol concentration (▲), and residual oxygen partial pressure (■) at different feed concentrations. Conditions as in Fig. 5.1 and $N = 20$ s⁻¹.

The oxygen excess to phenol and hence partial pressure has a pronounced effect on the rate of phenol oxidation as can be clearly seen in Fig. 5.4. The conversion of phenol and the selectivity to CO_2 increase with increasing oxygen flow rate up to a stoichiometric oxygen excess of 20%, followed by a decrease at higher oxygen flow rate. It was observed that although higher phenol conversion can be achieved at substoichiometric oxygen levels (S.E. of - 36%), the partial oxidation products are mainly carboxylic acids, including succinic and acetic acids, which were difficulty to oxidize at the experimental conditions. The rapid decline of the reaction rate at higher

S.E. again is explained by the over-oxidation of the platinum catalyst. Over-oxidation of platinum catalyst leads to the formation of p-benzoquinone and insoluble products attributed to polymers (Masende *et al.*, 2003).

It can be concluded from the experimental results that the oxygen load and hence the extent of oxygen coverage of the platinum catalyst has a great role on the performance of phenol oxidation. To quantify the performance of platinum catalysts within the optimum operation window (Masende *et al.*, 2003) a model that involves transport of oxygen and phenol to the catalyst is preferred.
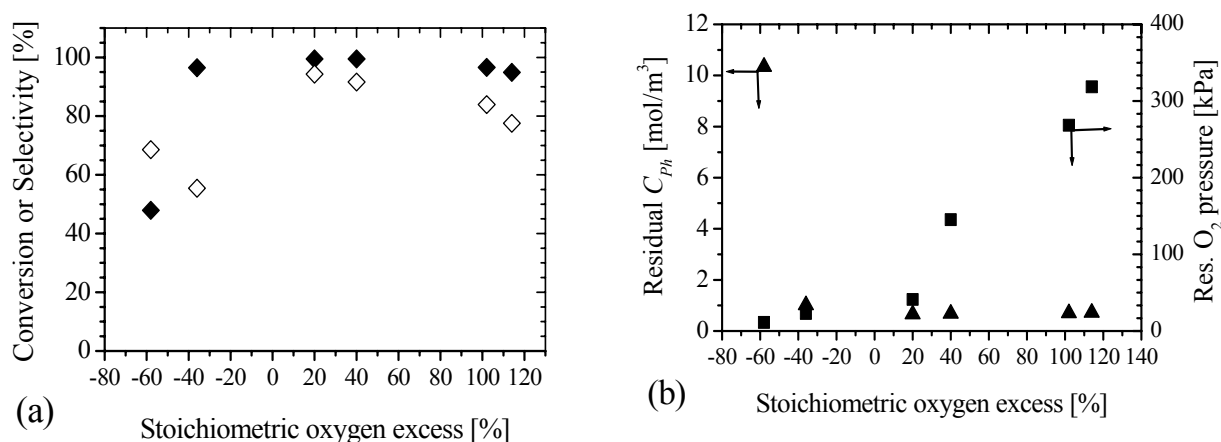
Fig. 5.4. Effect of stoichiometric oxygen excess (S.E.) on: (a) steady state phenol conversion (♦), selectivity to CO_2 (◊); (b) residual oxygen partial pressure (■) and residual phenol concentration (▲). Conditions: $W = 3.5$ g Pt/graphite, $N = 20$ s^{-1} and as in Fig. 5.1.

5.4.   Model development and evaluation

5.4.1. Mass-transfer equations for platinum catalysed phenol oxidation

The performance of the phenol oxidation reaction over the solid catalyst in a slurry reactor depends amongst others on interphase and intraparticle heat and mass transfer, mixing of the gas and liquid phases, and on the reaction kinetics. The model was constructed using the following assumptions:

  i. The reactor is perfectly mixed and isothermal;
  ii. The overall reaction for phenol oxidation is second-order, i.e. first order with respect to oxygen and first order to phenol;
  iii. Carbon dioxide and water are the only end products during phenol oxidation and products desorption from the external surface of the catalyst particles to the bulk liquid is not rate limiting;

iv.   The solubility of carbon dioxide at ambient conditions in acidic water is very low and is neglected;

v.   The amount of water vapour in the gas phase is very low and is neglected;

vi.   The concentration of water in the liquid phase is much higher compared to other reactants and therefore was considered as constant;

vii.   The concentration of phenol in the gas phase due to evaporation is neglected;

viii.   All gases entering and leaving the reactor behave ideally during the reaction.

Neglecting the gas phase transfer resistance at the gas side of the gas-liquid interphase, the transfer rate of oxygen at steady state condition is given by:

$$F_{O_2} = k_L \cdot a \cdot V_L \cdot \left(C_{O_2,i} - C_{O_2,b} \right) \tag{5.6}$$

The oxygen concentration in the liquid phase was calculated using the correlation of Battino (1981). The transfer rate of oxygen to the external surface of the catalyst particles is calculated as:

$$F_{O_2} = k_{s,O_2} \cdot a_s \cdot W \cdot \left(C_{O_2,b} - C_{O_2,s} \right) \tag{5.7}$$

The type of catalyst used (Pt/graphite) is an "egg-shell" catalyst where the active sites are located at the external surface. Therefore, diffusion inside the particle is negligible, that means, the effectiveness factor is considered to be unity. The transfer rate of phenol can be evaluated by considering the rate of mass-transfer from the bulk solution to the external surface of the catalyst particles as:

$$F_{Ph} = k_{s,ph} \cdot a_s \cdot W \left(C_{Ph,b} - C_{Ph,s} \right) \tag{5.8}$$

The mass transfer-coefficients from liquid to solid, $k_{s,O2}$ and $k_{s,Ph}$ are calculated from the Sherwood number as described by Sano *et al.* (1974). The overall rate of reaction at the catalyst particle surface is defined by:

$$R_{O_2} = 7 R_{Ph} = 7 k_w \cdot W \cdot C_{O_2,s} \cdot C_{Ph,s} \tag{5.9}$$

The overall expression for the rate of phenol oxidation and for the rate of transport of reactants, i.e. phenol and oxygen, to the catalyst particle surface can be established by combining equations (5.6) through (5.9). When oxygen transport is limiting ($C_{Ph,s} = C_{Ph,b}$), the rate equation is described by:

$$R_{O_2} = \frac{C_{O_2,i}}{\left[\dfrac{1}{k_L\, a V_L} + \dfrac{1}{k_{s,O_2}\, a_s W} + \dfrac{1}{7 k_w\, W\, C_{Ph,b}} \right]} \tag{5.10}$$

If phenol transport is limiting ($C_{O2,s} = C_{O2,i}$), then the reaction rate is given by:

$$R_{O_2} = \frac{7\, W\, C_{Ph,b}}{\left[\dfrac{1}{k_{s,Ph}\, a_s} + \dfrac{1}{k_w\, C_{O_2,i}} \right]} \tag{5.11}$$

However, if k_w is very large then either $C_{O2,s} \cong 0$ or $C_{Ph,s} \cong 0$, which means that a maximum transfer rate of either oxygen or phenol, respectively, to the catalyst surface is obtained. Taking into account these assumptions, the maximum oxygen transfer rate (for $C_{O2,s} \cong 0$) is obtained from Eq. (5.10) as:

$$R_{O_2,\max} = \frac{C_{O_2,i}}{\left[\dfrac{1}{k_L aV_L} + \dfrac{1}{k_{s,O_2} a_s W} \right]} \tag{5.12}$$

Similarly, the maximum transfer rate for phenol (for $C_{Ph,s} \cong 0$) was obtained from Eq. (5.8) as:

$$R_{Ph,\max} = k_{s,Ph} \cdot a_s \cdot W \cdot C_{Ph,b} \tag{5.13}$$

Experimental data for R_{O2}, calculated using Eqs. (5.2) and (5.5), were used to estimate the mass transfer and kinetic rate parameters, $k_L a$, k_s, and k_w in Eqs. (5.10) and (5.11).

Table 5.2
Mass transfer and kinetic rate parameters at T = 165 °C, P_T = 1.8 MPa , and N = 20 s^{-1}

Parameter	SI units	Graphical	Regression
$k_L a$	[s^{-1}]	0.14	0.16 ± 0.04
k_w	[m^3/kg.s]	-	10.4 ± 2.2
$k_{s,O2}$	[m/s]	$3.8.10^{-3}$	$4.7.10^{-3}$
$k_{s,Ph}$	[m/s]	-	$4.3.10^{-3}$
$k_{s,O2}a_s$	[m^3/kg.s]	2.11	2.61 ± 0.15
$k_{s,Ph}a_s$	[m^3/kg.s]	-	2.38 ± 0.01

5.4.2. Parameter estimation

The type of reactor used has a gas dispersion hollow impeller and two baffles in addition to the internals, which ensures sufficient mixing of reactants and catalyst particles. The mass transfer parameters $k_L a$, $k_{s,O2}a_s$, and $k_{s,Ph}a_s$ were determined from the experimental data by a graphical fitting method as well as by regression analysis. The regression analysis was performed using equations (5.10) and (5.11). The results are summarised in Table 5.2 in which the estimate for the reaction rate parameter k_w is also included.

The gas-liquid mass transfer coefficient, $k_L a$, was determined graphically assuming that the reaction rate constant k_w is very high. Therefore Eq. (5.12) is rearranged to give a plot of $ln [(V_L C_{O2,i}/R_{O2}) - (1/k_s a_s C_{cat})]$ versus $ln N$ (see Fig. 5.5a). A straight line with a slope of 3.1 is obtained which is the power with respect to varying stirring speed. The value of 3.1 is comparable to the theoretical value of 3.0 (Beenackers and van Swaaij, 1993).

Fig. 5.5(b) shows the influence of the impeller speed on $k_L a$ over the range of 600 to 1800 rpm. The gas-liquid mass transfer coefficient was compared with the correlations by Tekie *et al.* (1997) for a gas-inducing reactor (GIR). The estimated values are slightly lower than those obtained from the correlation of Tekie *et al.* (1997). The observed deviation could be due to different experimental environments, like presence of catalyst, reaction intermediates and end products, and the reactor geometry. Typical values for $k_L a$ are in the range of $0.1 - 0.5$ s^{-1} for both industrial and laboratory slurry reactors (Beenackers and van Swaaij, 1993).

(a)
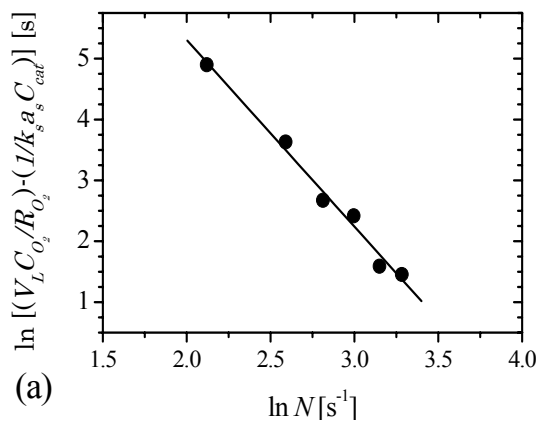
Fig. 5.5(a). Determination of $k_L a$ and dependency on the impeller speed; conditions see Fig. 5.1. The slope of the line is -3.1.

(b)
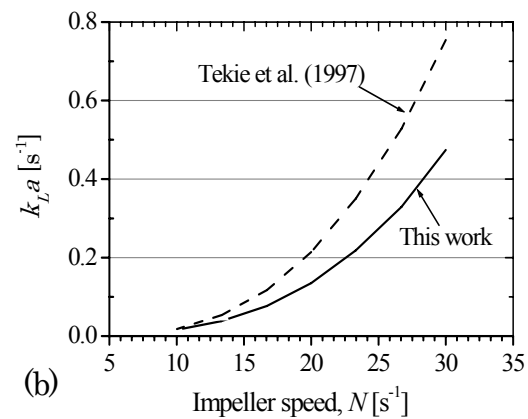
Fig. 5.5(b). Influence of impeller speed on $k_L a$; from this work the relationship $k_L a = 1.25 \times 10^{-5} N^{3.1}$ is obtained.

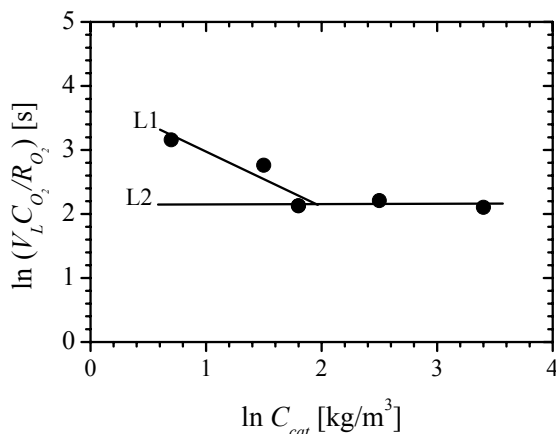

Fig. 5.6. Determination of $k_L a$, $k_s a_s$ and the power with respect to catalyst concentration: conditions see Fig. 5.2. The slope of line L1 is - 0.87, which is the power to the catalyst concentration.

In order to ascertain the contribution of the amount of catalyst on the phenol reaction rate, Eq. (5.12) was rearranged to fit the experimental data on a plot of $ln(V_L C_{O2,i}/R_{O2})$ versus $ln (C_{cat})$. Fig. 5.6 shows the best fit in which the power of - 0.87 fits the experimental data quite well. The y-intercept of 2.2 was obtained from the horizontal line and it is the contribution of both $k_L a$ and $k_{s,O2} a_s$ when the reaction becomes fully gas-liquid mass transfer controlled. The value of 2.11 m^3/kg.s for $k_{s,O2} a_s$ was obtained. This means, for the Pt/graphite particles used ($\rho_p = 720$ kg/m^3 and $d_p = 15$ μm), the a_s

value is 556 m^2/kg thus $k_{s,O2}$ becomes $3.8.10^{-3}$ m/s which corresponds to a Sherwood number of 3.1. This value is comparable to the value of 3.9 that is obtained from the correlation of Sano *et al.* (1974) at 1200 rpm.

The proposed model was evaluated from mass-transfer rate equations (5.10) and (5.12) in combination with mass balance equation for phenol and oxygen. Mass transfer parameters determined experimentally (Table 5.2) were used in the model simulations.
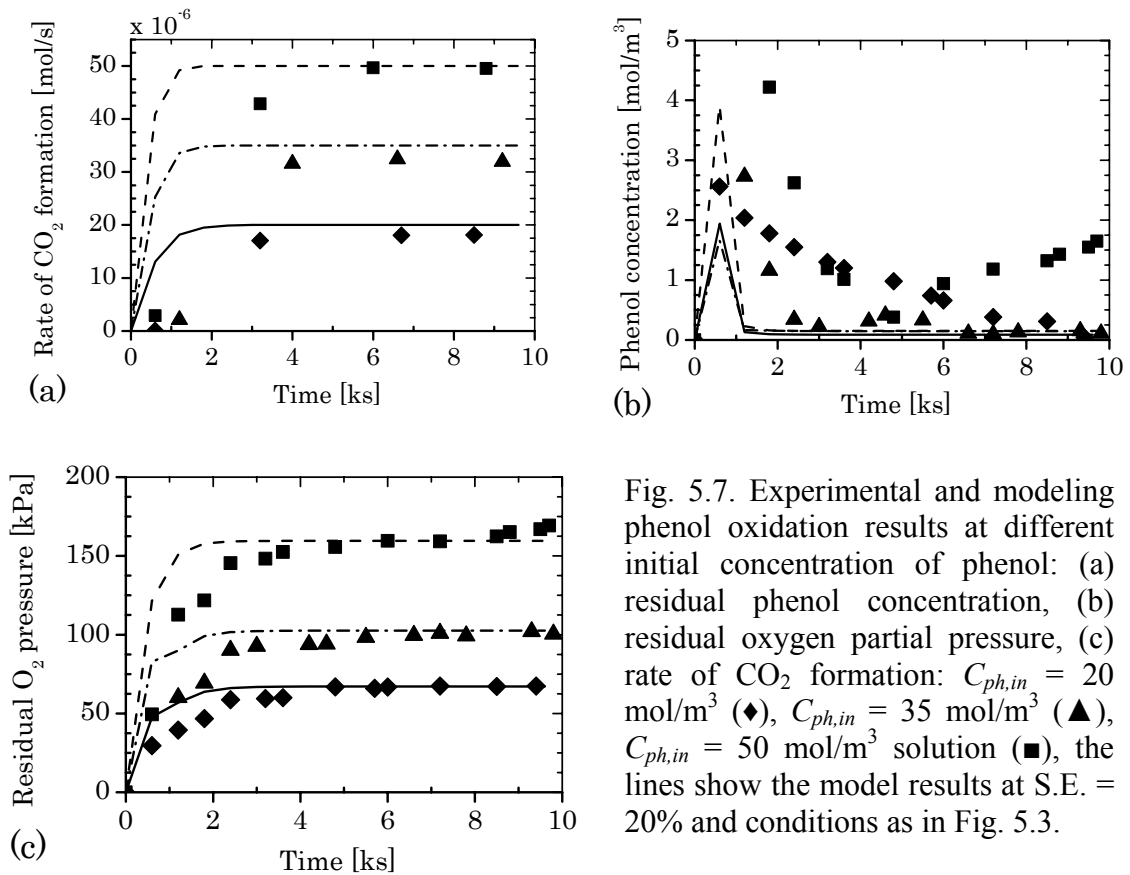

Fig. 5.7. Experimental and modeling phenol oxidation results at different initial concentration of phenol: (a) residual phenol concentration, (b) residual oxygen partial pressure, (c) rate of CO_2 formation: $C_{ph,in} = 20$ mol/m^3 (♦), $C_{ph,in} = 35$ mol/m^3 (▲), $C_{ph,in} = 50$ mol/m^3 solution (■), the lines show the model results at S.E. = 20% and conditions as in Fig. 5.3.

5.4.3. Simulation results

Model simulations were performed at different reactor conditions for the purpose of predicting the phenol conversion to CO_2, residual phenol concentration, and residual oxygen partial pressure. Fig. 5.7 shows the model predictions as well as experimental data for residual phenol concentration, residual oxygen partial pressure, and the rate of CO_2 formation. The predictions of the rate of CO_2 formation (Fig. 5.7a) and residual oxygen partial pressures (Fig. 5.7c) are in good agreement with the experimental data. However, the predicted residual phenol concentration is slightly different from experimental data (Fig. 5.7b), especially at measured residual phenol concentrations below 1 mol/m^3, which is less than 5% of the original concentration when 20 mol/m^3

phenol solution is used. The reason for the observed discrepancies is possibly two-fold; one being analytical errors for very low concentrations, and the other could be due to the effects of the reaction start-up procedure since the transient oxygen coverage of the platinum surface is not incorporated in the model.

Fig. 5.8 shows simulation results for the rate of CO_2 formation, residual concentration of phenol, and residual oxygen partial pressure at different oxygen flow rates, expressed in terms of stoichiometric oxygen excess. It is clear from Fig 5.8(a) that the model describes reasonably well the experimental data for the rate of CO_2 formation. Similar discrepancies in prediction however, are observed for residual phenol concentration during the first 2000 s as can be seen in Fig. 5.8(b). The model prediction for the residual oxygen partial pressure fits well with the experiemtnal data as can be seen in Fig. 5.8(c). Although the mass transfer model adequately describes the data, particularly at steady state conditions after 3000 s, the model needs to be extended to incorporate the transient oxygen coverage of the platinum surface.
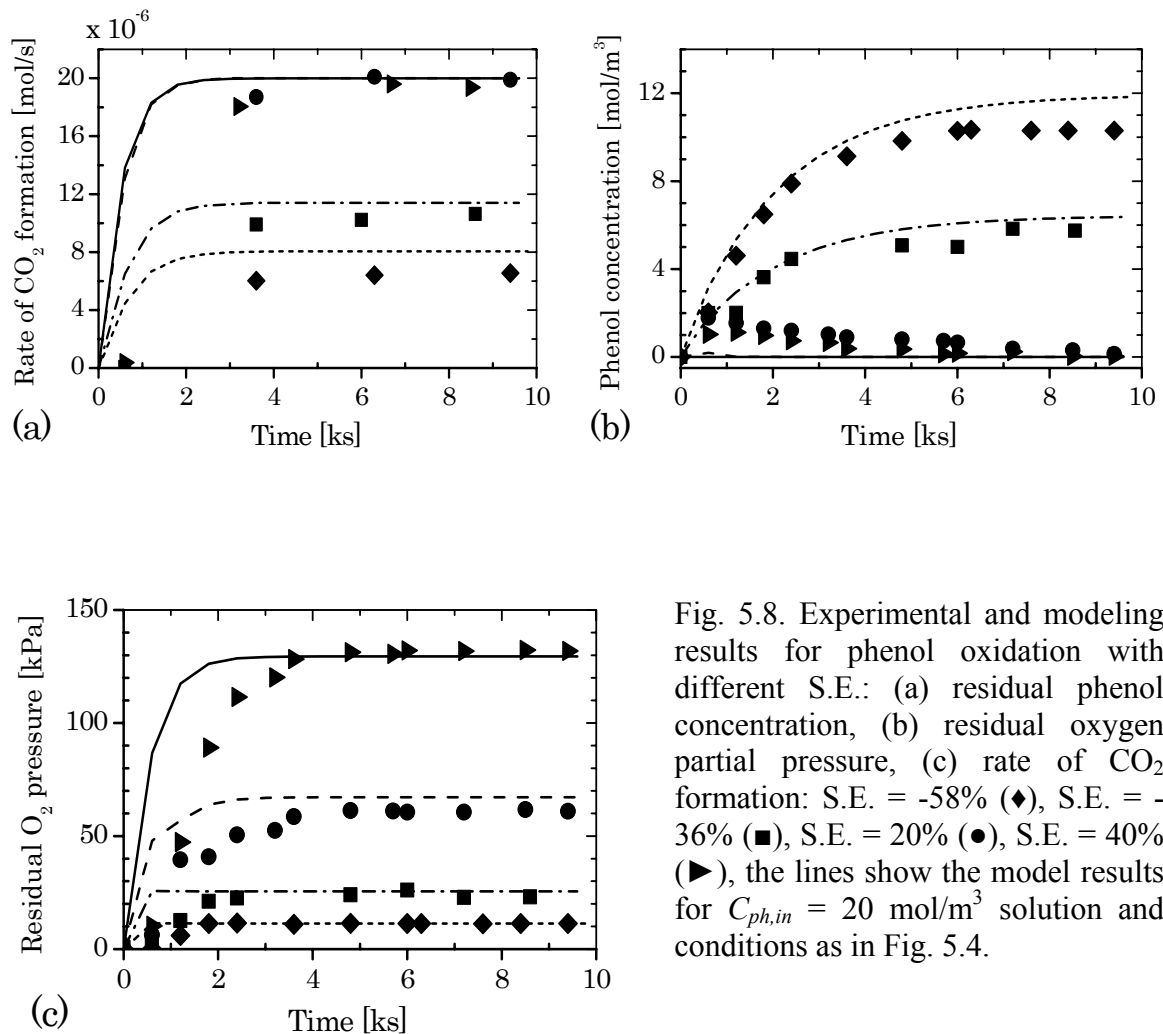

Fig. 5.8. Experimental and modeling results for phenol oxidation with different S.E.: (a) residual phenol concentration, (b) residual oxygen partial pressure, (c) rate of CO_2 formation: S.E. = -58% (♦), S.E. = -36% (■), S.E. = 20% (●), S.E. = 40% (►), the lines show the model results for $C_{ph,in}$ = 20 mol/m^3 solution and conditions as in Fig. 5.4.

5.5. Conclusions

The performance of Pt/graphite catalyst for liquid phase oxidation of phenol has been studied in a slurry phase CSTR. The effects of the main parameters such as stirrer speed, catalyst mass, and reactants concentrations have been discussed. Full phenol conversion and selectivity to CO_2 is obtained within stoichiometric oxygen excess to phenol from 0 to 20% (Fig. 5.4), and at residual partial pressure below 150 kPa. These boundaries of the operation window have been verified by the model predictions.

The impeller speed influences significantly the reaction rate (Fig. 5.1 & Fig. 5.5). The results indicate that oxygen transport to the catalyst, which determines the extent of oxygen coverage of the platinum surface, is a key factor in the reaction. The power, which expresses the contribution of the catalyst concentration during the reaction, is less than unity at low catalyst amount and decreases to reach zero order when excess amount of catalyst is used (Fig. 5.6). The values of the mass transfer parameters have been determined in this work. The gas-liquid mass transfer coefficient, $k_L a$, for oxygen was found to be 0.16 ±0.04 s^{-1} while the liquid–solid mass transfer coefficients, k_s, were $4.7.10^{-3}$ m/s and $4.3.10^{-3}$ m/s for oxygen and phenol respectively, at 1200 rpm.

The model developed in this paper predicts the performance of phenol oxidation over platinum catalyst in the mass transfer limited regime and within the practical operation window. The model fits well the experimental data, proving the hypothesis that platinum catalysed phenol oxidation to CO_2 takes place under oxygen transport controlled regime. The model, however, needs to be extended to predict the beginning of the reaction, where the reaction seems to be determined by both intrinsic kinetics and mass transfer.

Acknowledgements

Nomenclature

a gas-liquid interfacial surface area [m^2/m^3]

a_s weight specific liquid-solid interfacial surface area [m^2/kg]

C_i concentration of species i [mol/m^3]

C_{O2} oxygen concentration [mol/m^3]

C_{Ph} concentration of phenol in aqueous solution [mol/m^3]

d_p the powder size of the solid [m]

D_i diffusivity in water [m^2/s]

F_{O2} transfer rate of oxygen [mol/s]

F_{Ph} transfer rate of phenol [mol/s]

F_V volumetric flow rate [m^3/s]

k_La volumetric liquid-side mass transfer coefficient [1/s]

k_s liquid/solid mass transfer coefficient [m/s]

k_w weight specific reaction rate parameter [m^3/kg.s]

N impeller revolution speed [s^{-1}]

P pressure [Pa]

P_T total pressure in the reactor [Pa]

R_{O2} reaction rate of oxygen [mol/s]

R_{Ph} phenol reaction rate [mol/s]

V_L volume of the liquid in the reactor [m^3]

W total mass of dry catalyst in the reactor [kg]

Greek letters

ρ density [kg/m^3]

μ viscosity [kg/m.s]

σ surface tension [N/m]

Subscripts

b   bulk

G   gas

i   gas /liquid interface

in   inlet to reactor

L   liquid

out   outlet from reactor

p   particle

s   solid

T   total

w   weight specific

Abbreviations

cat   catalyst

CSTR   continuous stirred tank reactor

GIR   gas inducing reactor

GC   gas chromatography

HPLC   high performance liquid chromatography

max   maximum

Ph   phenol

Pt   platinum

sat   saturated

S.E.   stoichiometric oxygen excess [%]

References

Battino, R., Ed., 1981. IUPAC Solubility Data Series, Oxygen and Ozone. Pergamon Press, Oxford, 7.

Beenackers, A.A.C.M., van Swaaij, W.P.M., 1993. Mass transfer in gas-liquid slurry reactors. Chemical Engineering Science, 48, 3109-3139.

Harmsen, J.M.A., Jelemensky, L., van Andel-Schefer, P.J.M., Kuster, B.F.M., Marin, G.B., 1997. Kinetic modelling for wet air oxidation of formic acid on a carbon supported platinum catalyst. Applied Catalysis A: General, 165, 499-509.

Levec, J., Pintar, A., 1995. Catalytic oxidation of organics in aqueous solutions. 1. Kinetics of phenol oxidation. Journal of Catalysis, 135, 345-357.

Luck, F., 1999. Wet air oxidation: past, present and future. Catalysis Today, 53, 81-91.

Mallat, T., Baiker, A., 1994. Oxidation of alcohols with molecular oxygen on platinum metal catalysts in aqueous solutions. Catalysis Today, 19, 247-284.

Markusse, A.P., Kuster, B.F.M., Schouten, J.C., 2001. Platinum catalysed aqueous methyl α–D-glucopyranoside oxidation in a multiphase redox-cycle reactor. Catalysis Today, 126, 191-197.

Masende, Z.P.G., Kuster, B.F.M., Ptasinski, K.J., Janssen, F.J.J.G., Katima, J.H.Y., Schouten, J.C., 2003. Platinum catalysed wet oxidation of phenol in a stirred slurry reactor. A practical operation window. Applied Catalysis B: Environmental, 41, 247-267.

Matatov-Meytal, Yu.I., Sheintuch, M., 1998.Catalytic abatement of water pollutants. Industrial & Engineering Chemistry Research, 37, 309-326.

Maugans, C.B., Akgerman, A., 1997. Catalytic wet oxidation of phenol over a Pt/TiO$_2$ catalyst. Water Research, 31, 3116-3124.

Mishra, V.S., Mahajani, V.V., Joshi, J.B., 1995. Wet air oxidation. Industrial & Engineering Chemistry Research, 34, 2-48.

Sano, Y., Yamaguchi, N., Adachi, T., 1974. Mass transfer coefficients for suspended particles in agitated vessels and bubble columns. Journal of Chemical Engineering of Japan, 7, 255-261.

Savage, P.E., 2000. Heterogeneous catalysis in supercritical water. Catalysis Today, 62, 167-173.

Tekie, Z., Li, J., Morsi, B.I., Chang, M.Y., 1997. Gas-liquid mass transfer in cyclohexane oxidation process using gas-inducing and surface agitated reactors. Chemical Engineering Science, 52, 1541-1551.

Ukropec, R., Kuster, B.F.M., Schouten, J.C., van Santen, R.A., 1999. Low temperature oxidation of ammonia to nitrogen in liquid phase. Applied Catalysis B: Environmental, 23, 45-47.

6

KINETICS OF MALONIC ACID DEGRADATION IN AQUEOUS PHASE OVER Pt/GRAPHITE CATALYST

Abstract

This work aims at describing quantitatively the catalytic decarboxylation of malonic acid over a 5.0 wt% Pt/graphite catalyst. The study was carried out using a slurry phase CSTR at a temperature range of 120-160°C and at a reactor pressure of 1.8 MPa. The conversion of malonic acid during catalytic oxidation was found to proceed via decarboxylation to CO_2 and acetic acid, and also oxidation to CO_2 and H_2O. No indication of deactivation of the platinum catalyst was observed at a maximum residual oxygen pressure in the reactor up to 150 kPa. A reaction mechanism involving elementary steps has been suggested to explain the decarboxylation and oxidation of malonic acid. A kinetic model that accounts for both non-catalysed and catalysed decarboxylation of malonic acid has been developed and validated. The non-catalysed reaction is first order in malonic acid. The activation energies and adsorption enthalpies have been determined. The model is able to describe the experimental data adequately.

Keywords: Wastewater treatment; Malonic acid; Acetic acid; Decarboxylation; Kinetics; Platinum catalyst; Multiphase reactors

6.1. Introduction

The application of platinum metal catalysts in the oxidation of toxic organics in wastewater is gaining attention (e.g., Luck, 1999; Rivas *et al*., 1999; Harmsen *et al*., 1997; Gallezot, 1997). The advantages of using platinum catalysts in wet oxidation are: lowering the operating temperature employed in wet air oxidation, reducing the reaction or residence time as compared to wet air oxidation, and hence lowering investment costs. No leaching or dissolution of the Pt metal occurs, even in a hot and acid reaction medium, and the catalyst is easily separated from the cleaned water (Luck, 1999; Matatov-Meytal and Sheintuch, 1998; Mishra *et al*., 1995). So far, it has been shown that many organic wastes in water can be oxidised completely to CO_2 and H_2O (Masende *et al*., 2003a,b; 2004a; Gallezot, 1997).

The oxidation rate of organic wastes in aqueous phase and the activity of the platinum catalysts, depend on many factors. These include the concentrations of the reacting organic compounds and reaction products, the oxygen concentration, the catalyst amount, the temperature, the platinum particle size, the catalyst support material and the nature of the organic compound (ring, unsaturated acid, saturated acid, etc.) (Masende *et al*., 2003a,b; Besson and Gallezot, 2000). In addition, the mass transfer and hydrodynamic properties of the reactor system play an important role in liquid phase oxidation (Kluytmans *et al*., 2000). Although not well addressed in literature, the pH of the solution was found to greatly influence the reaction rate and activity of the platinum catalyst during wet oxidation of formic acid (Harmsen *et al*., 1997). Since low molecular weight carboxylic acids are formed as intermediates in wet oxidation, it is desirable to understand the mechanisms and process of their oxidation and the formation of refractory end products such as acetic acid. Malonic acid has been reported as an intermediate in the wet oxidation of phenol to CO_2 and acetic acid (Masende *et al*., 2003a,b). The diethyl ester of malonic acid is used in the syntheses of several vitamins, barbiturates and numerous other organic compounds. The manufacture of these products results in wastewater streams, which contain malonic acid.

The motivation of this work is to provide a quantitative description of the recent experimental results obtained during malonic acid reaction in aqueous phase (Masende *et al*., 2004a). It has been revealed that, in the presence of a catalyst and oxygen, the malonic acid reaction proceeds via homogeneous and catalytic decarboxylation, and catalytic oxidation. The decarboxylation route has been identified as the main route for the formation of acetic acid, which is difficult to oxidize at temperatures below 200°C.

A reaction mechanism to explain the observed data has also been proposed. To our knowledge, there is still little information on the kinetics of malonic acid degradation in wet oxidation, particularly in the presence of a platinum catalyst. In the present work a systematic evaluation of the kinetic data has been performed for the purpose of deriving a kinetic model, which can sufficiently describe the degradation of malonic acid in aqueous solution.

Table 6.1
Characteristics of the Pt/Graphite catalyst

Pt metal content	5% on dry basis
Type	Reduced/dry (287)
Carrier	Graphite powder
Catalyst particle size distribution[a]	> 15 μm (5%)
	> 10 μm (25%)
	> 5 μm (85%)
	> 2 μm (100%)
Total surface area (B.E.T.) [$m^2 \cdot g^{-1}$]	15.0
Metal dispersion[b] [%]	5.3
Metallic surface area[b] [$m^2 \cdot g^{-1}$ sample]	0.66
Metallic surface area[b] [$m^2 \cdot g^{-1}$ metal]	13.1
Porosity[c] [%]	69.3

[a]The particle size distribution using the Coulter LS 130 apparatus.
[b]Determined by means of CO chemisorptions using ASAP 2000 series equipment
[c]Mercury porosity measurement using AutoPore IV 9500 equipment

6.2. Experimental

The chemicals used in this research, including malonic acid and acetic acid, were pure analytical grade from Merck and were used as received. The solutions used in the oxidation experiments were prepared using deionised water. The liquid phase oxidation of malonic acid solution was investigated using a commercially available catalyst, Pt/graphite (5 wt%) from Johnson Matthey, and was used without any pre-treatment. Other information and specifications of Pt/graphite are shown in Table 6.1. The experiments were carried out in a continuous flow stirred slurry reactor (CSTR), a 500 ml autoclave (Autoclave Engineers, Zipperclave Hastelloy), which is equipped with a gas dispersion impeller. Details of the experimental set-up and reactor start-up procedures are reported elsewhere (Masende *et al*., 2003a; 2004a). Experiments were performed over a wide range of conditions. The reactor operating conditions are given in Table 6.2. Samples were analysed at a given interval of time for malonic acid as well as other end products.

Table 6.2
Standard reactor operating conditions

Parameter	Standard	Range
Temperature (°C)	150	120-160
Total pressure (MPa)	1.8	1.8
Oxygen partial pressure (MPa)	0.3	0-0.5
Oxygen flow rate (at room conditions) (ml/min)	40	8-50
Nitrogen flow rate (at room conditions) (ml/min)	150	150
Initial malonic acid concentration (mol/m^3)	20	20
Liquid flow rate (ml/min)	10	10
Liquid volume in the reactor (ml)	350	350
Catalyst (g)	3.5	3.5
Stirrer speed (rpm)	1200	350-1200
pH	Uncontrolled	2-7

The liquid samples were analysed by using a HPLC set-up (Merck-Hitachi) with a 300 x 8 ID mm RSpak KC-811 column and a refractive index detector (Waters R401). The composition of effluent gases (mainly O_2, CO_2 and N_2) was determined using an online gas analyser (Servomex, Xentra 4200) where nitrogen was used as an inert gas during reaction. The detailed analytical procedures for the gaseous and liquid effluents from the reactor have already been reported (Masende *et al.*, 2004a). The experimental results obtained from the CSTR were evaluated to give the disappearance rate of malonic acid, the rate of formation of end products, and carbon selectivity to CO_2 and acetic acid. More information on the reactor operation and data analysis procedures has been reported elsewhere (Masende *et al.*, 2003a).

6.3. Results and discussion

For a heterogeneous catalysed reaction to proceed, the reacting species have to be present at the catalytic active site. Oxygen has to be transferred from the gas phase to the liquid phase, through the liquid bulk to the catalyst particle and finally has to diffuse to the catalytic site inside the particle. The organic compound has to be transferred from the liquid bulk to the catalyst particle and to the catalytic site inside the particle. The reaction products have to be transferred in the opposite direction. Therefore, a mass transfer assessment for the reacting species was carried out in order to characterise the reaction regime in which the experimental data were obtained. Most of the experimental data have been reported elsewhere (Masende *et al.*, 2004a).

6.3.1. Assessment of mass transfer limitations

For the catalytic oxidation experiments, the concentrations of oxygen and malonic acid in the bulk liquid and at the catalytic site were determined using the steady state mass transport equations for oxygen and malonic acid. The mass transfer resistance for oxygen in the gas phase was considered to be negligible. In this work all experiments were carried out at an impeller speed of 1200 rpm. It has been previously verified during catalytic oxidation of phenol over Pt/graphite (Masende *et al.*, 2003a) that the rate of disappearance is independent of the speed of agitation when the impeller speed is set at 1200 rpm and above. Also the reactor used in this work was equipped with a special gas dispersion impeller. Therefore for a reactor that is perfectly mixed, the oxygen mass transport equals the consumption of oxygen by the oxidation of the organic component. The bulk liquid oxygen concentration ($C_{O_2,L}$) can be calculated from equation (6.1):

$$F_{O_2} = k_{GL}\, a_{GL}\, V_L \left(C_{O_2}^{sat} - C_{O_2,L} \right) = v_{O_2}\, V_L\, C_{cat}\, R_{w,MLO} \qquad (6.1)$$

The minimum value of $k_{GL}a_{GL}$ can be estimated when the concentration driving force is set at maximum, i.e. the bulk liquid concentration, $C_{O_2,L}$ is equal to zero for a given value of $C_{O_2}^{sat}$. The oxygen concentration in the liquid, which is in equilibrium with the gas phase, was calculated by using a semi-empirical correlation (Battino, 1981):

$$C_{O_2}^{sat} = 0.5483 \exp\left(-179.3439 + 8747.547/T + 24.45264 \ln(T)\right) P_{O_2} \qquad (6.2)$$

The criteria for checking the absence of mass transfer limitation was set at a minimum degree of oxygen saturation of 0.95 as reported in the literature (Fogler, 1999; Beenackers and van Swaaij, 1993). Therefore, a criterion for assessing the absence of gas-to-liquid mass transfer limitation was derived from Eq. (6.1) to get:

$$\frac{C_{O_2,L}}{C_{O_2}^{sat}} = \left(1 - \frac{v_{O_2}\, C_{cat}\, R_{w,i}}{k_{GL,O_2}\, a_{GL}\, C_{O_2}^{sat}} \right) \ge 0.95 \qquad (6.3)$$

It was verified that for the conditions employed in this study, whereby a stoichiometric oxygen excess (S.E.) above 10% was used, within the temperature range of 120 - 160°C, the reaction proceeded in the absence of any gas-to-liquid mass transfer limitation.

It was also important to verify the absence of mass transfer limitation from the liquid phase to the surface of the catalyst for malonic acid and for oxygen. For a perfectly

mixed bulk liquid, the oxygen mass transfer to the catalyst surface equals the consumption of oxygen by the oxidation of the organic compound. The transfer rate of malonic acid and oxygen from the liquid phase to the surface of the catalyst can be described by:

$$F_X = k_{LS,X}\, a_{LS}\, V_L \left(C_{X,L} - C_{X,S} \right) = \nu_X\, V_L\, C_{cat}\, R_{w,X} \tag{6.4}$$

where X= malonic acid or oxygen. The mass transfer coefficient from liquid to solid, $k_{LS,X}$, was calculated from the dimensionless Sherwood number (Sano *et al.*, 1974). The criterion for the absence of liquid-to-solid mass transfer limitation was derived from Eq. (6.4) to obtain:

$$\frac{C_{X,S}}{C_{X,L}} = \left(1 - \frac{\nu_X\, W\, R_{w,X}}{k_{LS,X}\, a_{LS}\, V_L\, C_{X,L}} \right) \geq 0.95 \tag{6.5}$$

Within the temperature range of 120 - 160°C, the diffusion coefficient (D_X) ranged from 8.35 x 10^{-9} to 1.28 x 10^{-8} m^2/s for oxygen and from 3.31 x 10^{-9} to 5.06 x 10^{-9} m^2/s for malonic acid, which were estimated in accordance with the Wilke-Chang equation (Perry *et al.*, 1999; Lide, 2003). The size of the catalyst particles, d_p, used was 15 μm, whereas the volumetric mass of the dry porous particle (ρ_p) was 720 kg/m^3. The $k_{LS,X}$ values for oxygen and malonic acid at 160°C are 3.0 x 10^{-3} and 9.45 x 10^{-4} m/s, respectively, for the minimum Sherwood numbers of 3.6 for oxygen and 2.8 for malonic acid, and with the volumetric liquid-solid interfacial surface area (a_{LS}) of 5556 m^{-1}. Similar calculations were performed under other conditions. It was found that the experimental data (e.g., $R_{w,X}$ and $C_{X,L}$) were obtained under the intrinsic kinetic regime since $C_{X,S}/C_{X,L} > 0.95$. Therefore, the experimental data could be used as input for kinetic model development and evaluation.

The significance of internal mass transfer limitation inside the catalyst was assessed using the Weisz-Prater criterion (Fogler, 1999):

$$C_{WP} = \frac{d_p^2}{16} \frac{\rho_p\, \nu_X\, R_{w,X}}{D_e\, C_{X,S}} \ll 1 \tag{6.6}$$

The effective diffusivity was estimated from $D_e = 0.25\, D_X\, \varepsilon_p$ (Fogler, 1999) with particle porosity, ε_p =0.68 (-), while the particle tortuosity factor was 4 (Vleeming, 1997). For the data under consideration, the maximum value obtained was C_{WP} = 0.075, indicating that no concentration gradients and no diffusion limitations existed. While the type of catalyst used is an "egg-shell" catalyst, where the active sites are mainly located in the outer shell, the criterion would be met even more easily.

6.3.2. Influence of reaction conditions

The effect of temperature on the non-catalysed degradation of malonic acid in an oxygen-free condition (only nitrogen) is shown in Fig. 6.1. The experimental data were obtained at a reactor pressure of 1.8 MPa with a constant malonic acid concentration of 20 mol/m^3 in the feed solution. The disappearance rate increases with an increase in temperature (Fig. 6.1a). The corresponding residual malonic acid concentration in the liquid phase is depicted in Fig. 6.1(b). The increasing trend of the residual concentration at the beginning of the reaction is due to the reactor start-up procedure where both malonic acid and oxygen were fed simultaneously into the reactor, when the reaction conditions were reached (Masende *et al.*, 2003a). In the gas phase, carbon dioxide was the only end product observed (Fig. 6.1c), whereas acetic acid was the only end product in the liquid phase, as shown in Fig. 6.1(d).
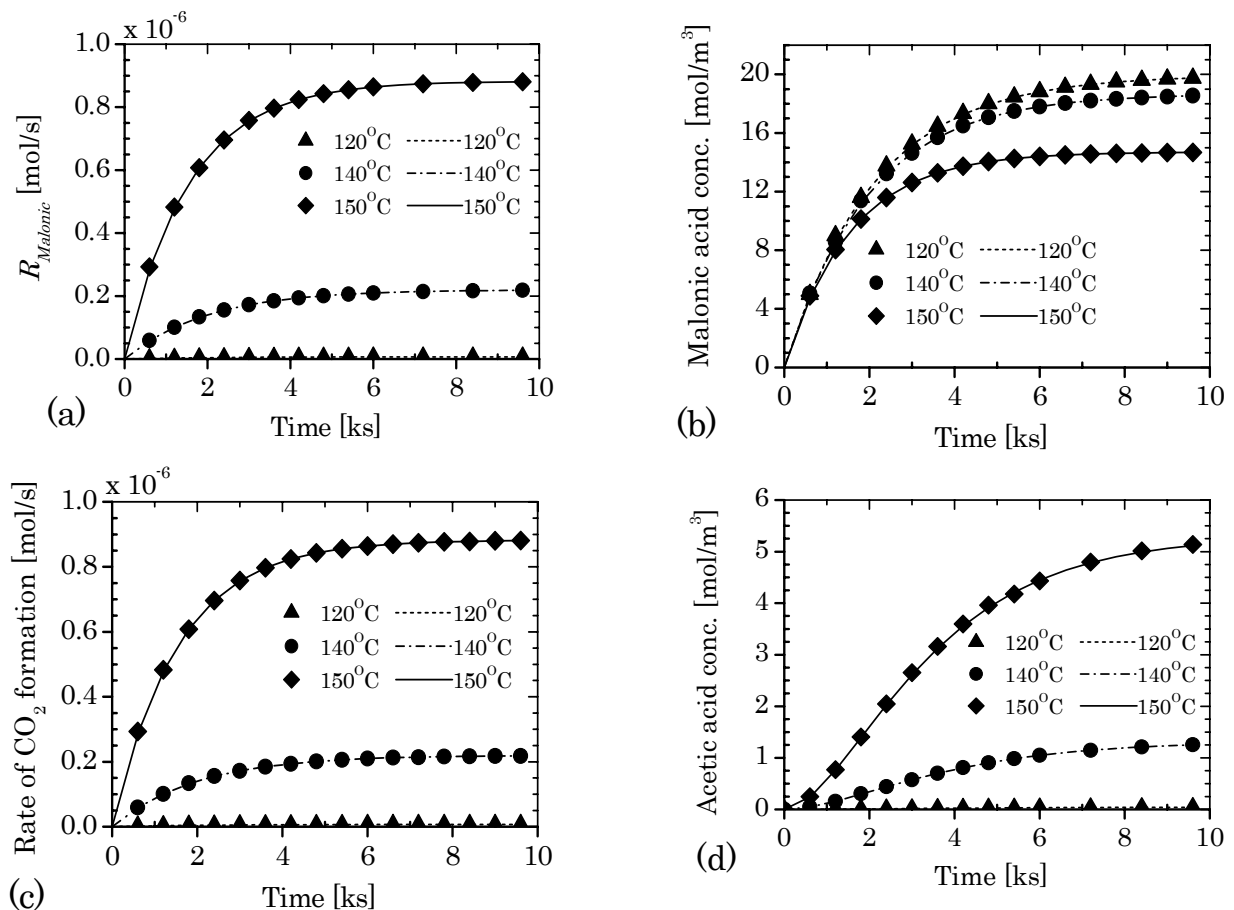
Fig. 6.1. Non-catalysed malonic acid reaction under oxygen-free conditions at different temperatures, 1200 rpm, and $C_{malonic}$=20 mol/m^3. Lines show calculated results with model Eq. (6.4.1) in Table 6.4 where A^0= 5.16 x 10^{23} ± 10^{21} s^{-1} and E_{ho}= 223.4 ± 10.4 kJ/mol; symbols show experimental data: (a) reaction rate for malonic acid, (b) malonic acid concentration, (c) rate of CO_2 formation, and (d) acetic acid concentration.

These results indicate that decarboxylation is the main reaction for malonic acid in the absence of a catalyst and at oxygen-free conditions. Furthermore, decarboxylation of malonic acid is enhanced with an increase in temperature. However, the catalytic effect of metal surfaces (e.g., reactor wall), and the acid-base catalysis cannot be excluded. Dissolved metal ions and metal complexes of organic compounds have been reported to have decarboxylative catalytic activity on carboxylic acids such as malonic acid (Marquié *et al*., 2001, Darensbourg *et al*., 1995). Decarboxylation of malonic acid can also occur as a result of nucleophilic addition by intramolecular acid catalysis (Mussons *et al*., 1999), which is favoured by the intramolecular hydrogen bond in the malonic acid (Pauling, 1948).

A comparative investigation of malonic acid conversion was carried out at 150°C with a feed concentration of 20 mol/m^3 for different reaction conditions: (i) no oxygen and no catalyst (called blank), (ii) with a catalyst, no oxygen, and (iii) both a catalyst and oxygen. It was found that the conversion rate of malonic acid to CO_2 and acetic acid was relatively low when a blank experiment was carried out as can be seen in Fig. 6.2.
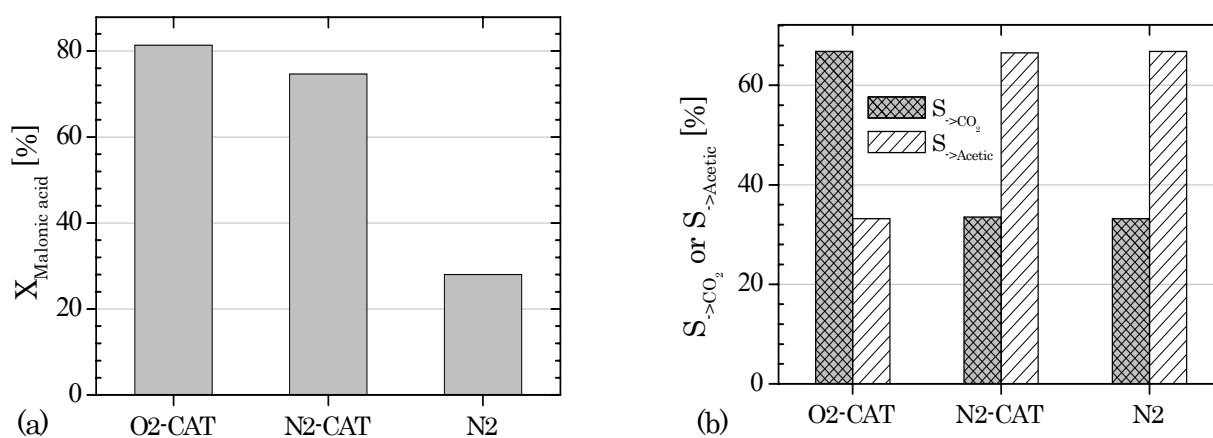
Fig. 6.2. Catalysed and non-catalysed reaction of malonic acid after 6.0 ks at 150°C, 1200 rpm, S.E.=100%, $C_{malonic}$=20 mol/m^3 and 10 kg$_{cat}$/m$_L^3$ Pt/graphite: (a) malonic acid conversion, and (b) selectivity to CO_2 and acetic acid.

The carbon selectivity to CO_2 and acetic acid were 34% and 66%, respectively. With a catalyst and in the absence of oxygen, the degradation to CO_2 and acetic acid increased, while the selectivity was the same as for the blank experiment. In the presence of a catalyst and oxygen, little increase of the disappearance rate for malonic acid was observed. The selectivity to CO_2 and acetic acid were 66% and 34%, respectively. It is evident from these results that both homogeneous and heterogeneous catalytic decarboxylation gave almost the same selectivity of the end products, CO_2

and acetic acid, however a high conversion rate of malonic acid was achieved when a platinum catalyst was added. Furthermore, in the presence of both oxygen and a Pt/graphite catalyst, more CO_2 was formed. When a Pt/graphite catalyst is used in decarboxylation of malonic acid, it is not yet obvious whether Pt metal or graphite or both are responsible for the catalytic activity. Graphite has been reported to show catalytic activity during thermal decomposition of carboxylic diacids (Marquié *et al.*, 2001).
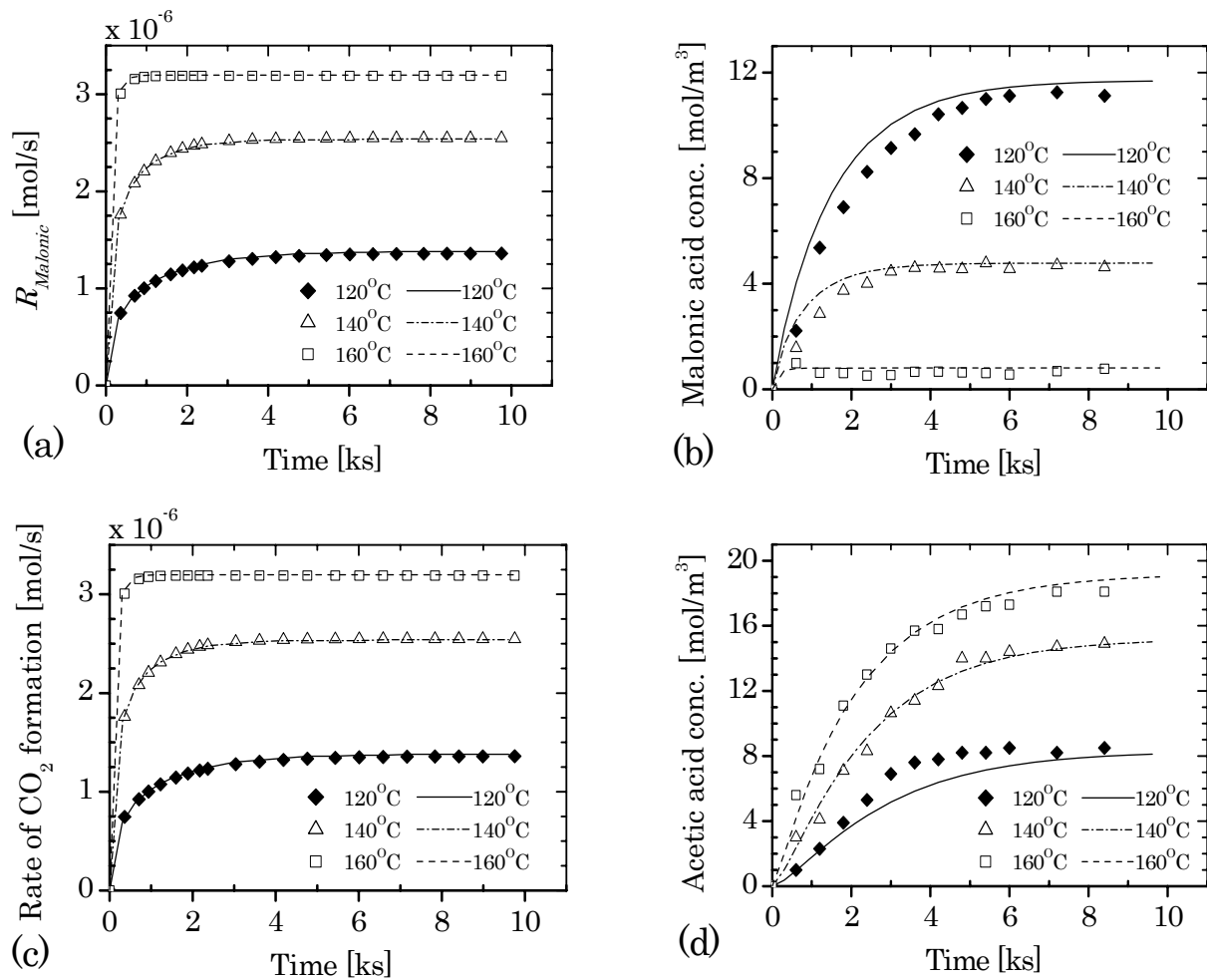

Fig. 6.3. Effect of temperature during malonic acid reaction without oxygen at 1200 rpm, $C_{malonic}$=20 mol/m^3 and 10 kg$_{cat}$/m$_L^3$ Pt/graphite. Lines show calculated results with model Eq. (6.4.3) in Table 6.4; symbols show experimental data: (a) reaction rate for malonic acid, (b) malonic acid concentration, (c) rate of CO_2 formation, and (d) acetic acid concentration.

The dependence of temperature was also investigated to determine its influence on the conversion of malonic acid and selectivity to CO_2 and acetic acid. The investigation was carried out with 10 kg$_{cat}$/m$_L^3$ of catalyst and in an oxygen-free environment (only nitrogen) to prevent oxidation. Fig. 6.3 shows an increase of the degradation rate for malonic acid as the temperature increases. The selectivities were again at 34% and

66% for CO_2 and acetic acid, respectively, even at a temperature of 160°C. It is clearly seen that a high temperature enhances the rate of disappearance of malonic acid.
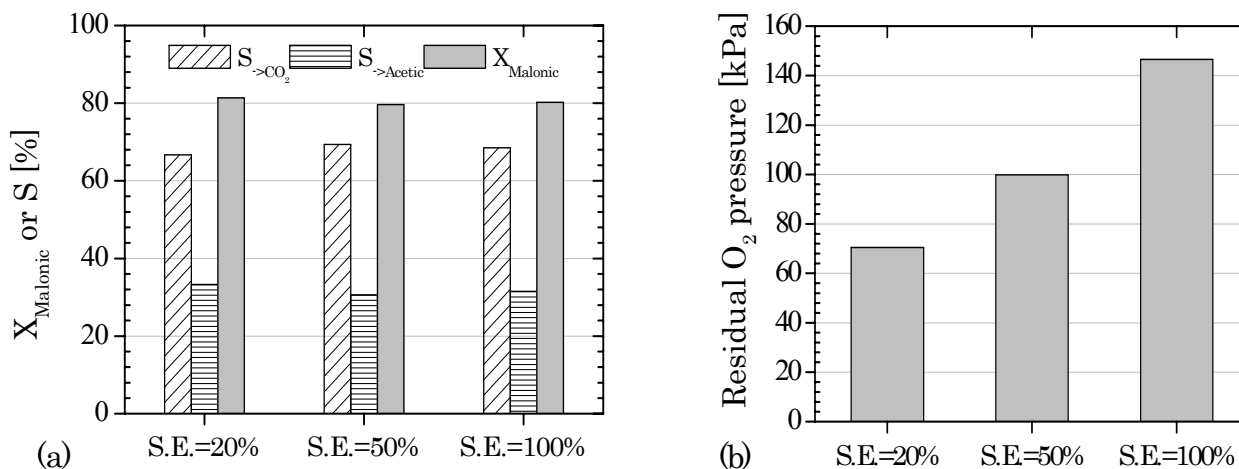

Fig. 6.4. Effect of oxygen partial pressure during malonic acid reaction at 150°C, 1200 rpm, $C_{malonic}$=20 mol/m^3 and 10 kg$_{cat}$/m$_L^3$ Pt/graphite after 6.0 ks; where O2-CAT: with catalyst and oxygen; N2-CAT: with catalyst and no oxygen; N2: no catalyst and no oxygen: (a) malonic acid conversion, selectivity to CO_2 and to acetic acid, and (b) residual oxygen partial pressure.

Fig. 6.4 shows the influence of oxygen concentration on malonic acid conversion at a temperature of 150°C with a catalyst concentration of 10 kg$_{cat}$/m$_L^3$. The concentration of malonic acid in the feed solution was 20 mol/m^3, whereas other parameters were kept at standard conditions (Table 6.2). It was found that when different oxygen molar flow rates, expressed as stoichiometric oxygen excess (S.E.), of 20, 50, and 100% were used, the conversion rate of malonic acid remained relatively the same with the selectivity to CO_2 and acetic acid of about 68% and 32%, respectively as shown in Fig. 6.4(a). The maximum residual oxygen partial pressure in the reactor was below 160 kPa (Fig. 6.4b), and no indication of catalyst deactivation could be seen from the data. Furthermore, the disappearance rate of malonic acid was slightly higher as compared to the case when a catalyst was used without oxygen.

This clearly indicates that although the addition of oxygen enhances slightly the conversion of malonic acid (Fig. 6.2), there is no change of the disappearance rate of malonic acid during oxidation experiments at S.E. from 20 to 100% (Fig. 6.4). However, it is also clear that the addition of oxygen in the presence of a Pt/graphite catalyst can change the selectivity towards the end products, CO_2 and acetic acid. In conclusion, it appears that when the catalytic reaction is carried out in the presence of oxygen, both reaction routes take place, i.e. homogenous and catalytic decarboxylation, and catalytic oxidation. The mechanistic interpretation and

explanation of the observed results have been reported in Chapter 3. In order to describe quantitatively the observed results, it is important to consider the elementary reactions steps, which are necessary in building kinetic models.

Table 6.3
Sequence of elementary steps proposed for the malonic acid reaction. The surface reaction is the rate determining. Malonic acid adsorbs physically on the catalytic site

Reaction	Rate equation	
"homogeneous" route		
$MLO \rightarrow AC + CO_2$	$R_1 = k_{nocat}\, C_{MLO}$	(I)
"heterogeneous" route		
$MLO + * \leftrightarrow MLO*$	$\theta_{MLO} = K_{MLO}\, C_{MLO}\, \theta_*$	(II)
$AC + * \leftrightarrow AC*$	$\theta_{AC} = K_{AC}\, C_{AC}\, \theta_*$	(III)
$MLO* \rightarrow CO_2 + [INT]*$	$R_4 = k_4\, \theta_{MLO}$ (rate-determining)	(IV)
$[INT]* \rightarrow AC + *$	fast	(V)
$[INT]* + 4[O] \rightarrow 2CO_2 + 2H_2O + *$	fast	(VI)
Site balance	$1 = \theta_* + \theta_{MLO} + \theta_{AC}$	(VII)

Note: $MLO = HOOC\text{-}CH_2\text{-}COOH$; $AC = CH_3COOH$; $[INT]=$ intermediate; $* =$ vacant catalytic site

6.3.3. Mechanisms for malonic acid degradation

The kinetic model for malonic acid degradation in the presence of a catalyst was developed taking into consideration the contribution of both homogeneous and heterogeneous catalytic routes. It was assumed that the catalytic sites on the surface are uniform, that is, the adsorption enthalpy of a molecule is the same for all the types of sites. In addition, the large molecules of malonic acid and acetic acid compete to occupy a single vacant site, whereas the adsorption of small species, like O- and H-atoms, was considered non-competitive, in order to accommodate the effect that the presence of oxygen does not change the rate-determining step. The elementary reaction steps proposed for the decarboxylation and oxidation of malonic acid are listed in Table 6.3.

The non-catalysed and homogeneous reactions are expressed by a first order reaction according to step (I). The catalytic model for decarboxylation was constructed by combining the elementary reaction steps (II), (III), and (IV) listed in Table 6.3. According to Langmuir-Hinshelwood kinetics malonic acid adsorbs on the catalytic site, as described in step (II). The surface reaction shown in step (IV) is considered to be first order in the adsorbed malonic acid surface concentration. In addition, the

surface reaction of the adsorbed malonic acid, i.e. decarboxylation, is considered to be the rate-determining step. During the reaction CO_2 is formed as the end product. In addition, an intermediate [INT] is also formed, which can recombine to form acetic acid according to step (V). When acetic acid is formed, it remains stable, especially at temperatures below 200°C. Similar to malonic acid, acetic acid is also adsorbed on the same catalytic site according to step (III).

The surface reaction between adsorbed oxygen and the intermediates formed in step (IV) takes place very rapidly to form CO_2 and H_2O (step VI). Although the reaction rate was slightly enhanced by the addition of oxygen (Fig. 6.2), the dependence of the disappearance rate of malonic acid on oxygen concentration (Fig. 6.4) is not sufficient to be incorporated in model development. The rate-determining step in this case remains the same, i.e. the decarboxylation of malonic acid (step IV). Based on the sequence of elementary steps and the site balance presented in Table 6.3, the kinetic rate equations were derived as described in the next section.

6.3.4. Kinetic models for malonic acid reaction

Kinetic models for the platinum catalysed reaction of malonic acid have taken into consideration the participation of both non-catalysed and catalysed routes to the end products. The non-catalysed decarboxylation of malonic acid can be obtained from the first-order rate equation:

$$R_{V,nocat} = k_{nocat} C_{MLO}, \qquad (\text{mol/m}^3.\text{s}) \tag{6.7}$$

where k_{nocat} is the reaction rate constant obtained from the experiments performed without a catalyst and in the absence of oxygen. The derivation of the kinetic rate equations for catalytic decarboxylation was based on a steady state approximation of the surface species and site balances. The coverage of malonic acid can be derived from the equilibrium equations in Table 6.3 and the site balance (VII) to obtain:

$$\theta_{MLO} = \frac{K_{MLO} C_{MLO}}{1 + K_{MLO} C_{MLO} + K_{AC} C_{AC}} \tag{6.8}$$

The reversible adsorption steps (II) and (III) were considered to be in fast equilibrium. For the decarboxylation of malonic acid at the surface, the following rate equation was obtained by combining reaction step (IV) in Table 6.3 with equation (6.8) to get

$$R_{V,4} = \frac{k_4 L_t C_{cat} K_{MLO} C_{MLO}}{1 + K_{MOL} C_{MLO} + K_{AC} C_{AC}}, \qquad (\text{mol/m}^3.\text{s}) \tag{6.9}$$

where L_t (mol/kg$_{cat}$), the total specific amount of catalytic sites for adsorption, and C_{cat} (kg$_{cat}$/m$_L^3$), the catalyst concentration. The terms in the denominator of Eq. (6.9) related to the surface reactions give the relative fractions of the different surface species with respect to the total number of the vacant sites.

Table 6.4
Kinetic models for malonic acid reaction where the unit for R_V is (mol/m^3.s)

Non-catalysed decarboxylation	
$\quad R_{V,nocat} = k_{nocat}\, C_{MLO}$	(6.4.1)
Catalysed decarboxylation	
$\quad R_{V,MLO} = R_{V,nocat} + \dfrac{k_c\, C_{MLO}}{1 + K_{MLO}\, C_{MLO} + K_{AC}\, C_{AC}}$	(6.4.2)
For very low K$_{AC}$	
$\quad R_{V,MLO} = R_{V,nocat} + \dfrac{k_c\, C_{MLO}}{1 + K_{MLO}\, C_{MLO}}$	(6.4.3)
For very low K$_{MLO}$	
$\quad R_{V,MLO} = R_{V,nocat} + \dfrac{k_c\, C_{MLO}}{1 + K_{AC}\, C_{AC}}$	(6.4.4)
For strong adsorption of malonic acid and acetic acid	
$\quad R_{V,MLO} = R_{V,nocat} + \dfrac{k_c^{'}}{1 + K_{EQ}\left(C_{AC}/C_{MLO}\right)}$	(6.4.5)
$\qquad$ where $K_{EQ} = K_{AC}/K_{MLO}$ (-) and $k_c^{'} = k_c/K_{MLO}$ (mol/m^3.s)	
For K$_{AC}$ << K$_{MLO}$ in (6.4.5)	
$\quad R_{V,MLO} = R_{V,nocat} + k_c^{'}$ where $k_c^{'} = k_c/K_{MLO}$ (mol/m^3.s)	(6.4.6)
For K$_{MLO}$ << K$_{AC}$ in (6.4.5)	
$\quad R_{V,MLO} = R_{V,nocat} + k_c^{'}\dfrac{C_{MLO}}{C_{AC}}$ where $k_c^{'} = k_c/K_{AC}$ (mol/m^3.s)	(6.4.7)
If $(K_{MLO}\, C_{MLO}, K_{AC}\, C_{AC}) << 1$ in (6.4.2)	
$\quad R_{V,MLO} = R_{V,nocat} + k_c\, C_{MLO}$	(6.4.8)

Several possible kinetic equations for decarboxylation of malonic acid were derived from Eqs. (6.7) and (6.9) and are listed in Table 6.4. Taking into consideration the homogeneous and heterogeneous catalytic contributions, the net disappearance rate for malonic acid is expressed by Eq. (6.4.2) in Table 6.4. The constants in the numerator of the final kinetic rate equations were lumped to give a kinetic rate constant, $k_c = k_4\, L_t\, C_{cat} K_{MLO}$, in (s^{-1}). To reduce the number of parameters in the denominator, a number of assumptions were considered. Taking into consideration that acetic acid does not strongly adsorb on the surface, Eq. (6.4.3) was obtained, whereas Eq. (6.4.4) was obtained by assuming weak adsorption of malonic acid on the catalytic site. Further simplification was also considered when both malonic acid and acetic acid

adsorb strongly on the catalytic site, i.e. by omitting 1 (due to large values of adsorption terms) in the denominator to obtain Eq. (6.4.5). Based on the assumption that acetic acid does not strongly adsorb on the catalyst, Eq. (6.4.6) with zero order in malonic acid was obtained. A further reduction of the number of parameters in Eq. (6.4.5) was carried out done by assuming weak adsorption of malonic acid to obtain Eq. (6.4.7). Eq. (6.4.2) was again simplified to obtain a first order Eq. (6.4.8) by assuming weak adsorption of malonic acid and acetic acid on the catalytic site surface. The kinetic rate equations were then compared and fitted to the experimental data for determination of kinetic parameters using Polymath Software.

6.3.5. *Model parameter estimation*

The derived kinetic models (Table 6.4) contain kinetic parameters which are related to the reaction temperature by the Arrhenius law (Eq. 6.10) for the kinetic rate parameters and by the Van't Hoff law (Eq. 6.11) for the reaction equilibrium parameters:

$$k_{T,j} = A_j^0 \exp\left(\left(-\frac{E_j}{R}\right)\frac{1}{T}\right), \tag{6.10}$$

$$K_{T,j} = K_j^0 \exp\left(-\left(\frac{H_j}{R}\right)\frac{1}{T}\right) \tag{6.11}$$

The adsorption enthalpy (H_j) always has an opposite sign with respect to the activation energy (E_j). In this work both activation energy and adsorption enthalpy (H_j) were taken as apparent parameters. Eqs. (6.10) and (6.11), in combination with the rate equations in Table 6.4, provide a means of correlating the dependence of the reaction rate on the temperature and on the malonic acid and acetic acid concentrations. Data obtained under a wide range of experimental conditions were used to determine the kinetic parameters; the activation energy and enthalpy, and the pre-exponential constants.

Regression analysis was carried out using a Polymath numerical computation package (Version 5.1). The program also calculates the correlation coefficients (R^2) and the 95% confidence intervals (C.I.), which were used as indicators of the best fit. The input data for regression were the experimental reaction rate, residual malonic acid concentration, and acetic acid concentration. The individual rate constants and equilibrium constants were obtained from isothermal data for each temperature. The pre-exponential factors, activation energies and adsorption enthalpies were obtained from Arrhenius plots.

The kinetic parameters obtained from the regression analysis are shown in Table 6.5. For the regression of the non-catalysed decarboxylation of malonic acid, model Eq. (6.4.1) was used. The values of the pre-exponential factor and activation energy for the non-catalysed reaction (Eq. 6.4.1) were 5.2 x 10^{23} s^{-1} and 223 kJ/mol, respectively. Since a constant catalyst concentration of 10 kg$_{cat}$/m$_L^3$ Pt/graphite was used, the values obtained for the non-catalysed reaction were kept constant during the determination of other kinetic parameters in the presence of a catalyst.

Table 6.5
Results of kinetic parameter estimation for models in Table 6.4

No.	Parameter/units	Value	C.I. (95%)	R^2	S.D.	Model equation
1	A_{ho}^0 (s^{-1})	5.16 x 10^{23}	10^{21}	0.998	0.176	Eq. (6.4.1)
2	E_{ho} (kJ/mol)	223.4	10.40			
3	A_c^0 (s^{-1})	4.28 x 10^{10}	10^9	0.991	0.190	
4	E_c (kJ/mol)	101.60	6.20			Eq. (6.4.2)
5	K_{MLO}^0 (m^3 mol^{-1})	1.45 x 10^7	10^7	0.972	0.214	
6	H_{MLO} (kJ/mol)	69.49	5.20			
7	K_{AC}^0 (m^3 mol^{-1})	2.17 x 10^{-29}	10^{-30}	0.997	0.114	
8	H_{AC} (kJ/mol)	- 204.20	26.40			
9	A_c^0 (s^{-1})	4.81 x 10^{11}	10^{10}	0.996	0.184	Eq. (6.4.3)
10	E_c (kJ/mol)	110.30	9.60			
11	K_{MLO}^0 (m^3 mol^{-1})	3.43 x 10^9	10^8	0.992	0.183	
12	H_{MLO} (kJ/mol)	77.32	6.60			
13	A_c^0 (s^{-1})	1.51 x 10^{10}	10^9	0.986	0.208	Eq. (6.4.4)
14	E_c (kJ/mol)	101.20	11.20			
15	K_{AC}^0 (m^3 mol^{-1})	3.92 x 10^{-20}	10^{-20}	0.912	0.535	
16	H_{AC} (kJ/mol)	- 139.40	18.2			
17	A_c^0 (s^{-1})	1.56 x 10^{12}	10^{11}	0.989	0.207	Eq. (6.4.8)
18	E_c (kJ/mol)	118.0	12.50			

Note: The (-) sign for adsorption enthalpy indicates an opposite sign with respect to the activation energy. C.I.: confidence interval; R^2: correlation coefficient; S.D.: standard deviation

When regression analysis was carried out for Eqs. (6.4.5), (6.4.6), and (6.4.7) listed in Table 6.4, no converged solutions were obtained from randomly selected initial values. The failure to obtain a converged solution for Eq. (6.4.5) could be a result of the assumption made which considers strong adsorption of malonic acid and acetic acid. A similar explanation holds for Eqs. (6.4.6) and (6.4.7), which were obtained after further simplification of Eq. (6.4.5). These model equations were therefore not considered for further analysis.
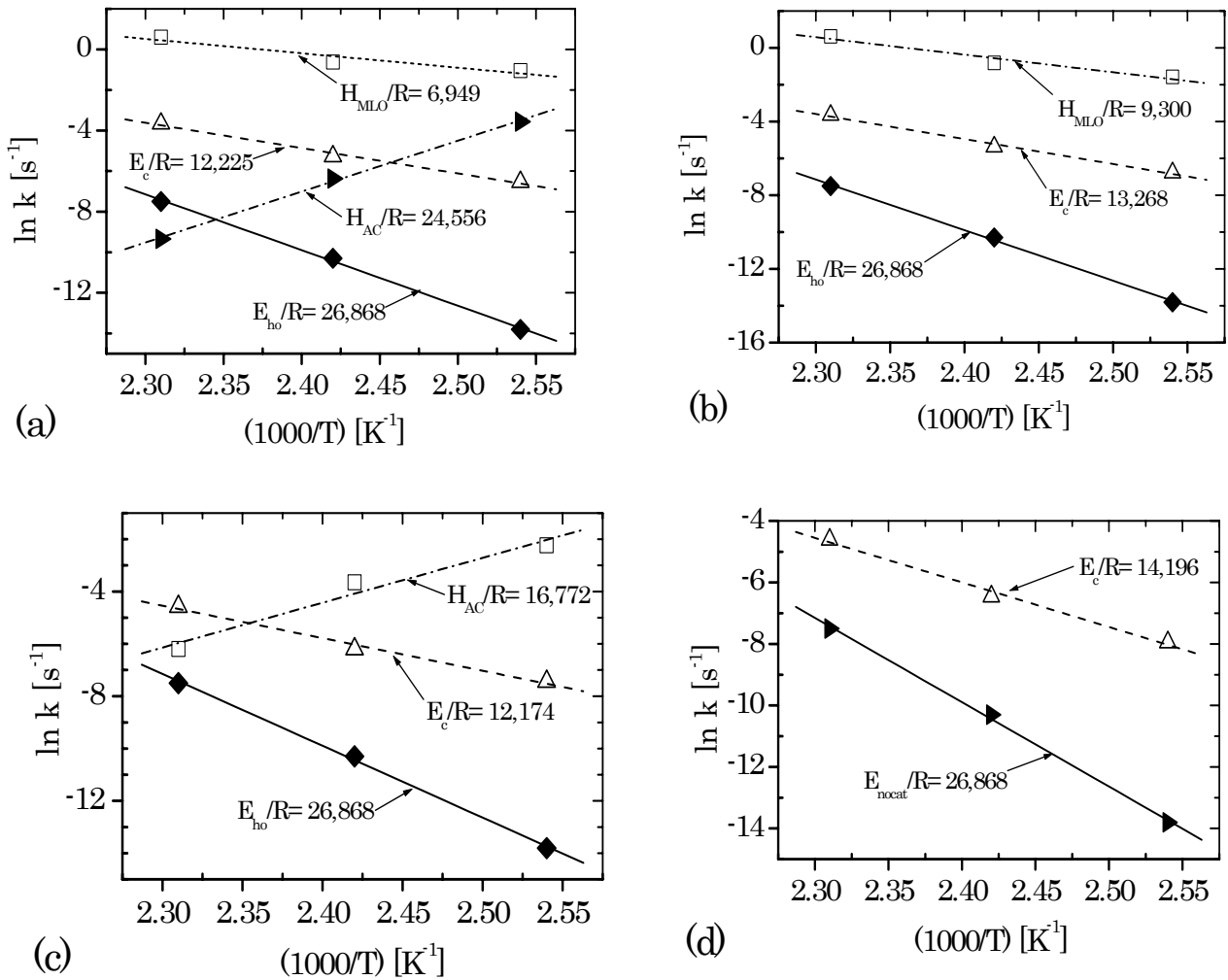
Fig. 6.5. Arrhenius plots for decarboxylation models for malonic acid: (a) model Eq. (6.4.2), (b) model Eq. (6.4.3), (c) model Eq. (6.4.4) and (d) model Eq. (6.4.8).

Similarly, the best fit values for the rate equations (6.4.2), (6.4.3), (6.4.4), and (6.4.8) were obtained from regression of the experimental data. The reaction rate parameters were determined from the Arrhenius plots presented in Fig. 6.5. A summary of the kinetic parameters, including the respective 95% confidence intervals and R^2 values, is shown in Table 6.5. The kinetic parameters for model Eq. (6.4.2) fit well the Arrhenius plot, as can be seen in Fig. 6.5(a). A best fit was also obtained for model Eq. (6.4.3), as can be seen in Fig. 6.5(b), which assumes weak adsorption of acetic acid. Model Eq. (6.4.4) gave a less good fit for the rate parameters (Fig. 6.5c) as indicated by the relatively low R^2 values. Good Arrhenius plots were obtained for the kinetic parameters for model Eq. (6.4.8) as shown in Fig. 6.5(d). This model did not consider the adsorption of malonic acid and acetic acid. A comparative analysis of the models was carried out as explained in the next section.
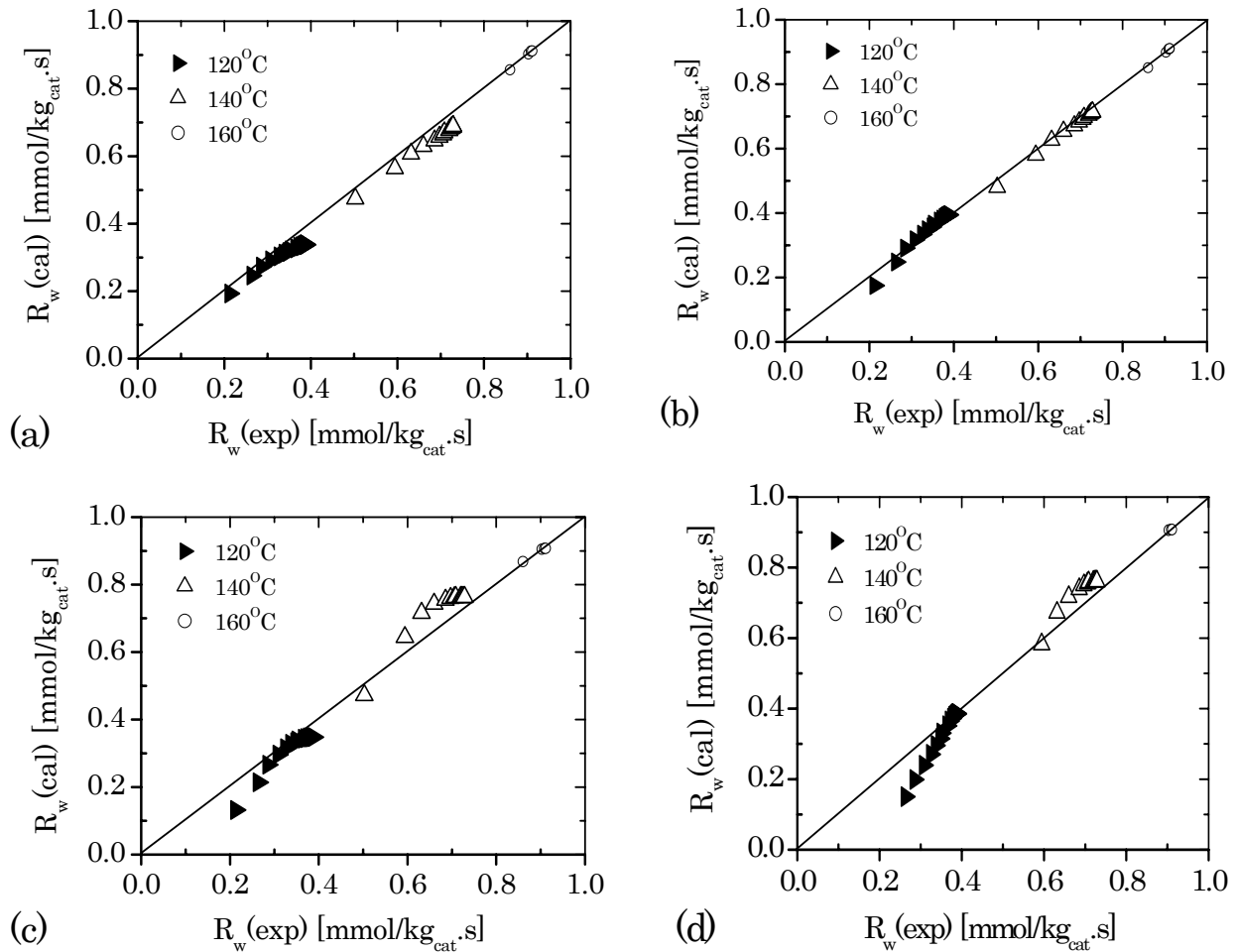
Fig. 6.6. Comparison between experimental and predicted disappearance rates of malonic acid during decarboxylation in the presence of Pt/graphite catalyst ($10\ kg_{cat}/m_L^3$): (a) model Eq. (6.4.2), $R^2 = 0.992$, S.D.$= 0.08$; (b) model Eq. (6.4.3), $R^2 = 0.999$, S.D.$= 0.02$; (c) model Eq. (6.4.4) $R^2 = 0.864$, S.D.$= 0.32$ and (d) model Eq. (6.4.8) $R^2 = 0.792$, S.D.$= 0.81$.

6.3.6. Reactor model simulation

A reactor model was developed with assumptions that the reactor is ideally mixed and is operated at isothermal conditions. This means that only the mass or mole conservation equations were considered. Differential equations were derived, as reported elsewhere (Masende *et al.*, 2004b) to describe the malonic acid and acetic acid concentrations in the liquid phase, the carbon dioxide, oxygen, and nitrogen concentrations in the gas phase as a function of time. Nitrogen gas was used to pressurise the reactor and the molar flow rate was kept constant throughout the reaction. The reactor model was obtained by combining each of the kinetic rate equations in Table 6.4 with the derived set of differential equations, which describe the mole balance in the slurry continuous flow reactor as a function of time. To solve the reactor model equations, a Polymath Script, which combines differential equations and

explicit equations was developed. The reactor model was solved to give a reaction rate, rate of CO_2 formation, residual concentration of malonic acid, and acetic acid concentration.

A comparison of the predicted data by model Eq. (6.4.1) and those observed during non-catalysed decarboxylation is shown in Fig. 6.1. It is seen that the model prediction fits well to the experimental data. To compare between experimental and calculated reaction rates for other model equations, a parity plot analysis was used. The parity plots of the experimental and calculated reaction rates for malonic acid are presented in Fig. 6.6. A fairly good fit of the experimental and calculated data was obtained from model Eq. (6.4.2), as can be seen in Fig. 6.6(a). The model however, predicts slightly lower values as compared to the experimental data especially at temperatures below 160°C. A better description of the experimental was obtained from model Eq. (6.4.3), as can be seen in Fig. 6.6(b). This suggests that acetic acid adsorption, which is not incorporated in model Eq. (6.4.3), seems to be weak in comparison to malonic acid adsorption. The parity plots of the calculated and experimental reaction rates for model Eq. (6.4.4) show high deviations (Fig. 6.6c) with very low R^2 values. A similar trend is observed for model Eq. (6.4.8), where high deviations are observed, as can be seen in Fig. 6.6(d). It is evident from the parity plots that a simple, first order rate equation Eq. (6.4.8) does not adequately describe the experimental data.

In Fig. 6.3, a comparison of the experimental data and the simulation results for model Eq. (6.4.3) is presented. As has been previously observed, the two model Eq. (6.4.2) and Eq. (6.4.3) were able to predict the reaction rates reasonably well. The small values of the standard deviations (S.D.) of the data points and R^2 values close to 1 obtained from the parity plots verify the accurate determination of the parameters and the reliability of the experimental data. To distinguish between the two models would require additional kinetic data.

6.3.7. *Assessment of kinetic parameters*

Since the kinetic parameters for malonic acid decarboxylation and oxidation over platinum catalysts are not available in the literature, a comparison with the current results was not possible. However, it is clear from the results that the kinetic parameters; namely, activation energies, adsorption enthalpies, pre-exponential factors, in the model Eqs. (6.4.2) and (6.4.3) are within the same order of magnitude. The activation energies for the catalytic reaction in Eq. (6.4.2) and Eq. (6.4.3) are also lower than those obtained for the non-catalysed reaction (Eq. 6.4.1). The range of 100

– 110 kJ/mol for activation energies corresponds to the values reported in the literature for carboxylic acids like acetic acid (Cybulski and Traweczyński, 2004; Klinghoffer *et al*., 1998; Gallezot *et al*., 1997). The overall kinetic rate constants at a given temperature for the non-catalysed reaction are lower than the catalytic reaction rate constants. For example, the reaction rate constant at 140°C is 2.87×10^{-5} s^{-1} for non-catalysed whereas the rate constants for the catalytic reaction are 6.04×10^{-3} s^{-1} and 5.40×10^{-3} s^{-1} for model Eq. (6.4.2) and Eq. (6.4.3), respectively.

The results also show that the adsorption of acetic acid does not greatly influence the rate of decarboxylation of malonic acid. Typical examples of the adsorption equilibrium constants for malonic acid and acetic acid obtained at 140°C are $K_{MLO}=$ 0.71 m^3/mol and $K_{AC}= 1.46 \times 10^{-3}$ m^3/mol, respectively. The corresponding values of the product of the equilibrium adsorption constant and the concentration after 6.0 ks were calculated as $K_{MLO}C_{MLO}= 3.92$ and $K_{AC}C_{AC}= 1.944 \times 10^{-2}$. This indicates that malonic acid, a di-carboxylic acid is the major occupant of the catalytic site (stronger adsorber). Beziat *et al*. (1999) also reported weak equilibrium adsorption for acetic acid ($< 5 \times 10^{-3}$ m^3/mol) as compared to succinic acid (di-carboxylic acid) (0.13 m^3/mol). Although the observed adsorption enthalpies for acetic acid seem to be high, i.e. from -139 to -204 kJ/mol, the actual equilibrium adsorption constants are low due to very small pre-exponential factors. The adsorption enthalpy of –8.6 kJ/mol for acetic acid on a CuO/γ-Al_2O_3 catalyst has been reported recently (Eftaxias *et al*., 2002). The insignificant adsorption of acetic acid is a good reason to prefer Eq. (6.4.3) over Eq. (6.4.2).

The adsorption enthalpy for malonic acid obtained is in the range of 69 to 77 kJ/mol, while a value of –28 kJ/mol has been reported in the literature (Eftaxias *et al*., 2002). Despite the good results from model Eq. (6.4.2) and Eq. (6.4.3), there are still uncertainties. For example, the adsorption equilibrium of malonic acid would be expected to decrease instead of increase with temperature. More experimental data will be needed to resolve these discrepancies, and to reveal the true chemical and physical mechanisms of the catalytic reaction.

6.4.   Conclusions

The kinetics of the catalytic reaction of malonic acid in aqueous phase over a Pt/graphite catalyst was studied. A systematic analysis of the experimental data was done for the identification of the appropriate mechanism and kinetic model equations. A model, which considers the contribution of a homogeneous route, and a

heterogeneous catalytic route, including the adsorption of malonic acid, was able to describe the experimental data adequately. The model Eq. (6.4.2) has the largest number of parameters to be estimated; however the best-fit values were easily obtained from the experimental data.

The kinetic and equilibrium parameters have been determined. The model is capable of describing the experimental data well. Although there are still uncertainties with regards to the adsorption enthalpy of malonic acid, the overall adsorption equilibrium is close to reported values for succinic acid and acetic acid for the $CuO/\gamma\text{-}Al_2O_3$ catalyst. The kinetic and equilibrium parameters indicate a strong adsorption of malonic acid and a weak adsorption of acetic acid. This indicates that dicarboxylic acids (e.g. malonic acid) are strongly adsorbed on platinum metal catalysts than mono-carboxylic acids (e.g. acetic acid). More kinetic measurements, however, are needed to refine the model Eqs. (6.4.2) and (6.4.3), which would also address the unresolved uncertainty on the malonic acid adsorption enthalpy.

Acknowledgements

Nomenclature

a_{GL}	volumetric gas-liquid interfacial surface area [m^2/m^3]
a_{GS}	volumetric gas-liquid interfacial surface area [m^2/m^3]
a_{LS}	volumetric liquid-solid interfacial surface area [m^2/m^3]
A^0	pre-exponential factor [s^{-1}]
C_X	concentration of the compound X [mol/m^3]
C_{O_2}	oxygen concentration [mol/m^3]
C_{WP}	Weisz-Prater criterion [-]
C_{cat}	concentration of catalyst [kg_{cat}/m_L^3]
d_p	the particle size of the solid [m]
$D_{e,X}$	effective diffusivity of X ($D_e = 0.25\,D_X\,\varepsilon_p$) [m^2/s]
D_X	diffusion coefficient of X in water [m^2/s]
E_j	apparent activation energy [kJ/mol]
F_X	molar flow rate of compound X [mol/s]
H_j	apparent enthalpy change [kJ/mol]

k_{GL}	gas-liquid mass transfer coefficient in the liquid phase [m/s]
k_{LS}	liquid-solid mass transfer coefficient [m/s]
k_j	reaction rate constant [s^{-1}]
K_j	adsorption equilibrium [m^3/mol]
L_t	total specific amount of sites for adsorption [mol/kg$_{cat}$]
P_{O_2}	partial pressure of oxygen [Pa]
R_i	reaction rate of compound i [mol/s]
$R_{V,i}$	volumetric reaction rate of compound i [mol/m^3.s]
$R_{w,i}$	specific disappearance or formation rate of compound i [mol/s.kg]
S_i	selectivity to compound i [%]
S.E.	stoichiometric oxygen excess to malonic acid [%]
Sh	Sherwood number [-]
T	temperature [K]
V	volume of the liquid in the reactor [m$_L$^{3}]
W	total mass of dry catalyst in the reactor [kg]
X_i	conversion of compound i [%]

Greek letters

ε_P	particle porosity [-]
θ_X	fraction of active site occupied by species X [-]
ρ_P	density of the dry particle [kg/m^3]
ν	stoichiometric number of oxygen for complete oxidation [-]

Superscripts
| 0 | initial |
| sat | saturated value |

Subscripts
AC	acetic acid
cat	catalyst
c	catalytic
ho	homogeneous
i	organic compound [-]
j	type of reaction or organic species [-]
L, l	bulk liquid
M	minimum value
MLO	malonic acid
nocat	non-catalysed reaction
p	particle
Pt	platinum
S, s	solid or the catalyst surface
T, t	total
w	weight specific
X	related to compound X

References

Battino, R., Ed., "IUPAC Solubility Data Series, Oxygen and Ozone", Pergamon Press, Oxford, 1981, p.459.

Beenackers, A.A.C.M. and van Swaaij, W.P.M., Chem. Eng. Sci. 48 (1993) 3139.

Besson, M. and Gallezot, P., Catal. Today 57 (2000) 127.

Béziat, J.C., Besson M., Gallezot, P. and Durécu, S., Ind. Eng. Chem. Res. 38 (1999) 1310.

Cybulski, A. and Trawczynski, J., Appl. Catal. B 47 (2004) 1.

Darensbourg, D.J., Holtcamp, M.W., Longridge, E.M., Khandelwal, B., Klausmeyer,K.K., and Reibenspies, J.H., J. Am., Chem. Soc., 117 (1995) 318.

Eftaxias, A., Font, J., Fortuny, A., Fabregat, A. and Stüber, F., Comp. Chem. Eng. 26 (2002) 1725.

Fogler, H.S., "Elements of Chemical Reaction Engineering", 3rd ed., Prentice Hall, Upper Saddle River NJ, 1999, p.577, 740.

Gallezot, P., Catal. Today, 37 (1997) 405

Gallezot, P., Chaumet, S., Perrard, A. and Isnard, P., J. Catal. 168 (1997) 104.

Harmsen, J.M.A., Jelemensky, L., van Andel-Schefer, P.J.M., Kuster, B.F.M.and Marin, G.B., Appl. Catal. A 165 (1997) 499.

Klinghoffer, A.A., Cerro, R.L., and Abraham, M.A., Catal. Today 40 (1998) 59.

Kluytmans, J.H.J., Markusse, A.P., Kuster, B.F.M., Marin, G.B. and Schouten, J.C., Catal. Today 57 (2000) 143.

Lide, D.R., Ed., "Handbook of Chemistry and Physics", 84th ed., CRC Press, LLC, 2004, p.6-49.

Luck, F., Catal. Today 53 (1999) 81.

Marquié, J., Laporterie, A., Dubac, J. and Roques, N., Synlett 4 (2001) 493.

Masende, Z.P.G., Kuster, B.F.M., Ptasinski, K.J., Janssen, F.J.J.G., Katima, J.H.Y. and Schouten, J.C., Appl. Catal. B 41 (2003a) 247.

Masende, Z.P.G., Kuster, B.F.M., Ptasinski, K.J., Janssen, F.J.J.G., Katima, J.H.Y. and Schouten, J.C., Catal. Today 79-80 (2003b) 357.

Masende, Z.P.G., Kuster, B.F.M., Ptasinski, K.J., Janssen, F.J.J.G., Katima, J.H.Y. and Schouten, J.C., Topics in Catal. (2004a) *Submitted.*

Matatov-Meytal, Yu.I. and Sheintuch, M., Ind. Eng. Chem. Res. 37 (1998) 309.

Mishra, V.S., Mahajani, V.V. and Joshi, J.B., Ind. Eng. Chem. Res. 34 (1995) 2.

Mussons, M.L., Raposo, C., Torre, M.F., Morán, J.R., and Caballero, M.C., Tetrahedron 55 (1999) 4077.

Pauling, L., Am. Sci., 36 (1948) 51.

Perry, R.H., Green, D.W. and Maloney, J.O., Eds., "Perry's Chemical Engineers' Handbook", 7th ed., McGraw-Hill, New York, 1999, p.5-48

Rivas, J., Kolaczkowski, S.T., Betran, F.J. and McLurgh, D.B., Appl. Catal. B 22 (1999) 279.

Sano, Y., Yamaguchi, N. and Adachi, T., J. Chem. Eng. Japan, 7 (1974) 255.

Santacesaria, E., Catal. Today 52 (1999) 113.

Vleeming, J.H., "Deactivation of carbon-supported platinum catalysts during carbohydrate oxidation", Ph.D. thesis, Eindhoven University of Technology, Eindhoven (1997), p. 156.

7

CATALYTIC WET OXIDATION OF MALEIC ACID OVER Pt/GRAPHITE CATALYST: MASS TRANSPORT AND REACTION KINETICS

Abstract

Catalytic wet oxidation (CWO) of maleic acid has been studied over a 5 wt.% Pt/graphite catalyst in a slurry phase CSTR. The influence of the catalyst concentration on the reaction rate was significant when small amounts of catalyst were employed. A high conversion of maleic acid to CO_2 and H_2O was obtained at an impeller speed of 20 s^{-1} with 10 kg_{cat}/m_L^3 Pt/graphite and stoichiometric oxygen excess to maleic acid between 0 and 100%. It is shown that high performance of the Pt/graphite catalyst, and hence high maleic acid conversion, was obtained when the reaction was carried out in the oxygen mass transport limited regime. The rate of reaction and hence CO_2 formation was found to increase with increasing impeller speed. A CWO model for maleic acid, based on mass transport of the reactants to the catalytic site, has been developed and validated. The model can be applied for the prediction of the reaction rate within the mass transport limited regime in which no deactivation of the catalyst takes place.

7.1.   Introduction

The use of noble metal catalysts in catalytic wet oxidation (CWO) of toxic organic compounds seems to be promising. The noble metal catalysts studied for phenol oxidation include ruthenium catalysts (Cybulski and Trawczynski, 2004; Vaidya and Mahajani, 2002) and platinum catalysts (Cao *et al*., 2003; Masende *et al*, 2003a, 2004a; Maugans and Akgerman, 1997) on different supports. The oxidation of aromatic organic wastes in water generally results in several intermediates, which include unsaturated carboxylic acids, like maleic acid, and saturated acids. Maleic acid has been identified in many studies as one of the major intermediates during phenol oxidation to either acetic acid or succinic acid, or to the desired end products CO_2 and H_2O via glyoxylic acid and oxalic acid (Matatov-Meytal and Sheintuch, 1998; Mishra *et al*., 1995). It is also well known that acetic acid, once formed, is difficult to oxidize at temperatures below 200°C. In industrial processes, maleic acid can be obtained by the hydration of maleic anhydride or from the wash water during maleic anhydride production. The primary use of maleic anhydride is in the manufacture of polyester and alkyd resins. The discharge of water from these processes often contains maleic acid or its degradation carboxylic acids, such as acrylic acid, acetic acid, and succinic acid. Therefore, it would be worth investigating the degradation of maleic acid in the presence of Pt/graphite catalyst.

Several reaction networks for maleic acid oxidation over different catalysts have been proposed in the literature (Oliviero *et al*., 2001; Gallezot *et al*., 1996; Devlin and Harris, 1984). Scheme 7.1 shows the main reaction intermediates and end products for maleic acid oxidation identified in different studies. According to the reaction scheme proposed by Devlin and Harris (1984), maleic acid can be oxidised either into glyoxylic acid to oxalic acid, which reacts easily to CO_2 and H_2O, or into acrylic acid, which leads to refractory acetic acid. Oliviero *et al*. (2001) also reported a reaction network for maleic acid oxidation over Ru/CeO$_2$ catalyst, which was similar to the non-catalysed network. The reaction network for maleic acid oxidation over platinum catalysts seems to be different. Gallezot *et al*. (1996) reported that maleic acid oxidation over a Pt/C catalyst does not proceed via acrylic acid, since no acetic acid was detected in their studies. In recent studies with Pt/graphite catalyst (Masende *et al*., 2003a,b, 2004a), it has been found that complete oxidation of phenol and also maleic acid to CO_2 and H_2O can be achieved when the reaction is carried out in the oxygen mass transfer controlled regime. During phenol oxidation it was further found that, under oxygen supply limited conditions, low molecular weight carboxylic acids including succinic acid and refractory acetic acid were formed, whereas at excess

oxygen aromatic compounds like *p*-benzoquinone, and insoluble matter attributed to polymeric products, were observed. The oxygen surface coverage determines the extent of reaction and the reaction network towards the desired end products (Masende *et al.*, 2003b). The formation of the refractory acids however, could be bypassed when the reaction was carried out within the proper operation window (Masende *et al.*, 2003a).

Scheme 7.1. An overview of the main intermediates and end products for maleic acid oxidation in liquid phase reported in the literature (Oliviero *et al.*, 2001; Gallezot *et al.*, 1996; Devlin and Harris, 1984).

Although several studies have been reported in the literature for catalytic wet oxidation of carboxylic acids using noble metal catalysts (Oliviero *et al.*, 2001; Rivas *et al.*, 1999; Gallezot *et al.*, 1997; Harmsen *et al.*, 1997; Gallezot *et al.*, 1996), the kinetics of CWO of maleic acid has not been extensively studied. There is still little information available in the published literature on the kinetics of CWO of maleic acid particularly, using Pt/graphite catalyst. Whereas kinetic data preferably are free from mass transport limitations (Perego and Peratello, 1999), in most of our studies we found that CWO using Pt/graphite catalysts proceeds to the desired end products, CO_2 and H_2O, when the reaction is carried out under oxygen transport limitation (Masende *et al.*, 2003a). Under intrinsic kinetic conditions, i.e. in the absence of mass transport limitations, the platinum catalyst exhibits fast deactivation.

Rivas *et al*. (1999) proposed a model for maleic acid oxidation over platinum/alumina catalyst, which considers a homogeneous non-catalysed and a heterogeneous catalytic contribution. The experiments were carried out in batch mode in a temperature range of 413-478 K and with oxygen partial pressure of 0.4-1.4 MPa. A conversion of 90% of maleic acid was obtained after a reaction period of 1 h at 443 K and no catalyst deactivation was reported. Previous studies on the performance of Pt/graphite catalyst (Masende *et al*., 2003a, 2004a) show that at high residual oxygen partial pressures above 150 kPa, deactivation of platinum catalyst occurs. For quantitative description of the performance of platinum catalyst during CWO of maleic acid, it is important to consider mass transport phenomena in the model development.

This work presents a systematic approach to obtaining a mass transport model for CWO of maleic acid over Pt/graphite. Maleic acid was chosen as a model compound since it has been identified as a major intermediate during phenol oxidation. A mass transport assessment, which is a good indicator of the proper reaction regime in which the experimental data are obtained, has been undertaken. A model that accounts for the mass transport of oxygen and maleic acid has been developed and evaluated.

7.2.   Experimental

The chemicals used in this research, including maleic acid, were pure analytical grade from Merck and were used as received. The solutions used in the oxidation experiments were prepared using deionised water. The liquid phase oxidation of maleic acid solutions was investigated using a commercially available catalyst, Pt/graphite (5 wt%) from Johnson Matthey, and was used without any pre-treatment. Other information and specifications of this Pt/graphite catalyst are shown in Table 7.1.

The experiments were carried out in a continuous flow stirred slurry reactor (CSTR), a 500 ml autoclave (Autoclave Engineers, Zipperclave Hastelloy), which is equipped with a gas dispersion impeller. Details of the experimental set-up and reactor start-up procedures are reported elsewhere (Masende *et al*., 2003a; 2004a). Experiments were performed over a wide range of reactor operating conditions (Table 7.2). Samples were analysed at a given interval of time for maleic acid as well as other end products. The liquid samples were analysed by using a HPLC set-up (Merck-Hitachi) with a 300 x 8 ID mm RSpak KC-811 column and a refractive index detector (Waters R401). The composition of the effluent gases (mainly O_2, CO_2, and N_2) was determined using an online gas analyser (Servomex, Xentra 4200) where nitrogen was used as an inert gas

during reaction. The detailed analytical procedures for the gaseous and liquid effluents from the reactor have been reported elsewhere (Masende *et al.*, 2004a).

The experimental results obtained from the CSTR were evaluated to give the disappearance rate of maleic acid, the rate of formation of end products, and carbon selectivity to CO_2. For all experimental data, the overall carbon balance and the oxygen balance were verified after every experiment, and were within the acceptable range of 95 - 100%. Detailed data analysis procedures are described elsewhere (Masende *et al.*, 2003a).

Table 7.1
Characteristics of the Pt/Graphite catalyst

Feature	Pt/graphite
Active metal content	5% on dry basis
Type	Reduced/dry (287)
Carrier	Graphite powder
Catalyst particle size distribution[a]	> 15 μm (5%)
	> 10 μm (25%)
	> 5 μm (85%)
	> 2 μm (100%)
Total surface area (B.E.T.) [$m^2 \cdot g^{-1}$]	15.0
Metal dispersion[b] [%]	5.3
Metallic surface area[b] [$m^2 \cdot g^{-1}$ sample]	0.66
Metallic surface area[b] [$m^2 \cdot g^{-1}$ metal]	13.1
Porosity[c] [%]	69.3

[a]The particle size distribution was confirmed using the Coulter LS 130 apparatus.
[b]Catalyst characterisation using ASAP 2000 series equipment
[c]Porosity measurement using AutoPore IV 9500 equipment

Table 7.2
Standard reactor operating conditions

Parameter	Standard	Range
Temperature (°C)	150	120 – 170
Total pressure (MPa)	1.8	1.8
Oxygen partial pressure (MPa)	0.3	0-0.5
Oxygen flow rate (at room conditions) (ml/min)	40	8-50
Nitrogen flow rate (at room conditions) (ml/min)	150	150
Initial maleic acid concentration (mol/m^3)	20	20
Liquid flow rate (ml/min)	10	10
Liquid volume in the reactor (ml)	350	350
Catalyst concentration (kg_{cat}/m_L^3)	10	0.6 –20
Stirrer speed (s^{-1})	20	6 – 20
pH	Uncontrolled	2-7

7.3.   Results and discussion

Catalytic wet oxidation of maleic acid was carried out in the presence of the heterogeneous Pt/graphite catalyst. Most of the experimental data have been reported elsewhere (Masende *et al.*, 2004a). In this paper only the data relevant for model development and validation, namely, the influence of such factors as stoichiomentric oxygen excess (S.E.), reaction temperature, catalyst concentration, and impeller speed are reported.
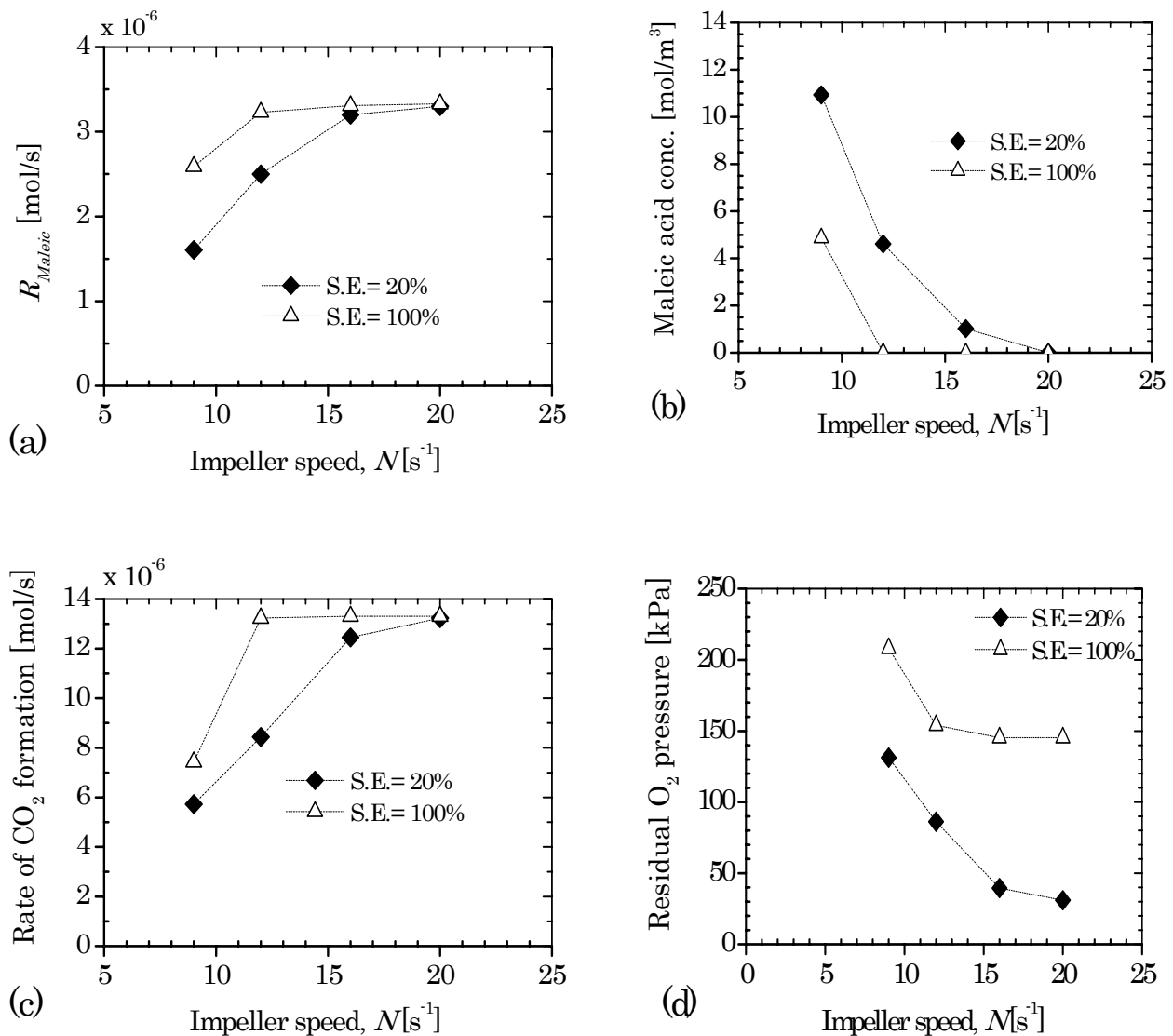
Fig. 7.1. Influence of impeller speed during maleic acid oxidation at 150°C, C_{maleic}=20 mol/m^3, and 6 kg$_{cat}$/m$_L^3$ Pt/graphite at steady state conditions after 6.3 ks run time: (a) disappearance rate of maleic acid, (b) concentration of maleic acid, (c) CO_2 formation, and (d) residual O_2 partial pressure.

7.3.1. Reaction conditions

The dependence of the rate of reaction on the impeller speed was investigated in the range 540 – 1200 rpm at 150°C and for 6 kg_{cat}/m_L^3 of Pt/graphite catalyst. The concentration of maleic acid in the feed solution was kept constant at 20 mol/m³, while two different oxygen molar flow rates, expressed as stoichimetric oxygen excess (Masende *et al.*, 2003a), that is, S.E. of 20% and 100%, were used. The slurry CSTR is equipped with a special gas dispersion impeller. When a transparent vessel was used, it was found that the minimum or critical speed at which gas bubbles are induced into the liquid was 9.6 s⁻¹ (575 rpm); below this value no gas could be induced into the liquid. High conversions of maleic acid (above 90%) were observed when the agitation speed was above an impeller speed of 15 s⁻¹ for a S.E. of 20%, whereas for a S.E. of 100% the rate of reaction was independent of the speed of mixing above 12 s⁻¹ as shown in Fig. 7.1. The results suggest that for high oxygen molar flow rates, a low agitation speed could give a sufficient rate of transport of oxygen to the catalyst surface, whereas for low oxygen molar flow rates such as S.E. of 20%, a high stirrer speed is required.
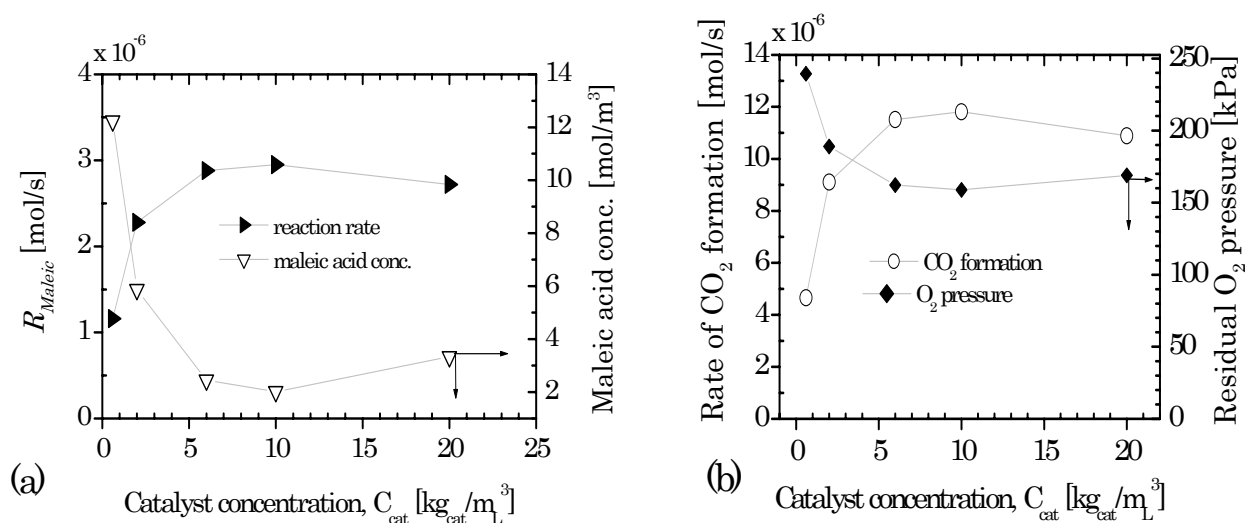
Fig. 7.2. Effect of catalyst concentration during oxidation of maleic acid solution at 140°C, S.E.=100%, 1200 rpm, and C_{maleic}=20 mol/m³ after 6.0 ks.

The effect of catalyst concentration on the rate of reaction was studied in the range 0.6-20 kg_{cat}/m_L^3 of Pt/graphite at 140°C and impeller speed of 20 s⁻¹. It was found that below a concentration of 6 kg_{cat}/m_L^3, the reaction rate and hence CO_2 formation increased with an increase in catalyst concentration. Within the concentration range of 6-10 kg_{cat}/m_L^3, no further increase in the reaction rate was observed as can be seen in Fig. 7.2. However, some decline in the reaction rate and also in the rate of CO_2

formation was observed at a catalyst concentration of 20 kg_{cat}/m_L^3. While there is a dependence of the reaction rate on the catalyst concentration below 6 kg_{cat}/m_L^3, the possibility of deactivation of the small number of active sites cannot be excluded, especially at the high oxygen molar flow rates used. The reason for the lower reaction rate observed at high catalyst concentration of 20 kg_{cat}/m_L^3 is not yet clear, however, the increased solid-to-liquid ratio can possibly affect the mass transport mechanisms for the reactant to the catalyst surface. For investigations of the dependence of maleic acid conversion on temperature and on oxygen molar flow rates (expressed as stoichiometric oxygen excess to maleic acid), the catalyst concentration of 10 kg_{cat}/m_L^3 was used as a standard.

7.3.2. *Effect of oxygen molar flow rate*

A number of experiments were carried out at a temperature of 150°C with a catalyst concentration of 10 kg_{cat}/m_L^3 to investigate the influence of oxygen concentration on maleic acid conversion. The concentration of maleic acid in the feed solution was 20 mol/m^3, whereas the molar flow ratio, expressed as stoichiometric oxygen excess (S.E.), was varied from –50% to 200%. Other parameters were kept at standard conditions (Table 7.2). The results shown in Fig. 7.3 indicate that the conversion of maleic acid increases with the increase in oxygen molar flow rate, whereby almost complete conversion to CO_2 and H_2O was achieved at S.E. of 20 and 100% as can be seen in Fig. 7.3(a). Similar trends were recorded for the residual maleic acid concentration (Fig. 7.3b) and for the rate of CO_2 formation (Fig. 7.3c).

The results indicate further that a high conversion of maleic acid could be obtained when the residual oxygen partial pressure in the reactor was below 150 kPa as shown in Fig. 7.3(d). At a high residual oxygen partial pressure of 300 kPa, a decline of catalyst activity was observed, especially at reaction times above 6.0 ks. This decline in catalyst activity can be due to over-oxidation of the platinum surface, which reduces the number of active sites available for the reaction. The over-oxidation of platinum catalyst during aqueous phase oxidation of organic compounds has been reported in other studies (Gallezot, 1997; Mallat and Baiker, 1995). These results are in agreement with our previous findings during phenol oxidation over platinum on graphite catalyst (Masende *et al*., 2003a). It is evident that when oxygen molar flow rates equivalent to S.E. of 20% are employed, complete conversion of maleic acid to CO_2 and H_2O could be achieved at a temperature of 150°C without deactivation of the catalyst. The observed results show that for complete conversion of maleic acid to the desired end

products, CO_2 and H_2O, without any loss of catalyst activity, the control of the oxygen concentration at the catalyst surface is crucial.
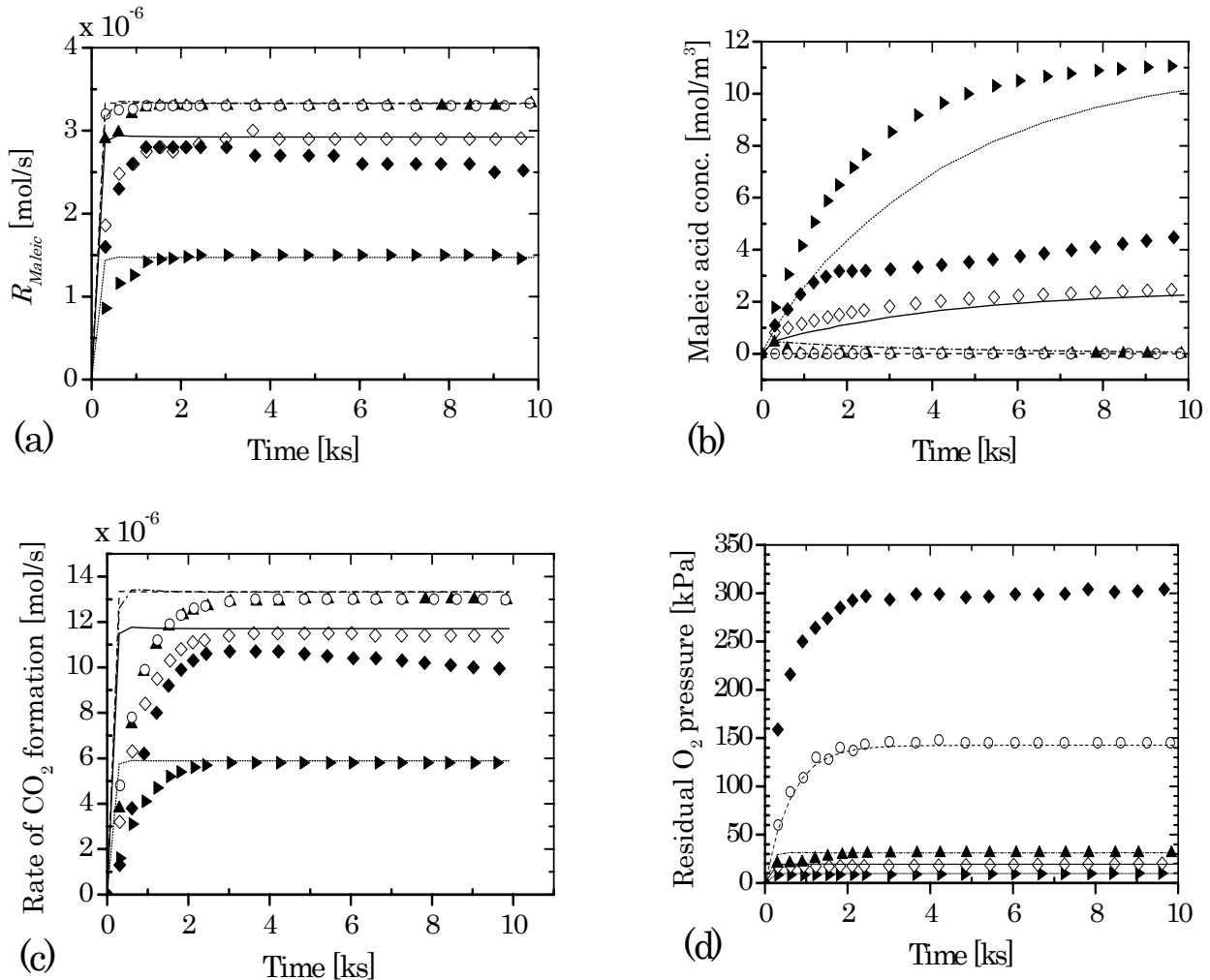
Fig. 7.3. Calculated and experimental results for maleic acid oxidation at different S.E. Symbols show experimental data for S.E. of: −50%(►), 0%(◊), 20%(▲), 100% (○), and 200%(♦), while lines show calculated results using equations (7.2)-(7.8) and data in Table 7.3. No modelling for data showing catalyst deactivation, e.g. S.E. of 200%: (a) reaction rate for maleic acid, (b) maleic acid concentration, (c) CO_2 formation, and (d) residual oxygen partial pressure.

7.3.3. *Effect of temperature*

The investigation of the temperature dependence of the reaction was carried out at a constant S.E. of 200% and 10 kg_{cat}/m_L^3 of Pt/graphite catalyst while other parameters were kept at standard conditions. The S.E. of 200% was chosen because it gives low conversion and showed catalyst deactivation at 150°C and therefore, the possibility for catalyst reactivation could be explored. It was found that a high temperature enhances the rate of conversion of maleic acid. Almost complete conversion of maleic acid to

CO_2 and H_2O was achieved at 170°C and no indication of catalyst deactivation was observed as can be seen in Fig. 7.4(a). At low temperatures, low conversions were obtained and a rapid decline of the catalyst activity was observed. It is clear from Fig. 7.4(b) that at high temperatures, the rate of consumption of oxygen is also increased which results into a relative decrease in the residual oxygen partial pressure. The increase in maleic acid conversion at high temperatures can be attributed to an increased catalytic activity of platinum catalyst that can handle high oxygen loads. To describe the observed results quantitatively, it is important to understand the reaction regime in which good performance of the catalyst was observed.
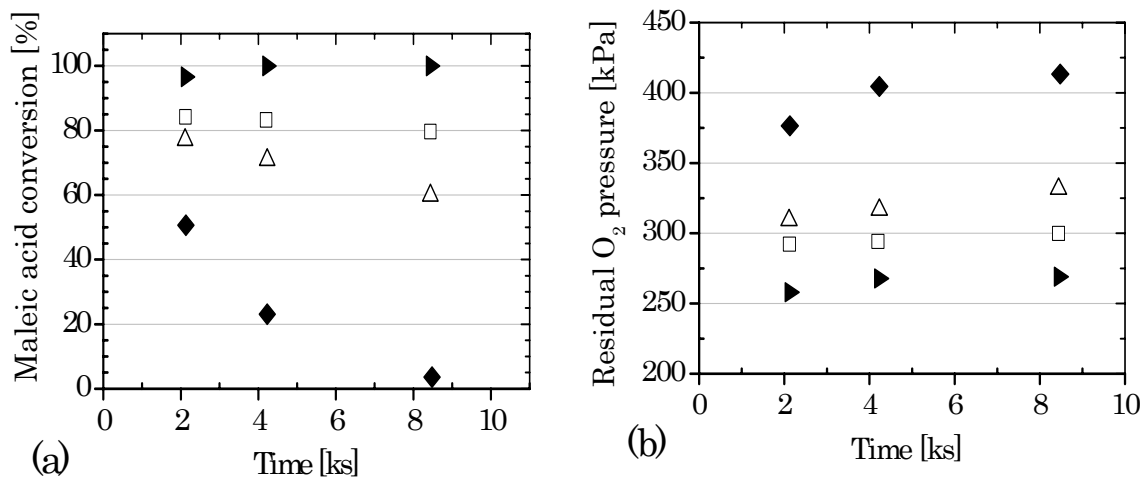
Fig. 7.4. Effect of temperature during maleic acid oxidation at S.E.= 200%, 1200 rpm, C_{maleic}=20 mol/m³, and 10 kg$_{cat}$/m$_L$³ Pt/graphite. Data points from each run were taken after 2.1 ks, 4.2 ks, and 8.4 ks. (a) conversion, and (b) residual O_2 pressure: Symbols: (♦) 120°C; (Δ) 140°C; (□) 150°C, and (▶) 170°C.

7.3.4. *Mass transport*

A mass transport assessment for the reacting species was undertaken for each experiment in order to characterise the reaction regime in which the experimental data were obtained. The data considered for mass transport limitation analysis were taken after 6.3 ks within one experimental run (corresponding to a reaction period of three times the average liquid residence time). Since the oxidation of maleic acid takes place at the catalyst surface, it was also necessary to determine the concentrations of oxygen and maleic acid at the catalyst surface. The mass transport equations for the reactants were based upon the film model, which assumes that the resistance to mass transfer is present in a thin film near a certain interface. The concentration only varies within this layer, and mass transfer through the film can be estimated for a known value of mass transfer coefficient. Therefore, sequential calculations were performed to determine

the concentrations in the bulk liquid and at the catalyst surface. Due to the high diffusivity of oxygen in the gas phase and its low solubility in water, the gas phase mass transfer resistance was considered to be negligible.

The criteria for checking the absence of gas-liquid mass transfer limitation was set at a maximum deviation of 5% or a minimum degree of saturation of 0.95 as reported in the literature (Fogler, 1999; Beenackers and van Swaaij, 1993). The experimental data are considered free of the gas-liquid mass transfer limitation if the ratio of the calculated bulk liquid concentration ($C_{O_2,L}$) to the equilibrium oxygen concentration ($C_{O_2}^{sat}$), is at least 0.95, that is the condition $C_{O_2,L}/C_{O_2}^{sat} \geq 0.95$ should be satisfied. The derivation of the mass transfer limitation criteria has been reported elsewhere (Masende *et al.*, 2003a, 2004b). The value of $k_{GL}a_{GL}$ used in the mass transfer evaluation was estimated using the correlation of Tekie *et al.* (1997) and is presented in Table 7.3. The oxygen concentration in the liquid, $C_{O_2}^{sat}$, which is in equilibrium with the gas phase, was calculated by using a semi-empirical correlation given by Battino (1981).

Similarly, for the absence of liquid-to-solid mass transfer limitation for maleic acid or oxygen, the ratio of the concentration at the catalyst surface ($C_{X,S}$) to the bulk liquid concentration ($C_{X,L}$) should be at least 0.95, that is the condition $C_{X,S}/C_{X,L} \geq 0.95$ needs to be satisfied. Within the temperature range of 120 - 170°C, the diffusion coefficient (D_X) ranged from 8.35 x 10^{-9} to 1.40 x 10^{-8} m^2/s for oxygen and from 3.06 x 10^{-9} to 5.13 x 10^{-9} m^2/s for maleic acid, which were estimated from the Wilke-Chang equation (Perry *et al.*, 1999; Lide, 2003). Data related to mass transport are presented in Table 7.3.

Table 7.3. Mass transfer data and kinetic parameters at 150°C, P_T= 1.8 MPa, 10 kg$_{cat}$/m$_L^3$ Pt/graphite, d_p= 15 μm, and impeller speed of 20 s^{-1}

Parameter	SI units	Oxygen	Maleic acid
$k_{GL}a_{GL}$ *	[s^{-1}]	0.120 ± 0.015	
a_{LS}	[m^2/m^3]	5556	5556
D_X	[m^2/s]	1.16 x 10^{-8}	4.23 x 10^{-9}
Sh_X	[-]	3.6	2.8
$k_{LS,X}$	[m/s]	2.78 x 10^{-3}	7.9 x 10^{-4}
$k_{LS,X}a_{LS}$	[s^{-1}]	4.4	15.5
k_w	[m^3/(kg.mol.s)]	8.4 ± 1.8	8.4 ± 1.8

*The $k_{GL}a_{GL}$ values at different stirrer speed (between brackets) are: 0.01 (9 s^{-1}), 0.028 (12 s^{-1}), and 0.068 (16 s^{-1}). The estimates are 15-32% lower than values obtained from the correlation of Tekie *et al.* (1997).

The significance of internal mass transport limitation was assessed using the Weisz-Prater criterion (C_{WP}), whereby pore diffusion is considered negligible if the condition $C_{WP} \ll 1$ is satisfied (Fogler, 1999). The effective diffusivity was estimated from $D_e = 0.25 D_X \varepsilon_p$, with particle porosity $\varepsilon_p = 0.68$ (-). For maleic acid and for the data under consideration, the maximum value obtained was $C_{WP} = 0.023$ (-), indicating that no intra-particle concentration gradients and no internal diffusion limitation existed. It was further found that for all experiments the maximum value for oxygen was $C_{WP} = 0.12$ (-), which again indicates the absence of concentration gradients and diffusion limitation. Because the type of catalyst used is an "egg-shell" catalyst, where the active sites are mainly located in the outer shell of the particle, the criterion is met even more easily.
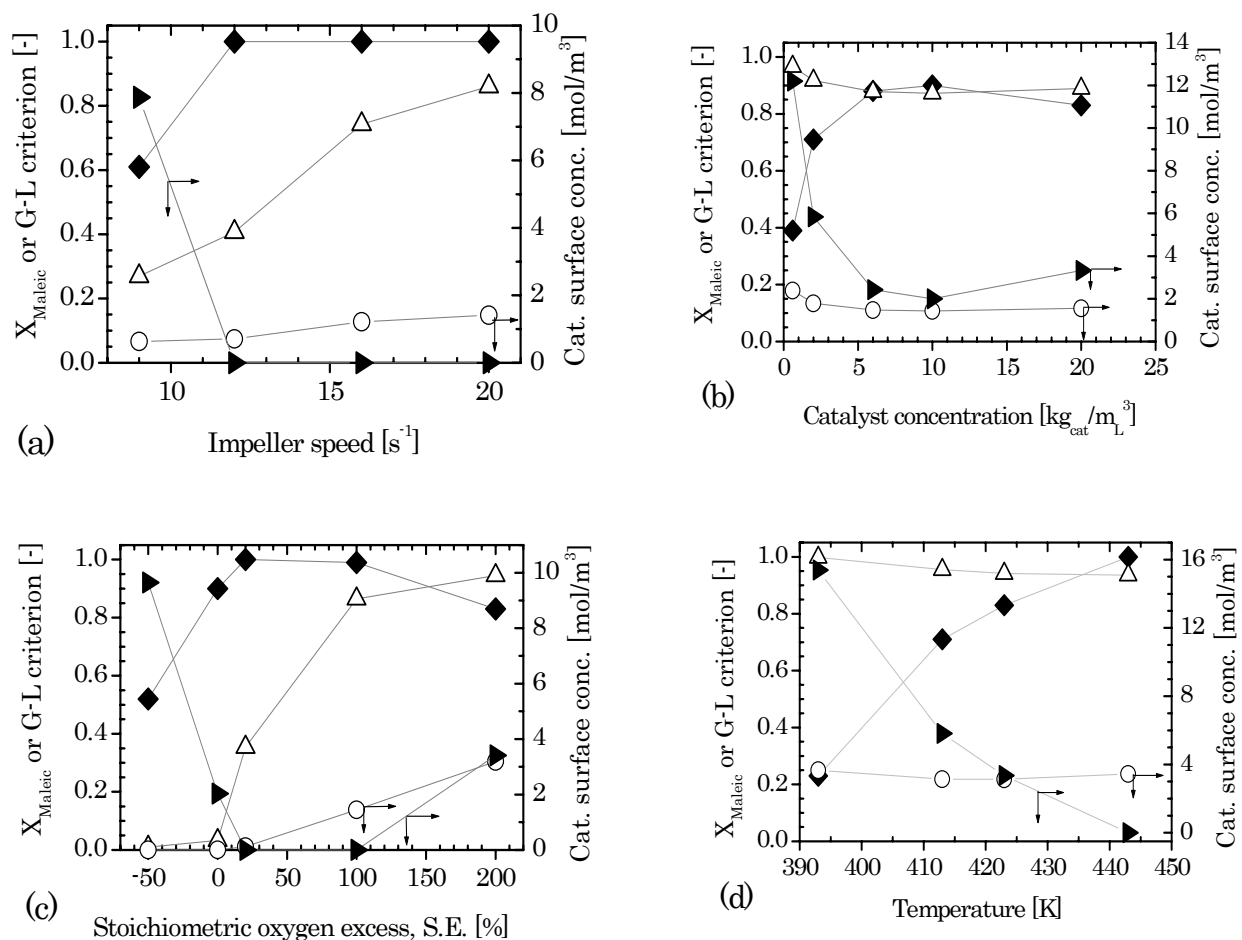
Fig. 7.5. Verification of mass transfer limitation criteria for experimental data: (a) effect of impeller speed at S.E.=100% and conditions as in Fig. 7.1, (b) effect of catalyst concentrations at conditions as in Fig. 7.2, (c) effect of stoichiometric oxygen excess at conditions as in Fig. 7.3, and (d) effect of temperature at conditions as in Fig. 7.4. Left y-axis: (♦) conversion, (Δ) G-L oxygen mass transfer criterion; right y-axis: (○) oxygen catalyst surface concentration, (►) maleic acid catalyst surface concentration.

An overview of the maleic acid conversion, the gas-liquid mass transfer criterion, and the reactant concentration at the catalyst surface is depicted in Fig. 7.5. It is clearly seen in Fig. 7.5(a) that at S.E. of 100% and with a catalyst concentration of 6 kg_{cat}/m_L^3, the ratio $C_{O_2,L}/C_{O_2}^{sat}$ was far below 0.95, which indicates that the data were obtained under oxygen gas-liquid mass transfer limitation. It is also clear that the conversion of maleic acid increased with an increase in impeller speed. At almost full conversion, the availability of maleic acid at the catalyst surface becomes limiting. A similar assessment was done for the data obtained from the study of catalyst concentrations at 140°C and S.E. of 100% with a constant impeller speed of 20 s^{-1}. In Fig. 7.5(b), with the exception of 0.6 kg_{cat}/m_L^3 where the catalyst concentration seems to be limiting, the other data were obtained at gas-liquid mass transfer limitation conditions (i.e. $C_{O_2,L}/C_{O_2}^{sat} < 0.95$). There was no liquid-solid mass transfer limitation for oxygen and maleic acid, and the concentrations at the catalyst surface were above 1 mol/m³ for the whole range of catalyst concentration.

Fig. 7.5(c) shows the mass transport evaluation at different stoichiometric oxygen excess at 150°C and a catalyst concentration of 10 kg_{cat}/m_L^3. At low S.E., the reaction is limited by the supply of oxygen, while at S.E. of 200%, deactivation of the catalyst was observed. It can be seen once again that at full conversion, maleic acid transfer is limiting. It is evident from these observations that complete conversion of maleic acid to CO_2 and H_2O was achieved when the reaction was carried out under oxygen mass transport limitation. A typical example can be seen for S.E. of 100% (T=423K, P_{O2}=145 kPa, C_{cat}= 10 kg_{cat}/m_L^3, C_{MA}= 6.6 x 10^{-4} mol/m³, and R_w= 9.43 x 10^{-4} mol/kg_{cat}.s), which gave $C_{O_2,L}/C_{O_2}^{sat} = 0.86$ indicating the presence of a gas-liquid mass transfer limitation. In Fig. 7.5(d) an assessment of the data for temperature dependence at S.E. of 200% is presented. It was verified that at temperatures above 420 K, the reaction is also under the oxygen gas-liquid mass transfer limitation albeit by a little, and at 443 K full conversion was achieved, causing maleic acid transfer to become limiting.

It can be concluded from the assessment that a high conversion of maleic acid to the desired end products, CO_2 and H_2O, can be achieved when the reaction is carried out in the oxygen transport controlled regime. It is also evident that there are no concentration gradients inside the catalyst pores. At a high conversion rate, the concentration of either oxygen or maleic acid at the catalyst surface can be very low. Therefore, wet oxidation of maleic acid in the presence of platinum catalyst can be

described quantitatively by considering the transport of oxygen and maleic acid to the catalyst surface.

7.3.5. Rate equations for maleic acid oxidation

The conservation equations for mass and energy are the basis for the reactor modelling. The oxidation of maleic acid in aqueous phase over Pt/graphite to the desired end products CO_2 and H_2O is described by the overall reaction:

$$COOH(CH)_2COOH + 3O_2 \rightarrow 4CO_2 + 2H_2O \qquad (7.1)$$
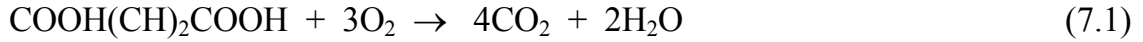
The reactor was assumed to work under isothermal conditions. Therefore, only mass balances must be solved. When a second-order reaction at the catalytic site (i.e. first-order in oxygen and first-order with respective to maleic acid) is considered, and the mass transfer resistance of oxygen in the gas phase is negligible, the volumetric reaction rate equation for oxygen (in mol m^3 s^{-1}) can be derived to obtain (Beenackers and van Swaaij, 1993):

$$R_{V,O_2} = \cfrac{C_{O_2}^{sat}}{\left[\cfrac{1}{(k_{GL}\,a_{GL})} + \cfrac{1}{(k_{LS}\,a_{LS})_{O_2}} + \cfrac{1}{\eta\,k_w\,C_{cat}\,C_{MA,L}}\right]} \qquad (7.2)$$

Eq. (7.2) is applicable when oxygen transport to the catalytic site is limiting ($C_{MA,S} = C_{MA,L}$). However, if maleic acid transport to the catalytic site is limiting ($C_{O_2,S} = C_{O_2,L}$), then the volumetric reaction rate (in mol m^3 s^{-1}) is given by:

$$R_{V,MA} = \cfrac{C_{MA,L}}{\left[\cfrac{1}{(k_{LS}\,a_{LS})_{MA}} + \cfrac{1}{(1/\nu)\eta\,k_w\,C_{cat}\,C_{O_2,L}}\right]} \qquad (7.3)$$

The effectiveness factor was taken equal to unity, i.e. $\eta=1$, which follows from the Weisz-Prater criterion in Section 7.3.4. Other symbols are described in the notation section.

To calculate the reaction rates from Eqs. (7.2) and (7.3) in a CSTR, first the mass-conservation equations for oxygen and maleic acid in the gas and liquid phases and at the catalytic site are described by Eqs. (7.4)-(7.8).

Oxygen in the gas phase:

$$\frac{V_G}{RT}\frac{dp_{O_2}}{dt} = F_{V,in}^g\,\frac{p_{O_2}^0}{RT} - F_{v,out}^g\,\frac{p_{O_2}}{RT} - (k_{GL}a_{GL})V_L(C_{O_2}^{sat} - C_{O_2,L}) \qquad (7.4)$$

Oxygen in the liquid phase:

$$V_L\frac{dC_{O_2,L}}{dt} = F_V^l(0 - C_{O_2,L}) + (k_{GL}a_{GL})V_L(C_{O_2}^{sat} - C_{O_2,L}) - (k_{LS}\,a_{LS})_{O_2}\,V_L(C_{O_2,L} - C_{O_2,S}) \qquad (7.5)$$

Assuming a steady-state approximation, the rate of oxygen transport (in mol m³ s⁻¹) equals the reaction rate at the catalyst surface:

$$R_{V,O_2} = (k_{LS}a_{LS})_{O_2}(C_{O_2,L} - C_{O_2,S}) = R_{w,O_2} C_{cat} \tag{7.6}$$

Assuming a constant liquid flow and a constant liquid volume, the concentration of maleic acid in the liquid phase is expressed by:

$$V_L \frac{dC_{MA,L}}{dt} = F_V^l(C_{MA,in} - C_{MA,L}) - (k_{LS}a_{LS})_{MA}V_L(C_{MA,L} - C_{MA,S}) \tag{7.7}$$

Similarly, for a steady-state reaction, the rate of transport of maleic acid (in mol m³ s⁻¹) to the catalytic site equals the rate of reaction:

$$R_{V,MA} = (k_{LS}a_{LS})_{MA}(C_{MA,L} - C_{MA,S}) = R_{w,MA}C_{cat} \tag{7.8}$$

The rate equations and the mole balance equations were solved using the Polymath package (Version 5.1). Model parameters were estimated using a sequential calculation procedure whereby the best-fit values could be obtained. The estimation of the gas-liquid mass-transfer parameter $k_{GL}a_{GL}$ and the liquid-solid mass-transfer parameters $(k_{LS}a_{LS})_{O_2}$ and $(k_{LS}a_{LS})_{MA}$, were performed through non-linear regression of the experimental data using Polymath (Version 5.1) whereby Eqs. (7.2) and (7.3) were used to obtain the best-fit values. Similarly, the reaction rate parameter k_w was determined from the regression of the experimental data.

7.3.6. Reactor model simulation

Estimates of all mass transfer and kinetic parameters are given in Table 7.3. The estimated values of $k_{GL}a_{GL}$ were found to be lower by 15%- 32%, within the range of impeller speeds of 9 s⁻¹ to 20 s⁻¹, as compared to values obtained from the correlation by Tekie *et al*. (1997). The gas-liquid mass transfer coefficient at an impeller speed of 20 s⁻¹ was found to be $k_{GL}a_{GL} = 0.12$ s⁻¹. The value for $(k_{LS}a_{LS})_{O_2}$ in Eq. (7.2) was 4.4 s⁻¹ which corresponds to a Sherwood number (*Sh*) of 3.6 (-), whereas the value for $(k_{LS}a_{LS})_{MA}$ in Eq. (7.3) was 15.5 s⁻¹ corresponding to *Sh* of 2.8 (-). The correlation of Sano *et al*. (1974) was used for the calculation of the Sherwood numbers. It is evident that the liquid-solid transport resistance of both maleic acid and oxygen is not as significant as the gas-liquid mass transfer resistance. In addition, the reaction parameter (k_w) of 8.4 m³ kg$_{cat}$⁻¹ mol⁻¹ s⁻¹ gave best-fit values for both Eqs. (7.2) and (7.3). The values for the liquid-solid mass transfer coefficients and the reaction parameter are considered to be minimum values since higher values gave no further influence on the reaction rate. For the reactor model simulation, the parameters in Table 7.3 were used.
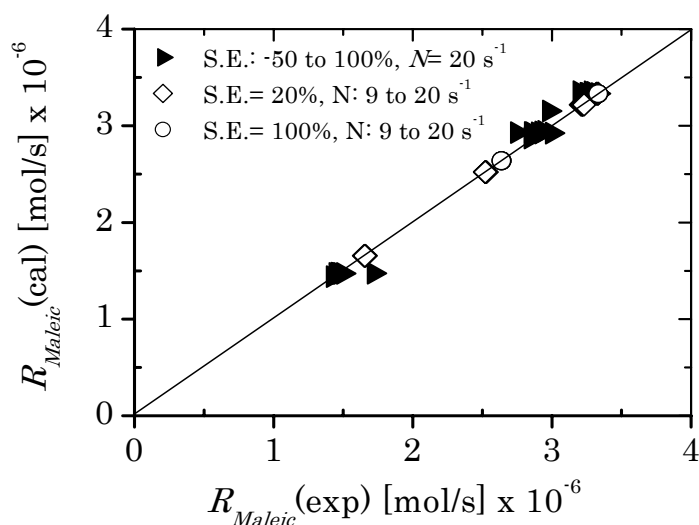
Fig. 7.6. Comparison between experimental and calculated disappearance rates for maleic acid during wet oxidation using Pt/graphite catalyst for different stoichiometric oxygen excess and different impeller speed.

Comparative analysis of the calculated and experimental disappearance rates of maleic acid for different reaction parameters is presented in Fig. 7.6. Only experimental data obtained at a steady state (after 6.3 ks) are compared to simulation results. It can be seen from the parity diagram that no significant bias between the experimental and calculated results exists. The experimental data obtained at different impeller speeds with S.E. of 20% and 100% have been satisfactorily described. The results confirm further that the contribution of the gas-liquid mass transfer rate to the overall reaction rate in both rate Eqs. (7.2) and (7.3) is crucial. Also a good fit with experimental data was observed when the model was applied at an impeller speed of 20 s^{-1} for different values of the stoichiometric oxygen excess.

In order to make a more detailed comparison, the reactor model was solved to give a reaction rate, residual concentration of maleic acid, CO_2 formation, and residual oxygen partial pressure as a function of time. Fig. 7.3 shows the model results and experimental data for stoichiometric oxygen excess of –50%, 0%, 20% and 100%. The predicted results for the disappearance rate of maleic acid are in good agreement with the experimental data. The deviation observed in Fig. 7.3(b) is due to the oxygen supply, since on the one hand a sub-stoichiometric amount of oxygen (-50%) was supplied to the reactor, whereas on the other hand the model does not account for partial oxidation since complete conversion of maleic acid to CO_2 and H_2O was assumed during the construction of the model. The deviations of the calculated rate of reaction which appear at the beginning of the experiments, are possibly due to experimental bias on starting the reactor due to stabilization of the liquid level control and due to the mixing volume between the reactor outlet and the sample port to the HPLC. It can be observed in Fig. 7.3(c) that a good agreement is also obtained for the

rate of CO_2 formation. The deviations observed at the beginning of the reaction can be explained by the dissolution of CO_2, which was assumed to be negligible. Fig. 7.3(d) shows a good fit of the predicted data with the observed residual oxygen partial pressure. It is clear from these results that the mass transport model can describe adequately the experimental data within the deactivation-free region, that is, where deactivation due to over-oxidation of catalyst was not identified.

7.4.   Conclusions

The performance of a Pt/graphite catalyst for the CWO of maleic acid has been investigated. The rate of reaction and hence CO_2 formation was found to increase with increasing impeller speed. This means gas-liquid mass transfer for oxygen, which depends on the impeller speed, controls the performance of the CWO of maleic acid. The dependence of the rate of reaction on catalyst concentration is significant when very small amounts of catalyst are employed. However, no clear relationship could be drawn between the increase in catalyst concentration and the reaction rate. It has also been found that a high conversion of maleic acid to CO_2 and H_2O is achieved when the stoichiometric oxygen excess to maleic acid is between 0 to 100% whereas the maximum residual oxygen pressure is below 150 kPa. At high oxygen residual partial pressure, deactivation of Pt/graphite catalyst occurs which results in a low conversion of maleic acid. Higher temperatures, however, enhance the catalytic activity of the catalyst.

A mass transfer analysis was found to be useful in revealing the operation regime in which experimental data were obtained. The catalyst was found to perform well when the reaction was carried out in the oxygen mass transport limited regime. A model, which accounts for the transport of the reactants to the catalytic site, has been developed and evaluated. The mass transfer coefficients and a minimum value for the reaction rate coefficient were obtained. The model results were in good agreement with the experimental data and can be used for prediction of the rate of reaction within the catalyst deactivation-free operation regime.

Acknowledgements

Nomenclature

a_{GL}	volumetric gas-liquid interfacial surface area [m^2/m^3]
a_{LS}	volumetric liquid-solid interfacial surface area [m^2/m^3]
C	concentration [mol/m^3] or active carbon support [-]
C_{cat}	concentration of catalyst [kg_{cat}/m_L^3]
C_{WP}	Weisz-Prater criterion [-]
C_X	concentration of the compound X [mol/m^3]
$D_{e,X}$	effective diffusivity of X [m^2/s]
d_p	particle size [m]
D_X	diffusivity of X in water [m^2/s]
F_V	volumetric flow rate [m^3/s]
k_{GL}	gas-liquid mass transfer coefficient in the liquid phase [m/s]
k_{LS}	liquid-solid mass transfer coefficient [m/s]
k_w	reaction rate constant [m^3 kg^{-1} mol^{-1} s^{-1}]
N	impeller speed [s^{-1}]
P_{O2}	partial pressure of oxygen [Pa]
P_T	total pressure in the reactor [Pa]
$R_{V,X}$	volumetric reaction rate of compound i [$mol/m^3.s$]
$R_{w,X}$	specific disappearance or formation rate of compound x [mol kgc_{at}^{-1} s^{-1}]
R_X	reaction rate of compound x [mol/s]
S.E.	stoichiometric oxygen excess to maleic acid [%]
Sh	Sherwood number [-]
T	temperature [K]
V_G	gas-phase volume in the reactor [m^3]
V_L	liquid-phase volume in the reactor [m^3]
W	total mass of dry catalyst in the reactor [kg]
X_{Maleic}	conversion of maleic acid [%]

Greek letters

ε_P	particle porosity [-]
η	effectiveness factor of the catalyst [-]
ρ_P	density of the dry particle [kg/m^3]
ν	stoichiometric number of oxygen for complete oxidation [-]

Superscripts

G, g	gas phase
L, l	liquid phase
0	initial condition
sat	saturation conditions

Subscripts

cat	catalyst

e	effective
in	incoming stream
L, l	bulk liquid
MA	maleic acid
out	outgoing stream
p	particle
Pt	platinum
S, s	solid or the catalyst surface
w	weight specific
WP	Weisz-Prater
X	related to compound X

References

Battino, R., Ed., "IUPAC Solubility Data Series, Oxygen and Ozone", Pergamon Press, Oxford, 1981, p.459.

Beenackers, A.A.C.M. and van Swaaij, W.P.M., Chem. Eng. Sci. 48 (1993) 3139.

Cao, S., Chen, G., Hu, X. and Yue, P.L., Catal. Today 88 (2003) 37.

Cybulski, A. and Trawczynski, J., Appl. Catal. B 47 (2004) 1.

Devlin, H.R. and Harris, I.J., Ind. Eng. Chem. Fundam. 23 (1984) 387.

Fogler, H.S., "Elements of Chemical Reaction Engineering", 3rd ed., Prentice-Hall, India, New Delhi, 2002, 1999, p. 738.

Gallezot, P., Catal. Today, 37 (1997) 405.

Gallezot, P., Laurain, N. and Isnard, P., Appl. Catal. B 9 (1996) L11.

Harmsen, J.M.A., Jelemensky, L., van Andel-Schefer, P.J.M., Kuster, B.F.M.and Marin, G.B., Appl. Catal. A 165 (1997) 499.

Lide, D.R., Ed., "Handbook of Chemistry and Physics", 84th ed., CRC Press, LLC, 2004, p.6-49.

Mallat, T. and Baiker, A., Catal. Today 24 (1995) 143.

Masende, Z.P.G., Kuster, B.F.M., Ptasinski, K.J., Janssen, F.J.J.G., Katima, J.H.Y. and Schouten, J.C., Appl. Catal. B 41 (2003a) 247.

Masende, Z.P.G., Kuster, B.F.M., Ptasinski, K.J., Janssen, F.J.J.G., Katima, J.H.Y. and Schouten, J.C., Topics in Catal. (2004a) *Submitted.*

Masende, Z.P.G., Kuster, B.F.M., Ptasinski, K.J., Janssen, F.J.J.G., Katima, J.H.Y. and Schouten, J.C., Catal. Today 79-80 (2003b) 357.

Masende, Z.P.G., Kuster, B.F.M., Ptasinski, K.J., Janssen, F.J.J.G., Katima, J.H.Y. and Schouten, J.C., Appl. Catal. B (2004b) *Submitted.*

Matatov-Meytal, Yu.I. and Sheintuch, M., Ind. Eng. Chem. Res. 37 (1998) 309.

Maugans, C.B. and Akgerman, A., Wat. Res. 31 (1997) 3116.

Mishra, V.S., Mahajani, V.V. and Joshi, J.B., Ind. Eng. Chem. Res. 34 (1995) 2.

Oliviero, L., Barbier, J.Jr., Duprez, D., Wahyu, H., Ponton, J.W., Metcalfe, I.S. and Mantzavinos, D., Appl. Catal. B 35 (2001) 1.

Perego, C. and Peratello, S., Catal. Today 52 (1999) 133.

Perry, R.H., Green, D.W. and Maloney, J.O., Eds., "Perry's Chemical Engineers' Handbook", 7th ed., McGraw-Hill, New York, 1999, p.5-48

Rivas, J., Kolaczkowski, S.T., Betran, F.J. and McLurgh, D.B., Appl. Catal. B 22 (1999) 279.

Sano, Y., Yamaguchi, N. and Adachi, T., J. Chem. Eng. Japan, 7 (1974) 255.

Tekie, Z., Li, J., Morsi, B.I. and Chang, M.Y., Chem. Eng. Sci. 52 (1997) 1541.

Vaidya, P.D. and Mahajani, V.V., Chem. Eng. J. 87 (2002) 403.

8
CONCLUDING REMARKS

8.1. Conclusions

Introduction

The work presented in this thesis is focused on the catalytic wet oxidation of organic waste using oxygen in the presence of platinum catalysts. Within the framework of the EVEN project (MHO/UDSM/EUT/EVEN), industrial wastewater containing non-biodegradable organic waste was identified as one of the major water pollution problems in Tanzania. The available conventional biological wastewater treatment in Tanzania, such as waste stabilization ponds (WSPs), is not suitable for this type of wastewater due to the inherent toxicity of organic wastes to micro-organisms. Heterogeneous catalytic wet oxidation, whereby the organic species in liquid phase reacts with oxygen in the presence of a catalyst, was identified as an alternative approach.

A literature review indicated that noble metal catalysts on different supports are effective for liquid phase oxidation as compared to non-noble metal and transitional metal oxides catalyst. The bottleneck for application of noble metal catalysts in liquid phase oxidation is their rapid deactivation. Platinum catalysts on different supports, namely, Pt/graphite, Pt/TiO$_2$, Pt/Al$_2$O$_3$, and Pt/AC were used in this work. Not many studies have been done on catalytic wet oxidation of organic wastes using platinum catalysts. The model compounds used in this work, namely, phenol (aromatic oxygenate), maleic acid (unsaturated acid), and malonic acid (saturated acid), represent a wide range of organic wastes. Valuable information such as, the practical operation window for platinum catalysts, the reaction networks of the model compounds, and on the mass transfer and reaction kinetics, has been obtained.

It has been shown that platinum catalysts are effective for catalytic wet oxidation of phenol and its intermediates to CO$_2$ and H$_2$O. Insight has been obtained into the

performance and effectiveness of platinum catalysts in liquid phase under different reaction conditions.

Experimental techniques

The slurry phase CSTR set-up has appeared to be useful for the investigation of the performance of the platinum catalyst in liquid phase oxidation of organic wastes. The use of mass flow controllers, online gas chromatography, and oxygen sensor or gas analyser, in combination with the volumetric gas meter provided accurate information on gas composition and flowrates. The high performance liquid chromatography (HPLC) whereby two columns were employed, one for phenol and aromatic intermediates, and another for carboxylic acids, was found to be a reliable and robust technique for identification and quantification of organic compounds in liquid phase. In order to get insight information on catalyst samples, characterisation techniques such as scanning electron microscopy (SEM), transmission electron microscopy (TEM), and CO chemisorption and mercury porosimetry, were found to be very useful.

Catalytic wet oxidation of phenol

The liquid phase oxidation of phenol over Pt/graphite has been studied in depth. The importance of a proper choice of the reactor start-up procedure in relation to the initial activity of the catalyst has been experimentally verified. A high activity of Pt/graphite catalyst was maintained when a reaction start-up method with 'simultaneous feed' of reactants (once reaction conditions are reached) was used. As the catalytic sites are exposed to both phenol and oxygen, deactivation of the catalyst is minimum when compared to the 'first phenol then oxygen' or the 'first oxygen then phenol' methods. Therefore, to maintain a high activity of the catalyst, a continuous stirred reactor is preferred where the ratio between liquid feed and oxygen can be easily controlled.

A wide range of factors was studied during catalytic wet oxidation (CWO) of phenol over Pt/graphite. It was found that complete oxidation of phenol to CO_2 and H_2O is achieved at 150°C when the reaction proceeds within the range of stoichiometric oxygen excess to phenol from 0 to 80%. By increasing the reaction temperature, the activity of the platinum catalyst, and also the reaction rate, was enhanced. At temperatures below 150°C, catalyst deactivation was observed with increased formation of polymeric products and lower selectivity to CO_2 and H_2O.

The oxidation mechanism of phenol over platinum catalyst appears to be different from the oxidation of phenol using non-noble metal oxide catalysts. The degree of oxygen coverage of the platinum surface has an influence on the activity of the Pt/graphite catalyst, and hence on the selectivity of the oxidation products. The activity of platinum catalyst remained high when the residual partial pressure of oxygen in the reactor was kept below 150 kPa at 1200 rpm. At higher residual oxygen partial pressure, the activity of platinum catalyst dropped as a result of deactivation by so-called over-oxidation. This type of deactivation was temporary and could be reversed at reducing conditions. The over-oxidation of the platinum surface, however, favoured the formation of *p*-benzoquinone leading to the formation of polymeric products, which resulted into permanent deactivation of the catalyst (poisoning). At conditions of limited supply of oxygen (a fully reduced platinum surface), the phenol oxidation reaction favours the formation of acetic and succinic acids which are difficult to oxidize.

Due to this phenomenon, a practical operation window (POW) was determined from the experimental data. Within the practical operation window a high phenol conversion and a high selectivity to CO_2 and H_2O can be achieved and deactivation of Pt/graphite catalyst is avoided. On the role of oxygen on the activity of platinum catalysts, four situations have been postulated, namely, over-oxidised, partly oxidised, free, and reduced platinum surfaces. It seems that the first role of oxygen is to raise the oxidation potential of the platinum necessary for releasing of a proton from the C-H bond ready for oxidation. A partly oxidised platinum surface favours full conversion of phenol to CO_2 and H_2O. At low oxidation potential, platinum active sites are vulnerable to poisoning by carbonaceous matter. The second role of oxygen is the protection of the platinum surface from irreversible poisoning by carbonaceous matter. The reaction pathway for platinum catalysed oxidation of phenol has been proposed. It was also found that glyoxylic acid is not a polymer precursor since it reacted rapidly to oxalic acid and to CO_2 in the presence of Pt/graphite catalyst. In addition, as both propanoic and muconic acid were never detected during phenol oxidation, it was evident that muconic acid is not an intermediate in the oxidation of phenol to end products.

The analysis of mass transport limitations revealed that higher conversions of phenol and high selectivities to CO_2 were favoured when the reaction was carried out in the mass transport limited regime. It was further found that when a high amount of catalyst was used, only part of the platinum catalyst participates in the reaction, while at a lower catalyst amount a non-linear dependence of the disappearance rate of phenol

on the catalyst concentration, was observed. Therefore, a model that predicts the performance of catalytic wet oxidation of phenol over platinum catalyst in the mass transfer limited regime, and within the practical operation window, has been developed and validated.

Malonic acid reaction

Malonic acid reaction has been chosen as a model reaction for saturated carboxylic acids, which have been reported in the literature during wet oxidation of phenol. It is also an important intermediate to CO_2 and to a refractory end product, acetic acid. The reaction of malonic acid in the presence of Pt/graphite catalyst was found to proceed via homogeneous and catalytic decarboxylation to CO_2 and acetic acid. It was also found that almost complete conversion of malonic acid to CO_2 and acetic acid was achieved at 160°C whereas a conversion of 28% was achieved at 150°C for non-catalysed decarboxylation in the absence of oxygen.

The results obtained in catalytic oxidation of malonic acid showed no significant improvement on the disappearance rate, whereas the selectivity to CO_2 increased. It seems that in the presence of catalyst and oxygen, the oxidation of malonic acid involves decarboxylation that gives intermediates, which can be oxidized at a highly oxidised platinum surface before desorption as acetic acid takes place. Without oxygen, the catalyst surface is in a reduced state and this favours the intermediates to recombine with H_{ads} to form acetic acid. Acetic acid, which was formed during catalytic decarboxylation, is a refractory compound that was difficult to oxidize at the conditions tested.

A number of kinetic models for the catalytic reaction of malonic acid have been developed based on the elementary steps in accordance to Langmuir-Hinshelwood kinetics. The adsorption steps for malonic acid and acetic acid on the catalytic site were assumed to be in a fast equilibrium. The pre-exponential factors, apparent activation energies and adsorption enthalpies have been determined from the experimental data. The optimum model that considers the contribution of a homogeneous and a heterogeneous route, including the adsorption of malonic acid, was able to accurately describe the kinetic experiments.

Catalytic wet oxidation of maleic acid

Catalytic wet oxidation of maleic acid is another model reaction used in this work. Maleic acid, an unsaturated carboxylic acid, is one of the major intermediates during phenol oxidation to either acetic acid or succinic acid, or to CO_2 and H_2O. Catalytic wet oxidation of maleic acid was investigated at different ranges of experimental conditions, including the influence of stoichiometric oxygen excess (S.E.) to maleic acid, temperature, agitation speed and catalyst concentration.

A study on the agitation speed shows that a high conversion of maleic acid to CO_2 and H_2O was obtained at an impeller speed of 1200 rpm and catalyst concentration of 10 kg_{cat}/m_L^3 Pt/graphite when the reaction was carried out at 150°C with S.E. between 0 and 100%. Deactivation of the Pt/graphite was observed at a S.E. of 200%. However, almost complete conversion of maleic acid to CO_2 and H_2O was achieved at 170°C when a high S.E. of 200% was used. This implies that at high temperatures the activity of the catalyst was enhanced. The influence of catalyst concentration on the conversion rate of maleic acid was significant when small amounts of catalyst were employed. The analysis of the experimental data for mass transfer limitations showed that a high activity of Pt/graphite catalyst and a high conversion of maleic acid to CO_2 and H_2O can be maintained when the reaction is carried out in the mass transport limited regime.

Based on mass transport of the reactants to the catalytic site, a CWO model for maleic acid was developed and validated. The mass transfer coefficients and the reaction rate coefficient have been determined from the experimental data. It has been shown that the mass transport model is capable of describing quantitatively the oxidation of maleic acid over Pt/graphite catalyst.

Influence of the catalyst properties

The influence of catalyst supports on the liquid phase oxidation of organic wastes was also investigated. The four catalyst samples used are: Pt/graphite, Pt/TiO_2, Pt/Al_2O_3 and Pt/AC. Throughout the range of experimental conditions, Pt/graphite catalyst was found to be the most effective and stable catalyst. The differences in activity of platinum catalysts in the liquid phase seem to be related to the metal dispersion and porosity of the catalyst support. A catalyst with a high metal dispersion and high porosity is vulnerable to rapid deactivation by over-oxidation and fouling. Pt/graphite, which has a metal dispersion of 5.3%, deactivates (over-oxidation) slowly compared to

Pt/TiO$_2$ (15.3%), Pt/Al$_2$O$_3$ (19.5%), and Pt/AC (19.0%). The corresponding porosity was Pt/graphite (69.3%), Pt/TiO$_2$ (73.8%), Pt/Al$_2$O$_3$ (76.9%), and Pt/AC (81.7%).

Deactivation by fouling or blocking of active sites is one of the consequences of over-oxidation, particularly during phenol oxidation whereby *p*-benzoquinone and polymer precursors are formed. Deactivation by fouling seems to be severe for "mixed" type catalysts, e.g., Pt/TiO$_2$, Pt/Al$_2$O$_3$ and Pt/AC, which also have relatively high percentage of porosity as compared to Pt/graphite catalyst. In conclusion, despite the differences of the morphological properties of the catalysts, the activity of platinum catalysts decreased in the order Pt/graphite > Pt/TiO$_2$ > Pt/Al$_2$O$_3$, as observed during phenol oxidation, and Pt/graphite > Pt/Al$_2$O$_3$ > Pt/AC during maleic acid oxidation.

8.2.   Process design considerations for Pt-CWO

The application of platinum catalysts in wet oxidation has shown that dangerous organic compounds like phenols can be oxidised to non- or less-toxic compounds at low temperatures (about 150°C) and pressure (< 1.8 Mpa). The low temperature, aqueous-phase heterogeneous catalytic oxidation of dissolved organic compounds is a potential mean for remediation of contaminated industrial effluents, and other wastewater streams. The ability for operation at substantially milder conditions of temperature and pressure, in comparison to supercritical water oxidation and wet air oxidation, is achieved through the use of supported platinum catalysts such as Pt/graphite.

However, the industrial applicability of platinum catalysed wet oxidation (Pt-CWO), like other wastewater technology, depends mainly on the nature of the target compounds, the pollution magnitude and concentration, geographical location of the pollution and catalyst performance. Due to the wide range of wastewater characteristics and non-biodegradable organic loads, accurate determination of the nature, quantity and composition is required. Platinum catalysed wet oxidation (Pt-CWO) is a heterogeneous process, which necessitates consideration to be given to mass transfer, and the kinetics and mechanisms of the chemical reaction. An understanding of how the reactor configuration and selected reaction conditions could influence these steps is therefore a key to optimisation of the process.

The purpose of this section is to identify the principal issues in the design of CWO using platinum catalysts and explore their impact on process design. The application ranges of platinum catalysed wet oxidation processes with respect to the quantity of

wastewater produced and the composition and concentration of pollutants it contains, are also discussed. The operational options and limitations, although this section is not exhaustive, are also outlined.

Selection of catalysts

The choice of the catalyst plays an important role in the possible industrial applicability of the catalytic wet oxidation of organic wastes to the desired end products carbon dioxide and water. In general the catalyst used should combine high activity with high selectivity and should preferably suffer little from deactivation in time. Platinum catalysts on different supports have the potential for effective removal of organic wastes. The catalyst support, which has not too high metal dispersion and a relatively low porosity, seems to maintain the highest activity and is less vulnerable to over-oxidation. The catalyst found to be effective for CWO is Pt/graphite catalyst with a metal dispersion of 5.3% and porosity of 69.3%. The performance of this catalyst was tested and proven for continuous oxidation of model organic compounds. However, improvements are still possible for Pt/TiO_2 catalyst, and other supports mentioned in the literature such as CeO_2, which require further testing.

Wastewater composition and organic pollutant loads

The model compounds tested, phenol, maleic acid, and malonic acid, are all oxygenate compounds, which represent a wide range of industrial wastewater. For an oxygenate organic pollutant P containing organically bound oxygen, the oxidation can be expressed as:

$$C_nH_aO_b + c\ O_2 \rightarrow n\ CO_2 + d\ H_2O \tag{8.1}$$

The stoichiometric coefficients for water and for oxygen are $d = a/2$ and $c = ((2n-b)+a/2)/2$, respectively. Based on the findings obtained from the model compounds, the catalyst chosen, Pt/graphite, is suitable for oxygenate compounds. However, the performance of platinum catalyst is limited with both the organic and the oxygen loads, which have been discussed in Chapter 2.

A high conversion of organic compound and selectivity to carbon dioxide can be obtained when low organic loads are employed. The concentration range studied was 5 – 70 mol/m^3 of phenol within the liquid flow rate of 5-20 ml/min. A continuous flow operation is preferable to batch-wise processing. This allows proper estimation of

oxygen loads based on the stoichiometric oxygen excess discussed in Chapter 2. The stochiometric oxygen excess to organic pollutant P is expressed as

$$S.E.(\%) = \frac{\left[(F_{O_2}/F_P) - c\right]}{c} \times 100 \qquad (8.2)$$

where F_{O2} and F_P are the molar flow rates of oxygen and compound P, respectively. It is advisable to select a S.E. of 20% and up to 100% at higher temperatures. The concentration of oxygen at the catalytic site depends also on the mixing speed and the residual oxygen partial pressure. The target organic pollutant conversion of the PCWO process can be set between 95 and 97%. However, on the one hand, this will depend on whether additional post-treatments, e.g. waste stabilization ponds (biological process), are available, while, on other hand the effluents discharge levels, environmental restrictions and legislation will be determining.

Reactor configuration for Pt-CWO

As platinum catalysed wet oxidation of organic wastes is a heterogeneous process, the mostly preferred reactor types are slurry reactors. Fixed bed reactors with structured catalyst packings can also be considered. However, further research on its performance is required. The use of a CSTR in this work has proved to be suitable for catalytic wet oxidation, especially for platinum catalysts. In order to keep the activity of the catalyst, the ratio of the surface concentration of oxygen ($C_{O_2,S}$) to organic compound ($C_{P,S}$) should be fixed. Thus a continuous slurry back mixing reactor is preferred when compared to batch mode in which the concentration changes with time or to a plug flow reactor where the concentration changes with distance from the feed point. The continuous slurry back mixing reactor has two significant advantages: it has a high volumetric capacity, and excellent heat control. It can be operated under isothermal conditions. Due to this, scaling up is not too difficult.

The combined effects of mass transfer and chemical reaction presented in this work can be used to estimate the quantitative effects of the CWO of organic wastes. It has been shown that for a high performance of platinum catalyst the reaction should be carried out within the mass transport regime. Effective gas dispersion is essential and can be easily controlled through proper choice of the agitation speed. The cost of separating the finely divided platinum catalysts from the liquid phase can be eliminated by the use of porous filter elements inside the reactor. A stainless porous filter (diameter of 28 mm) was used in laboratory scale at a liquid permeation velocity of 5.4×10^{-4} m^3 m^{-2} s^{-1}. These filters can be kept clean by reversing the flow of liquid

periodically. Using cross-flow membrane units outside the reactor, may also be an option, if higher permeation flows are required. Another good reactor configuration for platinum catalysed wet oxidation of organic wastes is the slurry bubble column, which might be the best option for large scale applications. The gas-liquid mass transfer and heat transfer properties of bubble columns are generally favourable, but less than in CSTR.

Reactor performance

The performance of the platinum catalysed wet oxidation depends not only on the process-technological complexity but also on the feed composition, the stability of the compounds, and the residual oxygen partial pressure in the reactor. Therefore, the process should be continuously monitored by chemical analytical measurement techniques on the processed wastewater flow to guard performance stability and also the partial pressure of oxygen. It has been shown that at high residual oxygen partial pressure, above 150 kPa, deactivation of platinum catalyst occurs. Also, at too low oxygen partial pressure, acetic acid is formed. While the dehydrogenation rate of the organic molecule is determining in which maximum rate can be achieved, oxygen mass transfer to the catalytic site should be precisely balanced. If other reactions are limiting, e.g. oxygen insertion, which is observed for oxalic acid, or decarboxylation, observed for malonic acid, then high oxygen loads will not significantly affect the rate.

The activity of the platinum catalyst is enhanced with increase in temperature. For example, during phenol oxidation (Chapter 2), the weight specific oxygen loads (S.O.L) were 0.35 and 0.67 $mol.s^{-1}.kg_{Pt}^{-1}$ at 150°C and 165°C, respectively. It follows that, for a given type of organic waste, the optimum reaction temperature needs to be determined. For low molecular weight organic compounds, higher temperatures must be chosen, since these are generally more stable. Once the temperature has been established the performance of the reaction is controlled by mass transport of the reactant to the catalytic site. This has been verified in Chapters 5 and 7.

Design assumptions

The design of a reactor for platinum catalysed wet oxidation of organic compounds requires a balanced concentration of the reactants at the catalytic site. For the case where oxidative dehydrogenation is dominating, the following assumptions can be made for derivation of the rate equations:

- ❑ A uniform reactor temperature
- ❑ The gas and aqueous phases are ideally mixed
- ❑ The ideal gas law can be applied for the gas stream
- ❑ The liquid feed flow contains no oxygen
- ❑ The mass transfer limitations of oxygen and organic compound are considered
- ❑ The effectiveness factor of the catalyst particles is 1
- ❑ Changes of the reactor volume due to changes in concentration of reactants, temperature or changes in the feed and outlet flow rate are negligible
- ❑ The organic compounds are not volatile
- ❑ The catalyst is retained in the reactor by a micro porous filter
- ❑ Catalyst deactivation other than over-oxidation can be neglected on a time scale of one day
- ❑ The physical properties of organic compounds are similar i.e. oxygenates
- ❑ Side products are neglected, a carbon dioxide selectivity of 100% is assumed

Rate equations

When oxygen transport to the catalytic site is considered limiting ($C_{P,S} = C_{P,L}$), the volumetric reaction rate equation for oxygen (in mol m^3 s^{-1}) can be expressed as:

$$R_{V,O_2} = \frac{C_{O_2}^{sat}}{\left[\dfrac{1}{(k_{GL}\, a_{GL})} + \dfrac{1}{(k_{LS}\, a_{LS})_{O_2}} + \dfrac{1}{\eta\, k_w\, C_{cat}\, C_{P,L}} \right]} = \frac{C_{O_2}^{sat}}{[A + B + C]} \qquad (8.3)$$

However, if the organic pollutant transport to the catalytic site is limiting ($C_{O_2,S} = C_{O_2,L}$), then the volumetric reaction rate (in mol m^3 s^{-1}) is given by:

$$R_{V,P} = \frac{C_{P,L}}{\left[\dfrac{1}{(k_{LS}\, a_{LS})_P} + \dfrac{1}{(1/c)\eta\, k_w\, C_{cat}\, C_{O_2,L}} \right]} = \frac{C_{P,L}}{[D + E]} \qquad (8.4)$$

The description of the symbols has been given in Chapter 7. The rate equations (8.3) and (8.4) can be combined with the mole balances for the type of the reactor used. The mass transfer coefficients have been determined for a CSTR with a gas inducing impeller. For other types of reactor and impeller, proper correlations for estimation of mass transfer coefficients should be used. The reaction temperature should be sufficiently high for k_w to be high, so that C<<(A+B) and E<<D.

8.3. Outlook

With regard to the obtained results described in this thesis, catalytic wet oxidation using platinum catalysts can be considered as a promising wastewater treatment process. The favourable conversion rates and stability of platinum catalysts in liquid phase observed in this work, justifies continuation of the research on catalytic wet oxidation. The topics of interest are described as follows.

The CWO mass transport model for phenol, which is similar for maleic acid, can be extended to incorporate the surface coverage. This will help to investigate from a theoretical point of view, several aspects of platinum catalysed wet oxidation (Pt-CWO) that have been determined practically. Such areas include the practical operational window, and reactor start-up and operation within and outside the operational window. The model can also be extended, by incorporating a mass transfer enhancement factor, if enhancement plays an important role during the catalytic wet oxidation of organic wastes.

The mass transport models describe the performance of platinum catalysts for liquid phase oxidation in the laboratory set-up. Hydrodynamic parameters of the system can change if the reactor is scaled up for industrial use. It would be useful to include reactor dimensions relevant for mass transfer in the model expressions that can enable its application to commercially available reactors.

Further studies on catalytic wet decarboxylation and oxidation of malonic acid can be useful. The interesting topic is to investigate the catalytic activity of graphite for malonic acid decarboxylation and oxidation. The role of oxygen and catalyst concentration in malonic acid oxidation needs to be clearly identified.

Towards industrial applications, the performance of CWO using platinum catalysts for high flow rate discharge and for high organic loads, scale-up and process stability should be studied. With regards to the choice of the catalyst an eggshell type of platinum catalyst with a relatively low metal dispersion and low percentage of porosity is preferred. The application of Pt/TiO_2 catalyst for wastewater treatment may be promising, however, further study is required. Another topic of interest would be the effect of hydrophilic characteristics of the supports, since these can significantly influence the mass transfer properties of the system, due to particle bubble adhesion.

ACKNOWLEDGEMENTS

CURRICULUM VITAE

Zacharia Peter Gikira Masende was born on August 18th, 1963 in Bariadi, Tanzania. In 1987 he started his university course at the Faculty of Engineering of the University of Dar es Salaam after having completed one year of National Service. In 1992 he obtained a B.Sc.(Eng.) degree with distinction from the Department of Chemical and Process Engineering of the University of Dar es Salaam. During his study, he was involved in various activities and responsibilities. Among others, he was a student representative and a member of the Board of the Faculty of Engineering. As part of co-curriculum activity, he had internships in several industries in Tanzania at different times, including Mwanza Textiles Ltd (1988), New Era Oil Mills Ltd (1989) and Lake Soap Industries Ltd (1991).

Since November 1992, he has been working at the Faculty of Engineering of the University of Dar es Salaam as a member of the teaching staff in chemical engineering. He was also involved in the design, installation and operation of laboratory facilities for a newly established course in the field of chemical engineering. In October 1996, he started a master's course in environmental engineering at the Faculty of Engineering of the University of Dar es Salaam. In November 1999, he received his master's degree in environmental engineering under the supervision of Prof. J.H.Y. Katima and Dr. E. Masanja on the topic of, "Utilization of water hyacinth biomass for production of ethanol". Immediately after this he started his Ph.D. research at the Eindhoven University of Technology in the Laboratory of Chemical Reactor Engineering, Department of Chemical Engineering and Chemistry, under the supervision of Prof.dr.ir. J.C. Schouten, Prof.dr.ir. F.J.J.G. Janssen, and Dr.ir. B.F.M. Kuster. During this study, he was also involved in the construction, installation and operation of a multiphase reactor set-up at the Department of Chemical and Process Engineering, University of Dar es Salaam. His Ph.D. research has resulted in this thesis.

PUBLICATIONS

Publications related to this thesis

Masende, Z.P.G., Kuster, B.F.M., Ptasinski, K.J., Janssen, F.J.J.G., Katima, J.H.Y. and Schouten, J.C., "Platinum catalysed wet oxidation of phenol in a stirred slurry reactor: A practical operation window", *Appl. Catal. B,* **41** (2003) 247.

Masende, Z.P.G., Kuster, B.F.M., Ptasinski, K.J., Janssen, F.J.J.G., Katima, J.H.Y. and Schouten, J.C., "Platinum catalysed wet oxidation of phenol in a stirred slurry reactor: The role of oxygen and phenol loads on reaction pathways", *Catal. Today,* **79-80** (2003b) 357.

Masende, Z.P.G., Kuster, B.F.M., Ptasinski, K.J., Janssen, F.J.J.G., Katima, J.H.Y. and Schouten, J.C., "Support and dispersion effects on activity of platinum catalysts during wet oxidation of organic wastes", *Topics in Catal.,* (2004) Submitted.

Masende, Z.P.G., Kuster, B.F.M., Ptasinski, K.J., Janssen, F.J.J.G., Katima, J.H.Y. and Schouten, J.C., "Platinum catalysed wet oxidation of phenol in a stirred slurry reactor: Mass transfer and reaction kinetics", *Chem. Eng. Sci.,* (2004) Submitted.

Masende, Z.P.G., Kuster, B.F.M., Ptasinski, K.J., Janssen, F.J.J.G., Katima, J.H.Y. and Schouten, J.C., "Kinetics of malonic acid degradation in aqueous phase over Pt/graphite catalyst", *Appl. Catal. B,* (2004) Submitted.

Masende, Z.P.G., Kuster, B.F.M., Ptasinski, K.J., Janssen, F.J.J.G., Katima, J.H.Y. and Schouten, J.C., "Catalytic wet oxidation of maleic acid over Pt/graphite catalyst: Mass transport and reaction kinetics", *Appl. Catal. B,* (2004) Submitted.

Other publications

Masende, Z.P.G., "Utilization of Water Hyacinth (WH) biomass for ethanol production", An MSc dissertation, University of Dar es Salaam, Tanzania, 1999.

Masende, Z.P., Katima, J.H.Y. and Masanja. E., "Ethanol from water hyacinth: Fermentability of WH hydrolysates from acid-catalysed hydrolysis process", *The Tanzania Engineer*, 6 (5) (1999) 27 – 39.